
# Cement Stabilized Materials with Use of RoadCem Additive

**P. Wu**

# Cement Stabilized Materials with Use of RoadCem Additive

**Proefschrift**

ter verkrijging van de graad van doctor
aan de Technische Universiteit Delft,
op gezag van de Rector Magnificus prof.ir. K.C.A.M. Luyben,
voorzitter van het College voor Promoties,
in het openbaar te verdedigen op maandag 21 september 2015 om 10.00 uur

door

**Pengpeng WU**

Master of Science in Bridge Engineering
Beijing Jiaotong University, China
geboren te Shandong, China

Dit proefschrift is goedgekeurd door de promotor:

Prof.dr. A. Scarpas

Copromotor:

Ir. L.J.M. Houben

Samenstelling promotiecommissie:

| | |
|---|---|
| Rector Magnificus | Technische Universiteit Delft, voorzitter |
| Prof.dr. A. Scarpas | Technische Universiteit Delft, promotor |
| Ir. L.J.M. Houben | Technische Universiteit Delft, copromotor |

Onafhankelijke leden:

| | |
|---|---|
| Prof.dr. J.T. Balbo | University of Sao Paulo, Brazil |
| Prof. D.N. Little, Ph.D., P.E. | Texas A&M University, USA |
| Prof. B. Birgisson, Ph.D., P.E. | Aston University, UK |
| Prof.dr. C. Jommi | Technische Universiteit Delft |
| Prof.dr.ir. H.E.J.G. Schlangen | Technische Universiteit Delft |

ISBN: 978-94-6203-866-0
Printed by: Wohrmann Print Service, Zutphen, the Netherlands


Section of Pavement Engineering, Delft University of Technology
E-mail: p.wu@tudelft.nl; pengwu.tu@gmail.com

# Summary

A cement stabilized road base is susceptible to especially transverse cracks which are mainly caused by the shrinkage during the cement hydration and the temperature decrease. Use of non-traditional additives in cement stabilization can be a potential alternative to eliminate or reduce the transverse cracks in cement stabilized road bases. This research is therefore focused on the characterization of the mechanical properties and deformation characteristics of cement stabilized materials, with or without use of a non-traditional additive, in relation to the mix variables, such as cement content and additive content. This additive, with product name "RoadCem", referred to as Rc additive, is mainly composed of alkali metal, alkaline earth metal substances and synthetic zeolites. The Rc additive is specifically used in cement stabilized soil materials. An extensive test program was carried out, in which the mechanical properties as well as the shrinkage behaviour and crack susceptibility were evaluated.

The laboratory investigation is the major part of this research which involves two types of soils (sand and clay) stabilized with different amounts of cement and Rc additive. For each mixture, a series of mechanical strength tests at various curing times were conducted, including compressive strength, flexural tensile strength, indirect tensile strength and fatigue tests. The laboratory test results give insight into the influence of the mixture variables (cement and Rc additive contents) on the properties of cement stabilized materials which showed that mechanical properties are much dependent on the mix proportions. For instance, adding Rc additive increases the mechanical strength of cement stabilized sand materials. Estimation models were developed to predict the mechanical strength of cement stabilized materials as a function of the mixture variables and the curing time. The estimation models show a good fit with the actual test data.

To verify the obtained laboratory results, a field study was established to evaluate the properties of the cement stabilized materials under field conditions and determine the difference between the laboratory-designed properties and the field performance. Field test sections were created by constructing a cement stabilized road base by using a variety of materials and applying variable mix designs. By comparing the mechanical strength of the field cores and the laboratory-prepared specimens, it is found that the compressive and indirect tensile strength of the field cores reach 30% to 70% of the strength obtained from the laboratory-prepared

specimens. This difference can be attributed to variations in the environmental conditions during hardening and the differences between laboratory-preparation methods and field construction techniques.

The deformation behaviour related to drying shrinkage and temperature variations was evaluated. The Rc additive was observed to have a significant influence on reducing the drying shrinkage of cement stabilized sand and clay materials. The Rc additive reduces the total shrinkage of clay-cement material by 50% at 28 days and the higher the Rc additive content, the less the drying shrinkage.

Finally, transverse crack patterns were analysed by using a mechanical model which relates the induced shrinkage and thermal tensile stress to the tensile strength of the materials. Adding Rc additive in cement stabilized materials reduces the total occurring tensile stress and thus reduces the potential of transverse cracks. Adding Rc additive reduces the width of the cracks and reduces the number of cracks approximately by 50% in cement stabilized materials. Further research is needed to develop the optimum mix design incorporating cement and Rc additive contents, to balance the mechanical properties and the cracking performance which can be beneficial for the design and performance of pavement structures with a cement stabilized base.

# Table of content

# List of abbreviations

| | |
|---|---|
| AASHTO | American Association of State Highway and Transportation Officials |
| CBM | Cement Bound Material |
| CTB | Cement Treated Base |
| CTE | Coefficient of Thermal Expansion |
| EN | European Norm |
| FTS | Flexural Tensile Strength |
| ITS | Indirect Tensile Strength |
| LL | Liquid Limit |
| PI | Plasticity Index |
| PL | Plastic Limit |
| SEM | Scanning Electron Microscopy |
| UCS | Unconfined Compressive Strength |
| USCS | Unified Soil Classification System |
| XRD | X-Ray Diffraction |

# CHAPTER 1

# INTRODUCTION

High quality road infrastructure is of utmost importance for economic development of any region in the world. As a consequence of economic growth, road traffic is increasing in vehicle numbers and in truck axle loads which requires extension of the road network, high quality road materials, adequate structural pavement design and correct construction methods. Both flexible and rigid pavement structures can be designed and constructed to address efficiency of these requirements. However, both types of pavements require a base course with good structural performance and a long service life below the surface layers.

For road bases (sub-bases), a variety of soils or granular materials are available for construction, but they may exhibit insufficient properties (e.g. low bearing capacity and susceptibility to volume change), which then could result in substantial pavement distress and reduction of pavement life. The properties of soil can be improved by addition of cement to form a durable hardened material which may be an alternative for pavement construction. Stabilization of soil or granular materials improves the soil gradation, reduces the plasticity index or swelling potential of soil, and increases the stiffness, strength and resistance to permanent deformation and thus contributing to pavement serviceability and high durability.

However, the hardened cement stabilized materials exhibit brittle behavior and are susceptible to shrinkage cracks due to the hydration process or a decrease of temperature. Cracks occurring in a cement stabilized base layer may reflect through the wearing course which would reduce the pavement serviceability and increase maintenance costs. Use of innovative additives in cement stabilization can be a

potential alternative to reduce or eliminate these disadvantages of cement stabilized road bases and could result in more durable and economic pavement structures.

## 1.1 Background and initiative of this research

A cement stabilized material is generally defined as a mixture of soil or aggregates with addition of cement and water, compacted to high density. As cement reacts with water, the hydration products bind the soil or aggregate particles together, resulting in enhanced strength and stiffness as well as improved durability and impermeability.

Cement stabilized material is primarily used as base material underlying asphalt or concrete pavements, which is normally known as a soil-cement base (ACI, 1990). A wide variety of soils or aggregates can be stabilized with cement, e.g. sand, silt, clay or gravel, even recycled concrete and waste materials (Croney, 1977). Thus, when high quality local materials are not available, stabilization of less suitable in-situ soils with cement could be a beneficial option which saves considerable natural resources and offers significant environmental benefit.

Cement stabilized soil or aggregates are known as materials which are susceptible to shrinkage cracks due to the moisture loss during hydration process or a decrease of temperature (Syed & Scullion, 2001; Molenaar, 2006; Bofinger & Williams, 1978; Adaska & Luhr, 2004). Shrinkage cracks that develop in the road base may reflect through the top layer, resulting in visible transverse cracks, as shown in Figure 1.1.

(a) Narrow reflection crack (b) Wide reflection crack

**Figure 1.1** Reflective cracks of cement stabilized road base (Adaska & Luhr, 2004)

Excessive reflective cracking may accelerate deterioration of the road structure and increases the susceptibility to moisture which eventually would lead to increased maintenance costs. Use of an excessive amount of cement may lead to a very stiff

stabilized layer which exhibits great potential of shrinkage cracks. On the other hand, an insufficient amount of cement might not provide adequate durability under expected traffic loads and environmental conditions (Guthrie et al, 2002). Therefore, seeking the appropriate mix design to balance the strength and the potential of cracking provides a great challenge for engineers and road agencies. However, use of non-traditional additives in cement stabilization can be a potential alternative to reduce or eliminate the transverse cracks and improve the properties of these materials.

Currently numerous non-traditional additives have been developed and increasingly promoted for use in stabilization. Santoni and Tingle (2002) divided these products into several categories, i.e. salts, acids, enzymes, lignosulfonates, petroleum emulsions, polymers, and tree resins. Many of these available products are advertised as low quantity in use, less construction time required or higher durability or higher overall performance compared with traditional stabilization additives (Tingle & Santoni, 2003). The effect of these products on the stabilization process has been evaluated in a few studies (Rauch et al., 2002; Tingle & Santoni, 2003; Santoni et al., 2005) which generally demonstrated that some products can provide some additional strength improvement, such as polymers, while some products failed to show observable changes or even resulted in a decrease of strength.

Despite the potential advantages of using these non-traditional additives, most transportation agencies and engineers hesitate to specify the use of these products (Rauch et al, 2002). Rauch (2002) attributed this lack of acceptance to the following issues:

- Principal concern is the lack of published, independent studies of these stabilizers, especially field performance data. Test results or field case studies provided by the product producers typically aim to demonstrate the benefits of these commercial products without showing data on the untreated control sections.
- The information provided by the stabilizer supplier is often not adequate. For instance, many manufacturers consider the chemical composition of their product to be proprietary, which makes it difficult to understand well the stabilization mechanism and forecast the potential field benefits.
- Lack of appropriate engineering expertise within supplier companies may result in the misapplication of the product and project failures.

Moreover, traditional cement stabilized materials have been extensively evaluated in many literature studies by investigating the mechanical strength, deformation behaviour and field performance (George, 1968; Sherwood, 1981; Lim & Zollinger, 2003; Guthrie & Rogers, 2010), and their specifications and construction techniques are also well documented (Williams, 1986; TRH 13, 1986; Little, 2009). Therefore, there is a growing need for in-depth research into the non-traditional additives which can provide a better understanding of the engineering properties of using these products and the potential benefits of their field applications.

Thus, this research was initiated to conduct an extensive test program to investigate the properties of a non-traditional additive in cement stabilization. One type of additive is evaluated, with trade name "RoadCem", manufactured by PowerCem Technologies in the Netherlands. In this thesis, this additive is referred to as Rc additive.

### 1.2 Introduction of RoadCem additive (Rc)

Rc additive is a fine grained white powder, mainly composted of alkali metal, alkaline earth metal substances (NaCl, KCl, $CaCl_2$ and $MgCl_2$), oxides, synthetic zeolites and activator. Figure 1.2 shows the Rc additive powder used in this study.

**Figure 1.2** RoadCem additive (Rc)

In road base construction, Rc additive is used by first mixing it with the in-situ soils and applying and mixing with cement and water. This type of additive has been used in construction of cement stabilized bases in many countries. Figure 1.3 shows some typical road projects constructed by using the Rc additive in the cement stabilized base course which have proven to be durable road stabilization.

(a) Brazil (b) Mexico

**Figure 1.3** Road projects by using Rc additive (www. powercem.com)

According to the supplier, use of the Rc additive in cement stabilization has the following advantages:

- Stabilization of all types of soils. Rc additive in combination with cement enables use of the in-situ soils including sand, clay, peat and even contaminated soils, etc. Rc additive has characteristics like ion exchanger, neutralizer, molecular sieve, catalyst and absorber.
- Increasing strength, stiffness and flexibility. Rc additive increases the strength and stiffness of cement stabilized soils, especially the early-age strength and thus the finished projects are normally allowed for traffic shortly after construction. Because the compounds of the Rc additive accelerate and increase the degree of cement hydration.
- Reducing the amount of shrinkage. Compared with the traditional cement stabilized road base, road bases with use of Rc additive don't show transverse cracks or much less cracks, which is mainly because the Rc additive can reduce the amount of shrinkage.

This study is initiated and aimed to systematically evaluate the effect of this additive and provide comparable test results with traditional cement stabilized materials.

### 1.3 Objective and scope of this research

The major objective of this research is to evaluate the influence of the Rc additive on the properties of cement stabilized soil materials under laboratory and field conditions. The basic mechanical properties (strength and stiffness) as well as the shrinkage of the materials are the main focus of this research.

First, investigation into the use of Rc additive was undertaken in terms of an extensive laboratory test program which mainly focused on the strength, stiffness and fatigue properties by evaluating variable mix designs for cement stabilized sand and clay. Based on the laboratory test results, estimation models were developed to predict the strength and stiffness of the stabilized materials with the combined effect of various factors such as cement content, Rc additive content and curing time. These prediction models will aid in designing an optimum mixture based on the required strength.

Furthermore, shrinkage tests were performed and by means of an analytical model the transverse crack pattern (i.e. crack spacing and crack width) developing in the cement stabilized layers was investigated.

In addition to the mechanical properties, the micro-properties of cement stabilized soil were also evaluated including observation of the microstructure of cemented crystals and chemical analysis of the hydration products, aiming to explain the observed mechanical behavior of using Rc additive. Moreover, the field performance of using Rc additive in cement stabilized bases was investigated and compared with the properties obtained in the laboratory condition.

### 1.4 Overview of the thesis

This thesis consists of 9 Chapters. Figure 1.4 shows the overview of the thesis.

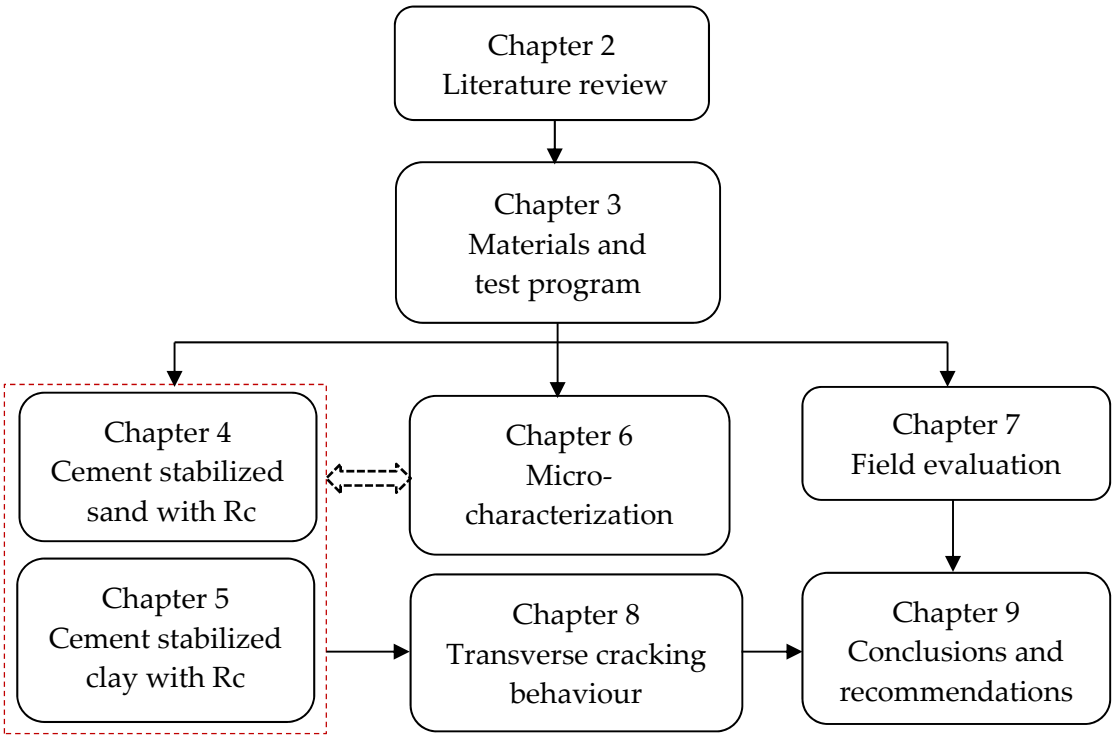


**Figure 1.4** Overview of this thesis

Chapter 2 reviews the literature on cement stabilized materials. This Chapter focuses on the compressive and tensile strength, modulus of elasticity, fatigue life as well as shrinkage behavior of traditional cement stabilized materials and will provide a good means of comparison with the properties of the materials evaluated in this study.

Chapter 3 presents the properties of the raw materials used for stabilization, the mix design and the test methods. Two types of soil were used, sand and clay, representing coarse-grained (non-cohesive) and fine-grained soils (cohesive) which behave quite differently in stabilization.

Chapter 4 focuses on the mechanical properties of cement stabilized sand with and without the use of Rc additive. An extensive laboratory test program consisting of compression, indirect tensile, flexural tensile and fatigue tests was conducted on 9 different mixtures. The properties of sand-cement were analyzed under the influence of variable cement and Rc contents and curing times. Based on this laboratory test data, estimation models were developed to predict the strength and stiffness of sand-cement materials. The models are based on the effects of cement content, Rc additive content, density of the specimens as well as curing time.

Similar to Chapter 4, the same test program and analyses were carried out on clay-cement materials with and without the addition of Rc additive in Chapter 5.

Based on Chapters 4 and 5 in which the influence of the Rc additive on the mechanical performance of soil-cement was investigated, Chapter 6 investigates the properties of these materials in the micro-scale aiming to explain the observed behavior in the previous two Chapters. This Chapter compared the microstructure and chemical analysis of cementitious materials with and without Rc additive.

Chapter 7 extends the research into the field performance of cement stabilized road bases with use of Rc additive. A new stabilized road base was constructed by using a wide range of soil types and applying different mix designs. In parallel, specimens using the same materials were prepared and cured in the laboratory in order to compare the properties with those of the core specimens collected in the field. Based on the field data, estimation models were developed to estimate the strength of cement stabilized materials in field conditions.

In Chapter 8 the shrinkage of cement stabilized sand and clay materials was measured for three mixtures with different amounts of Rc content and cured in two different conditions. The transverse crack pattern of the cement stabilized materials

was estimated by an analytical method, considering the development of the occurring tensile stress due to shrinkage and temperature changes, and the development of the tensile strength of the materials. The time of occurrence of the cracks, the crack spacing and the width of the cracks were calculated.

Chapter 9 summarizes the principle findings presented throughout this thesis and recommendations for further research are given.

## References

ACI. (1990). American Concrete Institute Committee 230. State-of-the-Art Report on Soil Cement. ACI Materials Journal, Vol. 87, No. 4, pp. 395–417.

Adaska, W.S. & D.R. Luhr. (2004). Control of reflective cracking in cement stabilized pavements, RILEM Publications.

Bofinger, H. E., H.O. Hassan & R.I.T. Williams (1978). The shrinkage of fine-grained soil-cement. TRRL supplementary report 398.

Croney. D. (1977). The Design and Performance of Road pavements. London, Transport and Road Resarech Laboratory, Crowthorne, UK.

George, K.P. (1968). Shrinkage Characteristics of Soil-Cement Mixtures, Highway Research Record 255, Washington D.C.

Guthrie, W.S. & M.A. Rogers (2010). Variability in Construction of Cement-Treated Base Layers. Transportation Research Record: Journal of the Transportation Research Board 2186(-1): 78-89.

Guthrie, W.S., Sebesta, S & Scullion, T. (2002). Selecting optimum cement contents for stabilizing aggregate base materials. No. FHWA/TX-05/7-4920-2, Texas Transportation Institute, Texas A & M University System.

Lim, S., & Zollinger, D.G. (2003). Estimation of the compressive strength and modulus of elasticity of cement-treated aggregate base materials. Transportation Research Record: Journal of the Transportation Research Board, 1837(1), 30-38.

Little, D.N. (2009). Recommended Practice for Stabilization of Subgrade Soils and Base Materials. NCHRP web-only document 144. Texas A&M University, Texas.

Marjanovic, P., Egyed, C.E.G., De La Roij, P and de La Roij, R (2008). The Road to the Future. Manual for Working with RoadCem. PowerCem Technologies, ISBN 978-90-79835-01-0.

Molenaar. A.A.A (2006). Structural Design of Pavement, Design of Flexible Pavement. Lecture Notes CT 4860, Delft University of Technology, the Netherlands.

Rauch, A.F., Harmon, J.S., Katz, L.E., & Liljestrand, H.M. (2002). Measured effects of liquid soil stabilizers on engineering properties of clay. Transportation Research Record: Journal of the Transportation Research Board, 1787(1), 33-41.

Santoni, R.L., Tingle, J.S., & Nieves, M. (2005). Accelerated strength improvement of silty sand with nontraditional additives. Transportation Research Record: Journal of the Transportation Research Board, 1936(1), 34-42.

Santoni, R.L., Tingle, J.S., & Webster, S.L. (2002). Stabilization of silty sand with nontraditional additives. Transportation Research Record: Journal of the Transportation Research Board, 1787(1), 61-70.

Syed, I.M., & Scullion, T. (2001). Performance evaluation of recycled and stabilized bases in Texas. Transportation Research Record: Journal of the Transportation Research Board, 1757(1), 14-21.

Sherwood, P.T. (1981). The properties of cement-stabilized materials, RRL Report LR 205, Crowthorne, UK.

Shon, C. S., Saylak, D., & Mishra, S. K. (2010). Combined use of calcium chloride and fly ash in road base stabilization. Transportation Research Record: Journal of the Transportation Research Board, 2186(1), 120-129.

Tingle, J.S., & Santoni, R.L. (2003). Stabilization of clay soils with nontraditional additives. Transportation Research Record: Journal of the Transportation Research Board, 1819(1), 72-84.

Tingle, J. S., Newman, J. K., Larson, S. L., Weiss, C. A., & Rushing, J. F. (2007). Stabilization mechanisms of nontraditional additives. Transportation Research Record: Journal of the Transportation Research Board, 1989(1), 59-67.

TRH 13 (1986). Cementitious Stabilizers in Road Construction South Africa. Pretoria, South Africa.

Williams, R.I.T. (1986). Cement-treated pavements: Materials, Design and Construction, London: Elsevier Applied Science Publishers Ltd.

# CHAPTER 2

# LITERATURE REVIEW
## BEHAVIOR OF CEMENT STABILIZED MATERIALS

The properties of cement stabilized materials in the laboratory conditions are influenced by several factors (ACI, 1990):

(a) Type of and proportion of soil, cementitious materials and water content;

(b) Compaction method;

(c) Uniformity of mixing;

(d) Curing conditions;

(e) Age of the compacted mixture, etc.

Because of these factors, a wide range of values for specific properties may exist. This Chapter provides an extensive literature survey on the structural properties of cement stabilized materials regarding how these factors influence various properties. The literature study begins with the materials used in cement stabilization, followed by the main part illustrating the structural properties of these materials. The properties discussed herein include the compressive strength, tensile strength and elastic modulus which are typically used for characterization of cement stabilized materials. The fatigue property and shrinkage behavior of these materials are discussed which are also important in the application of cement stabilized material in pavement construction. At the end, the literature of Rc additive is presented.

## 2.1 Traditional stabilizers

Stabilization of soil is an effective method to improve the soil properties and enhance the pavement performance, including:

(1) Increasing strength and stiffness;

(2) Increasing durability and resistance to erosion and frost attack;

(3) Reducing permeability and increasing volume stability to control the swell-shrink characteristics caused by moisture change.

Basically, there are two primary types of soil stabilization methods: mechanical and chemical. Mechanical stabilization involves the physical process of changing the soil properties, such as compaction or modifying the soil gradation by incorporating other types of soil. Chemical stabilization refers to addition of chemical stabilizers to improve the properties of soils. There are many types of chemical stabilizers that can be used, including cement, lime, fly ash and bitumen. The calcium-based stabilizers such as cement, lime and fly ash generally rely on cementitious/pozzolanic reactions to modify and/or stabilize soils while bitumen mainly involves physical binding of soil particles (Little, 1995; Sherwood, 1995).

- Cement stabilization

Cement stabilized material is defined as a mixture of cement, water and soil or aggregate, that after compaction results into hardened and durable material. When cement comes into contact with water, it forms calcium silicate hydrate (generally referred to as C-S-H) and calcium hydroxide ($Ca(OH)_2$). The C-S-H gel is the major portion of the hydration products and binds the material particles together, which creates the strength of hardened cement stabilized material (Raki et al., 2009; Selvam et al., 2009). Compared with the unbound soil, stabilizing soil with cement significantly increases the stiffness and strength, improves the durability and the resistance to environmental damage such as erosion or frost attack.

- Lime stabilization

Lime is most efficiently in stabilizing medium, moderately fine and fine-grained soils causing a decrease in plasticity and swell potential of expansive soils, and an increase in their workability and strength properties (Little, 2009). Soils with a Plasticity Index (PI) that exceeds 10 and have more than 25 percent particles passing the #200 sieve (0.075 mm) are considered desirable for lime treatment (Little, 2009). Lime has also been used to pretreat highly plastic soils to facilitate pulverization and mixing, followed by applying cement (Kersten, 1961). Lime increases the soil strength by

pozzolanic reaction but the resulting strength is generally much lower than that of cement stabilized soil with the same amount of stabilizers.

- Fly ash stabilization

Two major classes of fly ash are specified in ASTM C 618 on the basis of their chemical composition resulting from the type of coal burned: Class F and Class C. Class F is fly ash normally produced from burning anthracite or bituminous coal, and Class C is normally produced from burning subbituminous coal and lignite (Halstead, 1986). Class C fly ash usually contains more than 20% calcium compounds and thus exhibits self-cementing properties, whereas Class F is rarely cementitious and requires the addition of a cementing agent to achieve significant strength. Fly ash stabilization has been extensively evaluated and significant strength improvement of treated clay was reported in many studies (Solanki et al, 2010; Parsons & Milburn, 2003; Kolias et al., 2005). However, fly ash is a by-product and therefore the properties of fly ash can vary significantly depending on the source of the coal and the steps followed in the coal burning process (Little, 2009).

- Bitumen stabilization

Bitumen is obtained through distillation of crude oil in an oil refinery. It is sensitive to temperature changes. The stabilization of soils with bitumen differs greatly from cement and lime stabilization. Unlike cement and lime which act chemically with the material being stabilized, bitumen acts as a binding agent and simply sticks the soil or aggregate particles together and prevents the ingress of water (Sherwood, 1995).

In summary, as illustrated above, for each type of soil there is more than one traditional stabilizer that can be used. The choice between these types of stabilizers is dependent on the nature of the material to be stabilized and the desired function of the stabilized layer in the pavement structure (e.g. base or sub-base). Table 2.1 shows the efficiency of the stabilizers used for different soils.

In Table 2.1, it can be seen that cement is particularly effective in stabilizing coarse granular materials like gravel and sand. Lime is more efficient to improve fine-grained material like silt and clay. It is difficult to treat cohesive soils like clayey materials with cement owing to the high cement content required which will result in shrinkage cracking and the difficulty in pulverizing the cohesive soil and mixing the cement (TRH 13, 1986).

**Table 2.1** Application of traditional stabilization methods (Ingles, 1972)

| Designation | Fine clay | Coarse clay | Fine silt | Coarse silt | Fine sand | Coarse sand | Aggregate |
|---|---|---|---|---|---|---|---|
| Particle size (mm) | <0.0006 | 0.0006-0.002 | 0.002-0.01 | 0.01-0.06 | 0.06-0.4 | 0.2-2 | >2.0 |
| Volume stability | Very poor | Fair | Fair | Good | Very good | | |
| Lime | | | | | | | |
| Cement | | | | | | | |
| Bitumen | | | | | | | |
| | Range of maximum efficiency | | | | Effective, difficult quality control | | |

However, use of cement is more widespread than lime mainly due to the availability and much higher strengths that can be achieved by stabilization with cement. The following literature review will be focused on the properties of materials stabilized with cement.

## 2.2 Cement stabilized base layer in pavement structure

This study mainly focuses on the cement stabilizer. Cement stabilized material provides a strong, frost resistant base layer for flexible or rigid pavements, which is generally known as cement treated base (CTB). It can be used either in flexible or rigid pavements. Figure 2.1 gives examples of cement stabilized base in the pavement structure.

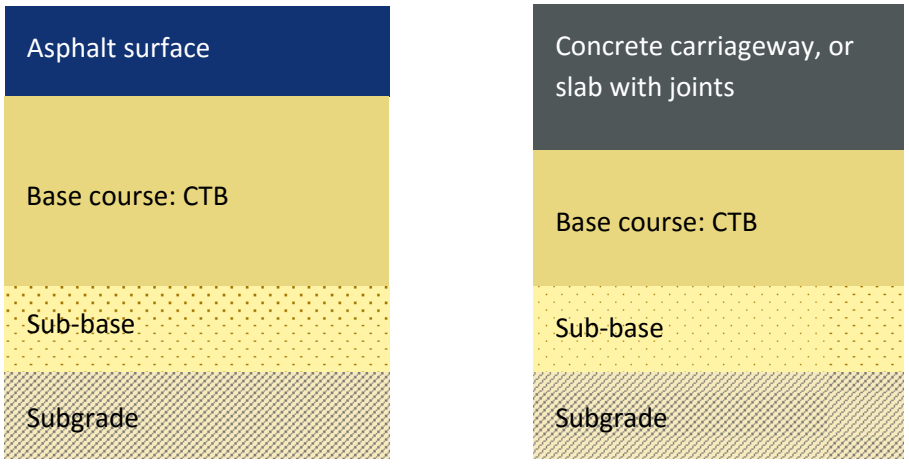


(a) Flexible (asphalt) pavement (b) Rigid (concrete) pavement

**Figure 2.1** Cement treated base in flexible and rigid pavement (after Williams, 1986)

A cement stabilized base acts as a structural layer in the pavement structure. Compared with an unbound base, the higher stiffness of the cement stabilized base

enables the loads to distribute over a wider area and hence considerably reduces stresses on the subgrade. Molenaar (2006) explained the load spreading capacity in a two-layer system consisting of a stiff top layer (modulus of elasticity E1) and subgrade (modulus of elasticity E2): when the modulus ratio E1/E2 is 100, the tensile stress in the second layer can almost be neglected and the vertical stress on the top of the second layer is significantly reduced.

Cement stabilized material is a general term to define a family of materials in which a common feature is that the addition of cement has made a material suitable for use in pavement construction (William, 1986). It is generally categorized into soil-cement, cement bound granular material (CBM) and lean concrete. The raw materials that can be used for processing in soil-cement include a wide range of materials, ranging from sandy and silty clays to more coarse grained materials. CBM can be regarded as a stronger form of soil-cement made with granular aggregate including gravel, crushed rock or slag. Lean concrete has a higher cement content than CBM and behaves more like concrete when large size aggregates are used (Croney, 1977). Figure 2.2 presents this "family" of cement based materials.

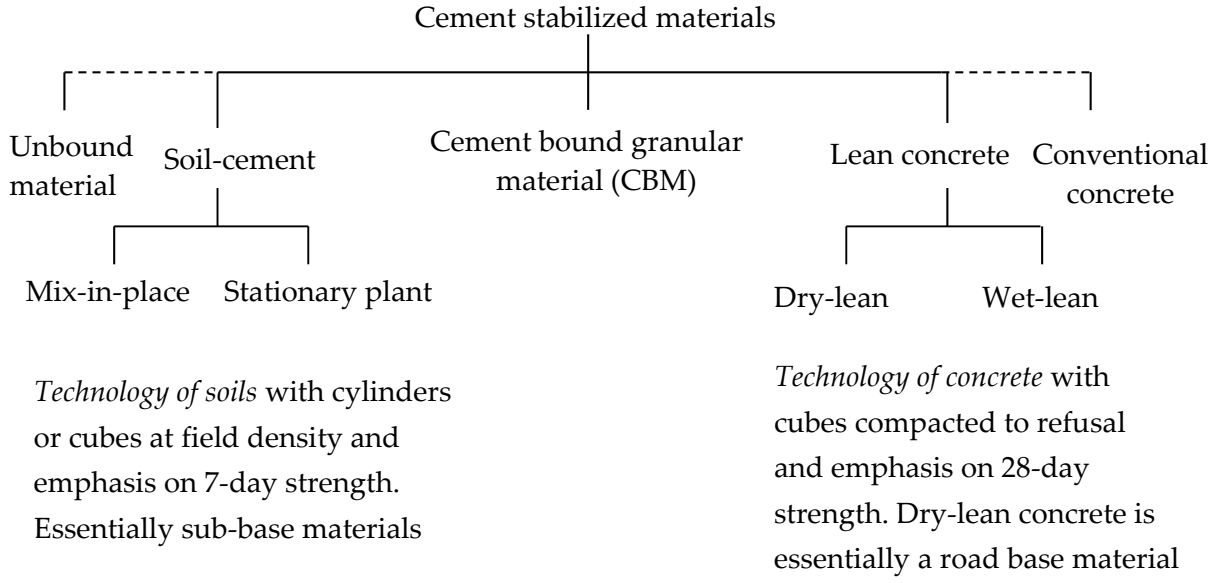


**Figure 2.2** The "family" of cement stabilized materials (Williams, 1986)

## 2.3 Materials for cement stabilization

### 2.3.1 Soil materials suitable for cement stabilization

Stabilization of soil with cement is an effective method to improve the soil properties and enhance the pavement performance. A wide range of soil or aggregate types, from coarse-grained materials like crushed gravel, sand to fine-grained soil like silt

or clay, can be stabilized with cement. Besides, tremendous amounts of recycled concrete or failed pavement materials have also been increasingly reused by stabilizing the crushed materials due to economic and environmental issues. Many guidelines give specifications regarding the suitable soil types for cement stabilization, summarized in Table 2.2.

**Table 2.2** Soil types suitable for cement stabilization

| | the Netherlands (Molenaar, 2010a) | South Africa (Croney, 1977) | UK (Watson, 1994) |
|---|---|---|---|
| Maximum LL | 50 | 45 | 45 |
| Maximum PI | 25 | 20 | 20 |
| Grading | % < 0.075 mm: <35%<br>% > 0.075 mm: >55%<br>Maximum grain size: <75 mm | The material should be well-graded with a coefficient of uniformity not less than 5. | Sieve size % passing<br>90 mm 85-100<br>10 mm 25-100<br>600 μm 10-100<br>63 μm 0-10 |

Coarse granular materials are commonly considered as the most suitable type to be stabilized with cement. Standard NEN-EN 14227-1 gives the aggregate grading suitable for cement bound granular mixture, indicated in Figure 2.3.

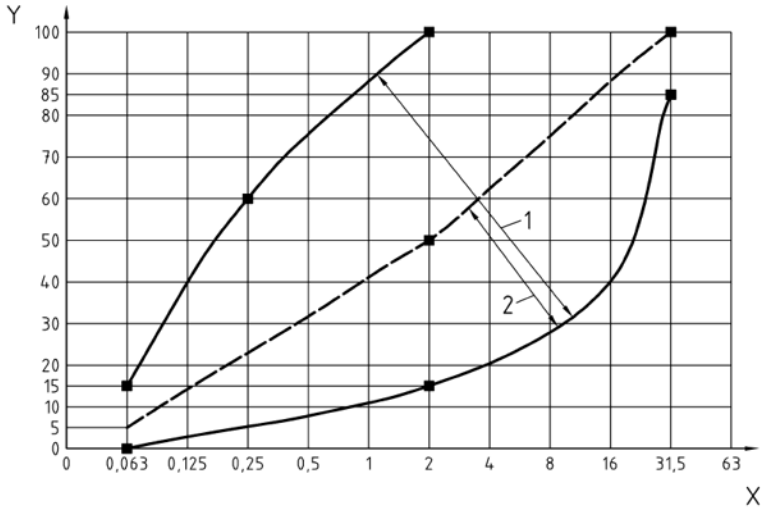


Key: Y–Percentage passing by mass; X–Sieve size, in millimeter (mm)
1–Envelope A; 2–Envelope B

**Figure 2.3** Aggregate gradation for cement bound granular mixture

The envelope in Figure 2.3 covers all the gradations with which practical experience in cement bound granular mixture exists. Gradations within envelop A include sands. Gradations within envelop B include well-graded coarse aggregates with limited contents of fines (< 0.063 mm).

### 2.3.2 Mix design for cement stabilization

In mix design of cement stabilized materials, the cement content plays a significant role in the properties of these materials. The proportion of cement alters the plasticity, volume change, susceptibility to frost heave, elastic properties, resistance to wet-dry and freeze-thaw cycles and other properties in different degrees for different soils (Kersten, 1961).

The selection of the cement content to be used is dependent on the soil property and the desired degree of improvement in soil quality. For example, relatively small amounts of cement can be used to modify the soil properties such as reducing the plasticity and decreasing the volume change of cohesive soils as the moisture varies. When it is desired to improve the strength and durability significantly, larger quantities are required (Donaldl, 1994). The former process is commonly referred to as cement-modified soil which describes a soil that is treated with a relatively small amount of cement in order to improve its soil properties. When more cement is used, the term is generally regarded as cement-treated base which refers to a strong, durable and frost resistant layer for the pavement structure (PCA, 2005a).

For stabilization, the quantity of cement required to give the specified strength for soil-cement varies with the soil types. Table 2.3 gives the cement contents likely to be required, by mass of the oven-dried soil.

**Table 2.3** Typical cement requirements for various soil types* (ACI, 1990)

| AASHTO Soil classification | ASTM soil classification | Typical requirement, % by dry mass | Requirement for durability tests, % by dry mass |
|---|---|---|---|
| A-1-a | GW, GP, GM, SW, SP, SM | 3-5 | 3-5-7 |
| A-1-b | GM, GP, SM, SP | 5-8 | 4-6-8 |
| A-2 | GM, GC, SM, SC | 5-9 | 5-7-9 |
| A-3 | SP | 7-11 | 7-9-11 |
| A-4 | CL, ML | 7-12 | 8-10-12 |
| A-5 | ML, MH, CH | 8-13 | 8-10-12 |
| A-6 | CL, CH | 9-15 | 10-12-14 |
| A-7 | MH, CH | 10-16 | 11-13-15 |

*Does not include organic or poorly reacting soils.

As indicated in research (Kersten, 1961; Donaldl, 1994; Molenaar, 2010a), a good quality mix is obtained with a cement content generally in a range of 8% to 14% by

mass (depending on the soil type). The compressive strength increases as the cement content increases. However, the higher the percentage of cement, not only the higher the costs but also the more severe the shrinkage cracking.

Before stabilization is used in road construction, laboratory test procedures are required to be carried out to determine the amount of water and cement to be added in order to achieve the specified strength. The optimum moisture content corresponds to the moisture content at which the maximum dry density of soil can be achieved (performed according to ASTM D 698 and D 1557). The cement stabilized specimens are normally prepared with the optimum moisture content. To determine the quantity of cement in mix design, two laboratory tests are normally required: the compressive strength (ASTM D1633) and the durability test by determining the weight losses under wet-dry (ASTM D559) and freeze-thaw tests (ASTM D560). The required cement content is the amount of cement at which the weight loss of the specimens subjected to 12 cycles of either wet-dry or freeze-thaw is not more than 14 percent for granular soils, 10 percent for more plastic silty soils, and 7 percent for clay soils (Thompson, 1998). Typical minimum compressive strength required in many specifications varies from 2.1 to 5.5 MPa at 7 days (PCA, 2005b). In the Netherlands, the mean compressive strength of cement stabilized sand (proctor made cylinders) should be at least 5 MPa at 28 days (Molenaar, 2006).

Water used in cement stabilized materials should be relatively clean and free of harmful substances such as salt, acids, or organic matter. Drinking water is satisfactory. However, seawater has been used satisfactorily when fresh water was unobtainable (Winterkorn & Pamukcu, 1991).

## 2.4 Properties of cement stabilized materials

### 2.4.1 Compressive strength

The compressive strength is the most commonly used mechanical property for evaluating cement stabilized materials, and is extensively used for the mix design and quality control (TRH 13, 1986). This type of test is easy to perform in the laboratory.

#### 2.4.1.1 Factors influencing the compressive strength

The compressive strength is closely linked to the cement content, soil type, degree of compaction, moisture content at compaction, as well as the curing regime.

These influencing factors are described hereafter:

(1) Effect of cement content and soil type

In the process of cement stabilization, cement reacts with water and produces calcium silicate hydrate and calcium aluminate hydrate gels, which bond the soil particles together. Most of the strength of a cement stabilized material comes from the physical strength of the matrix of hydrated cement (DFID, 2004). Therefore, cement content and soil type are the principle factors determining the properties of cement stabilized materials. A large amount of previous research documented the effect of cement content on the compressive strength. It generally revealed that the strength of cement stabilized materials increases as the cement content increases. Lay (1986/88) concluded that the compressive strength increase is approximately 0.5 to 1 MPa for each 1 percent of cement content added. Figure 2.4 illustrates the effect of cement content on different types of soil materials.

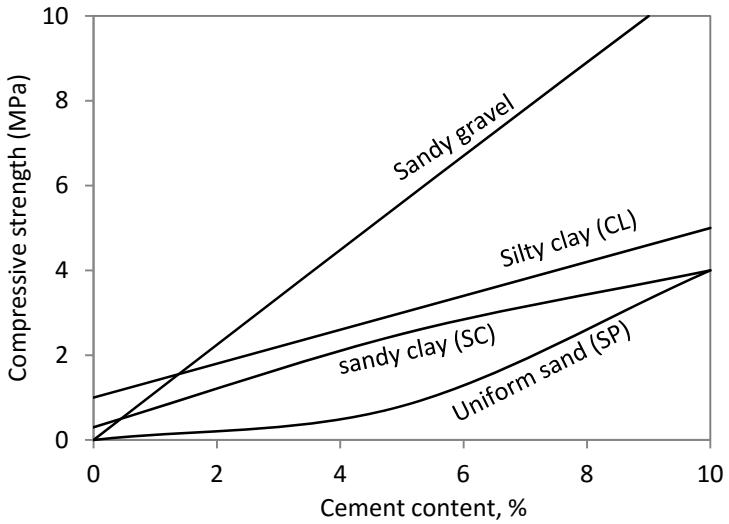


**Figure 2.4** Compressive strength at 7 days as a function of cement content for different soil types (Ingles & Metcalf, 1972)

As shown in Figure 2.4, the compressive strength increases almost linearly with the cement content and the rate is largely dependent on the soil type. Similar findings are also given in other research (TRH 13, 1986) which investigated stabilizing silt clay, sand and gravel with various cement contents and concluded that the compressive strength increases more or less linearly with the cement content but at different rates for different soils and that the larger the particle sizes of the soil, the higher the compressive strength of the stabilized material. Besides, Williams (1986) described that sandy and gravelly materials with 10 to 35% of silt and clay have the most favorable characteristics and generally require the least amount of cement for

adequate hardening because the fines can fill in the voids between the granular particles.

The improvement in compressive strength caused by cement content can be investigated by observing the microstructure of cement stabilized materials with different cement contents, as shown in Figure 2.5.

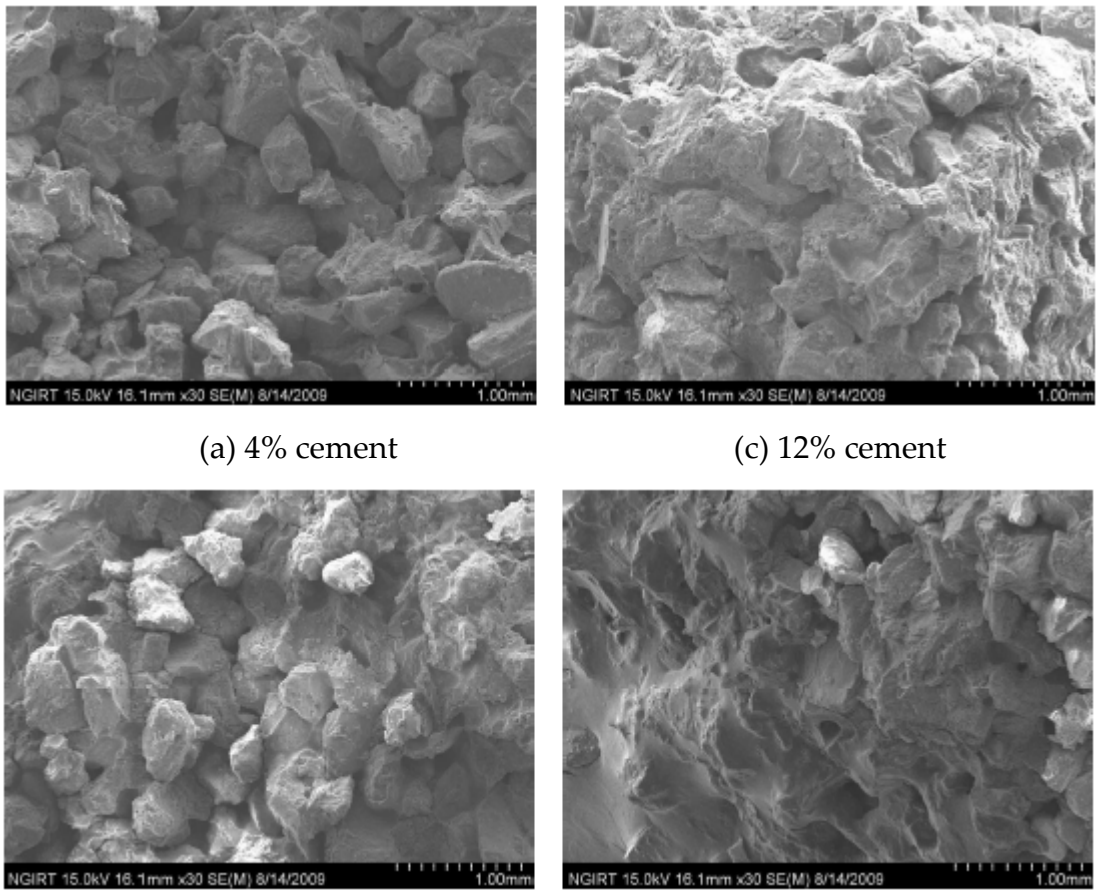


(a) 4% cement (c) 12% cement

(b) 8% cement (d) 16% cement

**Figure 2.5** SEM images of cement stabilized sand specimens with different cement contents, by dry mass of sand (Park, 2010)

As shown in the above images, for the specimens with a cement content of 4% and 8% by mass, the sand particles and some voids between these particles can be observed. However, for relatively high cement ratio such as 12% and 16% by mass, the voids between sand particles are filled with cement gel. Therefore, the higher the cement content, the more hydration products are produced, resulting in enhanced bonding strength.

(2) Effect of curing condition

Curing time is another important factor of controlling the compressive strength of cement stabilized materials. It is generally known that the compressive strength

increases with the curing time due to continued cement hydration. Figure 2.6 gives the results of compressive strength with curing time at different cement contents. This soil is classified as low plasticity sandy and clayey silt (ML), according to the USCS classification. It shows that the compressive strength increases rapidly during the first 7 days and after that the rate of increase is relatively low.

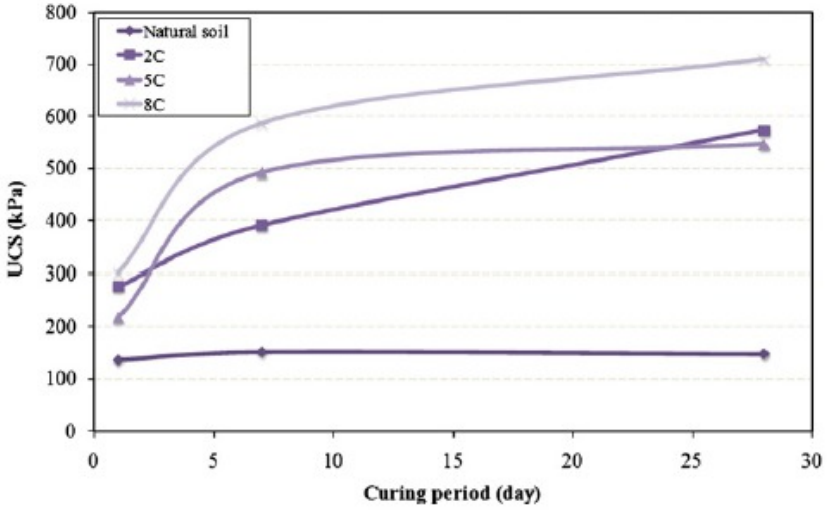


**Figure 2.6** Variation of strength at 1, 7 and 28 curing days of specimens (containing 2%, 5% and 8% cement, by mass) (Altun et al., 2009)

TRH13 (1986) described that the 28-days strength is between 1.4 and 1.7 times the 7-days strength. For estimation purposes a factor of 1.5 may be used. However, the strength of a stabilized material will often continue to increase for a period of several years from the time it is constructed (Croney, 1977). This strength development relation to the curing time can be explained by observing the change in the microstructure of cement stabilized materials (Horpibulsuk et al., 2010).

In addition to the curing time, the strength is also related to the curing temperature, which is essential for the cement hydration rate. The chemical reaction may slow down at low temperature and result into lower strength of the stabilized materials (Makusa, 2012). Increase in the ambient temperatures would enhance the compressive strength (Aliban et al., 1998). That means the higher the curing temperature, the faster the cement hydration. Figure 2.7 indicates the strength increases as the temperature increases and this effect has been used to develop accelerated test methods, i.e. curing at high temperature to give an early indication of the long-term strength.

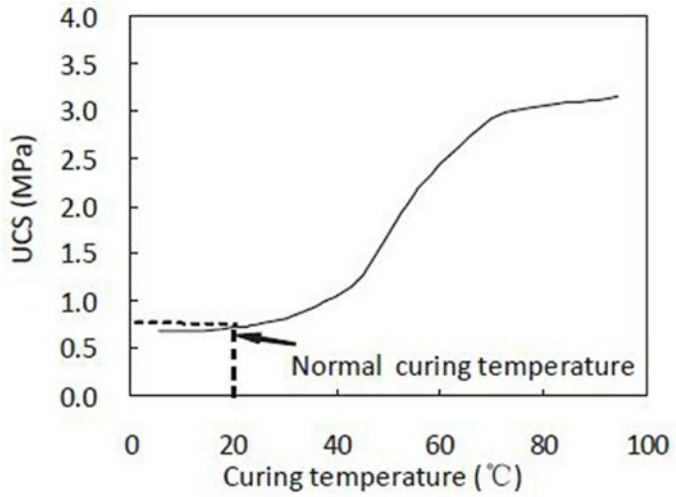


**Figure 2.7** Relationship between compressive strength and curing temperature for cement stabilized sand at 7 days (6% cement content by mass) (TRH 13, 1986)

Besides, curing methods like dry curing or immersing in water also influence the final strength. Bahar et al. (2004) investigated the strength of specimens (moderately plastic clay type A-6 according to AASHTO, 5% by mass cement) cured in water and found that after immersion in water for 48 hours, the strength of specimens decreased significantly compared to the dry specimens, because soaking reduces the bonding strength of the particles. Experiments by Kersten (1961) also showed that the compressive strength after 28 days immersion was in all cases lower than after 7-day immersion.

(3) Effect of density

The strength and durability of cement stabilized soil are strongly influenced by the density. The cement stabilized soil specimens must be heavily compacted in order to reduce the porosity and enhance the bonding strength. Basically, density of a specific material can be presented as the degree of compaction, related to the maximum dry density obtained from the Proctor test. A minimum density of 95% or 98% of standard or modified maximum Proctor density, depending on the role of the stabilized layer (base, sub-base or capping layer) in the pavement structure, is required in many specifications.

Additionally, it is well known that a cement stabilized mixture should be compacted as soon as the mixing procedure is accomplished. Delayed compaction will result in reduced strength and performance of the cement stabilized material. The cement reaction starts in the presence of water, resulting in a cementitious material, but as soon as the delayed compaction is done, the bound materials are broken and hence it leads to a reduced final strength. Figure 2.8 gives examples of delayed compaction

influencing the dry density (graph a) and strength (graph b) (TRH 13, 1986). It shows the loss in density and strength with increase in time between mixing and compaction. So it is essential to perform the compaction as soon as possible after mixing.

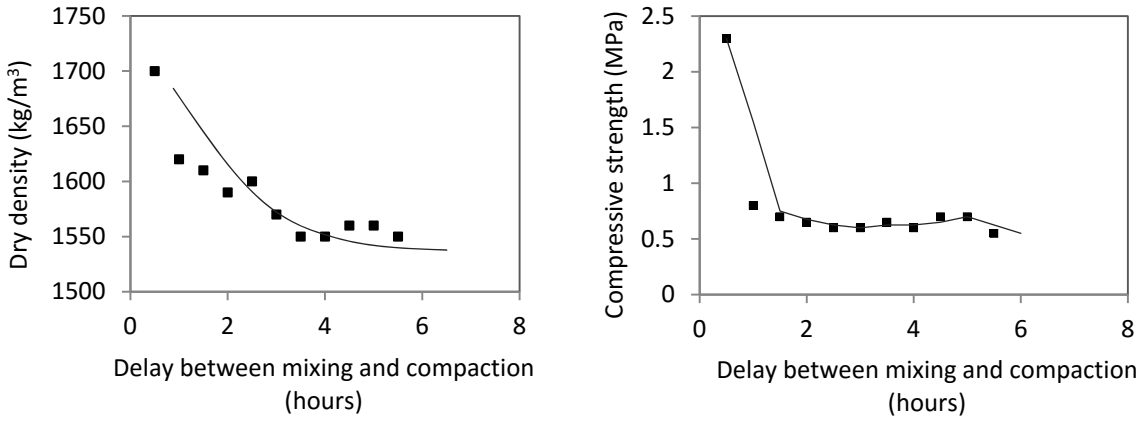


(a) (b)

**Figure 2.8** Effect of a time lapse between mixing and compaction on the dry density and unconfined compressive strength (after TRH 13, 1986)

(4) Effect of moisture content

Moisture content is also an important factor to determine the compressive strength because the optimum moisture content is essential to achieve the maximum dry density and to aid in cement hydration (Yoon & Abu-Farsakh, 2009). The dry density will be reduced at moisture contents above or below the optimum content (Kennedy, 1983).

Horpibulsuk et al. (2007) investigated cement stabilized coarse grained soils and found that compressive strength is related to the water to cement ratio. Yoon & Abu-Farsakh (2009) also examined the effects of the moisture content and the water/cement ratio on the compressive strength at 7 days, shown in Figure 2.9. The soil is classified as silty sand (SM) according to the USCS classification. As shown in Figure 2.9, the unconfined compressive strength has a positive correlation with the moisture content at the dry side of the optimum moisture content. The optimum water to cement ratios that correspond to the highest strength are about 0.75, 1.05 and 1.25 for the silty sand sample mixed with 12%, 10%, and 8% by mass of cement, respectively.

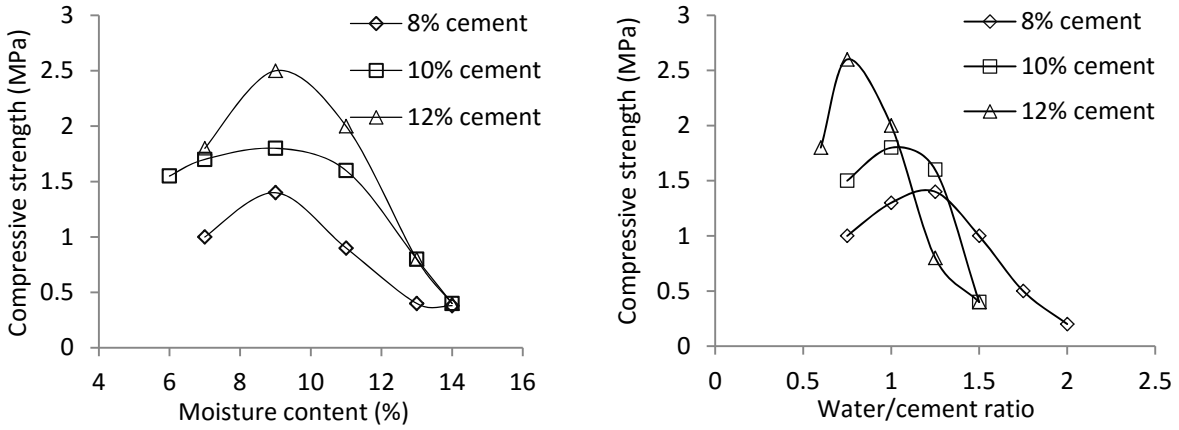


**Figure 2.9** Relationship of moisture content and water/cement ratio with UCS

Experimental work (Kersten, 1961) showed that the compressive strength increases to a maximum at a moisture content slightly less than the optimum moisture content for sandy soil and silty soil, and at a greater moisture content than the optimum moisture content for clay soil. However, the influence of the moisture content is more related to the workability and compatibility of materials to obtain a homogeneous mass than to the water requirement for hydration because adequate water for compaction ensures adequate water for hydration provided it is not lost during curing (Kersten, 1961).

#### 2.4.1.2 Estimation models for compressive strength (UCS)

Estimation models for unconfined compressive strength have been documented in a large number of previous studies. Table 2.4 summarizes the reported estimation models of compressive strength for cement-based materials. Most of these reported models correlate the compressive strength with various factors, including cement content, water content, density of specimens or curing time. The coefficients for these factors are experimentally determined and largely influenced by the soil type or compaction effort.

**Table 2.4** Prediction models of UCS for cement based materials (after Xuan, 2012)

| Material | Prediction model of UCS | Reference | Remarks |
|---|---|---|---|
| Cement stabilized materials | $UCS = a \cdot C$ | (Sherwood, 1968) | C=cement content, by mass; D=density W/C=water cement ratio; $C_v$=cement, by volume; M= crushed masonry content (by mass); t=curing time; a, b, k and s are experimentally determined. |
| | $UCS = k \cdot D^n$ | (Sherwood, 1995) | |
| | $UCS = \frac{a}{\left(\frac{W}{C}\right)^b}$ | (Horpibulsuk et al., 2007) | |
| | $UCS = 5.03 \cdot 10^4 \left[\frac{D}{(C_v)^{0.28}}\right]^{-3.32}$ | (Consoli et al., 2007) | |
| | $\mathrm{UCS} = 0.075\left(\frac{C}{W}\right) \cdot D^8 \cdot e^{0.0088M} \cdot e^{2.31 \cdot [1-(28/t)0.1]}$ | (Xuan, 2012) | |
| | $UCS\ (t) = UCS(t_0) + k \cdot \log\left(\frac{t}{t_0}\right)$ | (Terrel et al., 1979) | |
| | $UCS\ (t) = UCS(28)\frac{t}{a+b \cdot t}$ | (Lim & Zollinger, 2003) | |
| Concrete | $UCS(t) = UCS(28) \cdot e^{s\left(1-\left(\frac{28}{t}\right)^k\right)}$ | (EN 199-1-1, 2005) | |
| | $UCS(t) = UCS(28) \cdot \frac{t}{a+b \cdot t}$ | (ACI, 1998) | |

### 2.4.2 Tensile strength

#### 2.4.2.1 Flexural tensile and indirect tensile strength tests

Cement treated bases in pavement structures are subjected to tensile stresses and strains under traffic loads, so the tensile strength is an important parameter to characterize the properties of cement stabilized materials. The tensile strength is also critical for shrinkage cracking. Low tensile strength tends to exhibit greater shrinkage potential (Selvam, et al., 2009). The tensile strength obtained from a given material will vary depending on which type of tensile strength test is used (Thompson, 1998). In general, the direct tensile test, indirect tensile test and flexural tensile test are three main types of test that can be used to determine the tensile strength of cement stabilized materials.

In a direct tensile test, an axial tensile force is directly applied to a specimen (Hudson & Kennedy, 1968). Although such a test is simple in theory, serious difficulties are encountered in practical applications mainly due to the fact that the means of holding the specimens may create secondary stresses that influence the test results (Hudson & Kennedy, 1968; Thompson, 1998). Therefore, the indirect tensile test and the flexural tensile test are primarily used to characterize the tensile strength.

The indirect tensile strength test involves loading a cylindrical specimen with compressive loads distributed along two opposite generators. This test is widely used mainly due to the fact that it is easy to perform and the type of specimen and the testing equipment can be the same as used for compression test (Hudson & Kennedy, 1968). However, this test doesn't simulate the real behavior of a base layer under wheel loading (Thompson, 1998). Compared with this the flexural tensile strength test, which applies a bending load to a beam specimen, better simulates the manner in which a pavement layer is deflected by a wheel-loading.

On the basis of literature review, the tensile strength of cement stabilized material is also affected by variable factors including the cement content in the mix, soil type, degree of compaction, curing time, etc. Bahar et al. (2005) presented test results regarding the effect of the cement content on the indirect tensile strength of cement stabilized clay (A-6, according to AASHTO classification), see Figure 2.10.

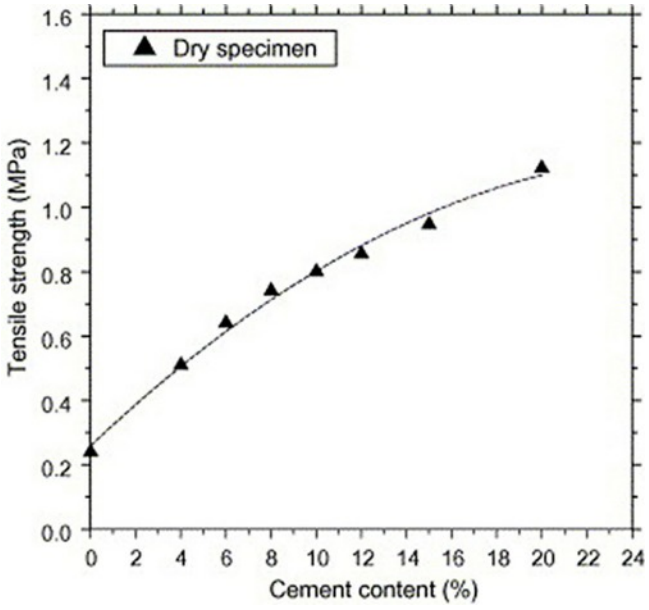


**Figure 2.10** Effect of cement content on indirect tensile strength (Bahar et al., 2004)

It is clear from Figure 2.10 that the indirect tensile strength increases significantly with the cement content up to about 10% and beyond that the rate of increase is slower. Besides, Consoli et al. (2011) indicated that a reduction of the porosity results in increased indirect tensile strength, because reduction of the porosity results in much more contact between the particles which enhances the bonding strength.

The correlation of tensile strength obtained from different tensile strength tests is described in many studies (Sherwood, 1981; Pretorius & Monismith, 1971; Williams, 1986) and it can be concluded that the flexural tensile strength is generally 1.5 times the indirect tensile strength and about 1.6 to 2 times the direct tensile strength.

According to standard NEN-EN 14227-1, the direct tensile strength can be derived as 80 percentage of the indirect tensile strength.

#### 2.4.2.2 Correlation between tensile strength and compressive strength

Based on literature studies, it can be found that tensile strength and compressive strength are well related and the correlations between these strengths have been established many times.

(1) Direct tensile strength and compressive strength

The correlation between direct tensile strength and compressive strength was investigated in a literature study (Kolias & Williams, 1978), indicated in Figure 2.11. Figure 2.11 addresses the test results from dry-lean concrete (materials A and D) to a fine-grained soil-cement (material C). B and E indicate the cement stabilized sandy soil. In Figure 2.11 it is shown that the strength ratio is to some extent dependent on the type of material processed and it can be postulated that the direct tensile strength is about 10 percent of the uniaxial compressive strength.

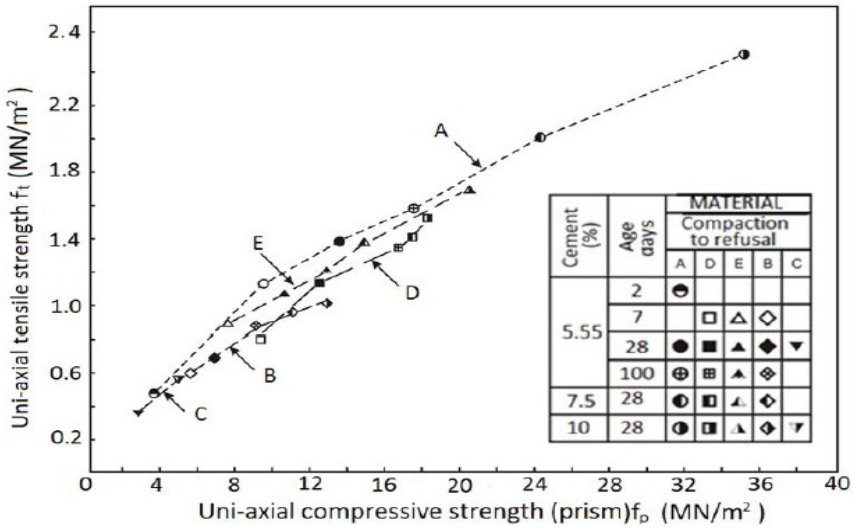


**Figure 2.11** Uniaxial tensile strength (direct tensile strength) plotted against uniaxial compressive strength (after Kolias & Williams, 1978)

(2) Indirect tensile strength and compressive strength

The relationship between indirect tensile strength and compressive strength has been investigated in extensive research. Generally a high compressive strength corresponds to a high indirect tensile strength (Shacklock, 1974).

Babic (1987) and Kennedy (1971) reported linear mathematical models which can be utilized to define the correlation between the compressive strength and the indirect tensile strength of cement stabilized materials, shown as the following correlations:

$$ITS = a \cdot UCS + b \quad \text{(Babic, 1987)} \quad (2\text{-}1)$$

$$ITS = a \cdot UCS \quad \text{(Babic, 1987)} \quad (2\text{-}2)$$

$$ITS = -11.38 + 0.1662 \cdot UCS \quad \text{(Kennedy et al., 1971)} \quad (2\text{-}3)$$

Where, *ITS* is indirect tensile strength (psi); *UCS* is the compressive strength (psi), a and b are the coefficients; 1psi ≈ 0.0069 MPa.

Thompson (1998) gave a detailed review on the correlation between compressive strength and indirect tensile strength which can be summarized as that the indirect tensile strength is about 10 to 13 percent of the compressive strength (Sherwood, 1968; Little, 1995; Thompson, 1966).

(3) Flexural tensile strength and compressive strength

Correlations between flexural tensile strength and compressive strength have also been reported by many investigators and in most of the research it is described that the flexural tensile strength is about 20 percent of the compressive strength. Research (Ronald et al., 1979) illustrated an almost linear relationship between flexural tensile strength and compressive strength, shown in Figure 2.12. Figure 2.12 indicates the flexural tensile strength was approximately 20 percent of the compressive strength.

Similar comparable data on unconfined compressive strength and flexural tensile strength of hardened cement-treated soils was also reported by Kersten (1961), which showed a nearly linear relationship at all cement contents and at all curing times. Molenaar (2006) also gave a linear relationship for cement treated fine-grained cohesive soil, shown below:

$$FTS = -0.0042 + 0.1427 \cdot UCS \quad (2\text{-}4)$$

Where, *FTS* is flexural tensile strength (MPa); *UCS* is compressive strength (MPa).

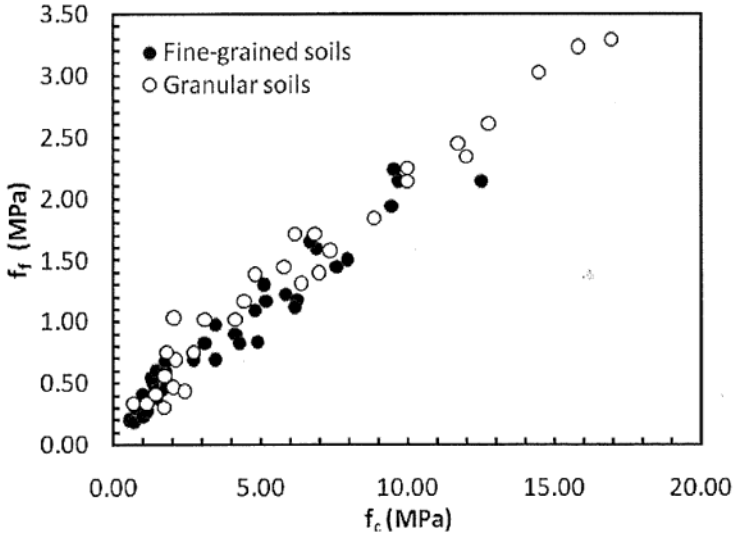


**Figure 2.12** Flexural tensile strength versus compressive strength (Ronald et al, 1979)

In a study (TRH 13, 1986) it is described that the flexural tensile strength of cemented materials is about one-third of the compressive strength for low-strength materials and about one-fifth of the compressive strength for high-strength materials. Kolias (1984) also reported data, based on 5 types of sandy soil ranging from silty sand to sand, which revealed that the flexural tensile strength is 20% of the compressive strength independent on the soil type.

Based on a large number of literature studies, generalized relationships between compressive strength and tensile strength are recommended for use in design (Thompson, 1998), expressed as follows:

$$ITS = 0.1 \text{ to } 0.15\ UCS \tag{2-5}$$

$$FTS = 0.2 \cdot UCS \tag{2-6}$$

Where, *ITS* is indirect tensile strength; *FTS* is flexural tensile strength; *UCS* is compressive strength.

### 2.4.3 Modulus of elasticity

The modulus of elasticity provides a measure for the stiffness of materials and indicates the load spreading ability of materials. The modulus of elasticity can be evaluated by the stress-strain performance. Figure 2.13 shows a typical normalized stress-strain curve for cement stabilized materials. The presented stress and strain are expressed as the percentage of the peak values. The modulus of elasticity is defined as the slope in the linear range of the curve.

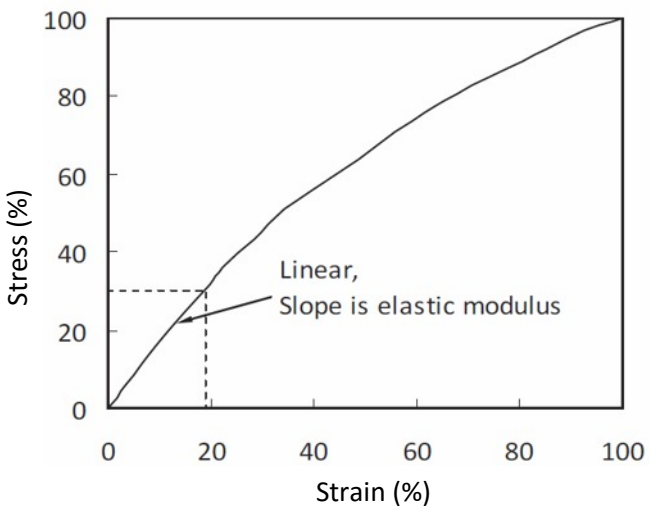


**Figure 2.13** Typical stress-strain curve for cement stabilized materials (TRH 13, 1986)

As can be seen in Figure 2.13, during the initial loading, the material behaves as linear-elastic but when loaded beyond a certain point, it becomes non-linear and non-elastic. As explained in TRH 13 (1986) when a cemented material is loaded beyond a certain limit, micro-cracking first develops at the interface between coarse particles and the matrix. The extent of micro-cracking increases during subsequent loading. It has also been reported that the micro-cracking starts at 25% of the ultimate strength and 35% of the strain at break during compression and flexural tests. In contrast, Galloway & Harding (1976**)** indicated that the initial stress-strain relationship becomes non-linear when the applied stress exceeds 40-70 percent of the failure stress.

#### 2.4.3.1 Static modulus of elasticity

Stabilizing soil with cement significantly increases the modulus of elasticity of the soil. Figure 2.14 presents the effect of addition of cement on the elastic modulus of specimens at the age of 28 days. The soil is classified as moderately plastic clay type A-6 according to the AASHTO classification.

In Figure 2.14 it can be seen that the cement stabilization increases the slope of the curve and hence the elastic modulus of the material increases from 189 MPa for un-stabilized soil to 251 MPa for soil stabilized with 10% cement.

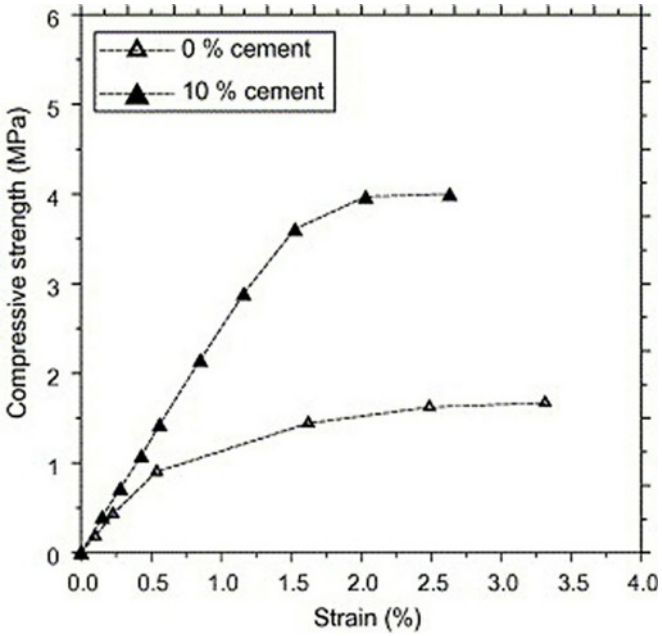


**Figure 2.14** Stress-strain curve for specimens under unconfined compression (Bahar et al., 2004)

The static modulus of elasticity can be determined in compression or tension tests. Williams (1972) reported that the static modulus of elasticity of cemented materials made with granular aggregates is nearly the same in compression and tension. Bofinger (1970) however found that the modulus of cemented silty clay in tension is only 10% of that in compression. The test results of the modulus of elasticity thus may vary in different test methods because materials behave differently in response to the tension or compression load.

Additionally, Molenaar (2010a) observed that cemented clayey materials also exhibit some degree of permanent deformation under repeated load and this deformation is more than that obtained in cemented gravel and sand materials and he concluded that the fewer fines are present in the soil-mixture the more the cement-treated soil will behave like concrete. Additionally, Kersten (1961) investigated the variation of the static modulus of elasticity of cement treated sand-clay mixtures with the clay content ranging from 0 to 100 percent and found that the static modulus decreased with increasing clay content. And thus it can be seen that the stress-strain performance is largely influenced by the nature of the soil material.

Many studies have reported correlations relating the elastic modulus with the strength of cement stabilized materials and concluded that a large variety of correlations do exist and they are influenced by the nature of the material being stabilized (Thompson, 1998). Figure 2.15 shows three strength-modulus relationship curves recommended for different material types.

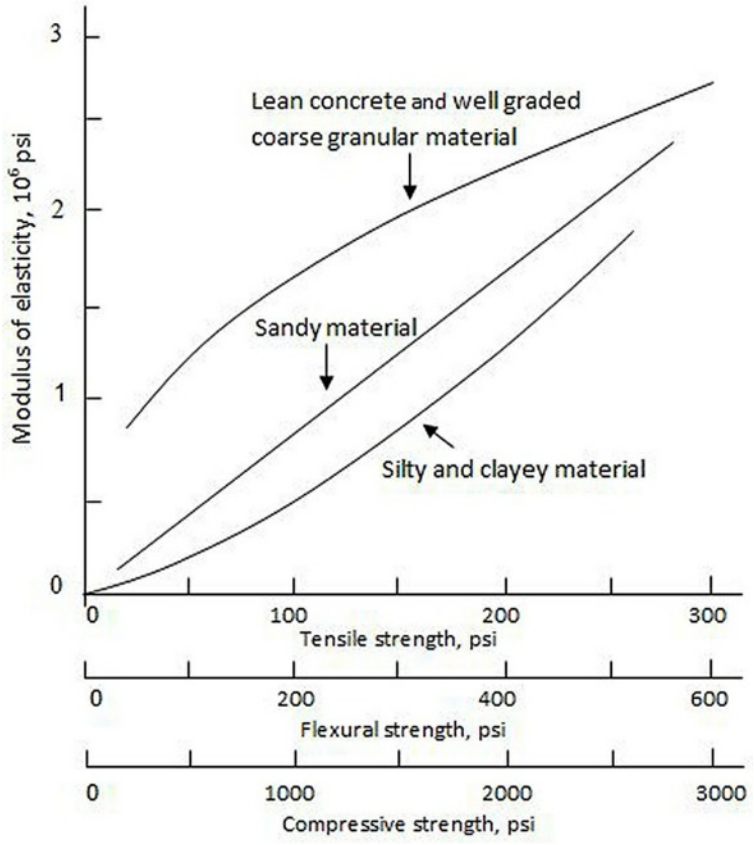


**Figure 2.15** Suggested curves for strength versus modulus of elasticity (Thompson, 1998).

In Figure 2.15 it can be seen that, for a given strength level, lean concrete has the highest modulus and the fine-grained soil cement has the lowest value. The equations governing these curves are expressed as:

For lean concrete and high quality coarse-grained materials:

$$E = 57500 \cdot (UCS)^{0.5} \tag{2-7}$$

For lower quality coarse-grained and sandy materials:

$$E = 1200 \cdot UCS \tag{2-8}$$

For silty and clayey fine-grained materials:

$$E = 440 \cdot UCS + 0.28 \cdot (UCS)^2 \tag{2-9}$$

Where, $E$ = the modulus of elasticity in psi, $UCS$ = compressive strength in psi.

According to the standard NEN-EN 14227-10, a cement bound granular mixture can be classified by the direct tensile strength $R_t$ and elastic modulus $E$, as shown in Figure 2.16. In Figure 2.16 the curves indicate the categories T5, T4, T3, T2 and T1. $R_t$ is the direct tensile strength which is considered as 80 percent of the indirect tensile

strength. E is the static elastic modulus which shall be measured in compression tests. Both properties are at the curing time of 28 days.

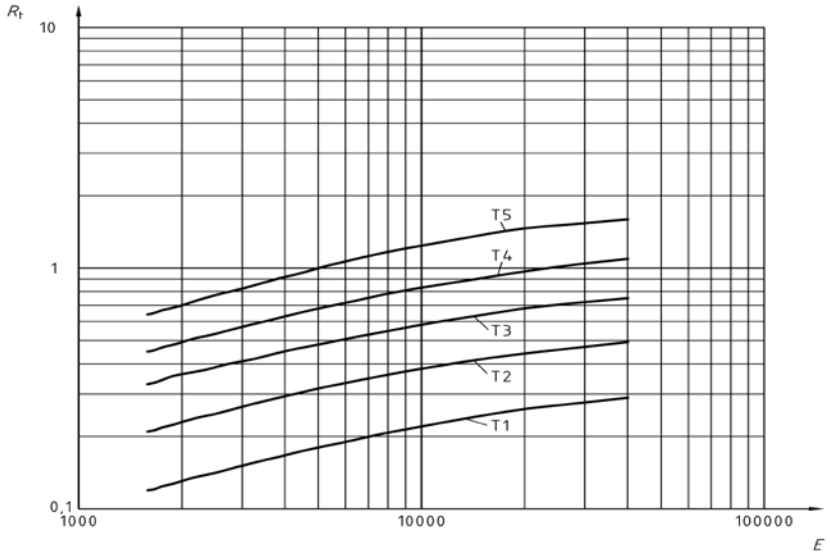


**Figure 2.16** Characterization of cement-bound granular mixture by direct tensile strength and static modulus of elasticity at 28 days

### 2.4.3.2 Dynamic modulus of elasticity

The dynamic modulus can be derived from the compression or tensile tests under dynamic loading and the applied load is generally much less than the ultimate failure strength. The range of stress used is between one-third and one-half of the compressive strength of the material, determined by separate test (Croney, 1977). There is also much discussion about whether to use dynamic or static modulus values in pavement calculations and often the average of both values is adopted in the structural pavement design (DFID, 2004; Croney, 1977). Table 2.5 lists some general values of the modulus of different materials used in structural analysis.

**Table 2.5** Modulus of elasticity for use in structural analysis

| | Ref.1 Croney (1977) | | Ref.2 Williams (1986) |
|---|---|---|---|
| Materials | Dynamic modulus (GPa) | Static modulus (GPa) | Modulus of elasticity (GPa) |
| Soil-cement (granular) | 18 | 10 | 3.5-20 |
| Soil-cement (silty PI<10) | 7 | 4 | |
| Soil-cement (clay PI>10) | 1 | - | |
| Cement-bound materials | 23 | 13 | 14-26 |
| Normal lean concrete | 27 | 19 | 26-36 |
| Stronger lean concrete | 30 | 23 | |

The relationship between dynamic and static modulus is established in a study (Croney, 1977), which is based on cemented granular materials and expressed as the following equation:

$$E_d = 1000 + 0.88 \cdot E_s \tag{2-10}$$

Where, $E_d$ and $E_s$ are the dynamic and static modulus (MPa), respectively.

The correlation between the dynamic modulus and the compressive strength has been documented in previous studies. Babic (1987) presented a non-linear relationship between the compressive strength and the dynamic modulus for different degrees of compaction (dry density), shown in Figure 2.17.

As indicated in Figure 2.17, the relationship between the compressive strength and the dynamic modulus of elasticity is mostly non-linear. The results can be described by a mathematical model in the following form:

$$E_d = \mathrm{a} \cdot \ln(b \cdot UCS) + c \tag{2-11}$$

Where, $E_d$ is dynamic modulus (GPa), U*CS* is compressive strength (MPa), a, b and c are experimentally determined coefficients.

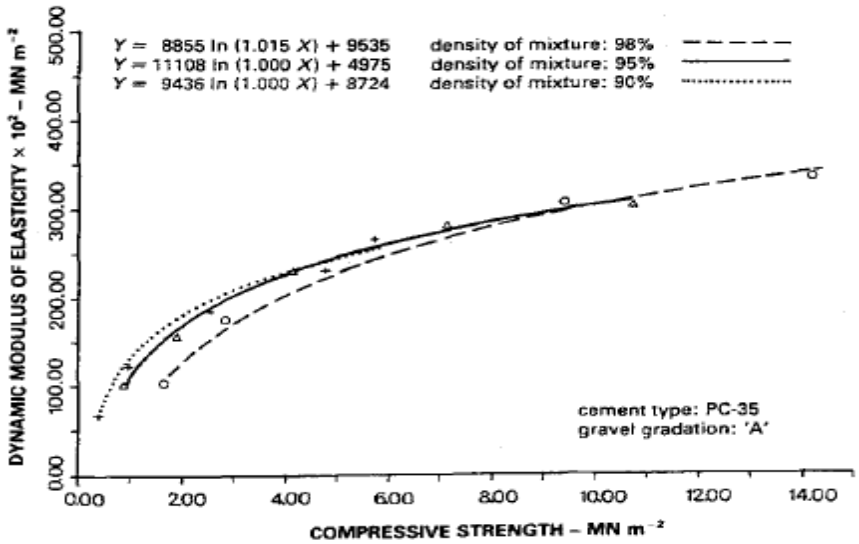


**Figure 2.17** 28-day compressive strength–dynamic modulus correlations (Babic, 1987)

The correlation between compressive strength and the dynamic modulus has also been proven to be different for various material types. Croney (1977) gave similar non-linear correlations for different soil types, shown in Figure 2.18.

In Figure 2.18 it can be seen that the correlation is significantly influenced by the material type and no single correlation for all types of mixtures is established. At a given compressive strength, the dynamic modulus decreases with increasing fines

content in the soil. Additionally, Kersten (1961) reported a linear correlation between dynamic modulus and the flexural tensile strength for cemented sand-gravel materials at 28 days.

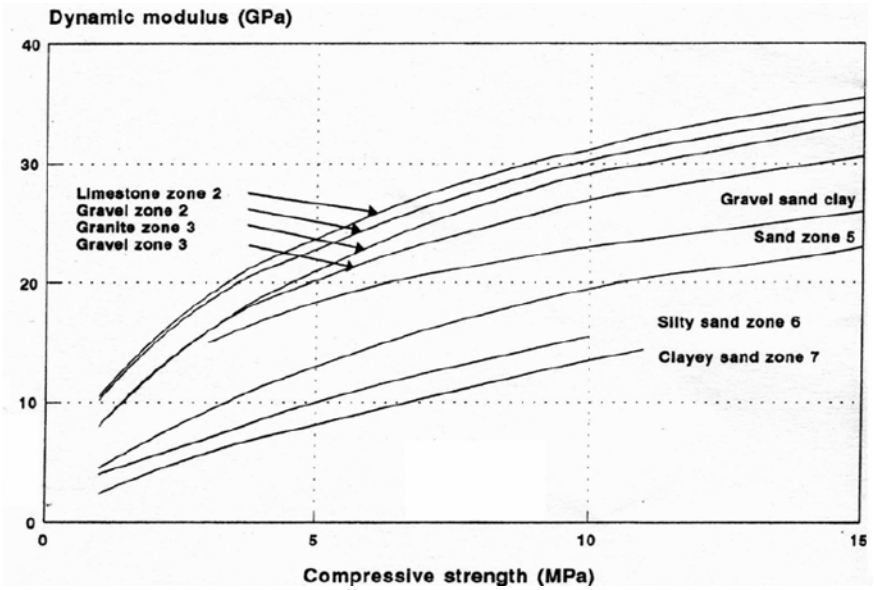


**Figure 2.18** Relationship between compressive strength and dynamic modulus

### 2.4.3.3 Estimation models of elastic modulus

Test procedures to determine an appropriate elastic modulus of cement stabilized material are somehow complicated, so it is always recommended to derive the modulus from the correlation between strength and modulus when only the compressive or tensile strength is available. Based on the previous research, the reported relationships are summarized in Table 2.6.

**Table 2.6** Estimation models for modulus of elasticity E

| Raw materials | Equations | Reference |
|---|---|---|
| Crushed stone | $E = 8000 \cdot FTS + 3500$<br>$E = 1816 \cdot (UCS)^{0.88} + 3484$ | (TRH 13, 1986) |
| Natural gravel | $E = 10000 \cdot FTS + 1000$<br>$E = 2239 \cdot (UCS)^{0.88} + 1098$ | (TRH 13, 1986) |
| Sand | $E = 1435 \cdot (UCS)^{0.885}$ | (HRB, 1962) |
| Fine sand and silty clay | $E = -34.367 + 2006.8 \cdot (UCS)^{0.78}$ | (Richardson, 1996) |
| Crushed concrete and masonry | $E = 366.8 \cdot D^{3.8} \cdot (UCS)^{0.56}$ | (Xuan, 2012) |
| Limestone and recycled concrete* | $E = 6.72 \cdot (UCS)^{1.5} \cdot (D)^{0.75}$ | (Lim&Zollinger, 2003) |
| Silty and clayey fine-grained material* | $E = 440 \cdot UCS + 0.28 \cdot (UCS)^2$ | (Thompson, 1998) |
| Low quality coarse-grained material* | $E = 1200 \cdot UCS$ | (Thompson, 1998) |
| High quality coarse-grained materials* | $E = 57500 \cdot (UCS)^{0.5}$ | (Thompson, 1998) |

Note: $FTS$ is the flexural tensile strength; $UCS$ is the unconfined compressive strength; $D$ is the density of the sample; * indicates the unit of $UCS$ and $E$ in psi.

### 2.4.4 Fatigue properties

Cement stabilized materials are subjected to the repeated flexural tensile stresses which are induced by the traffic loads. Under repeated loads, cracks may occur at the stabilized base layer and subsequently propagate through the pavement. This type of cracking caused by the accumulated traffic loads is normally referred to as fatigue cracking.

The failure starts as micro-cracking manifesting itself as a loss of bond at the interface between the aggregate and the matrix of the fine materials (Otte, 1979). Fatigue cracking is an indicator of pavement failure and can result in costly maintenance. Fatigue life under cyclic loading to predict the service life of the stabilized layer is considered as the main criterion in many pavement design methods (Crockford & Little, 1987). However, limited information regarding the fatigue properties of cementitious materials is reported due to the difficulties of testing, the rather brittle behavior and many variables influencing the results.

In the laboratory, the fatigue properties of cementitous materials are determined by subjecting a beam specimen to dynamic loads using a four-point bending test

machine. Two types of loading modes can be applied in a fatigue test: stress–controlled or strain-controlled, graphically indicated in Figure 2.19.

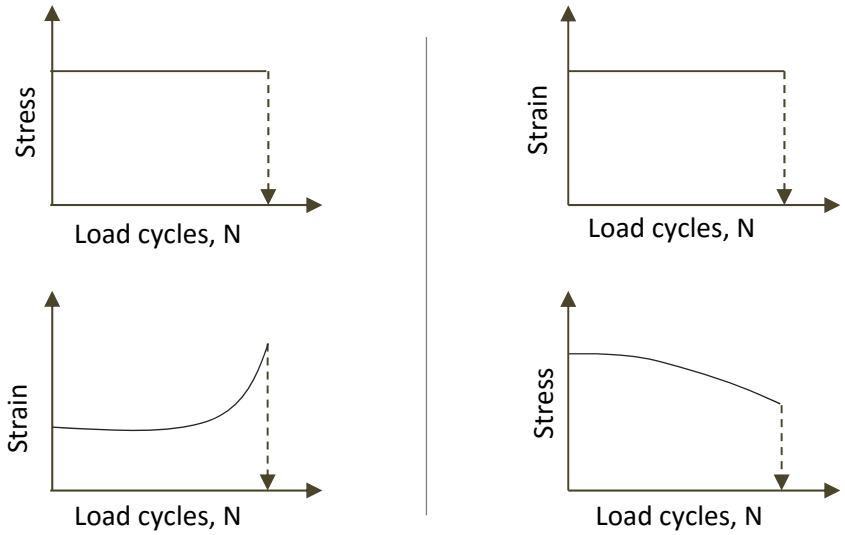


(a) Stress-controlled (b) Strain-controlled

**Figure 2.19** Graphical representation of loading modes (Monismith & Epps, 1971)

In stress-controlled mode, the amplitude of the applied load (stress) remains constant. As the stiffness of the material decreases under loading, the induced strain gradually increases. As soon as micro-cracking starts, cracking rapidly propagates through the beam specimen, resulting in rapid increase in strain till failure. So normally the failure criterion is defined as the moment when the specimen fractures. Whereas, for strain-controlled mode, the applied strain level stays constant, the stiffness reduces slowly and hence the required loading stress is decreasing. Under the decreased stress, the specimen may or may not facture completely. In this case, generally the failure point is arbitrarily assumed as the moment when the initial stiffness is reduced by 50%. The fatigue life obtained from strain-controlled test is much longer because it also includes the time of slow crack propagation. Therefore, the fatigue life in the laboratory condition is much dependent on the test method to be used. It is suggested by Pell (1978) to use stress-controlled testing conditions for engineering design approach because they give a conservative estimate of fatigue life.

Most of previous studies reported fatigue test results for cement stabilized materials are based on stress-controlled testing. Generally, the fatigue characteristics of cementitiously stabilized materials have been expressed in terms of stress ratio, commonly known as SN-N relation (equation 2-12).

$$SN = \mathrm{a} - \mathrm{b} \cdot \log N \tag{2-12}$$

Where, N − number of load cycles to failure, SN − Ratio of applied tensile stress and flexural tensile strength, a and b − experimentally determined coefficients.

Based on a large number of previous investigations, the reported fatigue relations exhibit a large variation, even for similar types of materials. Xuan (2012) summarized some fatigue lines based on different soil gradations and shown in Figure 2.20. As shown in Figure 2.20 (a), a large variation exists in the fatigue lines though the grain size distribution of these treated aggregates are quite similar.

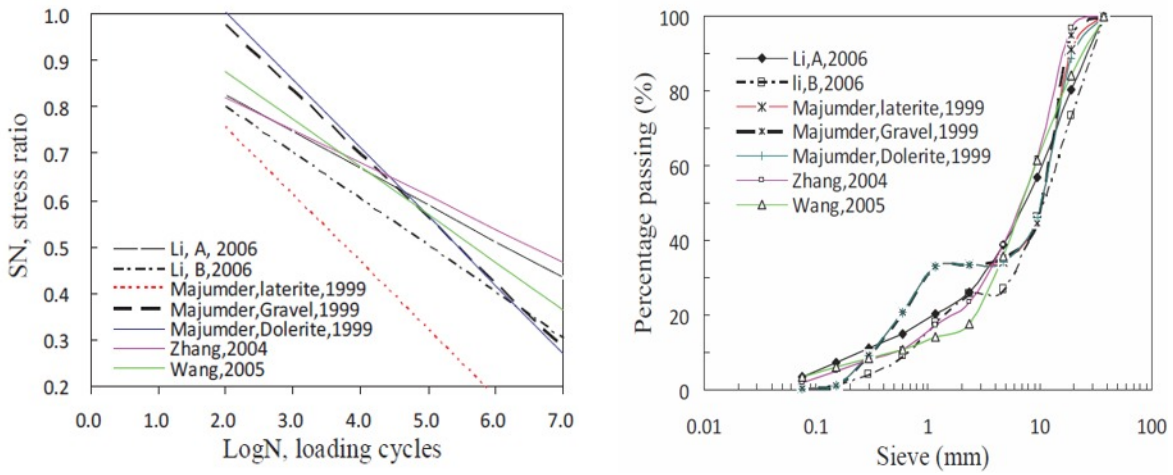


(a) Variation of SN-N relations (b) Grain size distribution of treated aggregates

Figure **2.20** Fatigue lines in literatures (Xuan, 2012)

Molenaar & Pu (2008) attributed the large variation of test results to the brittle nature of cemented materials, which means a small change in the applied tensile strain or stress can have a very large effect on the number of load repetitions to failure. Besides, these SN relations exhibit high values of the slope which indicates a rather brittle behavior.

Moreover, Balbo (1996) identified that the SN relation (stress ratio) ranges from 0.4 to 0.7 which leads to one million load cycles at failure, based on cement treated aggregate materials. Xuan (2012) combined more relations and concluded that this ratio could range from 0.18 to 0.70 for cemented granular materials. Williams (1986) gave a broad conclusion that a fatigue life of one million load applications can be expected when the stress level is restricted to 50% of the failure strength. Otte (1979) found that micro-cracking starts at a stress ratio of 0.35. That means there is no specific stress ratio for all the materials below which no fatigue damage will occur due to the variation of the grain size. Fatigue models based on flexural tensile strain

have also been reported in many investigations. Standard NEN-EN 12697-24 gives the following fatigue line related to the initial strain:

$$\ln(N) = a + b \cdot \ln(\varepsilon_0) \quad (2\text{-}13)$$

Where, $\varepsilon_0$ is the initial strain amplitude measured at the 100th load cycle.

Table 2.7 presents fatigue models related to the applied flexural tensile strain levels reported in different literatures. These models are related to the applied strain, strain ratio or modulus of elasticity.

**Table 2.7** Fatigue models based on strain levels

| Materials | Fatigue model | Reference | Remarks |
|---|---|---|---|
| Cemented materials | $\frac{\varepsilon}{\varepsilon_b} = 1 - 0.11 \log N$<br>$\frac{\varepsilon}{\varepsilon_b} = N^{-0.079}$ | (Otte, 1979) | $\varepsilon_b$ =flexural strain at break<br>$\varepsilon$ =applied strain level |
| Cement treated granular | $\log N = 9(1 - \frac{\varepsilon}{\varepsilon_b})$ | (Molenaar, 2006) | Used in south Africa<br>$\varepsilon_b$ =strain at break |
| A-1-a soil with 5.5% cement | $\log N = 9.110 - 0.0578\,\varepsilon$ | (Molenaar, 2006) | $\varepsilon$ =applied strain level |
| Cement-sand | $\log N = 8.5 - 0.034\,\varepsilon$ | (Molenaar & Pu, 2008) | $\varepsilon$ =flexural tensile strain at the bottom of stabilized base layer |
| Cement treated crushed rock | $\log N = 67.07 - 6.96 \log E - 18 \log(\varepsilon_t)$ | (Jameson, 1992) | $\varepsilon_t$ =maximum tensile strain<br>E=modulus (MPa) |
| Cement treated crushed asphalt | $\log N = 21.37 - 7.72 \log(\varepsilon_t)$ | (CROW, 2005) | $\varepsilon_t$ =maximum tensile strain |

### 2.4.5 Shrinkage behavior

A cement stabilized base is prone to dimensional changes mainly caused by the moisture loss during the cement hydration and decrease of temperature. When the cement treated material shrinks, the tensile stress will develop in the base layer due to the friction with the underlying layer. When the induced tensile stress exceeds the tensile strength of the cemented material, cracks will occur in the base layer and may reflect through the top layer, resulting in visible surface cracks.

TRH 13 (1986) gave a detailed explanation how the tensile strength development relative to the shrinkage tensile stress development affects the width and spacing of cracks, indicated in Figure 2.21. Figure 2.21 explains that if the shrinkage stress

exceeds the tensile strength at a relatively low strength then the cracks will be more numerous, narrower and more closely spaced (shown as Material A in Figure 2.21). If the material develops a greater tensile strength before the shrinkage stress exceeds the tensile strength, there will be fewer cracks, and they may be 2 to 3 mm wide and 4 to 6 m apart (shown as Material B). Material C has not cracked yet. However, subsequent changes in the widths of the cracks will be influenced by changes in the temperature and in the moisture within the layer (Bofinger, 1978).

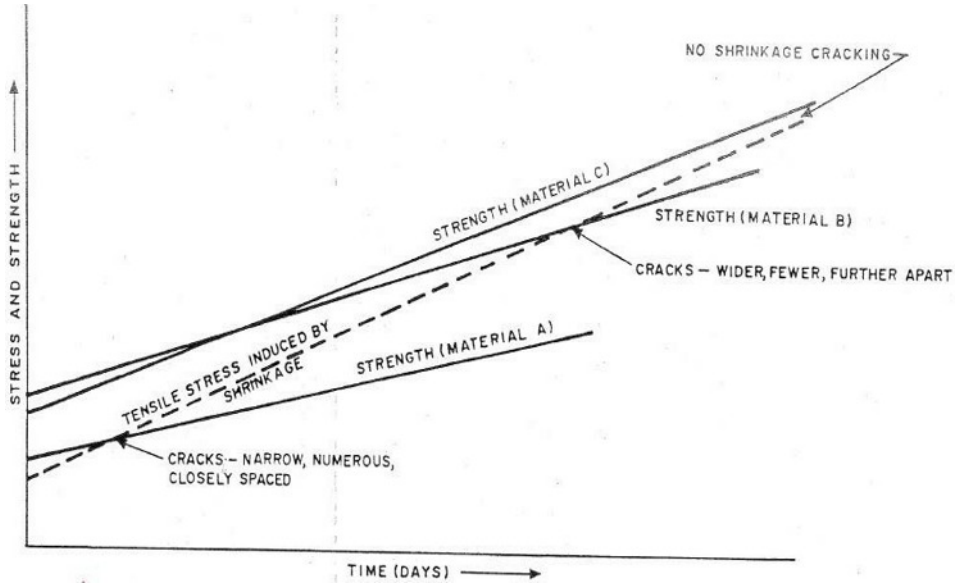


**Figure 2.21** Cracking as a result of the interrelationship between shrinkage stress, strength and time (TRH 13, 1986)

The cracks result from the restrained drying shrinkage and temperature variation, but when the stabilized soil is fine-grained, the cracking is mainly believed to be attributed to drying shrinkage (Bofinger, 1978). The shrinkage characteristic, as a major cause of cracking in cement stabilized materials, is mainly discussed hereafter. Shrinkage of soil-cement is mainly caused by the moisture loss due to the cement hydration as well as the evaporation. In the following discussion the effects of cement content, the type of soil, degree of compaction, and curing condition on the shrinkage behavior of cement stabilized materials are considered:

(1) Cement content

The cement content is most commonly considered as an important factor for controlling the shrinkage of cement stabilized materials. For natural soil, especially cohesive soil, addition of a small amount of cement can reduce its potential of swell and shrinkage, because the cement paste binds the soil particles, resulting a more rigid and stable structure than the untreated soil. But increasing the amount of

cement is traditionally believed to cause more shrinkage, because excessive cement content will consume more water, resulting in more drying shrinkage. Moreover, a higher cement content will lead to a higher tensile strength, which will result in a great potential of wide cracks at large spacing. Therefore, it is often suggested to reduce the potential of shrinkage cracking by lowering the cement content provided that an adequate minimum strength is maintained (Bofinger, 1978).

Figure 2.22 shows the final shrinkage at 300 days for cement treated recycled masonry and concrete. Figure 2.22 shows that in case the cement content increases from 2.5% to 5.5% by mass, the shrinkage increases from $302\times10^{-6}$ to $412\times10^{-6}$.

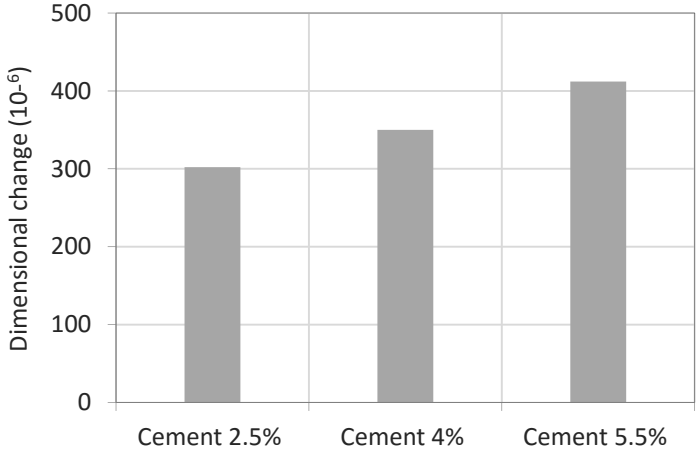


**Figure 2.22** Influence of cement content on the deformation of cement treated recycled granular materials (after Xuan, 2012)

However, contrary to the traditional thinking, different findings are presented in research (George, 1968; Bofinger, 1978) which indicated that there exists an optimum cement content at which the shrinkage was minimum, indicated in Figure 2.23. Besides, Bofinger (1978) also observed that the variation of cement content affected the shrinkage differently according to various methods of preparing specimens such as specimens moulded horizontally or vertically together with different compaction methods. However, no completely satisfactory explanation was offered in his study.

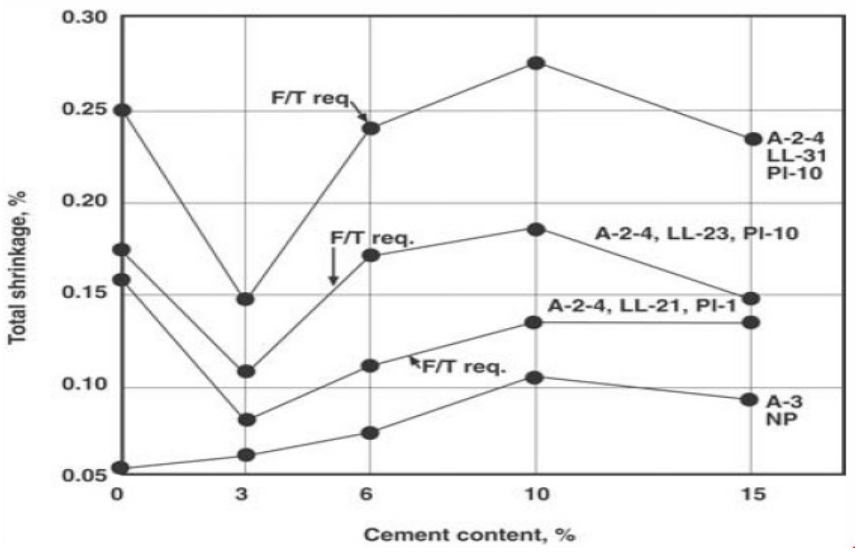


**Figure 2.23** Effect of cement content on shrinkage (George, 1968)

(2) Curing condition

Shrinkage cracks due to hardening and temperature variation might develop shortly after the pavement has been constructed. The development of shrinkage is time dependent. Bahar et al. (2004) investigated the effect of the curing time on the shrinkage, as shown in Figure 2.24. The soil, classified as moderately plastic clay type A-6 according to the AASHTO classification, is stabilized with different cement contents.

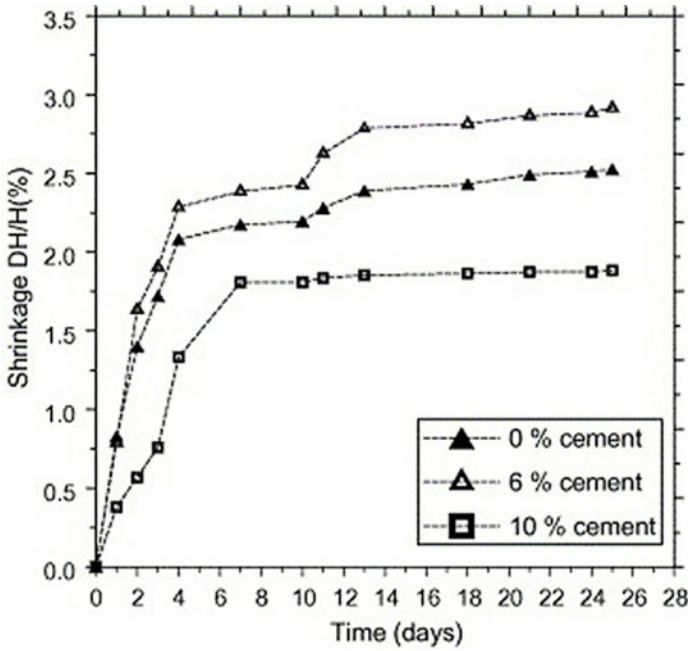


**Figure 2.24** Shrinkage development of cement stabilized A-6 clay with time (Bahar et al., 2004)

It can clearly be seen in Figure 2.24 that the shrinkage increases rapidly during the first 4 days, and then the rate of the shrinkage slows down. Hence, appropriate curing method during the first 4 days could be beneficial in reducing the total shrinkage.

Bofinger (1978) investigated the shrinkage behavior of cement stabilized soil (LL = 39, PI = 20) when moist cured for a short period and then exposed to drying environment, as shown in Figure 2.25. He found that regardless of the initial period of moist cure, almost all of the drying shrinkage occurs within 7 days after the moist curing period and its magnitude is reduced as the period of moist cure is increased.

Especially fine-grained materials are susceptible to the moisture loss when exposure to drying. Therefore, in practice an appropriate curing method for the completed base layer is essential to prevent the base surface from drying out and thereby reducing the amount of cracks.

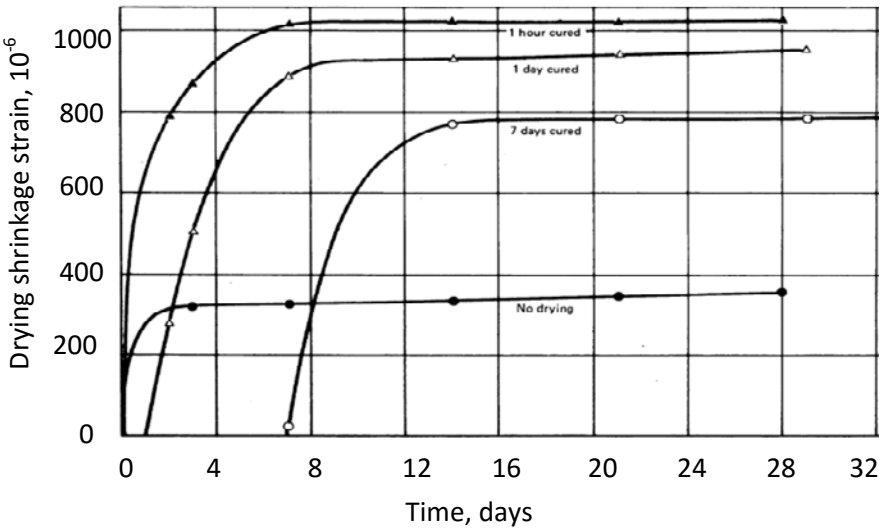


**Figure 2.25** Shrinkage of cement stabilized sandy clay with curing time (cement content 8%) (Bofinger, 1978)

(3) Moisture content

The degree of shrinkage is a function of the moisture loss during the cement hydration process. Therefore, minimizing the moisture content that is used for preparing specimens can be a significant factor for controlling the degree of shrinkage. Figure 2.26 presents the shrinkage at 28 days of cement stabilized sandy clay at variable moisture contents. The optimum moisture content of this soil obtained from standard Proctor test is 10%.

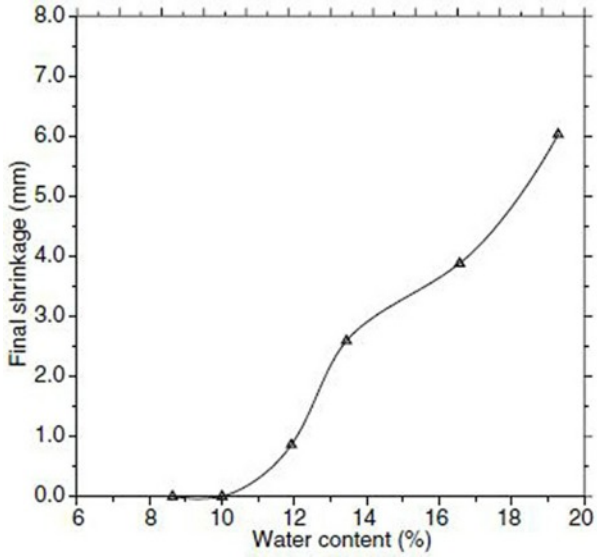


**Figure 2.26** 28-days shrinkage of cement stabilized sandy clay with different water contents (Kenai et al., 2006)

This figure shows that in case the water content used in preparing specimens increases the shrinkage increases rapidly. Because excessive moisture will remain in the pores of the soil-cement structure and will evaporate when the drying begins, causing the volume to shrink. In general, it is believed that shrinkage of soil-cement materials follows the capillary tension theory, i.e. when water is consumed for hydration or evaporates, the capillary tension force will develop in the pores, causing the overall volume shrinkage of the soil-cement structure.

Molenaar (2010a) reported that the specimens that were compacted at the dry side of the optimum moisture content showed less shrinkage. For practice this means that if one wants to limit problems due to shrinkage, compaction at a water content somewhat lower than the optimum moisture content is recommended.

(4) Compaction

A tight matrix of a well-compacted soil reduces the shrinkage potential, because the soil/aggregate particles are packed densely together, resulting in a reduced voids content. Good compaction also leads to better aggregate interlock if a crack does develop (Adaska & Luhr, 2004). Bhandari (1973) reported that compacting cement-stabilized soil at modified Proctor density reduced the shrinkage by more than 50% compared to stabilized soil compacted to standard Proctor density. In addition, the optimum moisture content at Modified Proctor compaction is typically less than that at standard Proctor compaction, which also helps to reduce shrinkage. Figure 2.27 shows that increased density and reduced moisture content result in less shrinkage of a cement-stabilized A-2-4 granular material. In Figure 2.27 it is shown that the

least amount of shrinkage is obtained for the stabilized material at highest density and lowest moisture content.

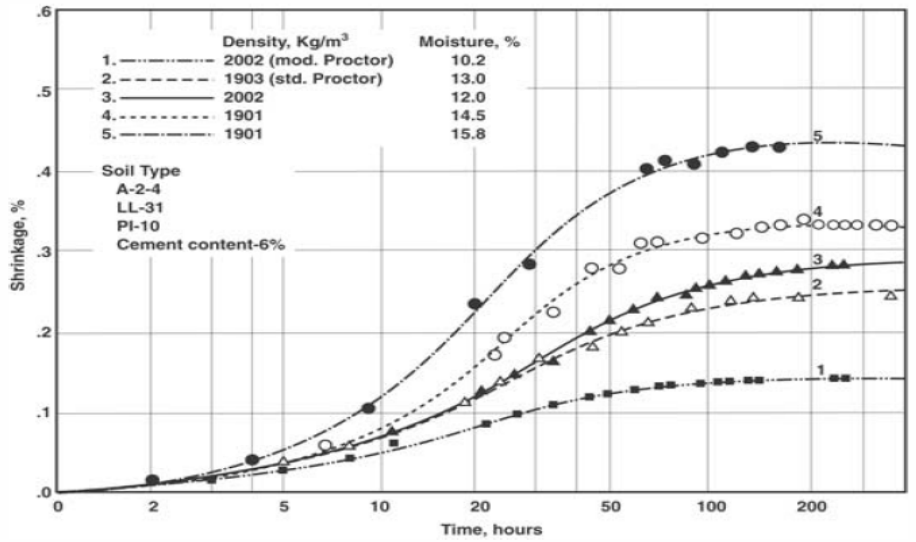


**Figure 2.27** Effect of density and moisture content on shrinkage of cement stabilized granular material (George, 1968)

Moreover, the effect of the compaction method was investigated by Bofinger (1978) and he concluded that shrinkage was maximum in specimens moulded by dynamic compaction for a clay-cement material and minimum when static compaction was used. He also mentioned that immediate compaction can also minimize the shrinkage.

(5) Soil type

Studies (George, 1968; Nakayama, 1965) showed that cement-stabilized fine-grained soils (e.g. clays) exhibit more shrinkage than cement-stabilized granular soils. That is because the granular materials can be adequately stabilized with a small amount of cement while fine-grained soils, which have larger particle surface areas, require more cement to achieve the specified strength (Adaska & Luhr, 2004). George (2002) presented an example of the effect of soil type on the crack pattern, as shown in Table 2.8.

**Table 2.8** Effect of fines content on soil-cement crack pattern (George, 2002)

| Type of soil | Crack width when last crack occurred, mm | Crack spacing, when last crack occurred, m | Crack width @ 7 days, mm | Terminal crack width, mm |
|---|---|---|---|---|
| #1 Silty sand | 1.5 @ 1.6 days | 13.0 | 3.40 | 6.0 @ 20 days |
| #2 Clayey sand | 2.9 @ 1.2 days | 6.0 | 6.00 | 10.8 @ 22 days |

In Table 2.8 it can be seen that the crack width is substantially affected by the fines content of the soil: the finer the soil particle, the larger the crack width. Because clay particles have a large surface area relative to their weight, so they hold a large amount of water, and have a high optimum moisture content, so the potential for shrinkage cracking is greater.

Shrinkage cracking is a natural characteristic of all cement-bound materials. However, if severe cracks occur at the surface, they will result in poor load transfer and pumping of the subgrade material due to water intrusion, and even structural failure of the pavement (Halsted, 2007; Little, 1987). Proper construction techniques and mix design methods can minimize these adverse effects. With respect to the construction process, following the proper construction techniques and providing good quality control during the field operation can minimize cracking (PCA, 2003).

A number of research studies (PCA, 2003; FM 5-410, 2012; Cho et al., 2006) present various methods to minimize shrinkage cracking, which include altering the mix design, proper construction process and techniques, use of "pre-cracking" method, and adding additives. Pre-cracking has been increasingly investigated. It is conducted by applying several passes by vibratory rollers to the cement-treated base at short curing times (typically 1 to 3 days after construction), to create closely spaced narrow cracks and thus to relieve the shrinkage stresses and to minimize the development of wide cracks (Litzka, 1995; PCA, 2003; Sebesta, 2005). A comprehensive field study conducted by Sebesta (2005) showed that pre-cracking reduces the severity of shrinkage cracks in the base, regardless of the cement content, and no damage occurred to the pavement when properly applied.

It is reported that the drying shrinkage of cement-treated soil can be significantly reduced by replacing a part of cement with fly ash (FM 5-410, 2012). Not only the maximum dry shrinkage is reduced, but also the rate of shrinkage is affected by the addition of fly ash. Figure 2.28 gives an example in which the addition of fly ash reduces the drying shrinkage (Cho et al., 2006).

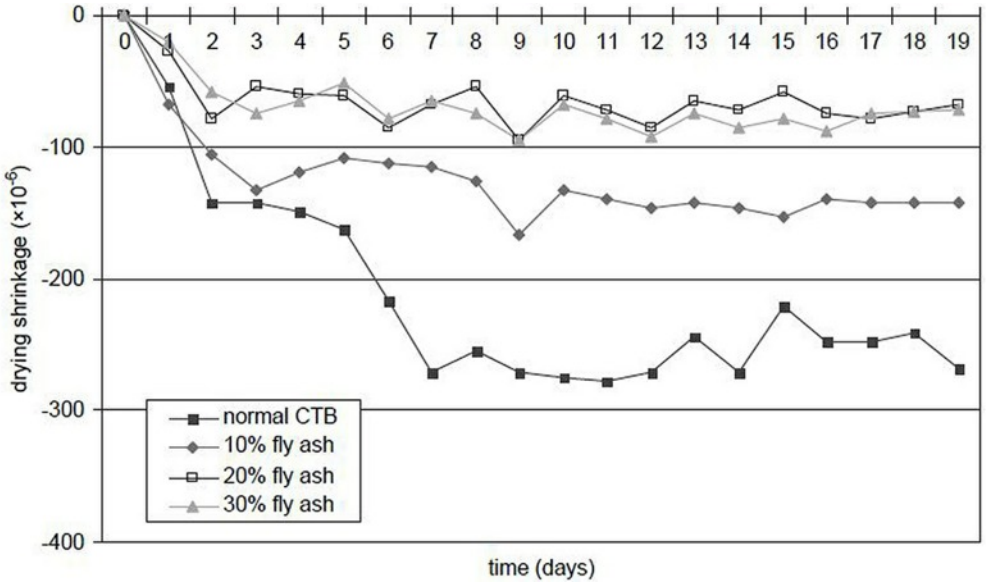


**Figure 2.28** Addition of fly ash to reduce drying shrinkage (Cho et al., 2006)

## 2.5 Non-traditional stabilizers

Apart from the traditional stabilizers like cement and lime, some non-traditional additives are currently used increasingly and marketed as efficient stabilizers for the soils. For instance, Little (2009) pointed out that some non-traditional stabilizers such as sulfonated oils, enzymes, ionic stabilizers may have a role in modifying or stabilizing soils with high sulfate contents when application of calcium-based traditional stabilizers is limited. Tingle et al. (2007) divided these non-traditional additives into seven categories: salts, acids, enzymes, lignosulfonates, petroleum emulsions, polymers and tree resins and summarized the proposed stabilization mechanisms as shown in Table 2.9. As can be seen in Table 2.9, stabilization of clay soil with these additives mainly involves either chemical or physical bonding.

Additionally, Tingle and Santoni (2003) compared the mechanical performance of stabilized clay specimens by using these 7 types of additives with the specimens stabilized by using cement or lime. Figure 2.29 shows the comparison of compressive strength of the stabilized clay specimens by using some of these additives. "Wet test" indicates the specimens are soaked in water for 15 minutes before testing to indicate the moisture susceptibility; "CL control" indicates the untreated soil sample without any stabilizer. Their study concluded that some of these non-traditional additives such as polymers and lignosulfonate significantly improved the UCS of clay materials, whereas other additives have no significant effect on the UCS and even showed large susceptibility to moisture.

**Table 2.9** Proposed stabilization mechanisms and suitability for stabilization application (Tingle et al., 2007)

| Stabilization additive | Proposed primary stabilization mechanism | Soil compatibility | Strength improvement | Volume stability | Water-proofing |
|---|---|---|---|---|---|
| Ionic | Cationic exchange and flocculation | Fine-grained soils | Low-medium | Low-medium | Low-medium |
| Enzymes | Organic molecule encapsulation | Fine-grained soils | Low | Low-medium | Low |
| Lignosulfonates | Physical bonding/cementation | Granular soils | Medium | Low-medium | Low-medium |
| Salts | Hygroscopy/cation exchange and flocculation/crystallization and cementation | All | Low-medium | Low | Low |
| Petroleum resins | Physical bonding/cementation | Granular soils | Medium | Medium | High |
| Polymers | Physical bonding/cementation | Granular soils | Medium-high | Medium | Medium-high |
| Tree resins | Physical bonding/cementation | Granular soils | Medium-high | Medium | Medium-high |

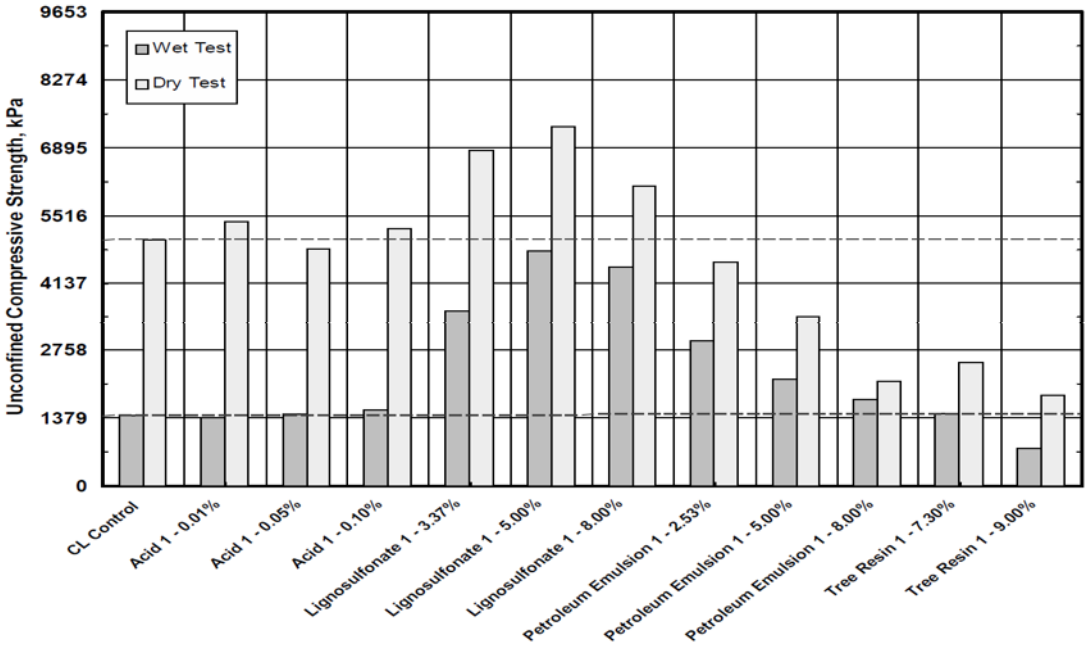


**Figure 2.29** Compressive strength of fat clay stabilized with acid, lignosulfonate, petroleum emulsion, or tree resin versus control (Tingle & Santoni, 2003)

Another study conducted by Parsons (2003) also found that these enzymatic stabilizers did not substantially improve the soil performance by comparing the

performance with other traditional stabilizers and enzyme-treated soils are susceptible to excessive moisture.

Similarly, Rauch (2002) investigated three liquid soil stabilizers which are categorized as ionic, acrylic polymer and enzyme. His study revealed that no marked changes in engineering properties (Atterberg limits, volume change and compressive strength) were found by stabilizing with these three stabilizers. Results from triaxial compression tests are shown in Figure 2.30, which indicates that there is no increase or even a decrease in strength by treating with these three stabilizers compared with the untreated soil. This study suggests that increasing the application rate of these additives (in excess of the supplier recommendation) might produce more significant and beneficial effects.

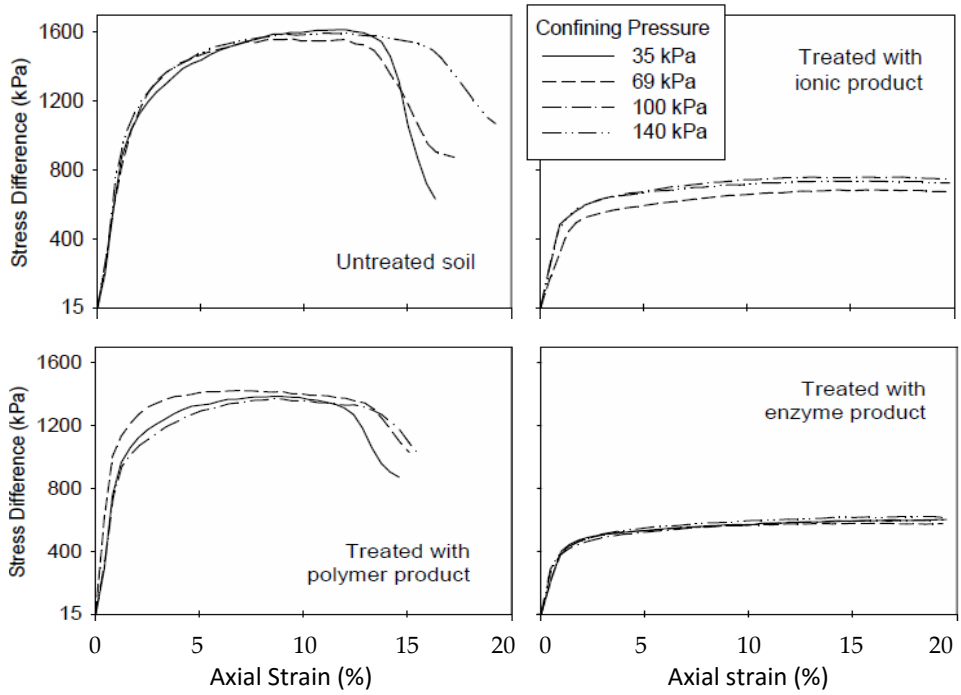


**Figure 2.30** Triaxial test result for stabilizing clay with different liquid stabilizers (after Rauch et al., 2002)

From the discussion above it can be concluded that some of these additives are reported to be efficient in enhancing the soil properties and some are not. The reason could be that the efficiency of these products is much dependent on the soil type or specific environment. That means, some products may work well in specific soil types in a given environment, but they probably perform poorly in another environment (Tingle & Santoni, 2003).

## 2.6 RoadCem additive (Rc) in soil stabilization

In this research, RoadCem additive (referred to as Rc) is employed to be used in stabilizing soil with cement. Unlike the above-mentioned additives which are used as stabilizer to replace cement or lime, Rc additive is designed as an additive used in conjunction with cement. Rc additive is a patented blend of alkali metal and alkaline earth metal substances and synthetic zeolites. Based on the compounds incorporated in Rc, this additive acts as a catalyst for cement hydration, ion exchange, absorbing and immobilizing the potentially harmful compounds, according to Powercem Synopsis (2008). According to a study by Gersonius and Egyed (2012), the macro economic advantages by using this additive are enormous.

Previous studies documented that Rc additive enhances the strength, stiffness and flexibility of cement stabilized materials and improves the overall performance of stabilized road layers (Marjanovic et al, 2008; Birgisson & Egyed, 2008; Mutepfa, 2010). For instance, Mutepfa (2010) showed that addition of Rc additive increases the compressive strength of cement stabilized sand materials from 2.5 to 4 MPa at the curing time of 7 days, when cement content 9% was used. The improvement on the mechanical properties can be attributed to the formed dense crystalline microstructure by adding this additive (Marjanovic et al, 2008). One example of SEM images (scanning electron microscopy) of cement treated sandy gravel is shown in Figure 2.32. In Figure 2.32, images A, B, C, and D indicate the ages of 1, 3, 5 and 8 months, respectively.

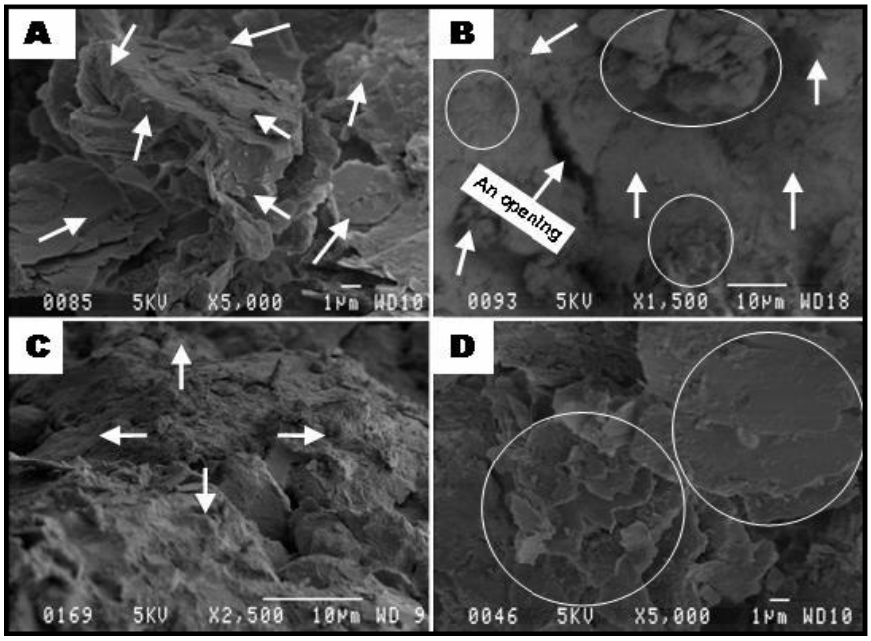


**Figure 2.32** SEM images of stabilized sandy gravel with cement content 7% and Rc additive 0.07% (by volume) (Moloisane, 2009)

In Figure 2.32, the images C and D illustrate the dense crystalline microstructure cured for 5 and 8 months. Especially image D shows a dense cemented matrix in the form of interlocked clusters (indicated by circles), which indicate an increase in linking soil particles and hence it contributes to the bond strength and strength gain. In this research, no comparison was made with the SEM results of mixtures without Rc additive, at the same cement level.

Moreover, addition of Rc additive in cement blended with pozzolanic materials such as fly ash and granulated blast furnace slag has also been evaluated (Ouf, 2012; Ventura & Koloane, 2005). Table 2.10 compares the compressive strength of stabilized sand soils with different amounts of stabilizers. The stabilizer contains 59% fly ash, 40% cement and 1% Rc additive. It shows that the compressive strength increases with rise of the stabilizer content.

**Table 2.10** Compressive strength of sandy soils treated with different amounts of stabilizer (Ventura & Koloane, 2005)

| Curing period (days) | Compressive strength (MPa) | | | | | |
|---|---|---|---|---|---|---|
| | Sand | | | 30% clay+70% sand | | |
| | Stabilizer content | | | Stabilizer content | | |
| | 8% | 12% | 18% | 8% | 12% | 18% |
| 1 | 1.33 | 1.55 | 1.91 | 0.66 | 0.80 | 1.35 |
| 2 | 1.55 | 1.70 | 2.01 | 0.80 | 0.98 | 1.50 |
| 7 | 1.94 | 2.50 | 3.57 | 1.51 | 2.00 | 2.91 |
| 14 | 2.38 | 3.52 | 5.00 | 2.52 | 3.23 | 4.25 |
| 21 | 2.85 | 4.22 | 6.01 | 3.00 | 3.85 | 5.25 |
| 28 | 3.47 | 5.00 | 7.00 | 3.41 | 4.26 | 5.86 |

Similar additives have been previously evaluated by Delft University of Technology (Houben & Poot, 2008a; Houben & Poot, 2008b) which generally showed promising results of strain at break and fatigue properties. These additives contain the similar compounds in Rc additive. Study by Houben and Poot (2008b) was conducted on the use of a similar additive in cement stabilized sand material (mixed with fly ash) which showed the strain at break of this material was 505 and 579 μm/m. The strain at break reported in these two studies is much higher than that of the traditional cement stabilized materials. Although the test results exhibited potential benefits of using these additives, these results are based on limited test data and lack comparison with the mixtures without using these additives. Therefore, this thesis is

initiated to conduct an extensive test program to evaluate the influence of Rc additive on the properties of cement stabilized materials.

## 2.7 Conclusions

This Chapter described the function of cement stabilized bases in the pavement structure, the mix components and the properties of cement stabilized materials. This Chapter focused on the properties of these materials, including compressive and tensile strength, modulus of elasticity, fatigue life as well as shrinkage behavior. In this Chapter, the main conclusions based on analysis of the large amount of previous studies can be drawn as follows:

1) More than one stabilizing agent can be used for individual soil type. The choice is dependent on the nature of the soil and the desired function of the stabilized layer as well as the overall cost. In general, cement is more suitable to stabilize granular materials like sand and gravel, while lime is more suitable to stabilize high plastic soils like clay.

2) Stabilizing unbound materials with cement significantly increases their strength and stiffness, and provides a durable base layer for flexible or rigid pavements. A cement stabilized base spreads the loads over a wide area and thereby considerably reduces the stress on the subgrade due to the traffic loads.

3) The mechanical properties of cement bound materials are largely influenced by cement content, soil type, degree of compaction, curing conditions and other environmental factors. The higher the cement content, the more coarse-grained the soil and the higher the degree of compaction, the higher the stiffness and strength of cement stabilized materials. Many estimation models have been reported to predict the compressive strength of cemented materials. Besides, correlations between the strength (compressive and tensile strength) as well as the elastic modulus have also been established in many literature studies.

4) With respect to fatigue properties, based on stress or strain controlled bending tests, most of the relationships are described by SN-N curves, which exhibit a large variation for various soil types.

5) Cement stabilized materials are susceptible to the shrinkage cracks due to moisture loss during hydration process or a decrease of temperature. The

degree of shrinkage is influenced by the cement content, soil type, moisture content and also the curing condition. Shrinkage cracks of cement stabilized base can be reduced by several methods, such as optimum mix composition and proper construction techniques.

6) The previous research shows promising results of using Rc additive in cement stabilized materials but lacks comparison with materials without using this additive. This study is initiated to extensively evaluate the influence of this additive on the properties of cement stabilized materials.

## References

ACI (1998). ACI Manual of concrete Practice: Part 1 (No. ACI 209R-92). U.S.A., Farmington Hills: ACI Committee 209.

ACI. (1990). American Concrete Institute Committee 230. State-of-the-Art Report on Soil Cement. ACI Materials Journal, Vol. 87, No. 4, pp. 395–417.

Adaska, W. S. & D.R. Luhr. (2004). Control of reflective cracking in cement stabilized pavements, RILEM Publications.

Aiban, S. A., Al-Abdul Wahhab, H. I., Al-Amoudi, O. S. B. & Ahmed, H. R. (1998). Performance of a stabilized marl base: a case study. Construction and Building Materials, 12(6), 329-340.

Altun, S., A. Sezer, et al. (2009). The effects of additives and curing conditions on the mechanical behavior of a silty soil. Cold Regions Science and Technology 56(2-3): 135-140.

Bahar, R., Benazzoug, M., & Kenai, S. (2004). Performance of compacted cement-stabilized soil. Cement and concrete composites, 26(7), 811-820.

Babic, B. (1987). Relationships between mechanical properties of cement stabilized materials. Materials and Structures 20(6): 455-460.

Balbo, J.T. & Cintra, J.P. (1996). Fatigue verification criteria for semi-rigid pavements. In National Meeting on Asphalt Mixture and Pavements, available online at: http://www, ptr. usp. br.

Bhandari, R.K.M. (1973). Shrinkage of Cement Treated Mixtures, Journal of the Australian Road Research Board, Vol. 5, No. 3.

Birgisson, B and Egyed, C.E.G. (2008). New Nano crystalline structure leads to visco-elastic behaviour of cement based materials.

Bofinger, H. E. & Sullivan, G. A. (1971). An investigation of cracking in soil-cement bases for roads. Road Research Laboratory, RRL Report LR 379, Crowthorne, UK.

Bofinger, H.E. (1970). The Measurement of the tensile properties of soil-cement. Ministry of Transport, RRL Report LR 365. Crowthorne, UK.

Bofinger, H. E., H.O. Hassan & R.I.T. Williams (1978). The shrinkage of fine-grained soil-cement. TRRL supplementary report 398.

Cho, Y. H., K. W. Lee & Ryu, S. W. (2006). Development of cement-treated base material for reducing shrinkage cracks. Transportation Research Record: Journal of the Transportation Research Board 1952(-1): 134-143.

Consoli, N.C., da Fonseca, A. V., Cruz, R. C., & Silva, S. R. (2011). Voids/Cement Ratio Controlling Tensile Strength of Cement-Treated Soils. Journal of geotechnical and geoenvironmental engineering, 137(11), 1126-1131.

Consoli, N.C., Foppa, D., Festugato, L., & Heineck, K.S. (2007). Key Parameters for Strength control of Artificially Cemented Soils. Journals of Geotechnical and Geoenvironmental Engineering, 133(2), 197-205.

Croney. D. (1977). The Design and Performance of Road pavements. London, Transport and Road Resarech Laboratory, Crowthorne, UK.

Crockford, W.W. and Little, D.N. (1987). Tensile fracture and fatigue of cement-stabilized soil. Journal of transportation engineering, 113(5), 520-537.

DFID (2004). Literature review stabilized sub-bases for heavily trafficked roads. Project report from the Department for International Development (DFID), of the UK and the Department of Public Works and Highways (DPWH), Philippines.

Donaldl. Basham, J. W. (Oct, 1994). Soil Stabilization for Pavements. The Unified Facilities Criteria.

FAA, Federal Aviation Administration (1981). AC No. 150/5370-10, U.S. Department of Transportation, April 21, 1981.

FM 5-410, 2012. Soil Stabilization for Roads and Airfields.
http://www.itc.nl/~rossiter/Docs/FM5-410/FM5-410_Ch9.pdf.

Galloway, J.W. & H.M. Harding (1976). Elastic modulus of a lean and a pavement quality concrete under uniaxial tension and compression. RILEM. Materials and Strucutre,13-18.

George, K.P. (1968). Shrinkage Characteristics of Soil-Cement Mixtures, Highway Research Record 255, Washington D.C.

George, K.P. (2002). Minimizing cracking in cement-treated materials for improved performance. No. R&D Bulletin RD123.

Gersonius, B & Egyed, C.E.G. (2012). Macro-economic Effect of Using the PowerCem Technology on Road Infrastructure in Flood Risk Areas, UNESCO – IHE, the Netherlands.

Guthrie, W.S. & M. A. Rogers (2010). Variability in Construction of Cement-Treated Base Layers. Transportation Research Record: Journal of the Transportation Research Board 2186(-1): 78-89.

Halstead, W.J. (1986). Use of fly ash in concrete. NCHRP 127. Washington: Transportation Research Board, National Research Council.

Halsted, G. E. (2006). Performance of Soil-Cement and Cement-Modified Soil for Pavements: Research Synopsis. Portland Cement Association, Skokie, USA.

HRB, Highway Research Board. (1962). The AASHO Road Test, Special Report 61. Washington D.C.

Horpibulsuk, S., Rachan, R., Chinkulkijniwat, A., Raksachon, Y., & Suddeepong, A. (2010). Analysis of strength development in cement-stabilized silty clay from microstructural considerations. Construction and building materials, 24(10), 2011-2021.

Horpibulsuk, S., Sirilerdwattna, W., Rachan. R & Katkan, W. (2007). Analysis of strength development in pavement stabilization: a field investigation. In: Proceedings of the 16th southeast Asian geotechnical conference, 579-583.

Houben, L.J.M. & Poot, M.R (2008a). Preliminary research into (fatigue) bending strength of stabilized harbor silt/sand stabilized with Immocem. Delft University of Technology Report 7-08-190-1 (in Dutch), the Netherlands.

Houben, L.J.M. & Poot, M.R. (2008b). 2-point bending tests to determine strength of Mexican material stabilized with ConcreCem. Delft University of Technology Report 7-08-190-2 (in Dutch), the Netherlands.

Hudson, W.R. & Kennedy T.W. (1968). An Indirect Tensile Test for Stabilized Materials. Research Report 98-1. Center for Highway Research, the University of Texas at Austin, USA.

Ingles, O.G, Metcalf, J.B. (1972). Soil Stabilization Butterworths, Sydney.

Jameson, G., Sharp, K. G., & Yeo, R. (1992). Cement-treated Crushed Rock Pavement Fatigue Under Accelerated Loading: The Mulgrave (Victoria) ALF Trial, 1989/1991 (No. ARR229).

Jeb S. Tingle & Santoni, R. L. (2003). Stabilization of clay soils with nontraditional additives. Transportation Research Record 1819 Paper No. LVR8-1136

Katz, L. E., Rauch, A. F., Liljestrand, H. M., Harmon, J. S., Shaw, K. S., & Albers, H. (2001). Mechanisms of soil stabilization with liquid ionic stabilizer. Transportation Research Record: Journal of the Transportation Research Board, 1757(1), 50-57.

Kersten, M.S. (1961). Soil Stabilization with Portland Cement. Washington, D. C., National Academy of Sciences National Research Council.

Kenai, S., R. Bahar, and M. Benazzoug. (2006). Experimental analysis of the effect of some compaction methods on mechanical properties and durability of cement stabilized soil. Journal of materials science 41, no. 21: 6956-6964.

Kennedy, J. (1983). Cement-bound Materials for Sub-bases and Road bases, Material Selection and Mix Design, Construction and Control Testing (No. 46.027 Monograph).

Kennedy, T.W., Moore, R.K. & Anagnos, J.N. (1971). Estimation of Indirect-Tensile Strengths for Cement-Treated materials, Record 351, Highway Research Board.

Kenai, S., Bahar, R., & Benazzoug, M. (2006). Experimental analysis of the effect of some compaction methods on mechanical properties and durability of cement stabilized soil. Journal of materials science, 41(21), 6956-6964.

Kolias, S., V. Kasselouri-Rigopoulou, et al. (2005). Stabilisation of clayey soils with high calcium fly ash and cement. Cement and Concrete Composites 27(2): 301-313.

Kolias, S. & Williams, R.I.T. (1978). Cement-bound road materials: strength and elastic properties measured in the laboratory. TRRL Supplementary Report 344, Transport and Road Research Laboratory, Crowthorne, UK.

Lay 1986/88 Lay, MG. (1986) Handbook of road technology. Includes chapter 10: stabilization (redrafted 1988). Published by Gordon & Breach, London, 1986.

Lim, S. & Zollinger, D.G. (2003). Estimation of the compressive strength and modulus of elasticity of cement-treated aggregate base materials. Transportation Research Record: Journal of the Transportation Research Board, 1837(1), 30-38.

Little, D.N. (1995). Handbook for stabilization of pavement subgrades and base courses with time, Dubuque: Kendall/hunt.

Little, D.N. (2009). Recommended Practice for Stabilization of Subgrade Soils and Base Materials. NCHRP web-only document 144. Texas A&M University, Texas.

Litzka, J., and W. Haslehner. (1995). Cold In-Place Recycling on Low-Volume Roads in Aultria. Proc., 6th International Conference on Low Volume Roads, Minneapolis, Minn.

Makusa, G.P. (2012). Soil stabilization method and materials, state of the art review, Lulea university of technology, Sweden.

Maclean, D.J., Robinson, P.J.M., & Webb, S.B. (1952). An Investigation of the Stabilization of heavy clay soil with cement for road base construction. Roads and road construction (London), 30:358, 287-92.

Marjanovic, P., Egyed, C.E.G., De La Roij, P and de La Roij, R. (2008). The Road to The Future. Manual for Working with RoadCem. PowerCem Technologies, ISBN 978-90-79835-01-0.

Mitchell, J.K. (1976). Fundamentals of soil behavior, John Wiley and Sons, Inc., New York.

Molenaar. A.A.A (2006). Structural Design of Pavement, Design of Flexible Pavement. Lecture Notes CT 4860, Delft University of Technology, the Netherlands.

Molenaar, A.A.A. (2010a). Road Paving Materials Part 1 Cohesive and non-cohesive soils and unbound granular materials for bases and sub-bases in roads. Lecture notes CT 4880, Delft University of Technology, Netherlands.

Molenaar (2010b). Road Paving Materials-Part II: Soil stabilization. Lecture Notes CT4880, Delft University of Technology, the Netherlands.

Molenaar, A. A. A. & Pu, B. (2008). Prediction of fatigue cracking in cement treated base courses. Proceedings of 6th RILEM International Conference on Cracking in Pavements (pp. 191-199).

Moloisane, R.Y. (2009). Evaluation of the long-term strength behaviour of unpaved roads stabilized with non-traditional stabilizers. Master thesis, University of Pretoria, South Africa.

Monismith, C.L., Epps, J.A., Kasianchuk, & McLean, D.B. (1971). Asphalt Mixture Behavior on Repeated Flexure. Report No. TE 70-5, University of California, Berkeley, USA.

Mutepfa, A.T. (2010). Laboratory Evaluation of the Effect of Cement Concentration, Water Salinity and the Roadcem Additive on Kalahari Soil Strength. Master thesis, University of Botswana, South Africa.

Nakayama, H., & Handy, R.L. (1965). Factors Influencing Shrinkage of Soil-Cement, Highway Research Record 86, Washington, D.C.

NEN-EN 14227-1 Hydraulically bound mixtures - Specifications-Part 1: Cement bound granular mixtures.

NEN-EN 14227-10 Hydraulically bound mixtures-Specifications-Part 10: Soil treated by cement. 2006.

NEN-EN 12697-24 Bituminous mixtures - Test methods for hot mix asphalt - Part 24: Resistance to fatigue.

Otte, E. (1979). Factors Affecting the Behavior of Cement Treated Layers in Pavements. In Australian Road Research Board Conference Proc (Vol. 9, No. 4).

Ouf, M.S. (2012). Effect of using pozzolanic materials on the properties of Egyptian soils. Life Sci J, 9(1), 554-560.

Park, S.S. (2010). Effect of Wetting on Unconfined Compressive Strength of Cemented Sands. Journal of geotechnical and geoenvironmental engineering 136(12): 1713-1720.

Parsons, R.L. & Milburn, J. P. (2003). Engineering behavior of stabilized soils. Transportation Research Record: Journal of the Transportation Research Board, 1837(1), pp.20-29.

PCA (2001). Suggested specifications for soil-cement base course construction. Portland Cement Association, Skokie, USA.

PCA (2003). Reflective cracking in cement stabilized pavements. Portland Cement Association, Skokie, USA.

PCA (2005a). Soil-Cement for commercial Sites, the low-cost alternative for heavy-duty industrial pavements. Portland Cement Association, Skokie, USA.

PCA (2005b). Soil-Cement technology for pavements: Different Products for different applications. Portland Cement Association, Skokie, USA.

Pell, P.S. (1978). Principles of material characteristics and pavement design. Lecture notes, Delft University of Technology, the Netherlands.

Pretorius, P.C. & Monismith, C.L. (1971). The prediction of shrinkage stresses in pavements containing soil cement bases, paper presented at the Annual Meeting of the Highway Research Board, Washington, D.C.

Raki, L., Beaudoin, J.J. & Alizadeh, R. (2009). Nanotechnology applications for sustainable cement-based products. In Nanotechnology in Construction 3 (pp. 119-124). Springer Berlin Heidelberg.

Rauch, A.F., Harmon, J.S., Katz, L.E., & Liljestrand, H.M. (2002). Measured effects of liquid soil stabilizers on engineering properties of clay. Transportation Research Record: Journal of the Transportation Research Board, 1787(1), 33-41.

Richardson, D.N. (May 1996). AASHTO Layer Coefficients for cement-stabilized soil bases, Journal of materials in civil engineering, Vol. 8, No.2, p. 83-87.

Sebesta, S. (2005). Part 1: Cementitious, Chemical, and Mechanical Stabilization: Use of Microcracking to Reduce Shrinkage Cracking in Cement-Treated Bases. Transportation Research Record: Journal of the Transportation Research Board, 1936(1), 1-11.

Shacklock, B.W. (1974). Concrete constituents and mix proportions. Cement and Consrete Association, London.

Selvam, R.P., Subramani, V.J., Murray, S. & Hall, K.D. (2009). Potential application of nanotechnology on cement based materials. No. MBTC DOT 2095/3004.

Sherwood, P.T. (1968). The properties of cement stabilized Materials. London: Road Research laboratory.

Sherwood, P.T. (1981). The properties of cement-stabilized materials, RRL Report LR 205, Crowthorne, UK.

Sherwood, P.T. (1995). Soil Stabilization with Cement and Lime. State of the Art review. London: HMSO Press.

Solanki, P., Zaman, M. M., & Dean, J. (2010). Resilient modulus of clay subgrades stabilized with lime, class C fly ash, and cement kiln dust for pavement design. Transportation Research Record: Journal of the Transportation Research Board, 2186(1), 101-110.

Terrel, R.L., Epps, J.A., Barenberg, E.J., Mitchell, J.K., & Thompson, M.R. (1979). Soil Stabilization in pavement Structures, a user's manual-Volume 1: pavement design and Construction Considerations (No. FHWA-IP-80-2). Washington D.C: Federal Highway Administration, Department of Transportation.

Thompson, M.R. (1998). Stabilized Base Properties (strength, modulus, fatigue) for mechanistic-based airport pavement design. University of Illinois at Urbana-Champaign, Illinois, USA.

Thompson, M.R. (1996). The Split-Tensile Strength of Lime-Stabilized Soils, Record 92, Highway Research Board.

Thompson, M.R. (1986). Mechanistic Design concepts for stabilized base pavements, Civil Engineering Studies, Transportation Engineering Series No. 46, Illinois Cooperative Highway and Transportation Series No.214, University of Illinois, Urbana-Champaign, Illinois, USA.

Tingle, J.S. & Santoni, R.L. (2003). Stabilization of clay soils with nontraditional additives. Transportation Research Record: Journal of the Transportation Research Board, 1819(1), 72-84.

Tingle, J.S., Newman, J.K., Larson, S.L., Weiss, C.A., & Rushing, J.F. (2007). Stabilization mechanisms of nontraditional additives. Transportation Research Record: Journal of the Transportation Research Board, 1989(1), 59-67.

TRH 13 (1986). Cementitious Stabilizers in Road Construction South Africa. Pretoria, South Africa.

Ventura, D & Koloane, T. (2005). Laboratory evaluation of Megatech's PowerCem blend to determine its suitability as a road building material stabilizer. Contract report. Johannesburg: CSIR Transport.

Watson, J. (1994). High way construction and maintenance. 2nd edition. Published by Longman group, Harlow, Essex.

Williams, R.I.T. (1972). Properties of cement stabilized materials. J. Instin. Highw. Engrs., 19(2), 5-19.

Williams, R.I.T. (1986). Cement-treated pavements: Materials, Design and Construction, London: Elsevier Applied Science Publishers LTD.

Winterkorn, H.F., & Pamukcu, S. (1991). Soil stabilization and grouting. In Foundation Engineering Handbook (pp. 317-378). Springer US.

Xuan, D.X. (2012). Cement Treated Recycled Crushed Concrete and Masonry Aggregates for Pavements. PhD dissertation, Delft University of Technology, Delft, the Netherlands.

Yoon, S. & Abu-Farsakh, M. (2009). Laboratory investigation on the strength characteristics of cement-sand as base material. KSCE Journal of Civil Engineering, 13(1),15-22.

# CHAPTER 3

# MATERIALS AND TEST PROGRAM

This research project aims to investigate the influence of Rc additive on the properties of cement stabilized materials. The test program is the main part of this research which is divided into two parts: laboratory tests and field evaluation. The entire program is designed in such a way that the properties of materials can be extensively evaluated and correlations between performance and material composition can be derived.

This Chapter illustrates the materials used in this study and the laboratory test program. On the basis of the literature studies, the compressive and the tensile strength are the two basic mechanical parameters to characterize cement stabilized materials. The laboratory test program consists of compression, indirect tensile and flexural tensile tests, stiffness and fatigue tests as well as shrinkage measurement. A variety of mix compositions with varying cement and Rc contents are used. Furthermore, the micro-properties of cement stabilized materials are examined by observing the morphology and via analysis of the chemical changes which can be linked to the mechanical test results. Figure 3.1 gives an overview of the entire test program.

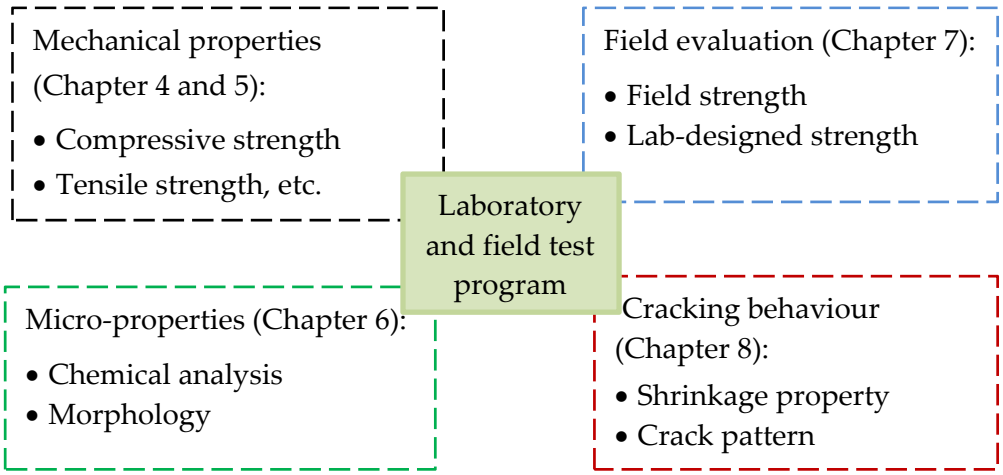


**Figure 3.1** Overview of the entire test program

## 3.1 Material characterization

### 3.1.1 Soils

The engineering properties of a cement stabilized material are largely determined by the nature of the raw material whether it is clay, silt, sand or coarse aggregate. The nature of material not only influences the choice of an appropriate stabilizer but also controls the structural properties of the end-product with this stabilizer. By nature, the variable soil properties are mainly attributed to the soil particle size distribution, shape of the grains, particle arrangement as well as the mineralogical composition (Molenaar, 2010). Soils and granular materials consist of an arrangement of particles, with the voids partly or completely filled with moisture. Figure 3.2 indicates three typical examples of particle arrangements.

(a) Aggregate with no fines

(b) Aggregate with sufficient fines for maximum density

(c) Aggregate with great amount of fines

**Figure 3.2** Three physical states of granular mixtures with fines content (Krebs & Walker, 1971)

In Figure 3.2 different fines contents are present in the particle structure which may lead to diverse material behaviors. A granular mixture containing no or low fines content (mixture a) usually has relatively low density and high voids content. For the mixture with sufficient fines content, the maximum density and lowest voids content can be obtained (mixture b). However, with a high fines content (mixture c) the material properties will be highly influenced by the moisture variation. For instance, mixture (c) will lose strength when it is wet and becomes rather strong when it is dry, whereas mixture (a) with no fines will not be affected by adverse water conditions. In this study, two types of soil for stabilization are evaluated which represent a granular material without fines and a soil with a great amount of fines:

- Sand (coarse-grained/non-cohesive soil)
- Clay (fine-grained/cohesive soil)

Figure 3.3 shows the sand and clay soil used in this laboratory research. Sand remains in loose state and individual sand grains can be seen. The clay is seen as dry flakes which are clay particle clusters with a small amount of natural moisture. Characterization of the soil materials was conducted by the sieve analysis, Atterberg limits, mineralogical test and Proctor test.


**Figure 3.3** Soil materials to be stabilized in this study

### 3.1.1.1 Sand

The classification of sand soil is mainly done in terms of particle size distribution, which is obtained by dry sieving according to ASTM C136-01. The cumulative

percentage passing is plotted against the corresponding sieve size, shown in Figure 3.4. Three sand samples were sieved. Figure 3.4 indicates that this type of sand is uniformly graded and a very small variation of individual sand specimens is observed. Coefficient of uniformity (Cu) and Curvature index (Cc) are 3.3 and 0.96, respectively. This type of sand is classified as poorly graded sand (SP) according to the USCS soil classification system (ASTM D2487).

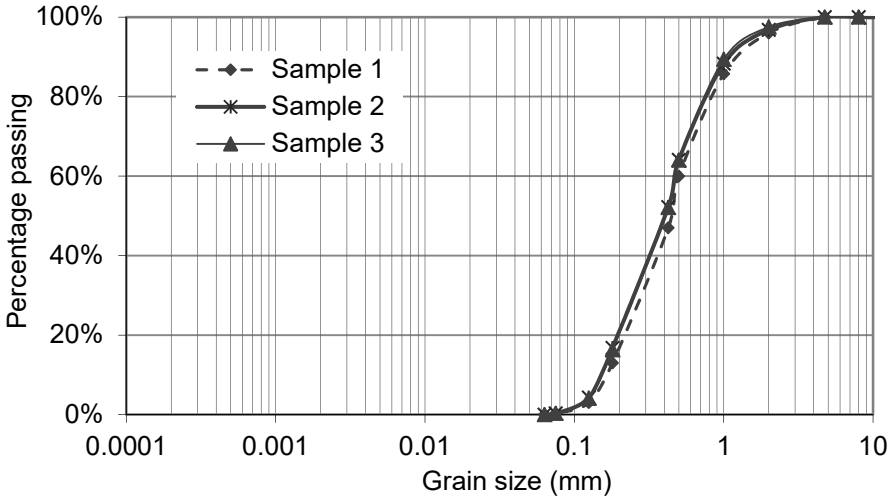


**Figure 3.4** Particle size distribution curve of sand

Besides, to characterize the sand mineral, the X-ray diffraction pattern is given in Figure 3.5 which shows the abundant quartz peaks and indicates that this type of sand is primarily composed of quartz mineral (Q).

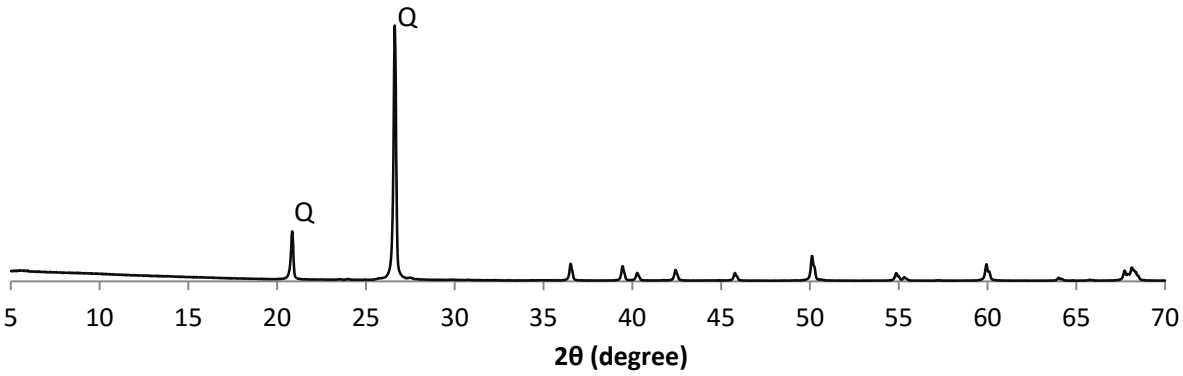


**Figure 3.5** X-ray diffraction pattern of sand

Additionally, the relationship between moisture content and dry density was investigated, and shown in Figure 3.6. Two compaction methods are used, Standard Proctor compaction (according to ASTM D698) and vibratory compaction by using a vibrating hammer (shown in Figure 3.13). The choice of these two compaction methods is based on some previous studies which documented that the traditional Proctor test method is not efficient in compacting granular materials for the reason

that granular material may displace or break down when struck by the impact rammer (Farrar, 2000; Felt, 1968).

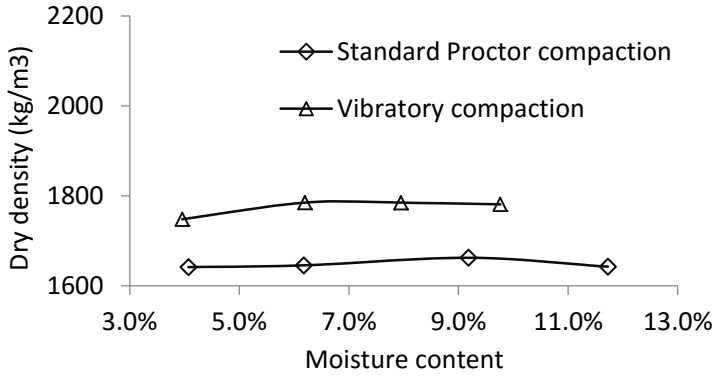


**Figure 3.6** Dry density versus moisture content of sand

In Figure 3.6 it can be seen that the dry density obtained from using the vibrating hammer is about 10% higher than from Proctor compaction at the same moisture content. That is because, when compacting the unbound sand material by the Proctor, the sand particles may displace and move loosely under the impact of the rammer, resulting in insufficient compaction. In contrast, during the compaction by the vibrating hammer the attached tamper almost fits into the internal diameter of the mould and thus provides confinement for the sand. More importantly, the vibratory loading results in a better arrangement of the sand particles and hence reduces the voids between them. However, from both curves it appears that the dry density is nearly constant and no obvious optimum moisture content and maximum dry density are observed. It indicates that the moisture content has no clear influence on the dry density of this uniformly graded sand, which was also mentioned by Molenaar (2010) that well-graded sandy or silty soils show a clearly defined peak to the compaction curve while the uniformly-graded soils, consisting of a narrow range of particle sizes, give a flatter compaction curve from which the optimum is not easy to define.

#### 3.1.1.2 Clay

The particle size distribution of clay was determined by a sedimentation process using a hydrometer (according to BS 1377: part 2:1990). The hydrometer analysis is a widely used method to obtain the distribution of particle sizes in the silt range (2-63 μm) and the percentage of clay particles (< 2 μm). The hydrometer analysis is based on the determination of the density of the suspension which will decrease as more particles settle, due to the differences in specific weight between soil and water (Molenaar, 2010). In this method a specific gravity hydrometer is used, shown in Figure 3.8 (a). The grain size distribution of clay from this hydrometer analysis is

shown in Figure 3.7. It can be seen in Figure 3.7 that the variation of the grain size distribution of the three tested clay samples is quite small.

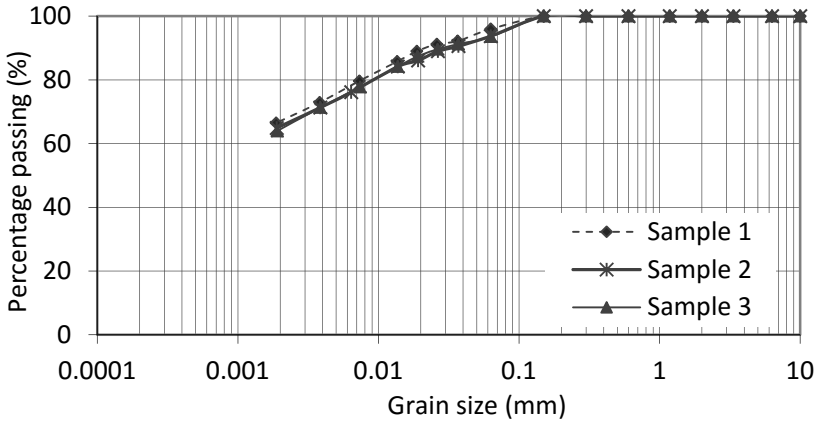


**Figure 3.7** Grain size distribution of clay

The water content greatly influences the behaviour of fine-grained materials. Atterberg limits including liquid limit (LL), plastic limit (PL) and shrinkage limit, provide a range of critical water contents at which the transition between the solid, plastic and liquid states occurs for a given soil. LL and PL tests for clay soil were conducted according to standard ASTM D4318, shown in Figure 3.8 (b) and (c).

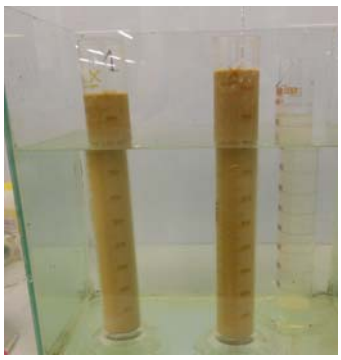

(a) Hydrometer test

(b) Liquid limit

(c) Plastic limit

**Figure 3.8** Tests for clay soil

For fine-grained soil, LL (liquid limit) and PI (plasticity index, the difference between LL and PL) are basically required in soil classification systems. The liquid limit (LL) and plasticity index (PI) of this investigated type of clay are 55.3 and 29.8, respectively. According to USCS soil classification, it is classified as fat clay (CH) which has a high plasticity.

Unlike sand, clay is composed of complex minerals which largely determine the engineering properties. There are three main groups of clay minerals commonly found in clay soil: kaolinite, illite and montmorillonite. Montmorillonite mineral is considered as the main factor determining the plasticity of clay. To identify the clay

minerals, X-ray diffraction pattern of the clay is given in Figure 3.9 which shows the identified minerals present in this type of clay: quartz (Q), kaolinite (K), illite (I) and montmorillonite (M).

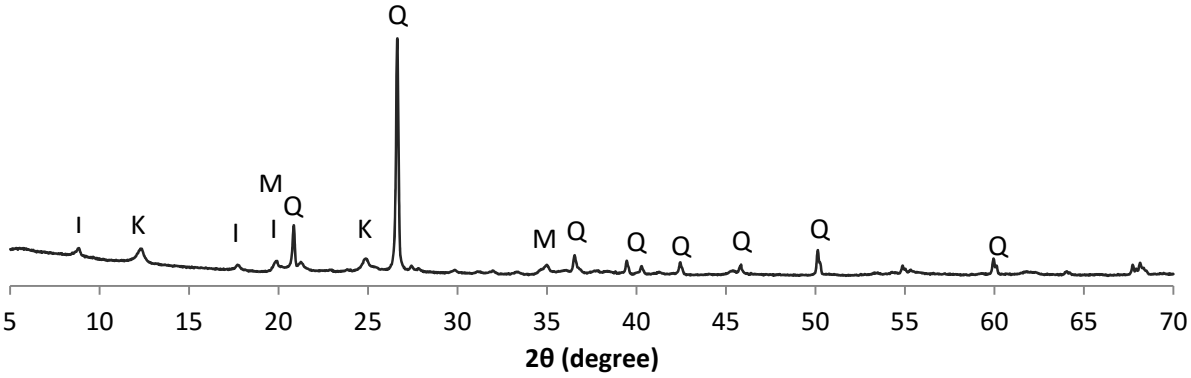


**Figure 3.9** X-ray diffraction pattern of clay

The chemical composition of the clay is given in Table 3.1.

**Table 3.1** Chemical compositions of clay (according to the supplier)

| Compound | Mass (%) | Compound | Mass (%) |
|---|---|---|---|
| $SiO_2$ | 63.3 | CaO | 0.6 |
| $Al_2O_3$ | 20.8 | MgO | 0.7 |
| $TiO_2$ | 1.3 | $Na_2O$ | 0.2 |
| $Fe_2O_3$ | 10.8 | $K_2O$ | 2.4 |

The relationship between the moisture content and the dry density of the clay is obtained by Modified Proctor test (according to ASTM D1557), shown in Figure 3.10. Compared with the Standard Proctor test conducted on sand soil, clay soil was compacted into 5 layers and more compacting effort was applied in the Modified Proctor test. An optimum moisture content of 16% is observed in the compaction curve which corresponds to the maximum dry density 1950 kg/m$^3$.

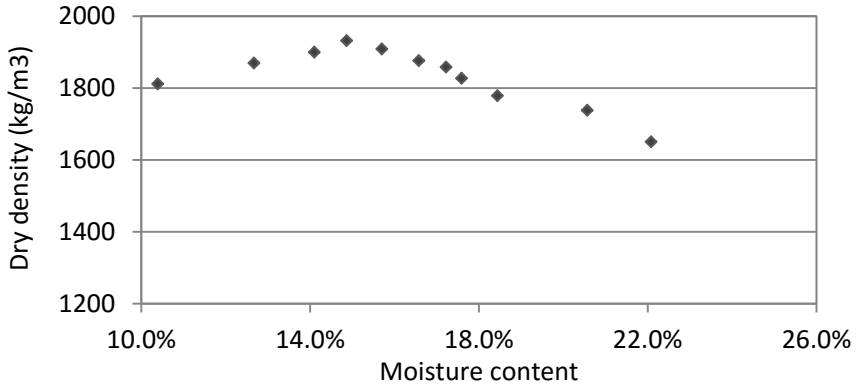


**Figure 3.10** Dry density versus moisture content of clay

### 3.1.2 Cement

Blast-furnace cement (CEM III/B 42.5 N LH) is used as the cement type. This type of cement contains 70% blast-furnace slag and 30% Portland cement clinker with low hydration heat. Blast-furnace cement is widely used in the Netherlands due to the availability and low cost and better chemical resistance and durability (Ferreira et al., 2004; Polder, 1996). The properties of this type of cement are listed in Table 3.2, together with the chemical composition, according to the manufacturer.

**Table 3.2** Properties of the used cement

| Engineering properties | | Chemical composition (%, by mass) | |
|---|---|---|---|
| Specific surface ($cm^2/g$) | 4820 | $SiO_2$ | 30 |
| Density ($kg/m^3$) | 2960 | CaO | 47 |
| 2-day compressive strength (MPa) | 13 | $Al_2O_3$ | 9 |
| 28-day compressive strength (MPa) | 58 | $Fe_2O_3$ | 1 |
| Initial setting time (min) | 230 | $Na_2O$ | 0.53 |
| Final setting time (min) | 300 | Sulphate $SO_3$ | 3.0 |
| 7d hydration heat (J/g) | 237 | Chloride | 0.04 |

This type of cement is characterized by longer initial setting time and a slower rate of strength development than Ordinary Portland cement (TRH13, 1986). The normal initial hardening rate ensures sufficient time for efficient mixing and compaction during manufacturing specimens in the laboratory.

### 3.1.3 Rc additive

Rc additive is a fine white powder. Regarding the chemical composition, Rc additive is mainly composed of:

(1) Alkali metal and alkaline earth metal substances (60–80%, by mass), including chloride sodium (NaCl), chloride potassium (KCl), chloride calcium ($CaCl_2$) and chloride magnesium ($MgCl_2$);
(2) Synthetic zeolites and oxides (5–10%, by mass);
(3) Activators (5–10%, by mass).

Rc additive is designed to be used in conjunction with cement to stabilize the in-situ soils. In cementitious process, Rc additive is believed to increase the degree of cement hydration and thus increases the mechanical strength (Marjanovic et al, 2008). For field application, this additive is usually used in low dosage, generally ranging from

1.2 to 2.4 kg/m$^3$, according to the supplier. The dosage of Rc additive can be increased based on local conditions such as the soil characteristics, opening time for traffic and climate conditions during construction.

Rc additive is highly soluble in water. In this study, Rc additive is firstly dissolved in water and then mixed with clay soil which can ensure the thorough distribution of the additive amongst the clay particles.

### 3.1.4 Water

Tap water from the region of Moerdijk (the Netherlands) is used for preparing all the specimens.

## 3.2 Test program

### 3.2.1 Test program

This study performed mainly through laboratory tests and a field evaluation. The laboratory research was carried out in three phases:

**Phase 1:** Evaluation of the mechanical properties of cement stabilized materials (e.g. stiffness, strength and fatigue property) by applying a wide range of mix proportions aiming to identify the effect of variable factors (e.g. Rc additive content and cement content) and obtain estimation models to predict the properties of cement stabilized materials with use of Rc additive.

**Phase 2:** Examination of the properties of cementitious materials in the micro-scale by using scanning electron microscopy (SEM) and X-ray diffraction analysis (XRD) in order to provide further insight into the microstructure of cement stabilized materials using the Rc additive.

**Phase 3:** Determination of the dry shrinkage under two different curing conditions and the coefficient of thermal expansion (CTE) to be used for the calculation of the transverse crack pattern due to drying shrinkage and temperature changes.

Figure 3.11 outlines the entire test program of the laboratory investigation of different mix compositions for non-cohesive soil sand and cohesive soil clay.

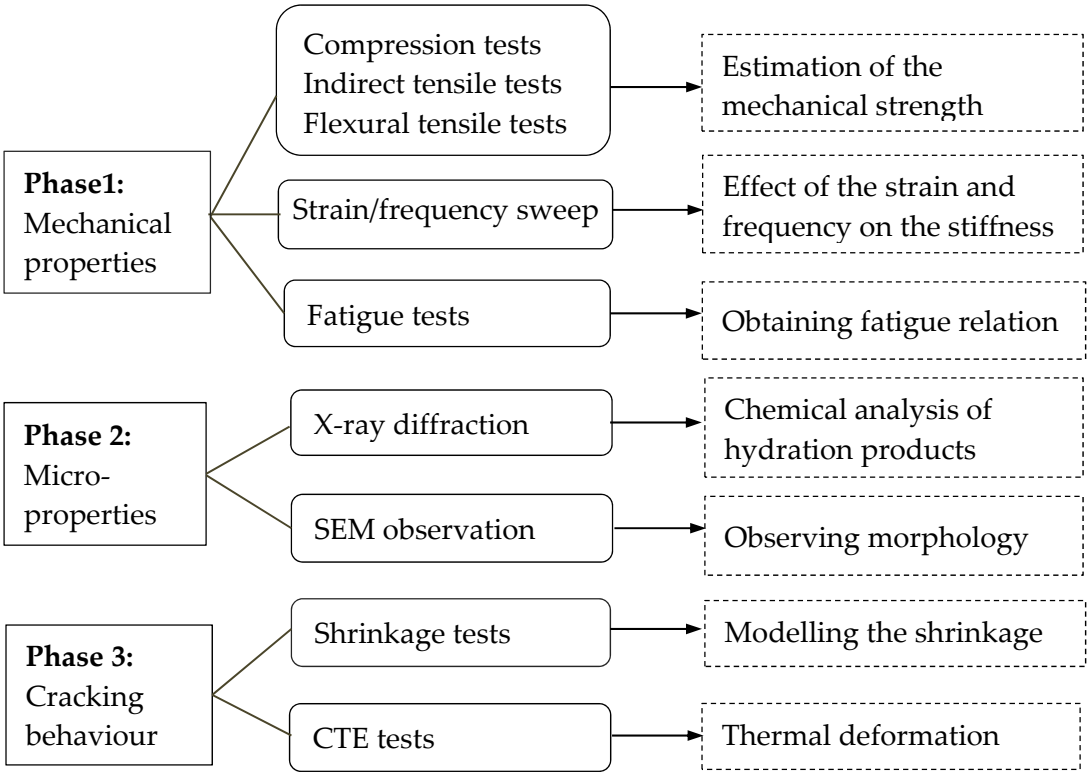


**Figure 3.11** Overview of the laboratory test program in this study

In addition to the laboratory research, a field validation was performed afterwards to evaluate the properties of stabilized materials under field conditions (e.g. field construction and weather conditions) and provide a comparison with the laboratory properties, which gives an insight into issues associated with the practical application. A cement stabilized road base was constructed by stabilizing a variety of raw materials with different mix compositions. This part of the research will be discussed in detail in Chapter 7.

Research on the structural properties of stabilized materials (Phase 1) forms the main part of the laboratory research, which covers the investigation of the strength, stiffness modulus, fatigue, etc. Table 3.3 lists the laboratory test methods and the corresponding specimen sizes as well as the curing times. In Table 3.3 the compression, indirect tensile and flexural tensile strength tests are carried out on all the investigated mixtures (described in section 3.2.2) to obtain the estimation models of these strength properties. The strain and frequency sweep tests were performed to evaluate the stiffness modulus of stabilized materials in flexural tests. At the end, drying shrinkage behavior and the coefficient of thermal expansion (CTE) were determined on three soil-cement mixtures with different amounts of Rc additive.

The following sections 3.2.2 and 3.2.3 focus on the mix design and the methods of preparing specimens for the laboratory tests, listed in Table 3.3. The laboratory test

results of these tests will be analyzed in Chapter 4, Chapter 5 and Chapter 8. The test program and analysis of the results of the micro-study (Phase 2) will be described in Chapter 6.

**Table 3.3** Laboratory test methods and specified curing time

| Test method | Size of specimen (mm) | | Mix design | Curing time (days) |
|---|---|---|---|---|
| Compressive strength | Cylinder | Ø101.6×116.4 | Mixtures in Table 3.4 | 3, 7, 28, 91 |
| Indirect tensile strength | Cylinder | Ø101.6×116.4 | | |
| Flexural tensile strength | Beam | 160×40×40 | | |
| Strain-seep | Beam | 400×50×50 | | 28 |
| Frequency-sweep | Beam | 400×50×50 | | 28 |
| Fatigue | Beam | 400×50×50 | | 28 |
| Shrinkage | Beam | 160×40×40 | 3 selected mixtures | 1 to 28 |
| CTE | Beam | 500×100×100 | | 180 |

### 3.2.2 Mix design

Properties of cement stabilized materials are controlled by the mix compositions mainly including soil, cement, water and additive. The mix design in this study concentrates on the factors of cement and Rc additive contents. Rc additive is used in combination with cement to modify and improve the properties of traditional cementitious material. The central composite design model is employed to indicate these two factors. This mix design method was adopted for use in many studies (Xuan, 2012; Robinson, 2000; Medani, 2000; Muraya, 2007). It is considered as a useful tool to evaluate the correlations between parameters of the mixture and the tested properties and is also able to reduce the number of trials to achieve a balance among the mix variables.

In this study, the cement and Rc contents both have five proportions in the mix design, illustrated in Table 3.4 which shows the coded terms and the absolute levels, and they are graphically shown in Figure 3.12. The mix compositions chosen for this laboratory research are related to the dry mass of soil, while in the field projects of using Rc additive, the mix design is usually applied based on the mass of soil with optimum moisture content, according to the supplier. Trial 1~4 are called star points representing the independent variables (1 and +1). Trial 5-8 are called corner points and the level of mix proportion is denoted as $\alpha$ (set as $\sqrt{2}$). The correlation between

each point is based on the equations (3-1) and (3-2). In many previous studies, it is generally recommended to use one sample for every star point and 5 specimens for the central point in such a way to reduce the number of test specimens. However, in this study three replicate specimens are designed to test at each point in order to achieve a higher reliability.

**Table 3.4** Coded terms for mix variables

| Trial | Code | Rc additive | Cement | Mixture (Rc, C), by dry mass of soil, in kg/m$^3$ |
|---|---|---|---|---|
| | | Rc | C | |
| 1 | $Rc_{-1}C_{-1}$ | -1 | -1 | (0.56, 159) |
| 2 | $Rc_{-1}C_{+1}$ | -1 | +1 | (0.56, 251) |
| 3 | $Rc_{+1}C_{-1}$ | +1 | -1 | (3.2, 159) |
| 4 | $Rc_{+1}C_{+1}$ | +1 | +1 | (3.2, 251) |
| 5 | $Rc_{-a}C_0$ | $-\alpha$ | 0 | (0, 205) |
| 6 | $Rc_{+a}C_0$ | $+\alpha$ | 0 | (3.8, 205) |
| 7 | $Rc_0C_{-a}$ | 0 | $-\alpha$ | (1.9, 140) |
| 8 | $Rc_0C_{+a}$ | 0 | $+\alpha$ | (1.9, 270) |
| 9 | $Rc_0C_0$ | 0 | 0 | (1.9, 205) |

$$\sqrt{2}\,(C_{+1} - C_0) = \frac{1}{2}\left(C_{+\alpha} - C_{-\alpha}\right) \tag{3-1}$$

$$\sqrt{2}\,(Rc_{+1} - Rc_0) = \frac{1}{2}\left(Rc_{+\alpha} - Rc_{-\alpha}\right) \tag{3-2}$$

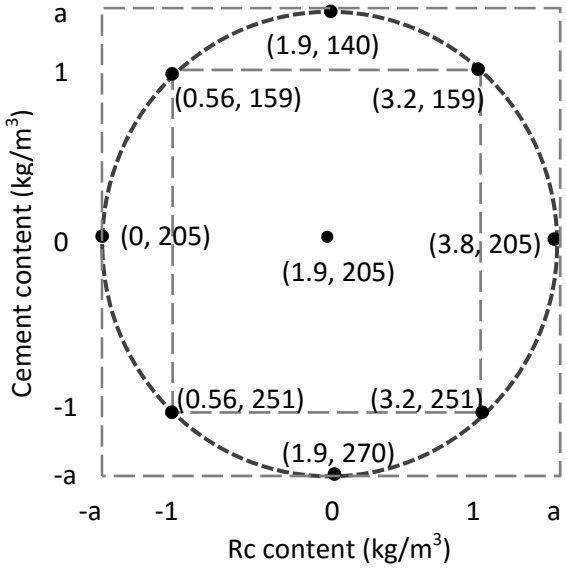


**Figure 3.12** Central composite mix design

As shown in the mix design in Figure 3.12, the cement content ranges from 140 to 270 kg/m$^3$, based on the dry mass of soil. The cement proportion is in a range from 7.9% to 15.1% of sand, and ranging from 7.2% to 13.8% of clay (by dry mass). The maximum amount of Rc additive is designed as 3.8 kg/m$^3$. The ratio of Rc additive to cement content is in a range from 0 to 2.01%, by mass.

Water content is another fundamental parameter to influence the performance of cementitious materials. Water serves two purposes for stabilization: it not only helps to obtain the maximum density during compaction but also enables cement hydration. In this study the mixture variables are focused on the cement and Rc additive contents. For each of these two investigated soil types, the water content is designed to be constant for all the evaluated mixtures. To obtain the appropriate water content for preparing the specimens, preliminary mixing of the soil-cement mixtures at a variety of water contents was carried out.

Although there is no clear optimum moisture content observed in the moisture-dry density curve of sand (Figure 3.6), the moisture content 8% appeared to be the proper content for mixing all the mixtures. A lower water content made the mixture with the highest amount of cement too dry because cement consumes a certain amount of water for hydration. When a higher water content was used, the mixture with a low amount of cement would experience excessive water leaking from the mould during compaction.

Since clay is known as a difficult material to be pulverized and mixed with cement, a variety of moisture contents were preliminarily assessed for mixing clay-cement materials, ranging from 16% to 35%. It was found that the water content 20.8%, which is 4% higher than the optimum moisture value of clay, would enable all the clay-cement mixtures to achieve relative homogenous mixtures and good workability for moulding. A lower or higher water content resulted in either too dry mixtures or more sticky lumps after mixing. Therefore, based on this pre-assessment, water contents 8% and 20.8% (related to the dry mass of the soil) are used to prepare sand-cement and clay-cement mixtures, respectively.

### 3.2.3 Specimen preparation and curing

Making specimens is in general carried out by first mixing all the components (soil, water, Rc additive and cement), followed by compaction and demolding. To achieve a good mixing of the stabilizer with soil is the most important factor affecting the quality of results, because the interaction between a stabilizer and the soil is influenced by the available surface area and adequate pulverization (Mitchell, 1981;

Prusinski & Bhattacharja, 1999). Granular material like sand is normally easy to mix which results in a homogeneous mixture. In contrast, cohesive soils are usually difficult to pulverize due to the high plasticity and hence some lumps will remain in the mixture. It is known that addition of cement can improve the workability of clay because the release of free lime ($Ca(OH)_2$) during cement hydration reduces the plasticity and improves the textural properties of the clay soil (Little, 2009).

In addition to the factor of cement, appropriate treatment of the clay soil also contributes to a homogeneous mixture. Research by Felt (1955) revealed that dry-lumps in the clay-cement mixture are found to be detrimental to the durability of materials (wet-dry and freeze-thaw tests) and he recommended to pre-wet the soil to ensure adequate moisture uniformly distributed in the lumps. Besides, Bofinger (1978) found that the shrinkage behavior of the clay-cement mixture is influenced by whether pre-treatment of clay is done or not. Thus, in this study the clay soil was pre-treated by wetting the soil for 16 hours prior to mixing with cement to ensure that moisture can be uniformly absorbed by the clay particles and eliminate the adverse influence of the dry lumps resulting from mixing.

The success of efficient mixing could also be influenced by the mixing equipment. In this study, H140 Hobart mixer with a 80-liter steel bowl was used. This mixer is attached with a spiral dough hook which provides the smooth mixing operation and with a bowl scraper to scrape the ingredients from the bowl sides, shown in Figure 3.13.

Compaction is another important procedure to be emphasized. The mixture was compacted by a vibrating hammer (Hilti TE1000-AVR). Studies (Kenai, 2006; Drnevich, 2007; Parsons, 1992) have shown promising results of using a vibrating hammer on cement stabilized materials. The vibrating hammer method is considered as a better option than the Proctor compaction because it also simulates the field compaction (Drnevich, 2007). Figure 3.13 shows the mixing equipment and vibrating hammer used in this study.


**Figure 3.13** Mixing and compacting equipment

The detailed procedures of preparing specimens are described in the following steps:

*Step 1 Mixing procedure*

Mixing of all the components was carried out in different ways for sand and clay due to the inherent different soil nature, which is illustrated as follows:

- Sand. After measuring the natural moisture content of the sand, additional water was added while mixing to raise the moisture content to the optimum value (8%). Subsequently, the required amount of Rc additive was added in the form of powder and mixed thoroughly. After mixing with Rc additive, the required amount of cement was added and mixed until a homogeneous mixture was obtained. The whole mixing process took approximately 15 minutes.
- Clay. The required amount of Rc additive was dissolved in a certain amount of water ($w_1$) which is 10 times (by mass) that of Rc. After thorough mixing the clay with optimum moisture content ($w_2$, 16% by mass), the dissolved Rc additive was added and mixed with the clay. After obtaining the uniform clay mixture with Rc additive, the mixture was stored in a container and slightly compacted by a vibrating hammer. The clay-Rc mixture was stored overnight to ensure that the added water and Rc additive distribute uniformly amongst the clay particles.

  After pre-treated for 16 hours, the clay-Rc mixture was mixed with the required amount of cement as well as additional water ($w_3$). This total amount of added water ($w_1$, $w_2$ and $w_3$) is equal to the required moisture content 20.8% (by mass) as noted previously.

The sand-cement mixtures appeared to be quite homogenous, while in the clay-cement mixtures a few percentage of small lumps (about 10-20 mm) remained which are unavoidable.

*Step 2 Compaction of the mixture*

- Compaction method. The steel mould was firstly oiled to prevent the sample would get attached to the sides of the moulds and then the homogeneous mixture was filled into the specified size of the steel mould. For cylindrical specimens, the mixture was compacted by the vibrating hammer at a frequency of 60 Hz. For making a beam specimen the mixture was compacted manually by a 1.5 kg-hammer.
- Compacting layers. The sand-cement mixture was compacted into 3 equal layers while the clay-cement was done with 5 layers due to the cohesiveness. Between layers, the surface was scratched to achieve good adhesion with the next layer. The entire compaction procedure for each batch was finished within two hours to avoid the detrimental effect of compaction delay. After compaction, the surface of the mould was leveled by a spatula.

*Step 3 Demoulding and curing of specimens*

- Sand-cement sample. After compaction and hardening for 24 hours, all the specimens were demoulded and placed in a moisture chamber with a temperature of 20±2˚C and a relative humidity of 90±5% for specified curing periods.
- Clay-cement sample. After compaction, the clay-cement specimens were demoulded immediately and placed in the same curing chamber because the clay-cement material maintained the moulded shape and achieved early strength as soon as the compaction was done. Immediate curing can prevent the significant moisture loss which is important since clay soil is susceptible to the moisture variation. Figure 3.14 shows the specimens after demoulding and curing in the climate chamber.

(a) Sand-cement specimens (b) Clay-cement specimens

**Figure 3.14** Specimens cured in the climate chamber

## 3.3 Conclusions

This Chapter characterized the properties of the materials used in this study and presented the chosen test program. The entire test program was divided into laboratory tests and field evaluation. Emphasis was placed on the laboratory program. The following aspects can be summarized:

- Two types of soil were used for stabilization: sand and clay, which represent non-cohesive and cohesive soils, respectively.
- For each type of soil, the central composite mix design model was applied by varying the cement and Rc additive contents, based on the dry mass of soil. The curing time of the mixtures was also taken into account as a variable factor. The moisture content is fixed for all the evaluated mixtures aiming to concentrate on the variable factors of cement and Rc additive.
- The laboratory test program to evaluate the structural properties included compression, indirect tensile and flexural tensile strength tests aiming to obtain estimation models to predict the mechanical strength of cement stabilized sand or clay materials, as a function of the cement and Rc additive contents and the curing time. Additionally, the stiffness, fatigue and shrinkage properties were also evaluated.
- Procedures of preparing specimens for the above-mentioned laboratory tests have been described with emphasis on the thorough mixing and pre-treatment of the clay.

## References

Bofinger, H.E., H.O. Hassan & R.I.T. Williams (1978). The shrinkage of fine-grained soil-cement. TRRL supplementary report 398.

Drnevich, V., A. Evans & A. Prochaska (2007). A Study of Effective Soil Compaction Control of Granular Soils. Purdue University, West Lafayette.

Felt, E.J. (1955). Factors influencing physical properties of soil-cement mixtures. Highway Research Board Bulletin.

Farrar, J.A. (2000). Bureau of Reclamation Experience with Construction and Control of Earth Materials for Hydraulic Structures. In D.W. Shankin, K.R. Rademacher & J.R. Talbot (Eds.), Construction and Controlling Compaction of Earth Fills, ASTM STP 1384. West Conshohocken: ASTM.

Felt, E.J. (1968). Laboratory Methods of Compacting Granular Soils. A.S.T.M. Special Technical Publication No. 239.

Ferreira, M., G.F. Liu & L. Nilsson. (2004). Blast furnace slag cements for concrete durability in marine environment. Concrete severe conditions: Environment & Loading Seoul, Korea.

Kenai, S., R. Bahar, et al. (2006). Experimental analysis of the effect of some compaction methods on mechanical properties and durability of cement stabilized soil. Journal of Materials Science 41(21): 6956-6964.

Krebs, R.D. (1971). Walker R.D. Highway Materials. McGraw-Hill Book Company, New York.

Little, D.N. (2009). Recommended Practice for Stabilization of Subgrade Soils and Base Materials. NCHRP web-only document 144. Texas A&M University, Texas.

Molenaar, A.A.A. (2010). Road Paving Materials Part 1 Cohesive and non-cohesive soils and unbound granular materials for bases and sub-bases in roads. Lecture notes CT 4880, Delft University of Technology, Netherlands.

Mitchell, J.K. (1981). Soil Improvement–state-of the Art report. Proc. 10th ICSMGE. Stockholm.

Muraya, P.M. (2007). Permanent Deformation of Asphalt Mixes. PhD Thesis, Delft University of Technology, Delft, the Netherlands.

Medani, T.O. (2000). Design Principles of Surfacings on Orthotropic Steel Bridge Decks. PhD dissertation, Delft University of Technology, the Netherlands.

Marjanovic, P., Egyed, C.E.G., De La Roij, P and de La Roij, R (2008). The Road to The Future. Manual for Working with RoadCem. PowerCem Technologies, ISBN 978-90-79835-01-0.

Prusinski, J.R. & Bhattacharja, S. (1999). Effectiveness of Portland cement and lime in stabilizing clay soils. Transportation Research Record: Journal of the Transportation Research Board, 1652(1), 215-227.

Parsons, A.W. (1992). Compaction of Soils and Granular Materials. A Review of Research Performed at Transport Research Laboratory, HMSO, London.

Polder, R.B. (1996). The influence of blast furnace slag, fly ash and silica fume on corrosion of reinforced concrete in marine environment. HERON, 41, 287-300.

Robinson, G.K. (2000). Practical Strategies for Experimenting. Wiley, Chichester, New York.

TRH 13 (1986). Cementitious Stabilizers in Road Construction South Africa. Pretoria, South Africa.

Xuan, D.X. (2012). Cement Treated Recycled Crushed Concrete and Masonry Aggregates for Pavements. PhD Thesis, Delft University of Technology, Delft, the Nethelands.

# CHAPTER 4

# CEMENT STABILIZED SAND WITH ROADCEM ADDITIVE

In many parts of the world, sand is readily available while good quality aggregates are not. In the Netherlands, sand is an important material for road construction. Stabilizing sand with cement significantly improves the strength, stiffness and reduces the permeability.

This Chapter aims to evaluate the influence of Rc additive on the properties of cement stabilized sand material including compressive and tensile strength as well as the fatigue property under repeated loadings. 9 different sand-cement mixtures (shown as the mix design in Figure 3.12) with variable cement and Rc additive contents were investigated and the influence of the cement and Rc contents was analyzed. Curing time is also taking into account in evaluating each property. Based on the laboratory test results, estimation models were developed to predict the mechanical behavior of sand-cement material by combining the effects of mix proportion, density of the specimen and curing time. Regarding the estimation models, different statistical functions were evaluated, such as linear, exponential or log-scale models.

## 4.1 Unconfined compressive strength

### 4.1.1 Test condition

Compressive strength is indicative of the degree of reaction in the soil-cement-water mixture based on the rate of hardening of the mixture (Little, 2009). The unconfined compressive strength test is performed by subjecting a cylindrical specimen to monotonic compressive loading at the rate of 0.05 MPa/s until failure. The unconfined compressive strength is defined as the peak load (F) divided by the area of the cross section of the cylindrical specimen. All the specimens were tested immediately after leaving the moist curing chamber to avoid the influence of variable humidity and temperature in the laboratory. Figure 4.1 shows the unconfined compressive testing in this study and the failure shape of a cylindrical specimen.

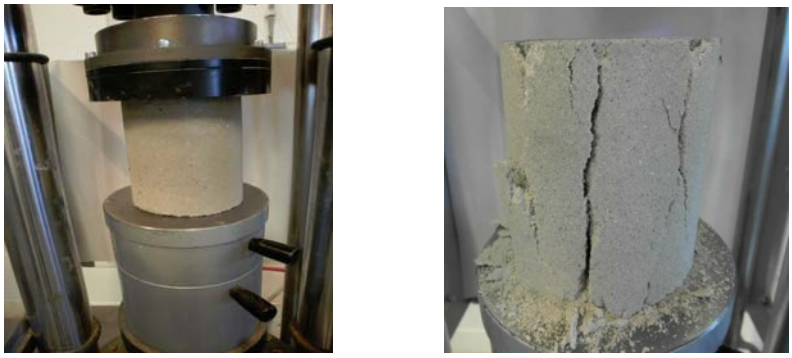

**Figure 4.1** Monotonic compressive testing and specimen after failure

As shown in Figure 4.1, the cylindrical specimens showed vertical cracking failure shape after compression testing. According to NEN-EN 13286-41, a satisfactory failure shape of the specimen was observed after testing. The compressive strength test data of all the evaluated mixtures are presented in Appendix A.

### 4.1.2 Test data and analysis with variable factors

In this study, cement and Rc contents are two independent factors which mainly contribute to the properties of the stabilized materials. In order to visualize the effect of cement and Rc contents on the compressive strength, Figure 4.2 presents the average compressive strength results for each mix design covering all curing times. Each data is the average value of three tested specimens and the highest strength at each curing time is indicated by the blue dot. Each mixture composition (Rc content and cement content, in kg/m$^3$) is indicated in this mix design model.

Besides, for the reason of data analysis, the compressive strength derived from the estimation model (equation 4-6), is also indicated herein by means of colors. The

compressive strength increases from the color of orange to yellow and reaches the highest values in the areas marked in dark colors (black for the curing time of 3 days, purple for 7 days and blue for 28 days and green for 91 days). These colors indicate the compressive strength is higher than 10, 17, 22 and 23 MPa, respectively. The estimation models for the compressive strength will be discussed in section 4.1.3.

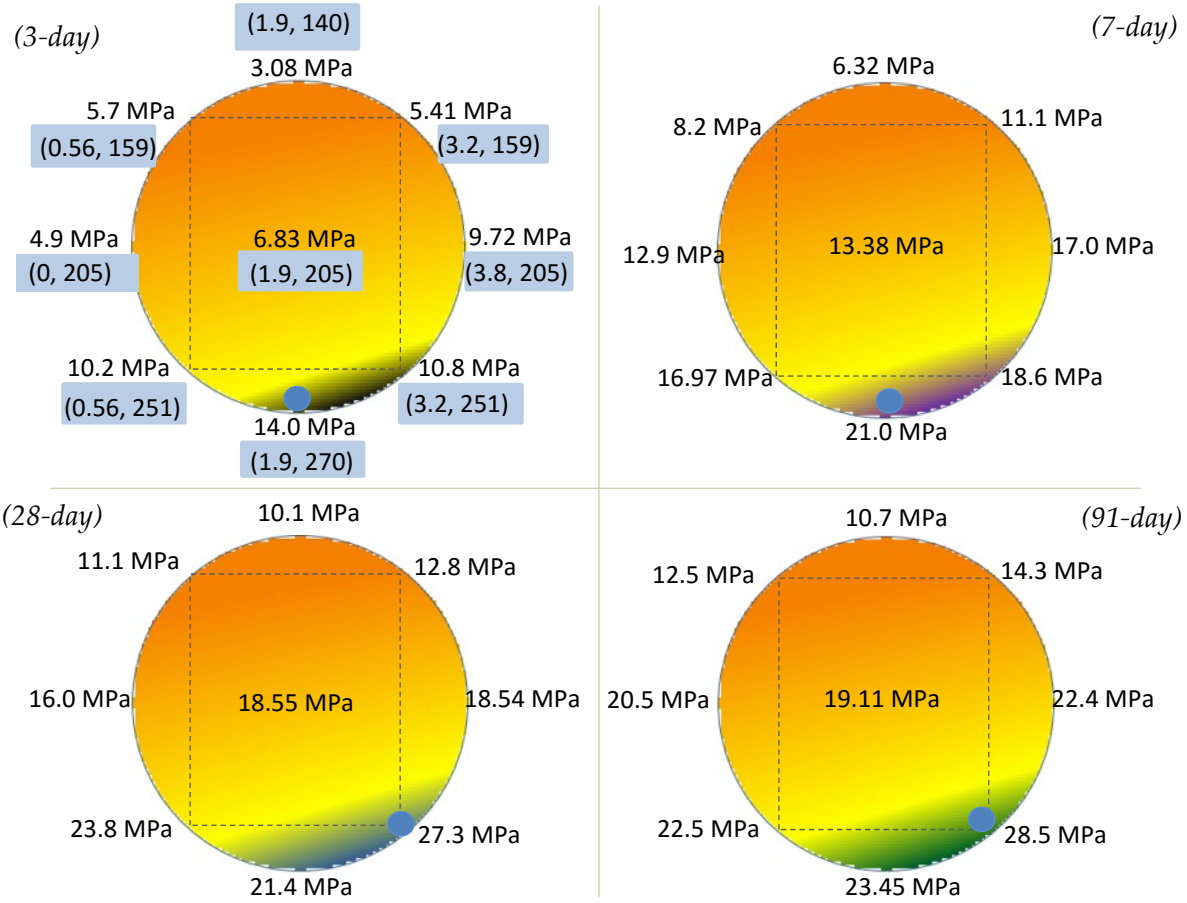


**Figure 4.2** Average compressive strength of all the sand-cement mixtures

Figure 4.2 clearly shows that, in the mix design model, the mixture which exhibits the highest compressive strength varies at different curing times. For instance, at the curing period of 3 and 7 days, the highest compressive strength exists in the mixture with the highest amount of cement (270 kg/m$^3$) and moderate amount of Rc additive (1.9 kg/m$^3$). But when the curing time increases, the highest compressive strength steadily shifts to the mixture with a lower cement content (251 kg/m$^3$) and a higher Rc content (3.2 kg/m$^3$). And one can see that the highest compressive strength at 28 and 91 days is both observed to be in the mixture (3.2, 251) (shown as the blue dot). In addition to this, the highest compressive strengths (indicated by the dark color areas) obtained from the estimation model are always in a mixture between (1.9, 270) and (3.2, 251) which have relatively high Rc and cement contents.

Moreover, at different cement content levels, the improvement caused by Rc additive is observed to be variable. For instance, for the mixtures with cement content 205 kg/m$^3$, the compressive strength at 3 days is increased nearly by 50% by adding Rc 3.8 kg/m$^3$ which indicates that use of Rc leads to a higher early strength, but when the curing continues to 91 days these three mixtures with variable Rc contents exhibit almost the same compressive strength and the 91-day strength is even slightly lower in the mixture with Rc content 1.9 kg/m$^3$. Compared with this, as the cement content increases to 251 or decreases to 159 kg/m$^3$ (8.9% or 14.1% by mass), the compressive strength of mixtures with variable Rc contents is approximately the same at 3 days, but the compressive strength at 91 days is increased by 26.7% and 15% as the Rc content rises from 0.56 to 3.2 kg/m$^3$.

The curing time is another important factor contributing to the properties of cement stabilized materials. Figure 4.3 illustrates the compressive strength of all the sand-cement mixtures as a function of the curing time. Each value represents the average compressive strength of the three tested specimens.

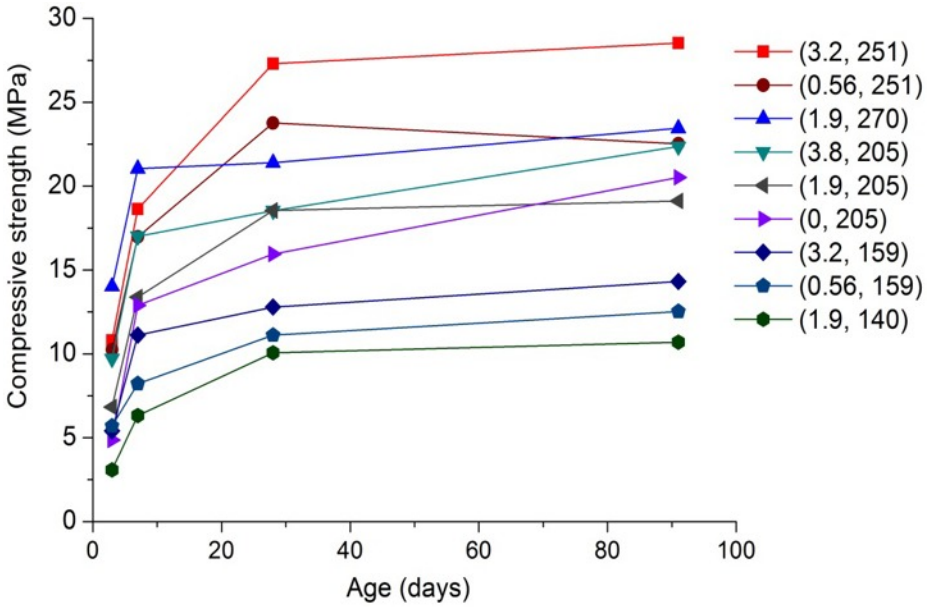


**Figure 4.3** Average compressive strength of sand-cement mixtures at different curing times

In Figure 4.3 it can be seen that the compressive strength increases substantially from 3 to 7 days, and then steadily increases until 28 days, but after 28 days the compressive strength remains almost constant which is observed in most of these mixtures. Nevertheless, variations occur in the curing period from 28 to 91 days. For instance, the compressive strength of mixture (0.56, 251) exhibits a slight decrease and the mixtures (0, 205) and (3.8, 205) exhibit an increase from 28 to 91 days.

Additionally, the mixture (1.9, 140) which has the lowest cement content exhibits the lowest compressive strength at all curing times. However, the highest amount of cement content in the mixture (1.9, 270) only leads to the highest early age strength within 7 days, while the 28-day and 91-day compressive strengths of this mixture are much lower than those of the mixture (3.2, 251) which has a higher Rc content and a lower cement content.

### 4.1.3 Estimation model of compressive strength

The variable factors evaluated in this research include the cement and Rc contents, density and curing time. Among these variables, the cement and Rc contents as well as the curing time are independent factors, while the density of different mixtures is mainly generated by different cement contents.

***(1) Influence of cement and Rc contents on the compressive strength***

Estimation models are obtained by firstly considering the effect of the mix variables at each curing time and then obtaining an overall models including the influence of curing time. Figure 4.4 shows the estimation models with combined effects of cement and Rc contents and density, which is based on all the tested mixtures at a curing period of 7 days. In this study, C, Rc and D represent the cement content, additive content and density of the specimen, respectively.

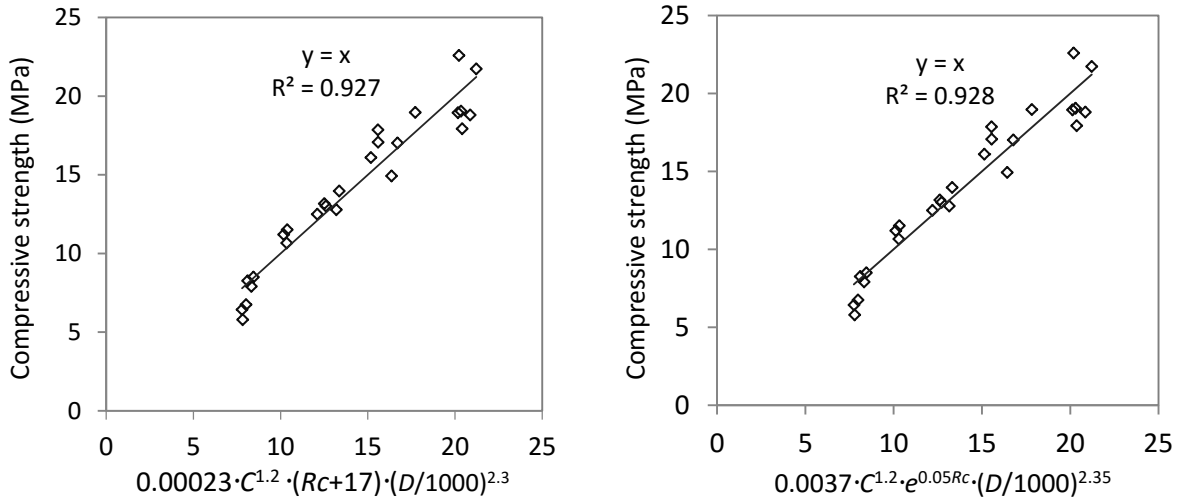


(a) Linear correlation (b) Exponential function

**Figure 4.4** Estimation models considering cement and Rc contents and density

In Figure 4.4 the influence of the Rc content is evaluated by two types of functions: linear and exponential relations, which can be described as follows:

$$UCS\ (7\text{d}) = 0.00023 \cdot C^{1.2} \cdot (Rc + 17) \cdot \left(\frac{D}{1000}\right)^{2.3} \qquad R^2=0.927 \qquad (4\text{-}1)$$

$$UCS\ (7\text{d}) = 0.0037 \cdot C^{1.2} \cdot e^{0.05Rc} \cdot \left(\frac{D}{1000}\right)^{2.35} \qquad R^2=0.928 \qquad (4\text{-}2)$$

Where, $UCS$ is unconfined compressive strength (MPa); $C$ is cement content (kg/m$^3$); $Rc$ is additive content (kg/m$^3$); $D$ is density of specimen (kg/m$^3$).

It can be found that these two models both fit the measured data quite well. The exponential model seems slightly better and thus is chosen to be employed for the estimation models of the compressive strength. Therefore, a general estimation model with exponential effects of cement and Rc contents can be adopted for use, expressed as the following equation:

$$UCS = \text{a} \cdot C^{n_1} \cdot e^{n_2 \cdot Rc} \cdot \left(\frac{D}{1000}\right)^{n_3} \qquad (4\text{-}3)$$

With consideration of curing time, the above estimation model is subsequently applied to approximate the tested data at individual curing time, shown in Figure 4.5.

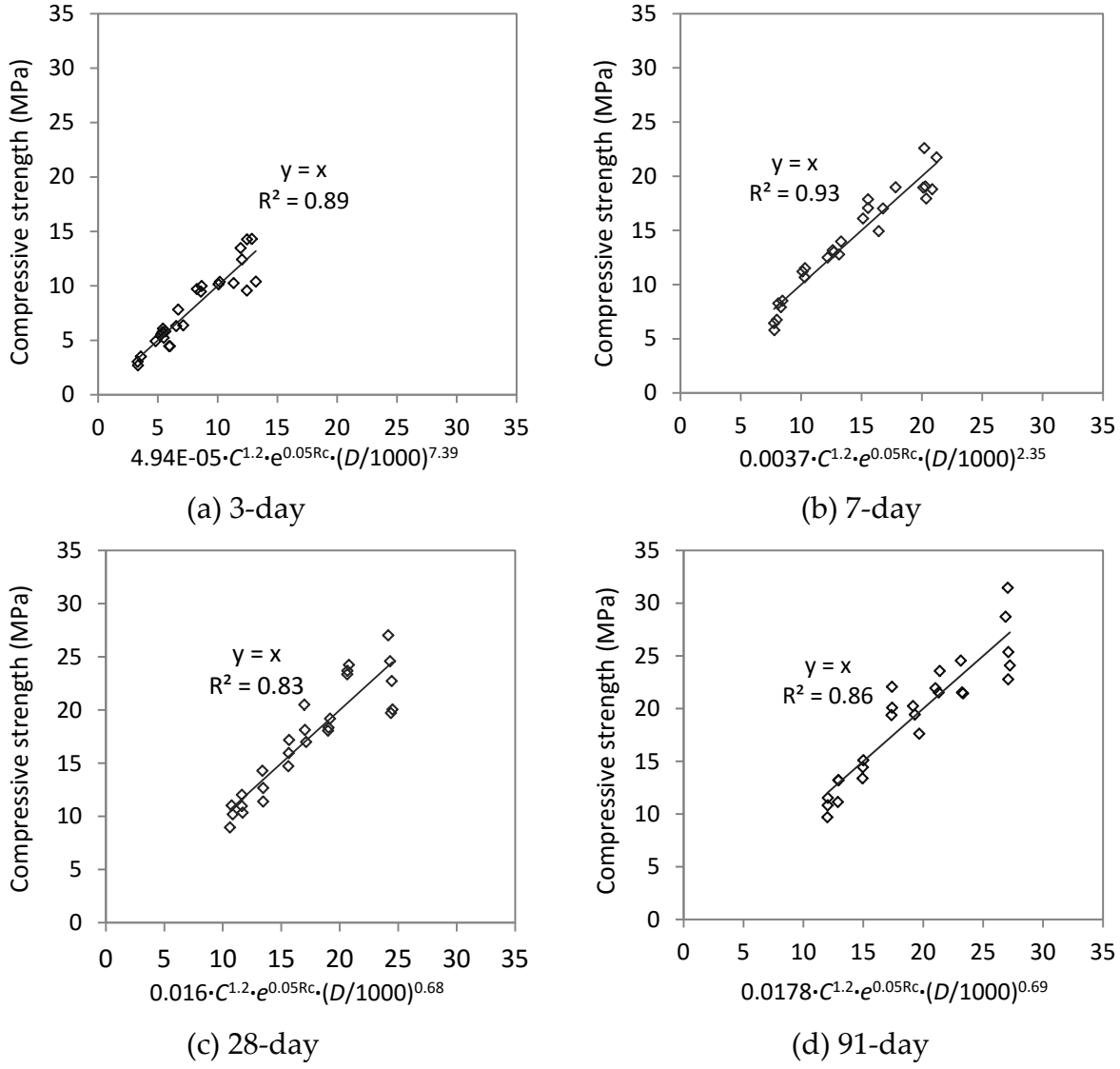


**Figure 4.5** Estimation models of compressive strength at different curing times

As shown in Figure 4.5, to achieve an acceptable $R^2$ coefficient of determination, the coefficient for each factor is variable at different curing times, which is illustrated in Table 4.1. In Table 4.1 the coefficients for the factors of cement and Rc contents exhibit constant values throughout 4 different curing times, which implies that the effects of the cement and Rc contents on the estimation models of compressive strength are not clearly correlated with the curing time. Therefore, the effects of cement and Rc contents on the compressive strength model can be expressed as the coefficients 1.2 and 0.05, respectively. In contrast, the coefficients "a" and "$n_3$" in equation (4-3) largely vary according to different curing times. So appropriate coefficients for "a" and "$n_3$" (for density) can be adjusted and obtained when incorporating the influence of the curing time.

**Table 4.1** Coefficients for the estimation models at different curing times

| Curing time | $UCS = \mathrm{a} \cdot C^{n_1} \cdot e^{n_2} \cdot (\frac{D}{1000})^{n_3}$ (4-3) | | | | |
|---|---|---|---|---|---|
| | a | $n_1$ | $n_2$ | $n_3$ | $R^2$ |
| 3-day | 0.0000494 | 1.2 | 0.05 | 7.39 | 0.88 |
| 7-day | 0.0037 | 1.2 | 0.05 | 2.35 | 0.93 |
| 28-day | 0.016 | 1.2 | 0.05 | 0.68 | 0.84 |
| 91-day | 0.0178 | 1.2 | 0.05 | 0.69 | 0.86 |

***(2) Influence of curing time on the compressive strength***

Figure 4.6 presents the estimation models for compressive strength including the influence of the curing time. The factor of curing time is evaluated by four different statistical models: log-scale, exponential, ACI and power-function models. The first three proposed models (graph a, b and c) are based on literature studies (Terrel et al., 1979; EN 199-1-1, 2005; ACI, 1998), which are previously investigated in research by Xuan (2012). Each graph includes the tested data of all the sand-cement mixtures at all evaluated curing times. These four estimation models shown in Figure 4.6 are described as the following equations:

$$UCS = 0.0084 \cdot C^{1.2} \cdot e^{0.05 \cdot Rc} \cdot \left(\frac{D}{1000}\right)^{1.5} \cdot \left(1 + 0.442 \cdot \log\left(\frac{t}{28}\right)\right) \quad R^2 = 0.86 \qquad (4\text{-}4)$$

$$UCS = 0.000126 \cdot C^{1.2} \cdot e^{0.05 \cdot Rc} \cdot \left(\frac{D}{1000}\right)^{1.5} \cdot \left(\frac{t}{0.0527 + 0.012t}\right) \quad R^2 = 0.90 \qquad (4\text{-}5)$$

$$UCS = 0.0091 \cdot C^{1.2} \cdot e^{0.05 \cdot Rc} \cdot \left(\frac{D}{1000}\right)^{1.5} \cdot e^{0.068 \cdot \left(1 - \left(\frac{28}{t}\right)^{1.155}\right)} \quad R^2 = 0.91 \qquad (4\text{-}6)$$

$$UCS = 0.004 \cdot C^{1.2} \cdot e^{0.05 \cdot Rc} \cdot \left(\frac{D}{1000}\right)^{1.5} \cdot t^{0.2} \qquad R^2 = 0.83 \qquad (4\text{-}7)$$

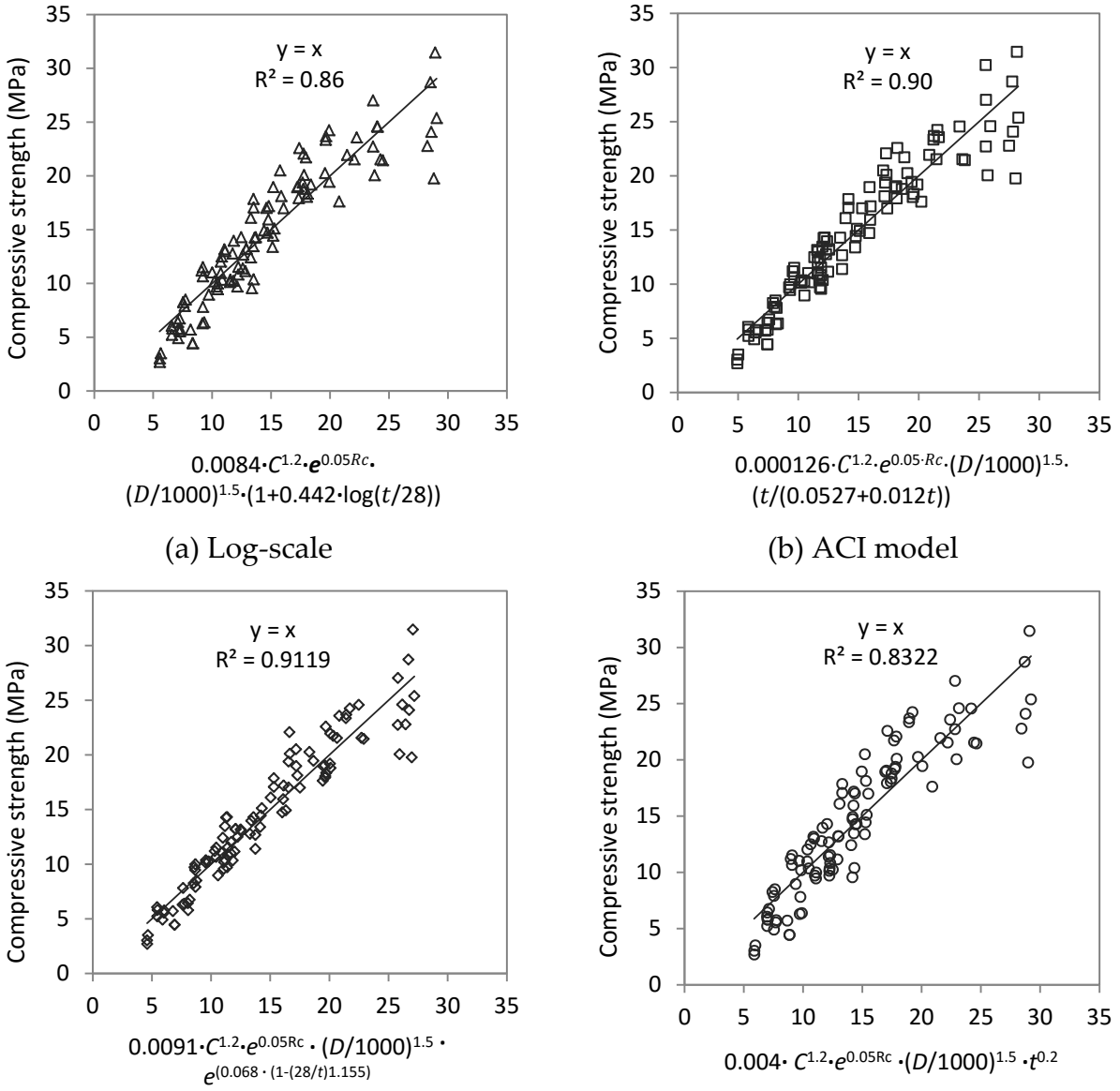


(a) Log-scale (b) ACI model

(b) Exponential model (d) Power-function model

**Figure 4.6** Estimation models of compressive strength with curing time

It can be seen that the exponential function (equation 4-6) exhibits the best fit to the real data with high $R^2$ which reaches 0.91. Therefore, the exponential model can be adopted to estimate the compressive strength of stabilized sand material with the combined effects of cement and Rc contents, density and curing time.

In order to illustrate the contribution of the cement and Rc contents in the estimation model (equation 4-6) on the compressive strength at curing time of 28 days, the response surface and contour plot are developed and shown in Figure 4.7. As can be seen from Figure 4.7 the cement content is the main controlling factor for the

compressive strength. The higher the cement content, the higher the compressive strength. Moreover, the Rc additive has an additional effect on the improvement of the compressive strength.

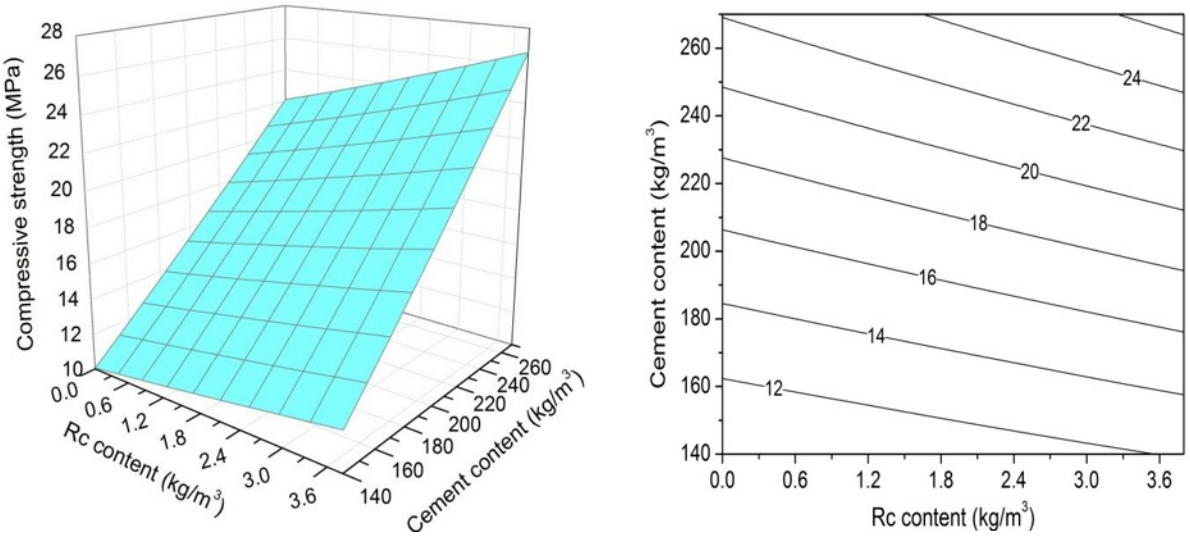


(a) Response surface (b) Contour plot

**Figure 4.7** Effect of cement and Rc contents on the compressive strength (t = 28 days)

## 4.2 Indirect tensile strength

### 4.2.1 Test condition

The indirect tensile strength test is performed by subjecting a cylindrical specimen to a compression force applied by two opposite generators (NEN-EN 13286-42). This loading configuration develops tensile stress perpendicular to the direction of the applied load, which ultimately causes the specimen to fail by splitting along the vertical diameter. It is usually required to pack strips which can be plywood or steel material along the generators in order to distribute the load to prevent local failure due to the compressive stresses at the loading point. The loading configuration is indicated in Figure 4.8.

The specimen used for indirect tensile strength test can be the same size as that for compression test and an indirect tensile strength test is easy to perform. Therefore, it is commonly adopted for use rather than direct tensile strength test which has the problems of gripping specimens (Williams, 1986). However, shortcomings of indirect tensile strength test have also been documented, for instance, it doesn't simulate the real loading condition in the field. Research (Hudson & Kennedy, 1968) also reported that the type of material used for loading strip and the width of the strip may have potential influence on the testing results especially in measurement of the vertical

deformation. However, the indirect tensile test is still considered as the appropriate test currently available for determining the tensile properties of highway materials (Hudson & Kennedy, 1968).

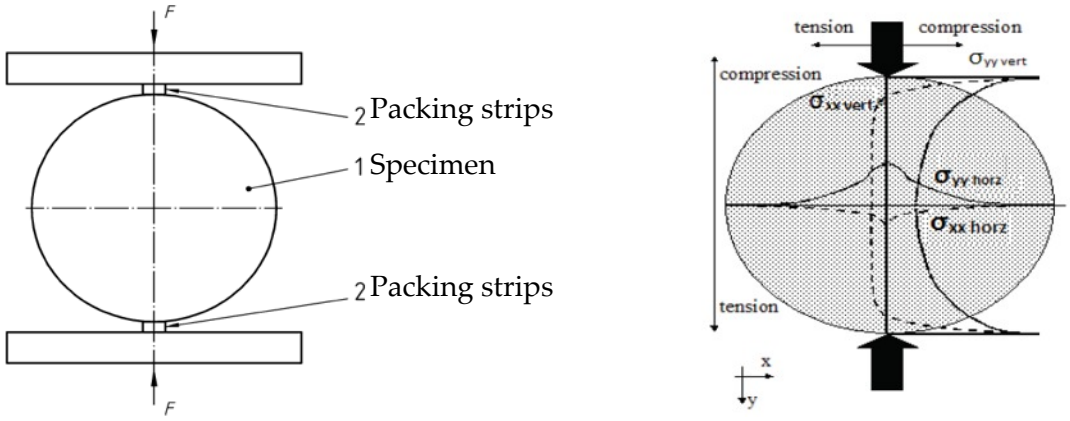


(a) Loading configuration (NEN-EN 13286-42) (b) Stress distribution

**Figure 4.8** Diagram of indirect tensile strength test

In this study, the size of the specimens used for indirect tensile strength test is Ø101.6×116.4 mm, the same as that for compression test. The specimen was loaded in the vertical axis at a constant stress rate. Two plywood strips with length 130 mm, width 20 mm and thickness 3 mm were centrally placed between specimen and the generators to distribute the load. Figure 4.9 shows the indirect tensile strength test setup and the specimen after fracture. The laboratory test data of the indirect tensile strength tests, which include all the evaluated mixtures at different curing times, are illustrated in Appendix A.

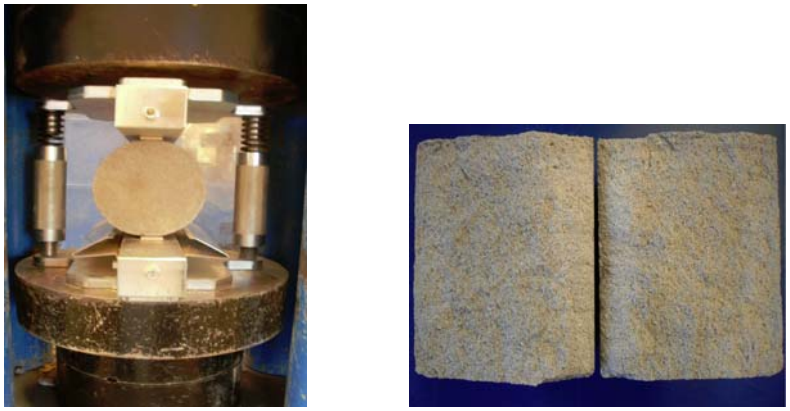

**Figure 4.9** Indirect tensile strength test setup and the specimen after failure

The indirect tensile strength is calculated from the failure force F using the following formula:

$$ITS = \frac{2F}{\pi HD} \quad (4\text{-}8)$$

Where, *ITS* is the indirect tensile strength (MPa); *F* is the failure force (N); *H* is the length of the specimen (mm); *D* is the diameter of the specimen (mm).

During testing, the failure crack propagates through the vertical diameter. According to research by Hudson and Kennedy (1968), the tension failure in the indirect tensile strength test is caused by the tensile stress acting perpendicular to the loaded diameter. The fracture is initiated along the loaded diameter and propagates through the interface between matrix and the sand particles. On the basis of the literature (Xuan, 2012; Hudson & Kennedy, 1968), the failure pattern in the indirect tensile strength test depends on the mix components and thus failure originates either through the matrix such as the bonding layer between aggregate particles or through crushing the granular particles.

### 4.2.2 Test data and analysis with variable factors

The indirect tensile strength test results for each mix design are presented together with the mix design, shown in Figure 4.10. It covers the indirect tensile strength results for all the mixtures at different curing times and each data indicates the average value of three specimens. The blue dot represents the mix design which produces the highest indirect tensile strength at each curing time. Meanwhile, similar to the analysis of compressive strength, the indirect tensile strength based on the estimation model (equation 4-13) (discussed later in this section) is also shown herein and the dark color areas (black for 3 days, purple for 7 days, blue for 28 days and green for 91 days) indicate the indirect tensile strength higher than 1, 1.5, 2 and 2.2 MPa, respectively.

As shown in Figure 4.10, the indirect tensile strength exhibits a similar pattern as the compressive strength. The curing time affects the mixture which achieves the highest indirect tensile strength. It can be seen that the mixture with Rc additive 1.9 kg/m$^3$ and highest amount of cement achieves the highest 3-day indirect tensile strength, but as the curing time rises to 91 days, the highest strength value is obtained for the mixture (3.2, 251) with a higher Rc content and a lower cement content. Among all these mixtures, the highest indirect tensile strength values always occur in the mixtures between (1.9, 270) and (3.2, 251) (shown in the dark color area) and the

highest strength from testing also occurs in this range. This finding is consistent with the compressive strength.

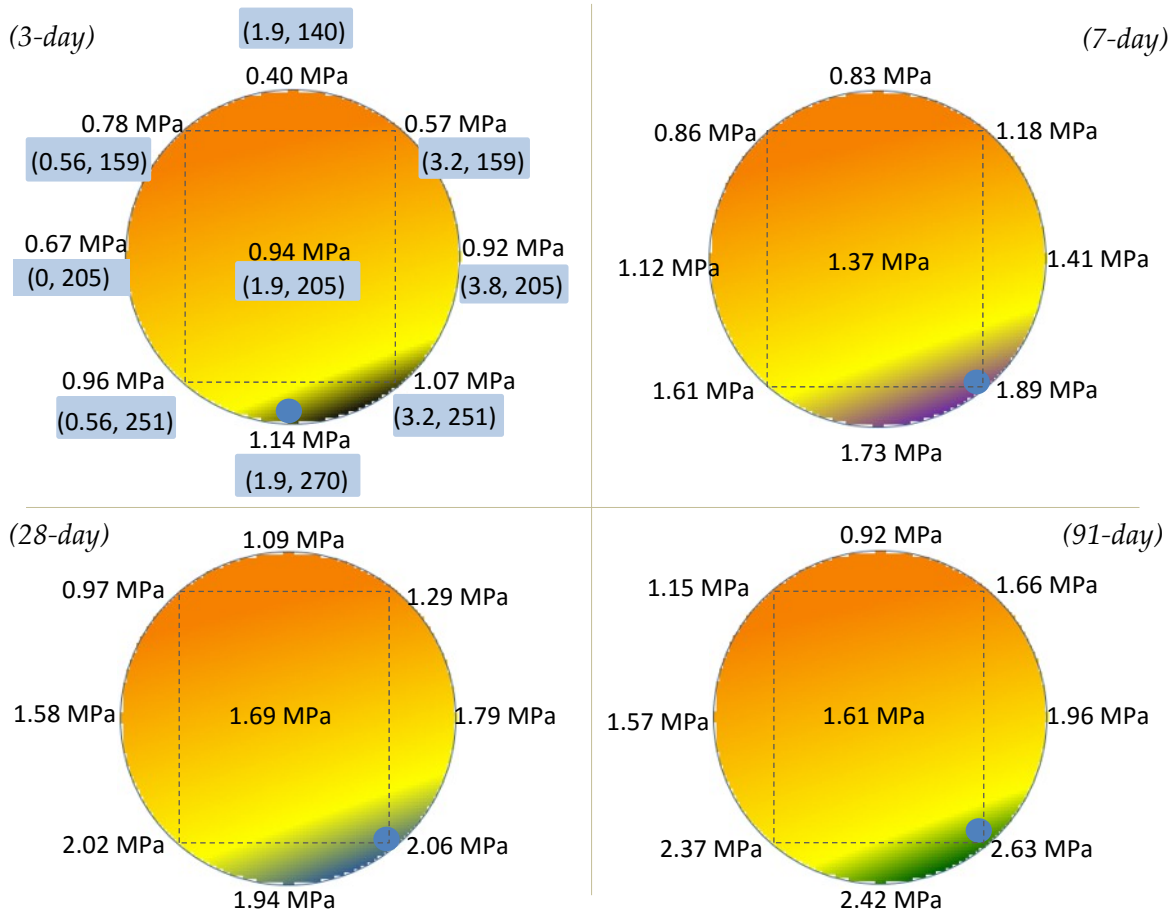


**Figure 4.10** Average indirect tensile strength of all the sand-cement mixtures

It can also be seen that the mixtures with higher Rc contents (indicated in the right side of the mix design) generally exhibit a higher indirect tensile strength at all curing times. Regarding the influence of cement, it can be observed that the indirect tensile strength significantly increases as the cement content increases (the cement content is increasing in the vertical direction), which is also documented in literature studies (Kolias et al., 2005; Consoli et al., 2011).

With respect to the influence of the curing time, Figure 4.11 gives the development of indirect tensile strength of all tested sand-cement mixtures as a function of the curing time.

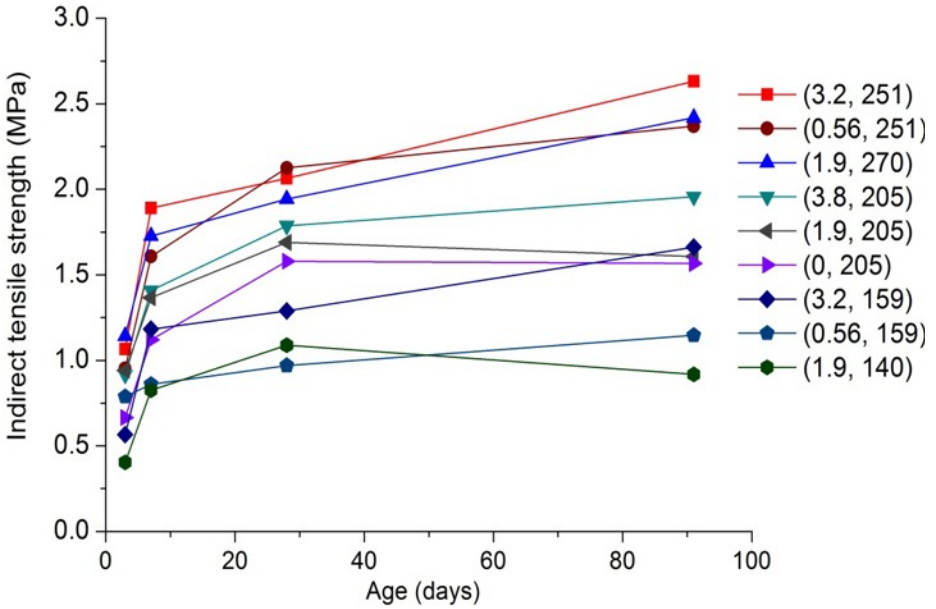


**Figure 4.11** Indirect tensile strength of sand-cement mixtures at different curing times

In Figure 4.11 it can be seen that the relation of the indirect tensile strength with the curing time is similar to that of the compressive strength (see Figure 4.3). The indirect tensile strength substantially increases from 3 days to 7 days. For instance, for most of the mixtures the 7-day strength is at least 50% higher than the 3-day strength and in some mixtures, such as mixtures (3.2, 159) and (3.2, 251), the 7-day strength is even almost two times higher than the 3-day strength. But when the curing time increases from 28 days to 91 days, the trend of the indirect tensile strength development considerably varies for the different mixtures. For instance, mixtures with cement content 159 and 251 kg/m$^3$ all showed a 10~30% higher indirect tensile strength, but the rest of the mixtures exhibited either constant or slightly decreased 91-day strength. Again, mixture (3.2, 251) with a relatively high Rc content achieves the highest indirect tensile strength at 91 days and the mixture with the lowest amount of cement shows the lowest indirect tensile strength at 91 days.

### 4.2.3 Estimation model of indirect tensile strength (ITS)

***(1) Influence of cement and Rc contents on the indirect tensile strength***

Similar to the compressive strength, the estimation of the indirect tensile strength is also investigated in different statistical models. With respect to the influence of the Rc content, both linear and exponential models are evaluated, shown in Figure 4.12.

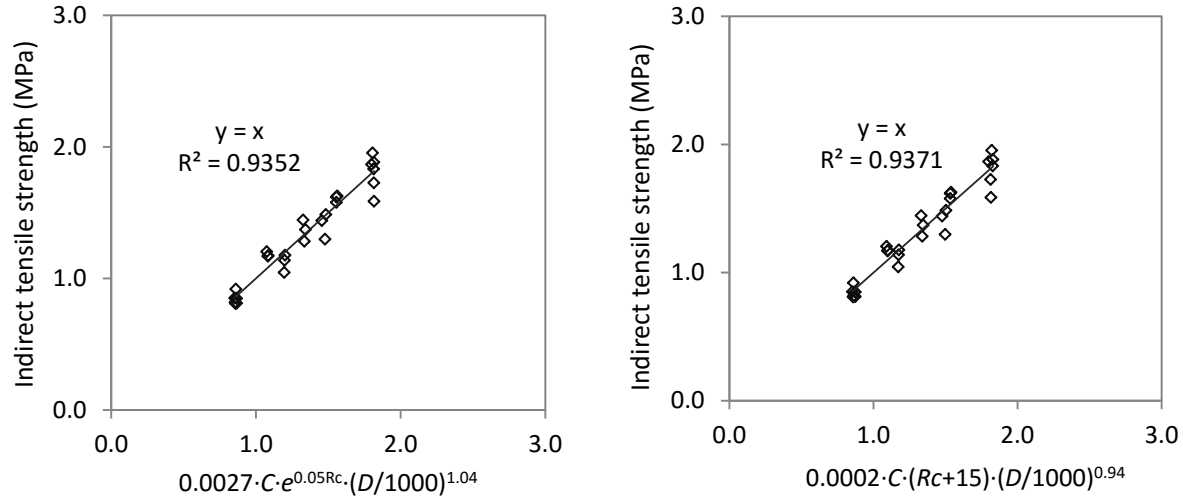


(a) Exponential function (b) Linear correlation

**Figure 4.12** Estimation models of indirect tensile strength with effects of cement and Rc contents and density (t = 7 days)

The models indicated in Figure 4.12 are expressed as the following equations:

$$ITS = 0.0027 \cdot C \cdot e^{0.05Rc} \cdot (\frac{D}{1000})^{1.04} \qquad R^2 = 0.935 \qquad (4\text{-}9)$$

$$ITS = 0.0002 \cdot C \cdot (Rc + 15) \cdot (\frac{D}{1000})^{0.94} \qquad R^2 = 0.937 \qquad (4\text{-}10)$$

Where, $ITS$ is indirect tensile strength (MPa); $C$ is cement content (kg/m$^3$); $Rc$ is additive content (kg/m$^3$); $D$ is density of specimen (kg/m$^3$).

In Figure 4.12 it can be observed that, these two models both approximate the test data quite well. Both models have a $R^2$ value 0.94, which implies that satisfactory estimation models are achieved. In order to stay consistent with the estimation model of the compressive strength, the exponential function of the Rc content is also chosen for the indirect tensile strength.

Figure 4.13 shows the estimation models of the indirect tensile strength at different curing times by utilizing the exponential function for the Rc content. The coefficients of these estimation models are summarized in Table 4.2. In Table 4.2 it can be seen that the coefficients of cement and Rc contents for estimation models of indirect tensile strength both exhibit constant values regardless of the curing time, which is similar to the estimation models of the compressive strength. Nevertheless, the curing time greatly influences the coefficients of "a" and "$n_3$" (for density D). Therefore, the coefficients of "$n_1$" and "$n_2$" can be fixed as 1 and 0.05, respectively, while "a" and "$n_3$" will be optimized by incorporating the effect of curing time.

**Table 4.2** Coefficients for the estimation models of indirect tensile strength

| Curing time | $ITS = \mathrm{a} \cdot C^{n_1} \cdot e^{n_2 \cdot Rc} \cdot \left(\frac{D}{1000}\right)^{n_3}$ | | | | |
|---|---|---|---|---|---|
| | a | $n_1$ | $n_2$ | $n_3$ | $R^2$ |
| 3-day | 0.001 | 1 | 0.05 | 1.71 | 0.77 |
| 7-day | 0.0027 | 1 | 0.05 | 1.04 | 0.94 |
| 28-day | 0.0053 | 1 | 0.05 | 0.416 | 0.80 |
| 91-day | 0.00083 | 1 | 0.05 | 3.11 | 0.86 |

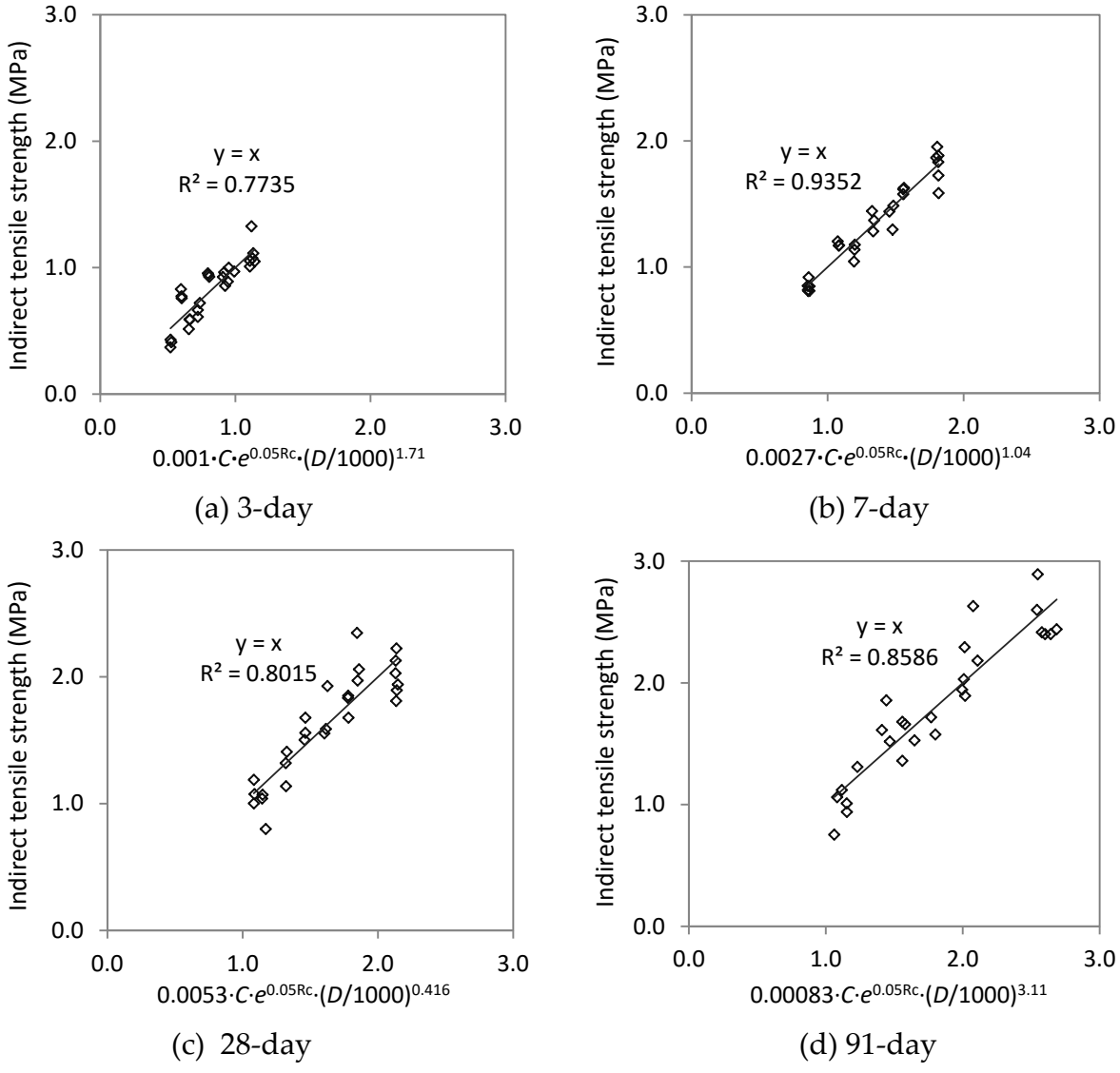


**Figure 4.13** Estimation models of indirect tensile strength at different curing times

***(2) Influence of curing time on the indirect tensile strength***

The influence of the curing time on the estimation model of indirect tensile strength is also verified by four proposed statistical models which are used previously for

estimating the compressive strength. Figure 4.14 presents the test data and the approximation models for indirect tensile strength. The following figures are based on the laboratory test results on all evaluated sand-cement mixtures covering all curing times.

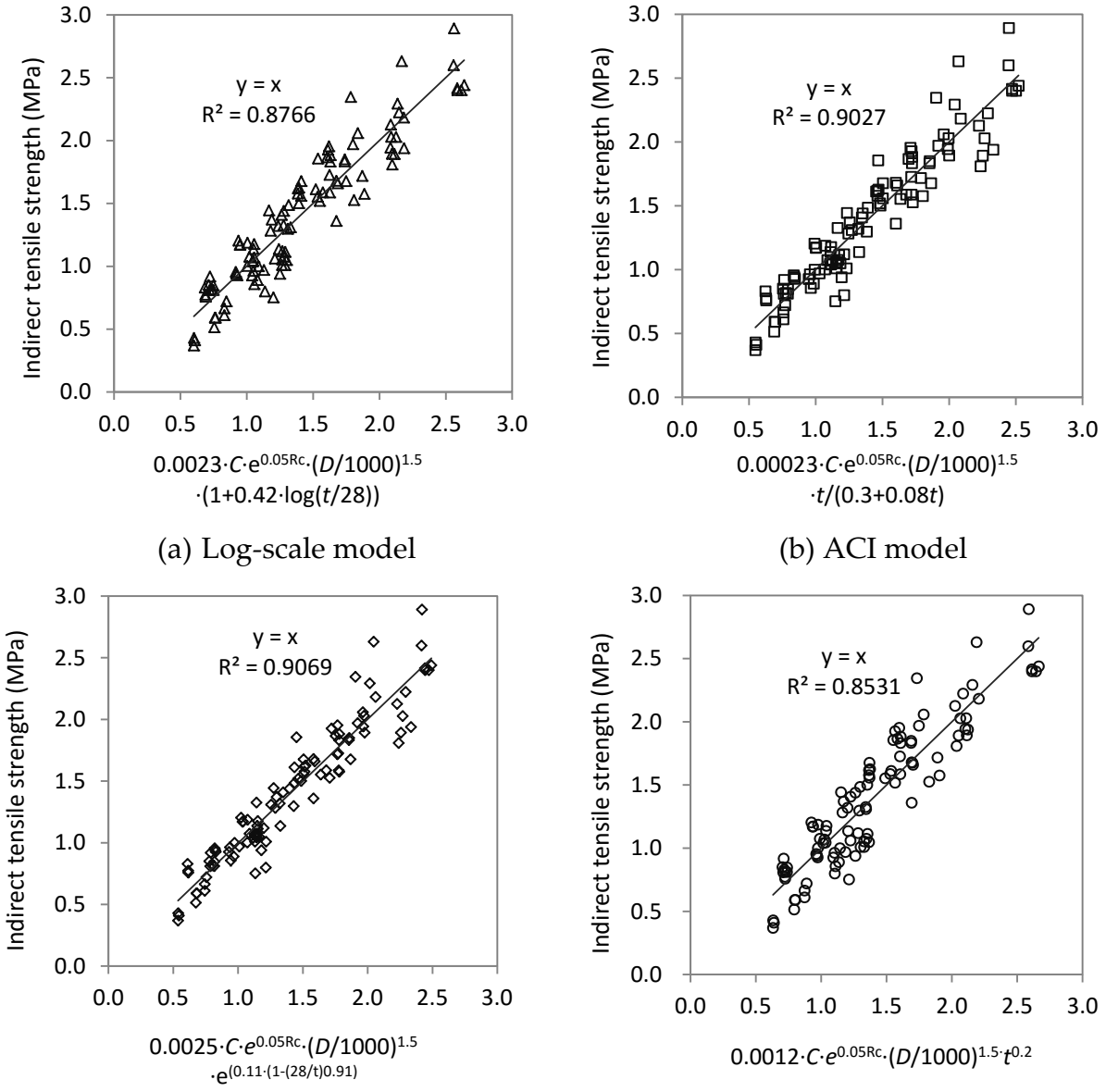


(a) Log-scale model (b) ACI model

(c) Exponential model (d) Power-function model

**Figure 4.14** Estimation models of indirect tensile strength with influence of curing time

The estimation models of indirect tensile strength shown in Figure 4.14 can be described as follows:

$$ITS = 0.0023 \cdot C \cdot e^{0.05Rc} \cdot \left(\frac{D}{1000}\right)^{1.5} \cdot \left(1 + 0.42 \cdot \log\left(\frac{t}{28}\right)\right) \qquad R^2 = 0.88 \qquad (4\text{-}11)$$

$$ITS = 0.00023 \cdot C \cdot e^{0.05Rc} \cdot \left(\frac{D}{1000}\right)^{1.5} \cdot \left(\frac{t}{0.3+0.08t}\right) \qquad R^2 = 0.90 \qquad (4\text{-}12)$$

$$ITS = 0.0025 \cdot C \cdot e^{0.05Rc} \cdot \left(\frac{D}{1000}\right)^{1.5} \cdot e^{0.11\left(1-\left(\frac{28}{t}\right)^{0.91}\right)} \qquad R^2 = 0.91 \qquad (4\text{-}13)$$

$$ITS = 0.0012 \cdot C \cdot e^{0.05Rc} \cdot \left(\frac{D}{1000}\right)^{1.5} \cdot t^{0.2} \qquad R^2 = 0.85 \qquad (4\text{-}14)$$

Obviously, the exponential model with $R^2 = 0.91$ shows the best approximating trend and thus it can be utilized for prediction of indirect tensile strength of cement stabilized sand materials. These estimation models indicate that the indirect tensile strength of cement stabilized sand material is positively correlated to the cement and Rc contents, the density of the specimen as well as the curing time.

To illustrate the influence of cement and Rc contents on the indirect tensile strength the response surface and contour plot are developed, shown in Figure 4.15. This model is based on the estimation model (equation 4-13) at curing period of 28 days.

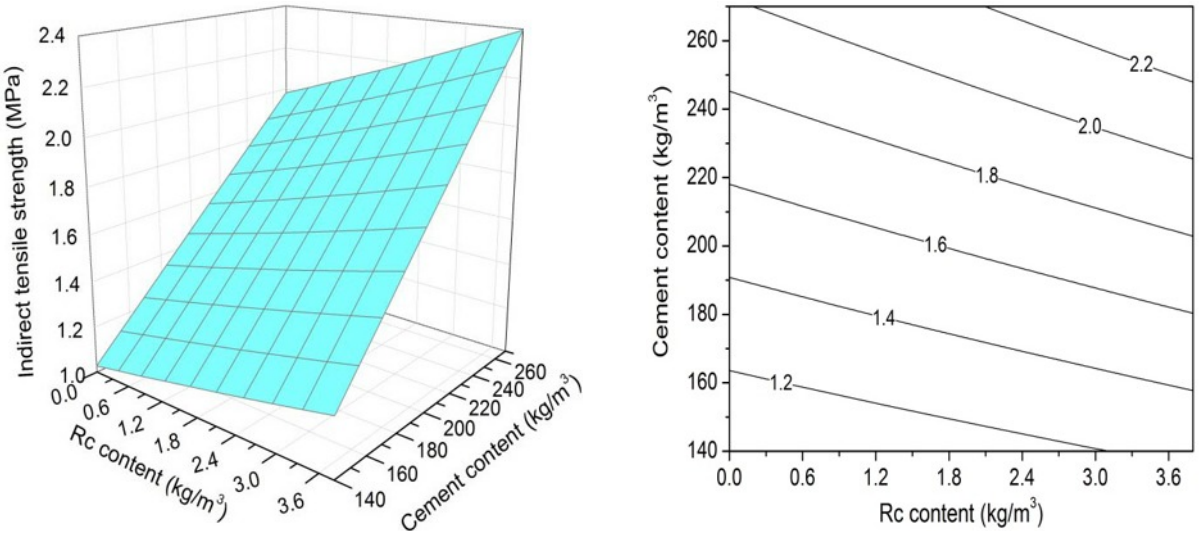


(a) Response surface (b) Contour plot

**Figure 4.15** Influence of cement and Rc contents on the indirect tensile strength of cement stabilized sand (t = 28 days)

In Figure 4.15 it can be observed that the cement content significantly promotes the increase of the indirect tensile strength. Also the Rc content improves the indirect tensile strength. Besides, by comparing the lines in the contour plots of Figure 4.7 and Figure 4.15 it can be noted that the Rc additive has a similar influence on the indirect tensile strength and the compressive strength.

## 4.3 Flexural tensile strength

### 4.3.1 Test condition

The flexural tensile strength is measured by monotonic three-point bending test which applies a load through upper and lower rollers. Compared with the indirect tensile strength test, the flexural test has certain advantage of simulating the manner in which a pavement layer is deflected by wheel-loading (Williams, 1986). For this bending test, the size of specimen is 160 × 40 × 40 mm. The beam specimen was simply supported and subjected to a single concentrated load at the midpoint at a constant loading rate of 0.05 MPa per second, shown in Figure 4.16. The loading span I is 120 mm.

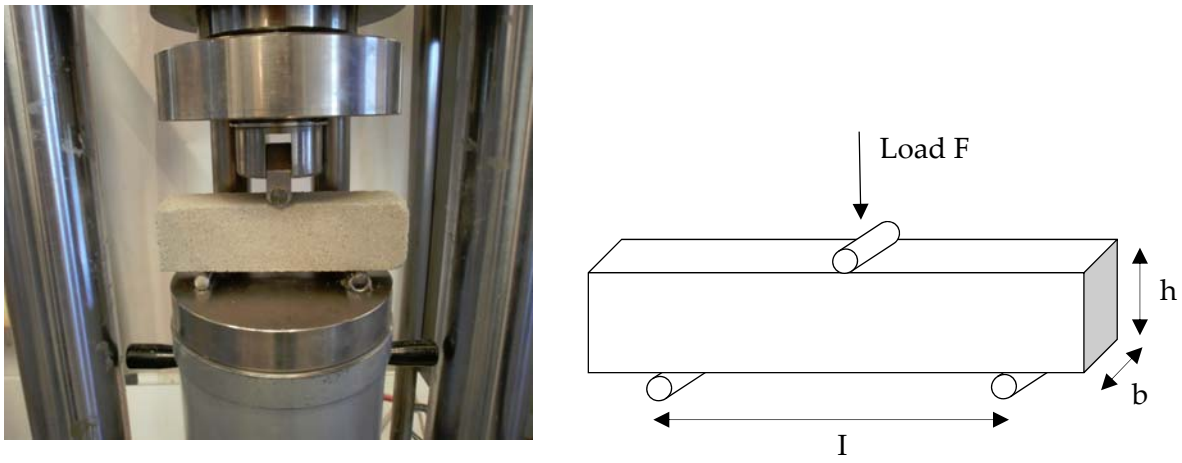


**Figure 4.16** Flexural tensile strength test

The flexural tensile strength is calculated by the following equation:

$$FTS = \frac{3FI}{2bh^2} \tag{4-15}$$

Where, $FTS$ is the flexural tensile strength from three-point bending test (N/mm$^2$); $F$ is the maximum load (N); $I$ is the supporting span (mm); $b$ is the width of the test beam (mm); $h$ is the height of the test beam (mm).

The flexural tensile strength is calculated by the standard flexure formula using the dimensions of the beam and the applied load at the moment when the beam fails. This formula, however, assumes that stress is proportional to the distance from the neutral axis which assumes a linear elastic behaviour under compression and tension (Hudson & Kennedy, 1968; Williams, 1986). Because it is easy to conduct and the loading conditions are similar to the field condition of the pavement layer, this test is favoured for use (Hudson & Kennedy, 1968).

### 4.3.2 Test data and analysis with variable factors

The test data of the flexural tensile strength tests on all stabilized sand mixtures is presented in Appendix A. Similar to the analysis of the compressive strength and the indirect tensile strength, the results of the flexural tensile strength are also represented together with the mix design, given in Figure 4.17. Each data is the average value of three tested prismatic specimens and the blue dot represents the mixture which exhibits the highest flexural tensile strength at each curing time. Again, the results derived from the estimation model of flexural tensile strength (based on equation 4-20) are indicated herein in Figure 4.17. The dark color areas, black for 3 days, purple for 7 days, blue for 28 days and green for 91 days, represent the flexural tensile strength higher than 2.5, 3, 3.5 and 4 MPa, respectively.

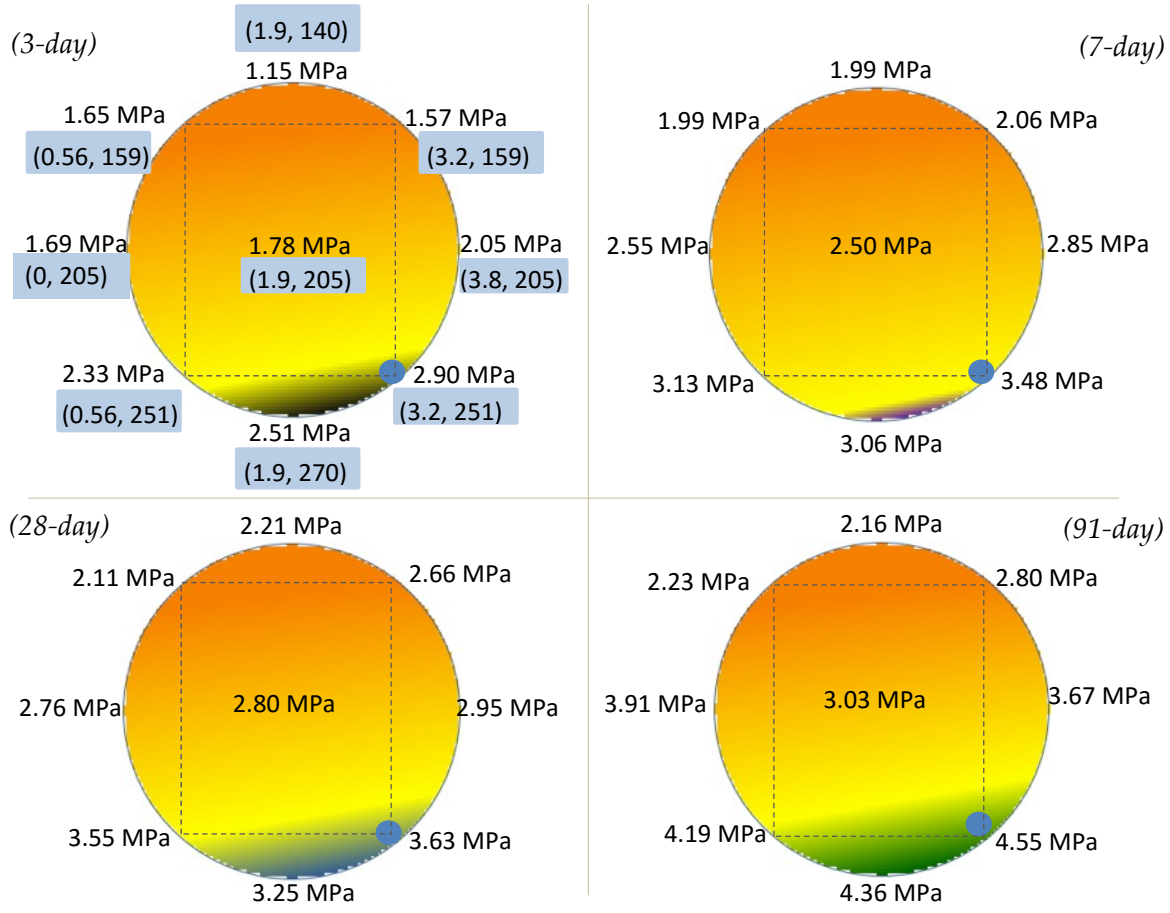


**Figure 4.17** Average flexural tensile strength of all the sand-cement mixtures

In Figure 4.17 the highest flexural tensile strength from the test data is always found in the mixture (3.2, 251) at all curing times. Whereas, based on the estimation model, the mixtures to obtain the highest flexural tensile strength is in the range from (3.2, 251) to (1.9, 270) (indicated by the dark colors). Again, for the mixtures with cement content 159 and 251 kg/m$^3$, increasing the Rc content can contribute to a higher

flexural tensile strength. For instance, the 91-day strength of the mixtures with these two cement contents increases approximately by 25% and 9%, respectively, by adding more Rc additive.

Figure 4.18 presents the flexural tensile strength of all stabilized sand mixtures correlated to the curing age. As can be seen from Figure 4.18, the flexural tensile strength shows a significant increase within 7 days mainly due to the rapid cement hydration in the early age. But the flexural tensile strength at 28 days is generally only slightly higher than the 7-day strength and some mixtures showed almost the same strength at 28 days. But after 28 days, some of the mixtures showed an increase in flexural tensile strength around 30% until 91 days and the other mixtures showed a constant strength at 91 days.

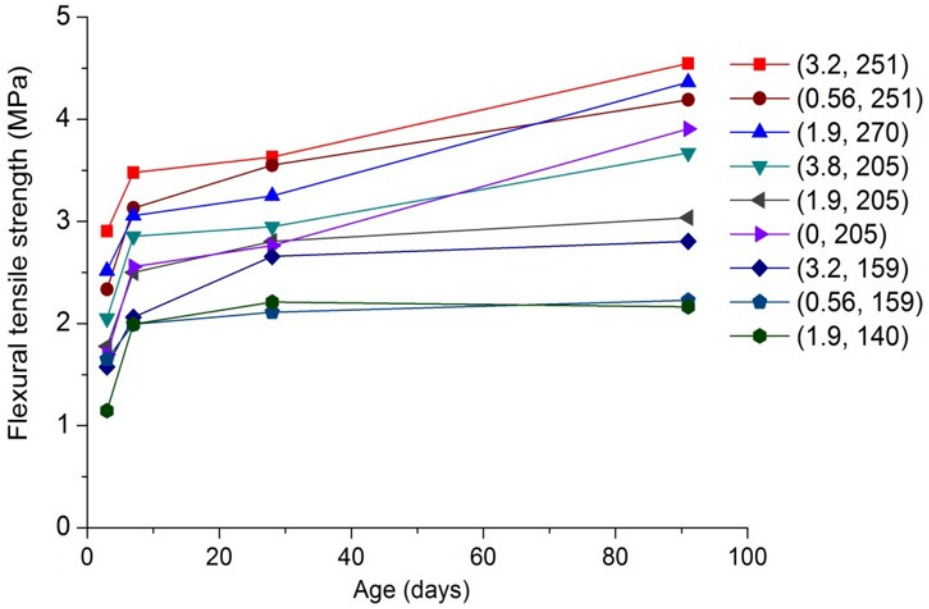


**Figure 4.18** Flexural tensile strength of sand-cement mixtures at different ages

### 4.3.3 Estimation model of flexural tensile strength (FTS)

Estimation of the flexural tensile strength follows the same procedure as applied on the compressive and the indirect tensile strength.

***(1) Influence of cement and Rc contents on the flexural tensile strength***

Figure 4.19 shows the estimation models of flexural tensile strength with consideration of the effect of cement and Rc contents. Again, two different models are assessed on the factor of Rc contents.

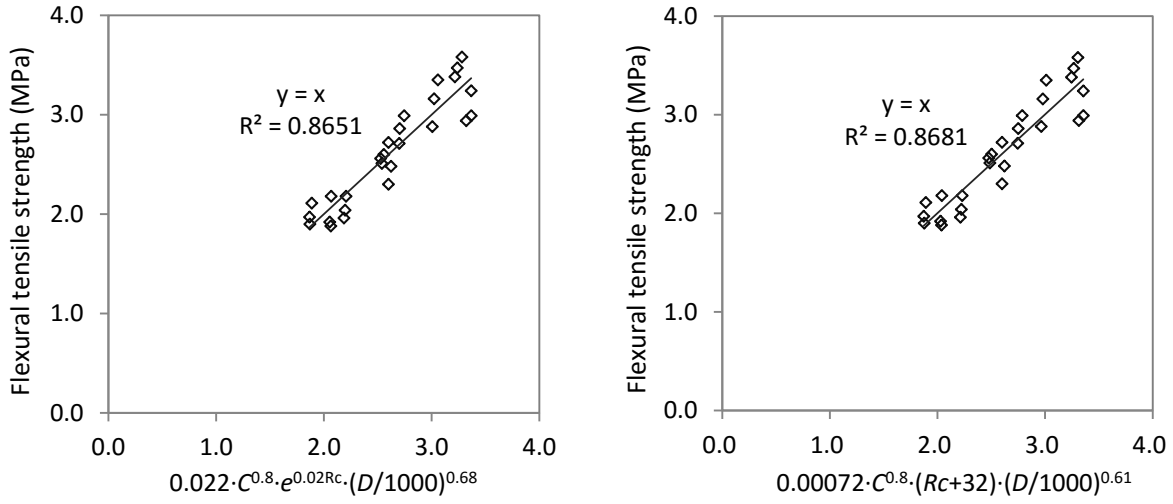


(a) Exponential function (b) Linear correlation

**Figure 4.19** Estimation models of *FTS* under effects of cement and Rc contents (t = 7days)

The models indicated in Figure 4.19 are expressed as the following equations:

$$FTS = 0.022 \cdot C^{0.8} \cdot e^{0.02Rc} \cdot (\frac{D}{1000})^{0.68} \qquad R^2 = 0.865 \qquad (4\text{-}16)$$

$$FTS = 0.00072 \cdot C^{0.8} \cdot (Rc + 32) \cdot (\frac{D}{1000})^{0.61} \qquad R^2 = 0.868 \qquad (4\text{-}17)$$

Where, $FTS$ is flexural tensile strength (MPa); $C$ is cement content (kg/m$^3$); $Rc$ is additive content (kg/m$^3$); $D$ is density of specimen (kg/m$^3$).

As shown in the equations above, the influence of the Rc content can be expressed as either an exponential or linear function. Both of these models fit the test data well. Till now it can be concluded that exponential and linear correlations can both be employed to approximate the effect of the Rc content on the mechanical strength of cement stabilized sand materials and both approximation models can achieve nearly the same $R^2$. This finding is applicable for UCS, ITS and FTS. In this study the exponential function of Rc content is mainly used in the estimation models. Figure 4.20 gives the estimation models at each curing time based on the exponential relationship of Rc.

As expected, the coefficients for each model are variable according to the different curing times, listed in Table 4.3.

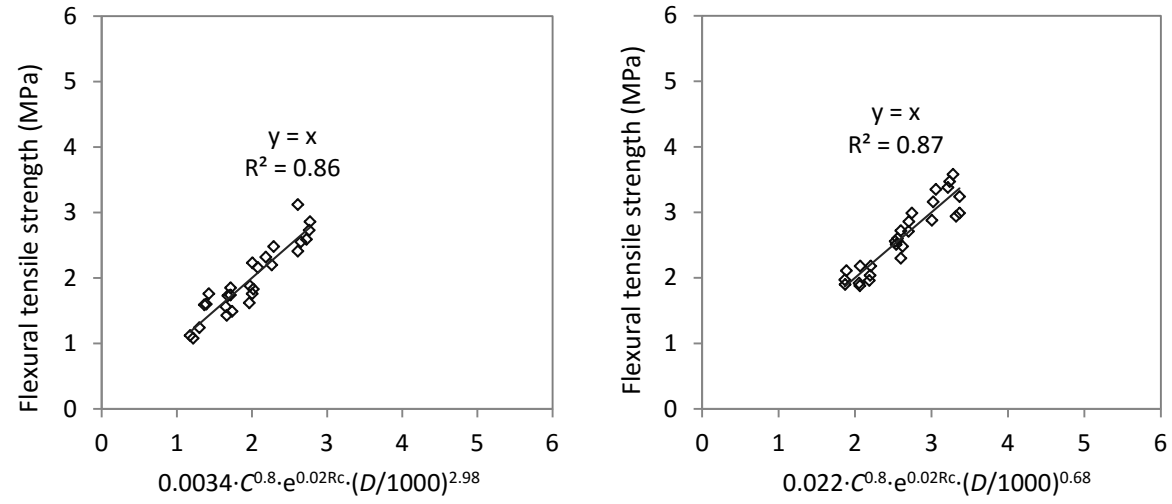


(a) 3-day (b) 7-day

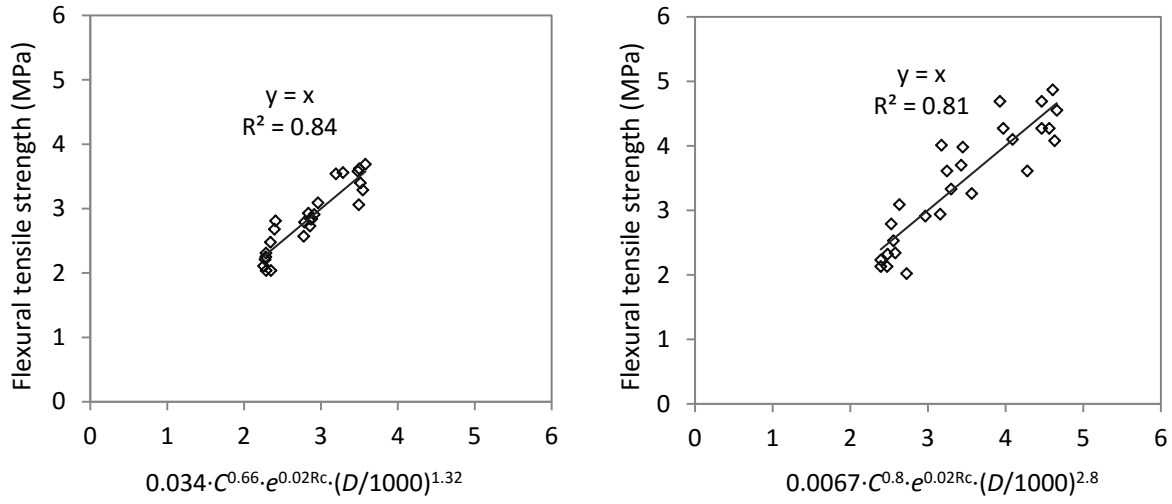


(c) 28-day (d) 91-day

**Figure 4.20** Estimation models of flexural tensile strength at different curing ages

**Table 4.3** Coefficients for the estimation models of flexural tensile strength at different ages

| Curing time | $FTS = \mathrm{a} \cdot C^{n_1} \cdot e^{n_2 \cdot Rc} \cdot (\frac{D}{1000})^{n_3}$ | | | | |
|---|---|---|---|---|---|
| | a | $n_1$ | $n_2$ | $n_3$ | $R^2$ |
| 3-day | 0.0034 | 0.80 | 0.02 | 2.98 | 0.86 |
| 7-day | 0.022 | 0.80 | 0.02 | 0.68 | 0.87 |
| 28-day | 0.034 | 0.66 | 0.02 | 1.32 | 0.84 |
| 91-day | 0.0067 | 0.80 | 0.02 | 2.8 | 0.81 |

As shown above, the coefficients for cement and Rc contents ($n_1$ = 0.8, $n_2$ = 0.02) fit the test data well at all curing times with exception of the age of 28 days ($n_1$ = 0.66, $n_2$ = 0.02). However, to obtain the estimation models comprising all the tested mixtures, the coefficients "$n_1$" and "$n_2$" are fixed as 0.8 and 0.02 at each curing time.

Additionally, the coefficients of "a" and "$n_3$" are variable and will be modified based on the influence of curing time.

***(2) Influence of curing time on the flexural tensile strength***

For estimation models of flexural tensile strength, the influence of curing time is also evaluated by four types of models. As discussed previously, these models all achieve a satisfactory approximation for compressive strength and indirect tensile strength. Figure 4.21 shows the estimation models of flexural tensile strength under the influence of curing time.

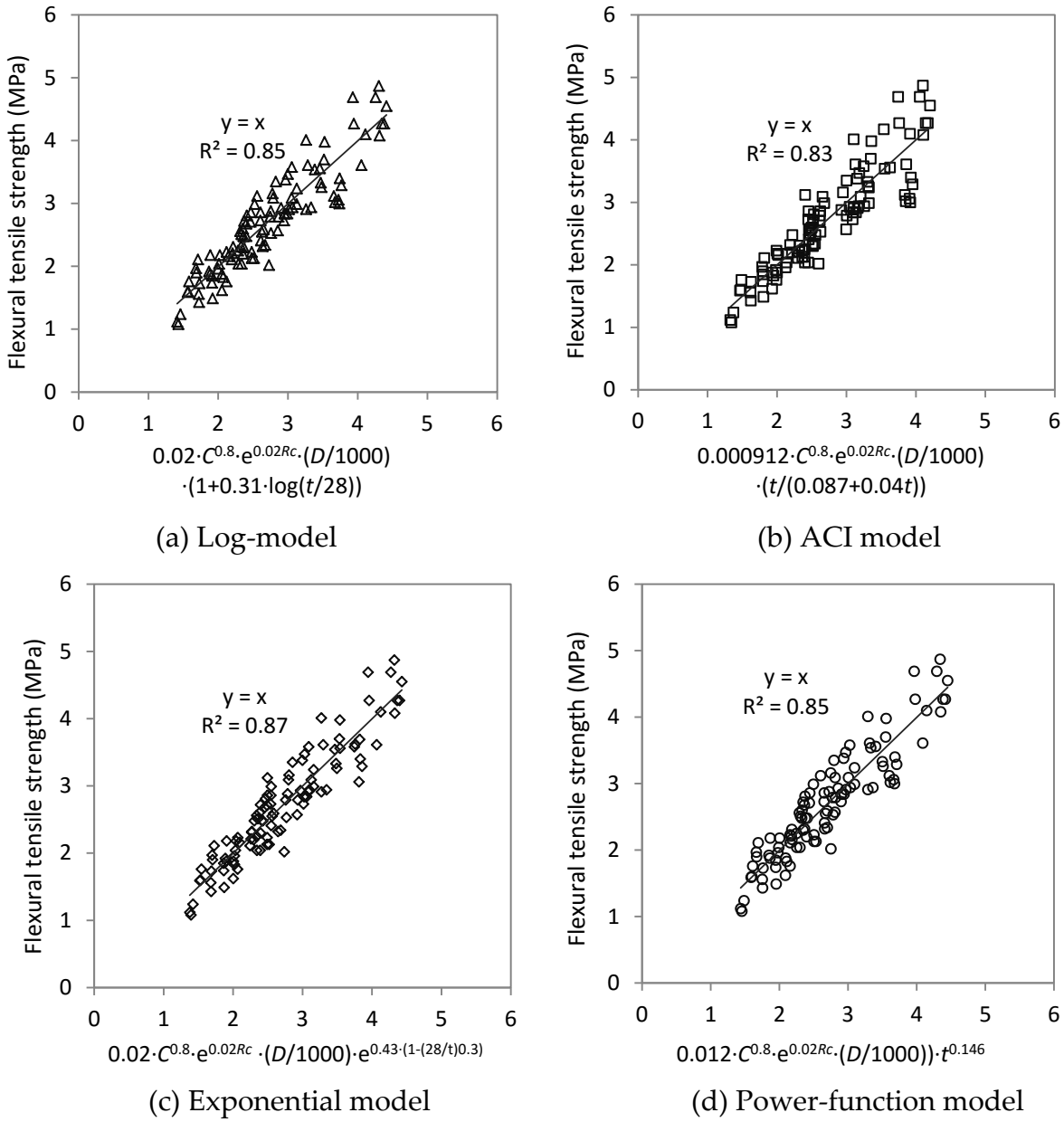


**Figure 4.21** Estimation model of flexural tensile strength with influence of curing age

As shown in Figure 4.21 the exponential model shows the best fit for the test data and all these four estimation models of flexural tensile strength are described as follows:

$$FTS = 0.02 \cdot C^{0.8} \cdot e^{0.02Rc} \cdot \left(\frac{D}{1000}\right) \cdot \left(1 + 0.31 \cdot \log\left(\frac{t}{28}\right)\right) \qquad R^2 = 0.85 \qquad (4\text{-}18)$$

$$FTS = 0.000912 \cdot C^{0.8} \cdot e^{0.02Rc} \cdot \left(\frac{D}{1000}\right) \cdot \frac{t}{0.087 + 0.04t} \qquad R^2 = 0.83 \qquad (4\text{-}19)$$

$$FTS = 0.02 \cdot C^{0.8} \cdot e^{0.02Rc} \cdot \left(\frac{D}{1000}\right) \cdot e^{0.43 \cdot \left(1 - \left(\frac{28}{t}\right)^{0.3}\right)} \qquad R^2 = 0.87 \qquad (4\text{-}20)$$

$$FTS = 0.012 \cdot C^{0.8} \cdot e^{0.02Rc} \cdot \left(\frac{D}{1000}\right) \cdot t^{0.146} \qquad R^2 = 0.85 \qquad (4\text{-}21)$$

Compared with the estimation models of compressive strength and indirect tensile strength, the $R^2$ value of flexural tensile strength is somewhat lower. Effects of cement and Rc contents on the flexural tensile strength are indicated by response surface and contour plot (based on the model 4-20), shown in Figure 4.22. In Figure 4.22 it can be clearly found that the rise of cement content can considerably increase the flexural tensile strength. Moreover, addition of Rc also leads to the higher flexural tensile strength. Again, the Rc additive has an additional effect on the improvement of flexural tensile strength.

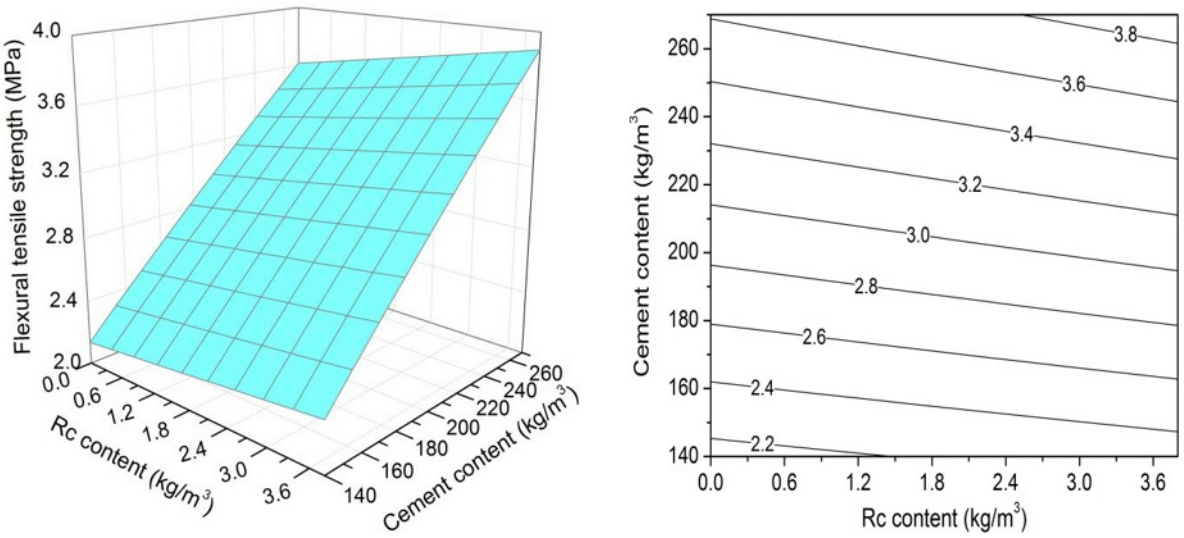


(a) Response surface (b) Contour plot

**Figure 4.22** Influence of cement and Rc contents on the flexural tensile strength (t = 28 days)

## 4.4 Stiffness modulus in four-point bending test

In this study, the stiffness modulus was investigated by means of cyclic four-point bending test by applying variable strain and frequency levels which are described as strain-sweep and frequency-sweep tests, according to standard NEN-EN 12697-26. Beam specimens with size 400×50×50 mm were subjected to cyclic loading in a four-point bending fatigue machine with a temperature controlled cabinet, shown in Figure 4.23.

**Figure 4.23** Four-point bending test setup

The strain sweep test was performed by applying an increasing strain level from 50 until 400 μm/m at a fixed frequency of 10 Hz. As for the frequency sweep test, frequencies with a range from 0.4 to 20 Hz were increasingly applied at a constant strain of 50 μm/m. These two tests were displacement-controlled and applied with sinusoidal loading wave. During testing, the deflection of the beam at the mid span was measured with a linear variable displacement transformer (LVDT). The data acquisition software recorded the load and the deformation of the specimen per load cycle. The stiffness modulus, the maximum tensile stress and maximum tensile strain at each load cycle were calculated based on the load and measured deflection. During each sweep stage (each strain or frequency level), 200 load cycles were applied and the stiffness modulus was taken as the average value of the last 10 cycles. In both sweep tests, all the beam specimens were cured for 28 days and tested at a controlled temperature of 20°C.

### 4.4.1 Strain-sweep test data and analysis of results

**(1) Strain-sweep test data**

In a strain-sweep test, the stiffness of the sand-cement material in flexure is evaluated under various strain levels. Thus, the stiffness modulus as a function of the strain levels can be obtained which can indicate how the material resists the applied strain. Besides, the correlation between the tensile stress and the applied strain at each stage is also obtained. Figure 4.24 gives examples of the test data on three replicate specimens, including the stiffness-strain and stress-strain curves, based on the mixture (1.9, 205), i.e. cement 205 kg/m$^3$ and Rc 1.9 kg/m$^3$.

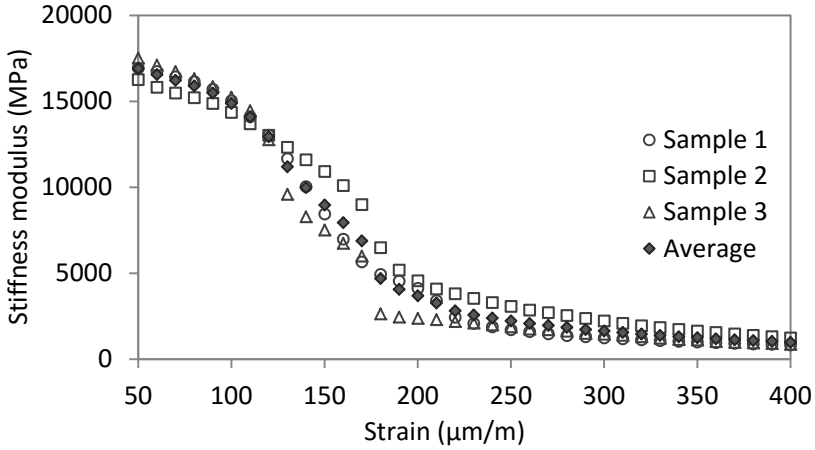


(a) Stiffness modulus versus strain

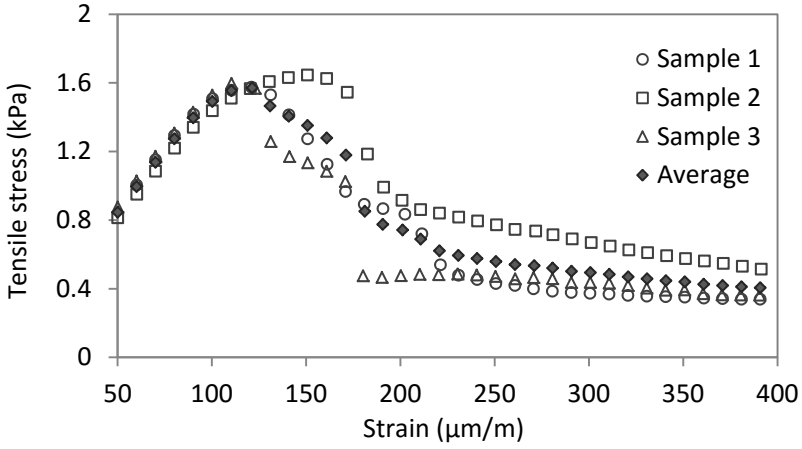


(b) Tensile stress versus strain

**Figure 4.24** Strain-sweep test results for mixture (1.9, 205)

In Figure 4.24 (a) it can be seen that the stiffness of sand-cement material gradually decreases when subjected to increased strain levels. The results of three specimens show small variation. As shown in Figure 4.24 (b) initially the stress is nearly linearly related to the increased strain but as the strain exceeds a certain limit which could indicate the micro-cracking occurs, the stress non-linearly sharply decreases. Herein,

the peak tensile stress, which is on average 1.6 MPa, is defined as the flexural strength. Note that the failure strength obtained from the three-point bending test is described as flexural tensile strength, aiming to distinguish these two parameters. Besides, the maximum strain where this peak tensile stress occurs, is defined as the strain at break. Based on this mixture, the strain at break ranges from 110 to 150 μm/m which indicates a large variation in the test results.

Table 4.4 summarizes the test data from the strain-sweep tests consisting of the initial stiffness modulus, flexural strength as well as the strain at break. The initial stiffness modulus is obtained from the stiffness under the applied strain level of 50 μm/m.

**Table 4.4** Strain-sweep test data

| Specimen code | Mix design (by dry mass of soil) | | Stiffness at strain level 50 μm/m | Flexural Strength | Strain at break |
|---|---|---|---|---|---|
| | Rc | Cement | | | |
| | kg/m$^3$ | kg/m$^3$ | MPa | MPa | μm/m |
| $Rc_0C_0$-1 | 1.9 | 205 | 16944 | 1.58 | 120 |
| $Rc_0C_0$-2 | 1.9 | 205 | 16271 | 1.67 | 150 |
| $Rc_0C_0$-3 | 1.9 | 205 | 17513 | 1.60 | 120 |
| $Rc_0C_{-a}$-1 | 1.9 | 140 | 11938 | 1.35 | 141 |
| $Rc_0C_{-a}$-2 | 1.9 | 140 | 12600 | 1.14 | 111 |
| $Rc_1C_{-1}$-1 | 3.2 | 159 | 12860 | 1.48 | 141 |
| $Rc_1C_{-1}$-2 | 3.2 | 159 | 12021 | 1.24 | 151 |
| $Rc_1C_{-1}$-3 | 3.2 | 159 | 11816 | 1.39 | 191 |
| $Rc_aC_0$ -1 | 3.8 | 205 | 16540 | 1.78 | 120 |
| $Rc_aC_0$ -2 | 3.8 | 205 | 14876 | 1.69 | 130 |
| $Rc_aC_0$ -3 | 3.8 | 205 | 17005 | 2.10 | 140 |
| $Rc_1C_1$-1 | 3.2 | 251 | 18659 | 1.48 | 220 |
| $Rc_1C_1$-2 | 3.2 | 251 | 16906 | 2.44 | 170 |
| $Rc_1C_1$-3 | 3.2 | 251 | 18581 | 1.87 | 120 |
| $Rc_0C_a$-1 | 1.9 | 270 | 19939 | 2.99 | 170 |
| $Rc_0C_a$-2 | 1.9 | 270 | 18936 | 2.40 | 150 |
| $Rc_0C_a$-3 | 1.9 | 270 | 19810 | 2.54 | 160 |
| $Rc_{-1}C_1$-1 | 0.56 | 251 | 19627 | 2.49 | 140 |
| $Rc_{-1}C_1$-2 | 0.56 | 251 | 19063 | 1.94 | 110 |
| $Rc_{-1}C_1$-3 | 0.56 | 251 | 17538 | 1.99 | 133 |
| $Rc_{-a}C_0$ -1 | 0 | 205 | 13131 | 1.64 | 140 |
| $Rc_{-a}C_0$ -2 | 0 | 205 | 15414 | 1.81 | 141 |
| $Rc_{-a}C_0$ -3 | 0 | 205 | 14250 | 1.73 | 142 |
| $Rc_{-1}C_{-1}$-1 | 0.56 | 159 | 13400 | 1.21 | 100 |
| $Rc_{-1}C_{-1}$-2 | 0.56 | 159 | 14964 | 1.71 | 140 |
| $Rc_{-1}C_{-1}$-3 | 0.56 | 159 | 12154 | 1.02 | 100 |

**(2) Analysis of results from strain-sweep test**

***a) Stiffness modulus in the strain-sweep test***

Figure 4.25 presents the stiffness modulus obtained from the cyclic bending test as a function of the applied strain level of the cement stabilized sand beams with variable Rc contents.

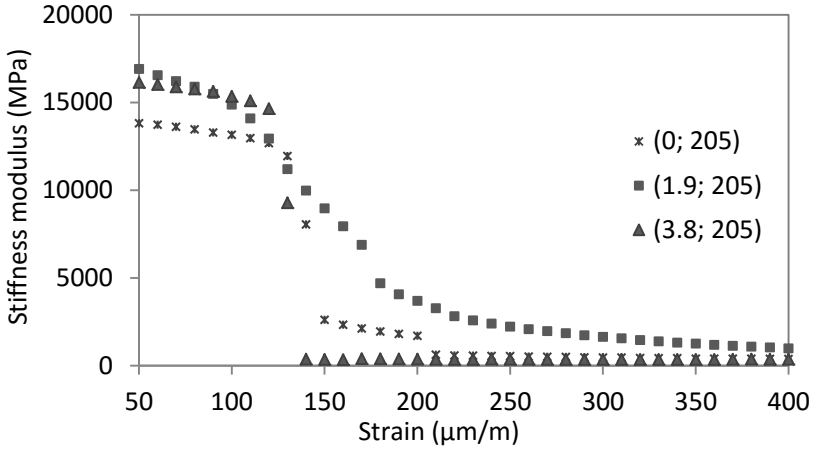


(a)

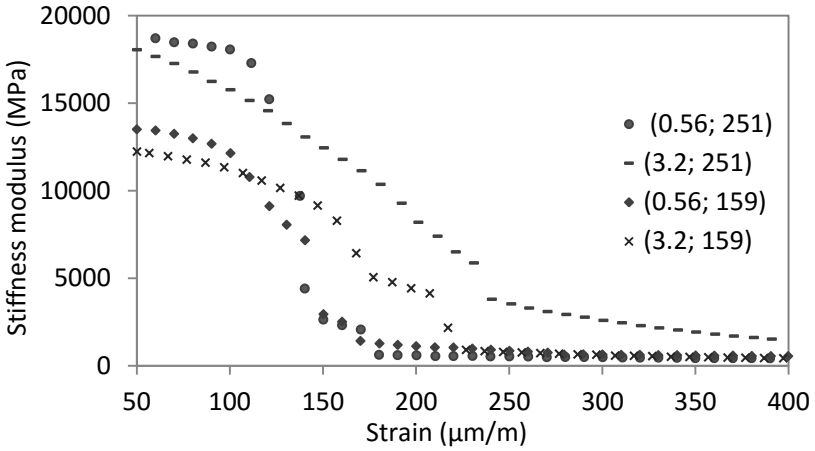


(b)

**Figure 4.25** Influence of Rc additive content on the stiffness modulus

In Figure 4.25 it can be seen that the stiffness modulus of cement stabilized materials is strongly dependent on the applied strain. As the strain increases, the stiffness modulus significantly decreases until failure. Based on the cement content of 205 kg/m$^3$, the mixture with Rc content 1.9 kg/m$^3$ obviously exhibits the highest stiffness modulus that steadily decreases with increasing strain level and at the end of the test the material didn't suddenly break. In contrast, the beams without Rc and with an excessive amount of Rc act like very brittle materials and the stiffness modulus of these two mixtures sharply decrease at an applied strain around 140 μm/m, which indicates that cracking occurred in the tested beams. In the second graph, which

shows stiffness of mixtures with cement contents of 159 and 251 kg/m$^3$, it can be noted that as the Rc content increases from 0.56 to 3.2 kg/m$^3$, the beam can withstand higher strain levels before failure.

Regarding the influence of the cement content on the development of the stiffness modulus, Figure 4.26 shows the stiffness modulus curves of three sand-cement mixtures with different cement contents and the same Rc content 1.9 kg/m$^3$.

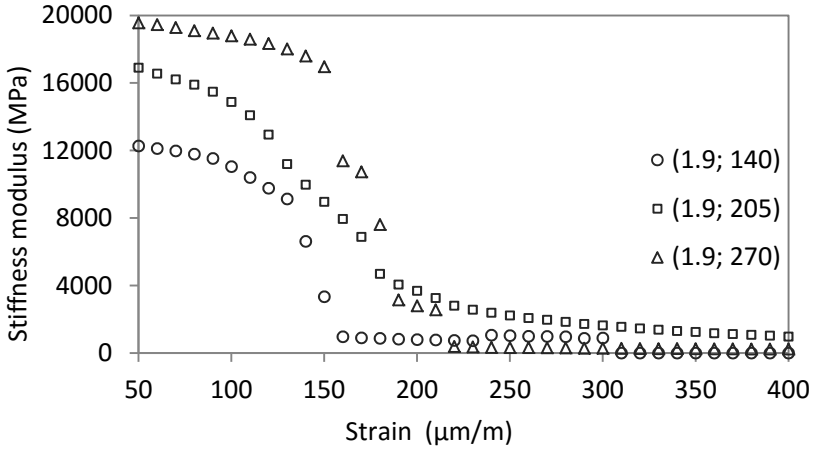


**Figure 4.26** Influence of cement content on the stiffness modulus

As shown in Figure 4.26, when the cement content increases to 270 or decreases to 140 kg/m$^3$, the stiffness of these two mixtures both reduce significantly at the applied strain around 150 μm/m. The mixture of cement content 205 kg/m$^3$ together with addition of Rc 1.9 kg/m$^3$ gives more flexible development which implies that appropriate amounts of cement and Rc additive can improve the flexibility of the cement stabilized sand materials.

As discussed above, the stiffness modulus of sand-cement decreases under the increased strain levels which means micro-cracking may occur as the applied strain exceeds a certain limit or fatigue damage may happen under repeated loadings. Thus, the initial stiffness which is obtained at the first strain level 50 μm/m, is adopted to evaluate the influence of mix variables on this parameter. In order to quantify the effect of cement and Rc contents on the values of flexural stiffness, estimation models are developed for the stiffness modulus when subjected to strain level 50 μm/m, shown in Figure 4.27. Two statistical models are considered, with combined effect of cement and Rc contents as well as density of the specimen. The cement content and density of the specimen are evaluated in a power function and the Rc content is evaluated in two functions: exponential and linear.

In Figure 4.27 linear and exponential functions are applied for the effect of Rc content and these two models fit the test data quite well and showed exactly the same $R^2$.

From the estimation models it can be seen that the stiffness modulus is positively influenced by the cement content. Whereas, the coefficient of Rc additive in these two models are rather low which indicates a limited influence. These two models show a good fit with the test data.

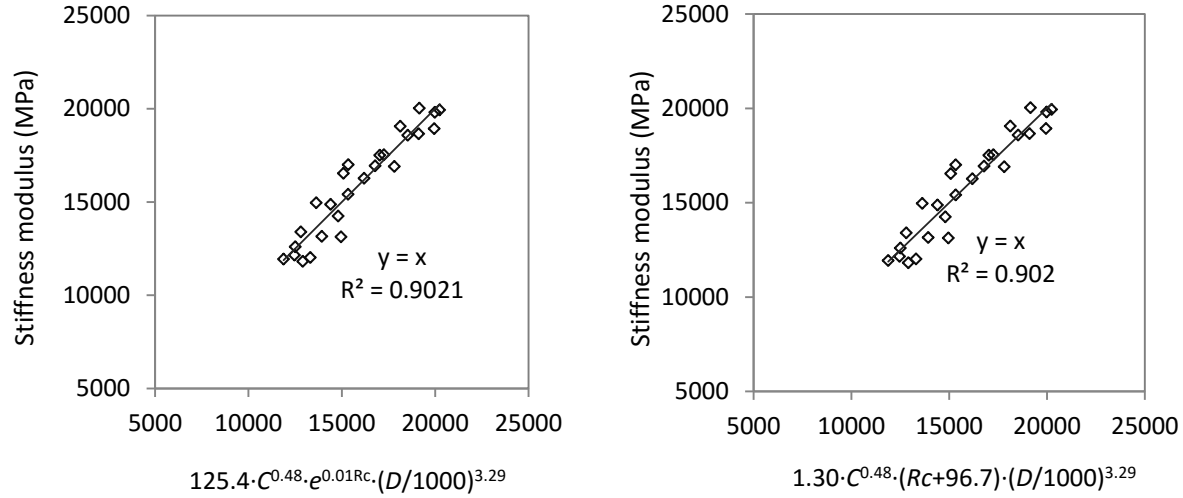


(a) Exponential function (b) Linear function

**Figure 4.27** Estimation models of stiffness modulus

***b) Strain at break and flexural strength in the strain-sweep test***

Figure 4.28 shows the strain at break obtained from all the sand-cement mixtures. An error bar is given to indicate the variation of three test results. Strain at break and flexural strength are obtained from the stress-strain curve (example shown in Figure 4.24).

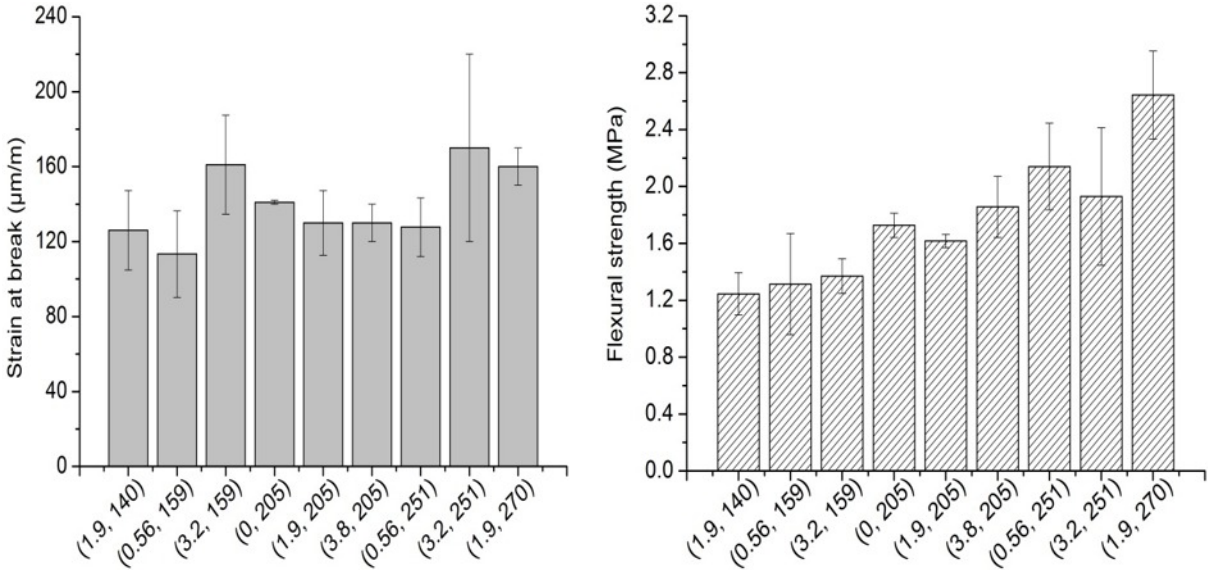


(a) Strain at break (b) Flexural strength

**Figure 4.28** Strain at break and flexural strength in the four-point bending test

In Figure 4.28 (a) it can be seen that the three mixtures with cement content 205 kg/m$^3$ have nearly the same strain at break. In contrast, the Rc content plays an obvious role in the mixtures with cement contents of 159 and 251 kg/m$^3$, where the strain at break increases on average by 40% as the Rc content increases from 0.56 to 3.2 kg/m$^3$. Additionally, the cement content doesn't appear to have a clear influence on the strain at break. Conversely, rise of the cement content increases the flexural strength (graph b). For instance, the mixture with the highest amount of cement produces the highest flexural strength and the lowest flexural strength appears in the mixture with the lowest cement content. The Rc additive content doesn't show significant effect on the flexural strength.

Attempts are also made to develop the estimation models aiming to predict the flexural strength and strain at break of cement stabilized materials, shown in Figure 4.29. Figure 4.29 presents the flexural strength and the strain at break for all tested mixtures. An exponential function for the effect of the Rc content is applied in the estimation models.

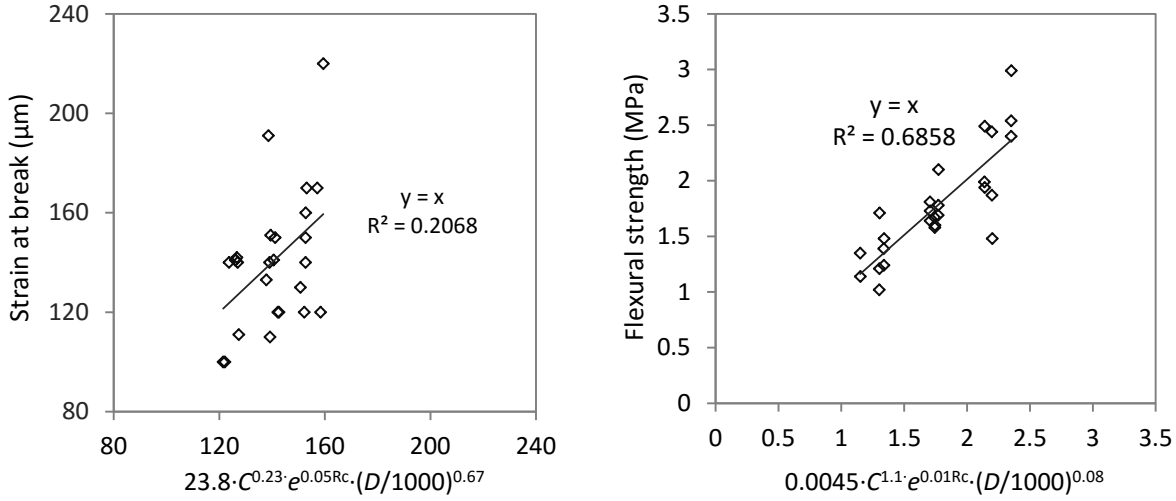


(a) Strain at break (b) Flexural strength

**Figure 4.29** Estimation models of strain at break and flexural strength

In Figure 4.29 the estimation models of strain at break and the flexural strength exhibit rather low $R^2$ values, which are 0.21 and 0.69, respectively. It is because a large variation occurred in the test data. However, it gives an indication that the Rc content has a certain positive influence on the strain at break while the flexural strength is more closely related to the cement content.

*c) Maximum wheel load from linear-elastic multilayer calculation*

In this section, the linear-elastic multilayer program BISAR is used to back-calculate the heavy traffic load under which the maximum tensile strain would occur at the bottom of the cement stabilized layer. This load indicates the wheel load which induces the maximum tensile strain (strain at break) at the bottom of the stabilized base layer and may cause immediate cracking of the base. The basic idea of back-calculation is to determine the target wheel load which leads to the strain at break of the stabilized base layer.

This BISAR calculation is done for an assumed two-layer pavement structure and the input parameters for each layer is illustrated in Table 4.5. The stiffness modulus and the expected strain at break were adopted referring to the result for the individual mixtures (shown in Table 4.4) and the average value of three test data was used.

**Table 4.5** Input parameters for BISAR calculation

| Pavement Structure | Materials | Input parameters | | | | | Calculated |
|---|---|---|---|---|---|---|---|
| | | Thickness | Poisson's ratio | Stiffness | Tire pressure | Wheel load | Strain at break |
| | | m | - | MPa | MPa | kN | μm/m |
| Layer 1 | Sand-cement | 0.25 | 0.25 | Table 4.4 | 1 | Target | Table 4.4 |
| Layer 2 | Unbound subsoil | _ | 0.35 | 100 | _ | _ | _ |

The obtained maximum wheel load for each mixture is presented together with the mix design and shown in Figure 4.30.

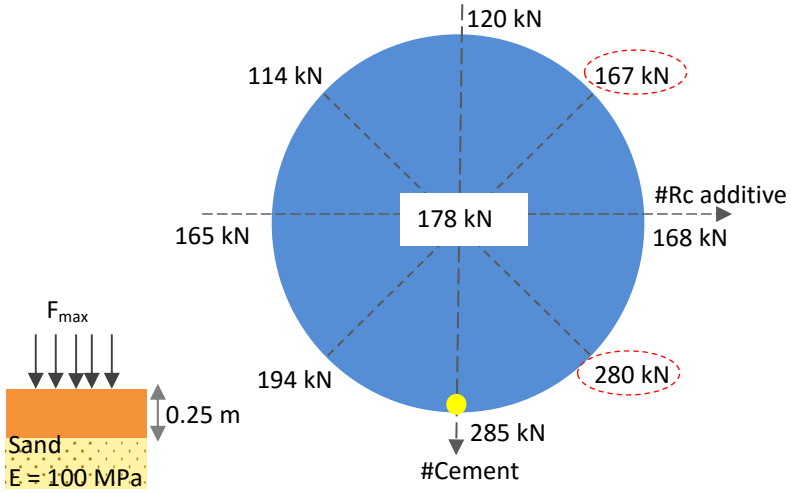


**Figure 4.30** Highest wheel load of the sand-cement base layer before breaking

The yellow dot in Figure 4.30 indicates the mixture which resists the highest load, which is observed in the mixture with the highest amount of cement. Increasing the

Rc content in sand-cement mixtures is also found to be capable of withstanding a higher traffic load before the stabilized base cracks, indicated in the red circle. For example, for the mixtures with cement content 159 and 251 kg/m$^3$, as the Rc content increases from 0.56 to 3.2 kg/m$^3$, the maximum load increases on average by 45%.

### 4.4.2 Frequency-sweep test data and analysis of the results

As for the frequency sweep test, frequencies with a range from 0.4 to 20 Hz were subsequently applied and the applied strain was constantly fixed as 50 μm/m, which is approximately 30% of the strain at break for the sand-cement materials. During each sweep stage, 200 load cycles were applied and the stiffness modulus was taken as the average value of the last 10 cycles. For the frequency-sweep test, 3 specimens were tested for each mix composition. Figure 4.31 gives an example of the frequency-sweep test data from three specimens (mix design with cement 205 kg/m$^3$ and Rc 1.9 kg/m$^3$).

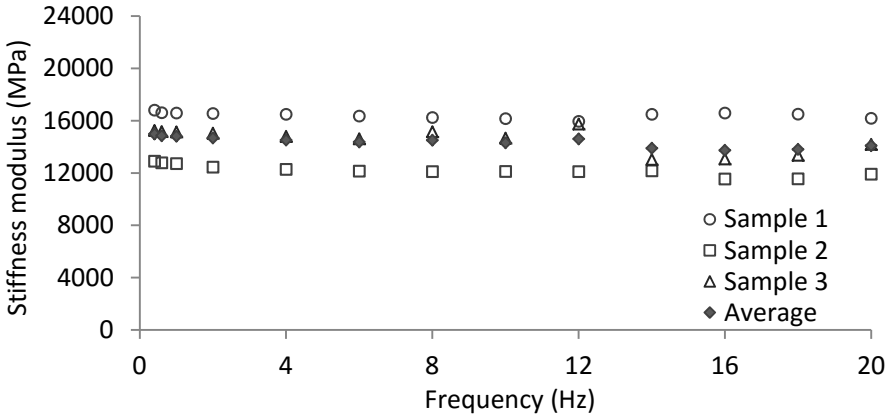


**Figure 4.31** Frequency-sweep test results from 3 test repetitions

As shown in Figure 4.31 the frequency of cyclic loading doesn't seem to influence the stiffness of sand-cement materials. Besides, the variation of the three specimens is relatively small. The influence of the frequency of dynamic loading on the stiffness modulus of cement stabilized sand is evaluated on all the mixtures, shown in Figure 4.32. The specimen was subjected to the constant strain 50 μm/m at various load frequencies. Each stiffness curve is plotted as a function of the frequency levels, based on the mean value of three specimens.

As can be seen from Figure 4.32, the stiffness modulus of the cement stabilized sand materials remains nearly constant at different frequency levels, which is observed in all the tested mixtures. Therefore, the conclusion can be drawn that the frequency of dynamic loading has no obvious influence on the stiffness modulus of cement

stabilized materials. Figure 4.32 again shows that a higher cement content generally yields a higher stiffness.

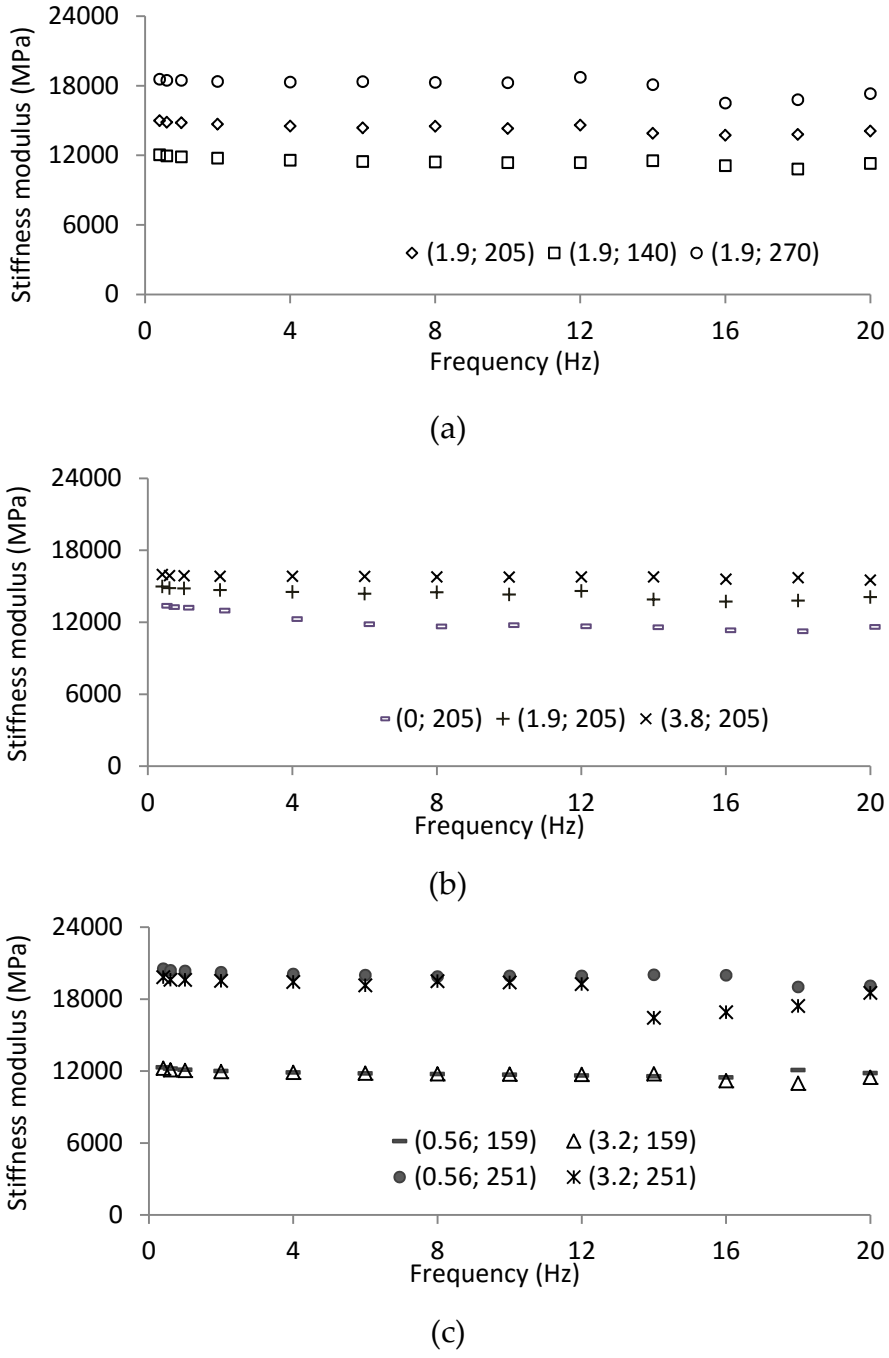


**Figure 4.32** Influence of load frequency on the stiffness modulus of sand-cement

## 4.5 Fatigue property

### 4.5.1 Fatigue test condition

The fatigue life under cyclic loading is the appropriate type of failure to predict the life of the stabilized layer in the pavement structure (Crockford & Little, 1987). The

fatigue property is determined by subjecting the beam specimen to various stress levels and the resulted number of load repetitions at failure is plotted against the applied stress. The four-point bending test machine was used (see Figure 4.23). At each applied stress level, the stress-controlled loading mode was applied and hence the amplitude of the applied load was held constant during testing. The stress level to be applied is lower than the flexural strength obtained from the four-point bending test. Table 4.6 describes the test conditions for the fatigue test.

**Table 4.6** Fatigue test conditions (according to standard NEN-EN 12697-24)

| Items | Test conditions |
|---|---|
| Loading mode | Stress-controlled |
| Loading wave | Sinusoidal wave |
| Frequency | 10 Hz |
| Temperature | 20°C |
| Age | 28 days |

Figure 4.33 gives an example of a fatigue test result at different stress levels which shows a typical plot of stiffness modulus ratio (defined as the ratio of the occurring stiffness modulus to the initial value) versus the number of load repetitions. The initial stiffness modulus is obtained as the average value during the initial 90$^{th}$ to 100$^{th}$ load applications, which is used as a reference to determine the development of the stiffness.

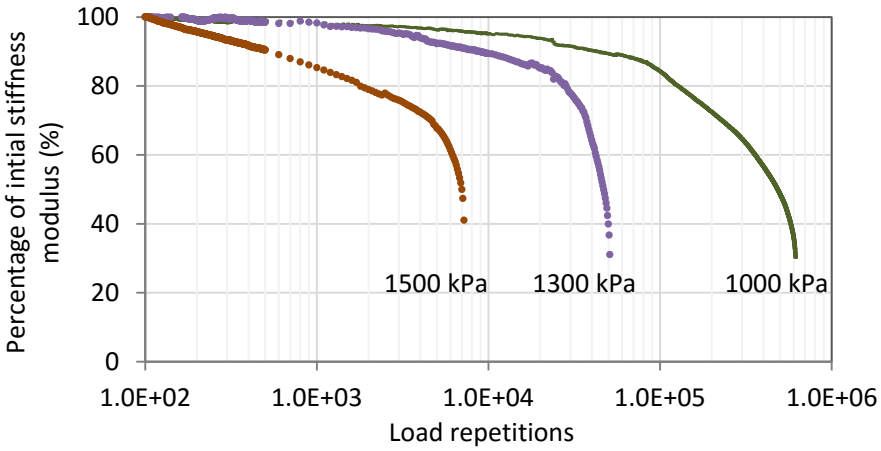


**Figure 4.33** Ratio of stiffness versus load cycles based on mixture (1.9, 205)

As shown in Figure 4.33, under repeated loading the stiffness modulus ratio decreases gradually while at the end of the test the stiffness modulus decreases rapidly until fracture occurs. During the stress-controlled loading mode, a constant stress is applied and the stiffness modulus is decreasing after many load repetitions,

so in such condition that the strain of the specimen increases as the stiffness decreases until failure. As soon as the crack is initiated, the crack will rapidly propagate through the specimen and cause the complete fracture. The failure point is defined as the moment when the beam gets completely fractured. Besides, it can be seen that the higher the stress level that is applied, the smaller the number of load repetitions the beam can withstand.

### 4.5.2 Fatigue relation of all the tested mixtures

According to standard NEN-EN 12697-24, the fatigue line is plotted as a function of the initial strain (strain amplitude at 100$^{th}$ cycle) against the number of load repetitions at failure. Based on this study (stress-controlled loading mode), the fatigue life N in relation to the various applied stress levels is also evaluated, expressed as the following two equations:

$$N = k_1 \cdot (\sigma)^{-k_2} \text{ or } N = k_1 \cdot (\varepsilon)^{-k_2} \quad (4\text{-}22)$$

Where, N is the number of load cycles at failure; σ is the applied stress (kPa); ε is the initial strain (μm/m); $k_1$ and $k_2$ are experimentally determined coefficients.

Figure 4.34 shows as an example of the relationship between the fatigue life with applied stress levels and the strain, based on mixture (1.9, 205), i.e. Rc additive 1.9 kg/m$^3$ and cement 205 kg/m$^3$. In Figure 4.34 the number of load cycles N and applied stress level σ and initial strain ε are all presented on a log-log scale aiming to illustrate the slope $k_2$ of the fatigue line.

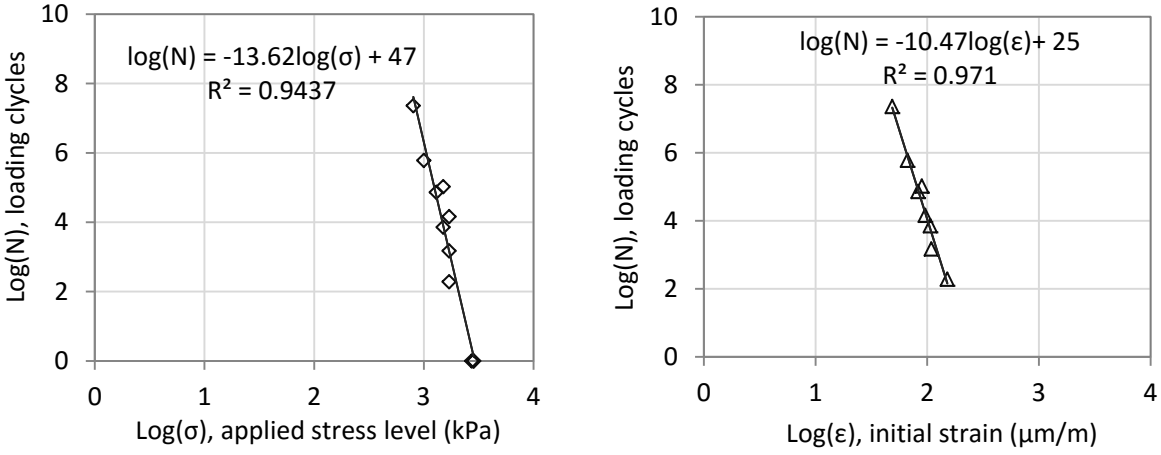


(a) Stress-based fatigue relation (b) Strain-based fatigue relation

**Figure 4.34** Fatigue relation of the tested mixture (1.9, 205)

As demonstrated in Figure 4.34, good correlations between the number of load cycles and the initial strain or stress levels are established, and these two types of relations showed similar $R^2$ values. The fatigue relations for all the stabilized mixtures are

given in Table 4.7, presented by the coefficients $k_1$ and $k_2$. Stiffness is defined as the ratio of stress to strain, so the stress-based relations can be replotted as initial strain-based relations, therefore, these two types of correlations are both considered. In Table 4.7 it can be seen that the fatigue relation for mixture $Rc_{-1}C_{-1}$ (0.56, 159) shows a very low $R^2$ value and thus it is excluded from the following analysis. Large variations of the $k_1$ and $k_2$ values are observed, which are largely dependent on the mix composition.

**Table 4.7** Parameters for fatigue relations of all the sand-cement mixtures

| Mix code | Mix design (by dry mass of soil) | | Fatigue life, log(N) | | | | | |
|---|---|---|---|---|---|---|---|---|
| | | | Stress-based relation | | | Strain-based relation | | |
| | Rc | Cement | log($k_1$) | $k_2$ | $R^2$ | log($k_1$) | $k_2$ | $R^2$ |
| | [kg/m³] | [kg/m³] | [-] | [-] | | [-] | [-] | |
| $Rc_0C_0$ | 1.9 | 205 | 47 | 13.62 | 0.94 | 25 | 10.47 | 0.97 |
| $Rc_0C_{-a}$ | 1.9 | 140 | 43 | 12.45 | 0.93 | 22 | 8.92 | 0.32 |
| $Rc_{+1}C_{-1}$ | 3.2 | 159 | 45 | 14.02 | 0.60 | 16 | 6.45 | 0.67 |
| $Rc_{+a}C_0$ | 3.8 | 205 | 41 | 11.49 | 0.81 | 18 | 6.85 | 0.78 |
| $Rc_{+1}C_{+1}$ | 3.2 | 251 | 55 | 15.84 | 0.97 | 30 | 13.01 | 0.86 |
| $Rc_0C_{+a}$ | 1.9 | 270 | 53 | 15.18 | 093 | 28 | 12.01 | 0.89 |
| $Rc_{-1}C_{+1}$ | 0.56 | 251 | 52 | 15.04 | 0.94 | 26 | 11.16 | 0.88 |
| $Rc_{-a}C_0$ | 0 | 205 | 47 | 13.59 | 0.98 | 34 | 15.07 | 0.96 |
| $Rc_{-1}C_{-1}$ | 0.56 | 159 | 10 | 2.29 | 0.10 | 6 | 1.51 | 0.11 |

To visualize the difference, Figure 4.35 presents the fatigue lines of all the sand-cement mixtures, expressed in log-log scale. In Figure 4.35 generally it can be seen that the fatigue lines are largely dependent on the mix compositions and these two types of fatigue relations show different trends. For instance, the stress-based relations are rather parallel between mixtures, in other words the variation of the slope ($k_2$-value) of the fatigue lines is relatively small. In contrast, the slope of the strain-based fatigue lines is more variable. Besides, it can be noted that mixture (3.2, 159) shows a large deviation in both types of relations and indicates a rather low number of load repetitions at the given stress or strain levels compared with the rest of the mixtures.

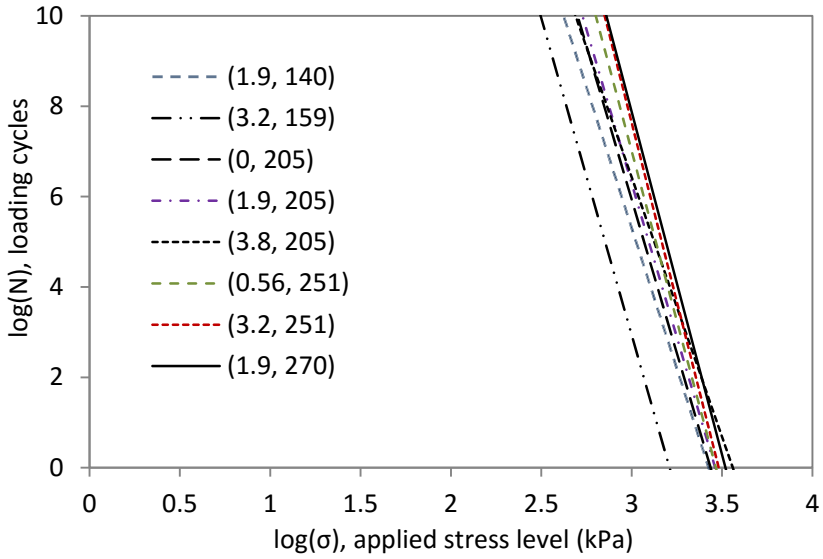


(a) Stress-based fatigue relations

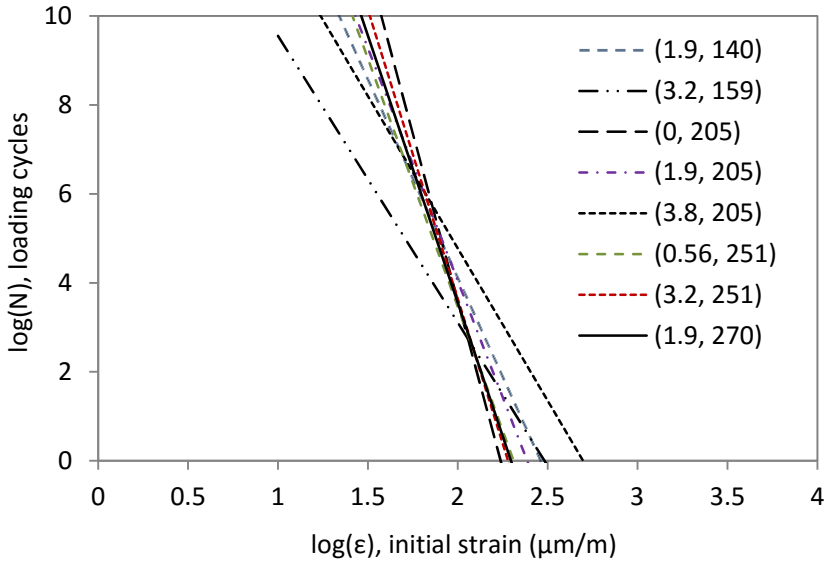


(b) Strain-based fatigue relations

**Figure 4.35** Fatigue line for all the sand-cement mixtures

Moreover, as can be seen for the stress-based relations, the $k_2$ value ranges nearly from 12 to 16 indicating a large slope and rather brittle behavior of cement stabilized sand materials, which can be compared with $k_2$ for asphalt mixtures generally ranging from 3 to 6 (Ghuzlan & Carpenter, 2002). A literature study by Ghuzlan and Carpenter (2002) concluded that the wide range of $k_1$ and $k_2$ values are attributed to factors including testing mode of loading (stress-controlled/strain-controlled), specimen size and mixture variables, etc. However, it is found that $k_1$ and $k_2$ are well correlated, shown in Figure 4.36.

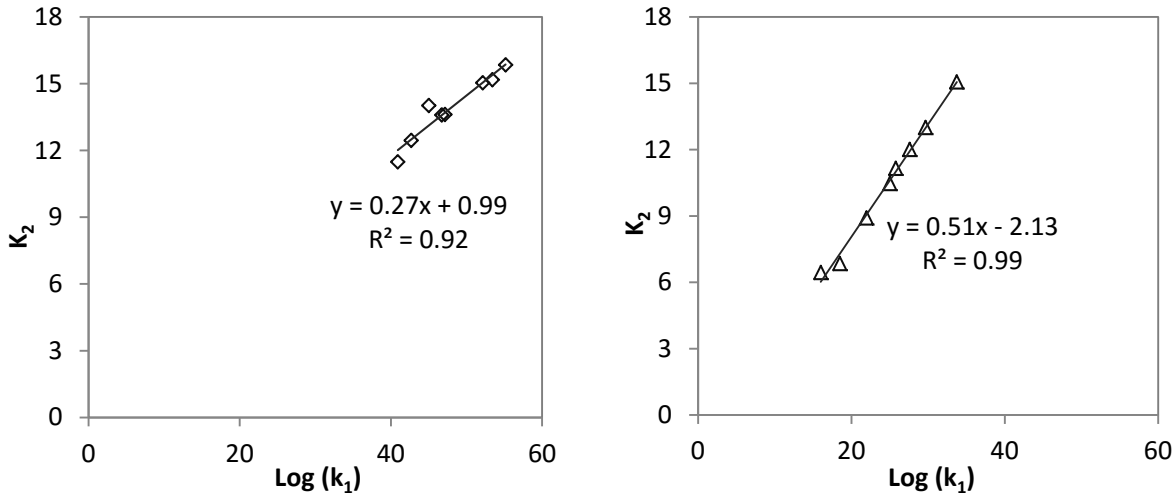


(a) Stress-based fatigue relations (b) Strain-based relations

**Figure 4.36** Correlation between $k_1$ and $k_2$

Figure 4.36 includes all the $k_1$ and $k_2$ values in the fatigue models from all the mixtures and $k_1$ is indicated by its log. It can be found that $k_1$ and $k_2$ are highly correlated in both types of fatigue models. $k_2$ is linearly correlated to $\log(k_1)$ independent of the mix design. Although different mixtures alter the values of $k_1$ and $k_2$, the relation between $k_1$ and $k_2$ is consistent. But the coefficients of the linear relationship are quite different in these two types of fatigue relations, given in the following equations:

$$k_2 = 0.27 \cdot \log(k_1) + 0.99 \qquad R^2=0.92 \quad \text{stress-based fatigue relations} \qquad (4\text{-}23)$$

$$k_2 = 0.51 \cdot \log(k_1) - 2.13 \qquad R^2=0.99 \quad \text{strain-based fatigue relations} \qquad (4\text{-}24)$$

Similarly, research by Ghuzlan and Carpenter (2002) also gives the $k_1$ and $k_2$ relation for asphalt concrete materials, which is based on 84 different mixtures and it is emphasized that the uniform relationship between $k_1$ and $k_2$ doesn't change in different mixtures and it may have a potential use in pavement design, shown as follows:

$$k_2 = 0.3269 \cdot \log(k_1) - 1.1857 \qquad R^2 = 0.94 \qquad \text{(Ghuzlan \& Carpenter, 2002)}$$

In order to identify the influence of cement and Rc additive on the fatigue resistance, the stress level (or strain level) that corresponds to one million load cycles is analyzed in this section. On the basis of the literature, the similar concept is referred to as endurance limit (also as fatigue strength) which illustrates the stress or strain level (or stress ratio, which is related to the ultimate strength) that can be applied to material without causing fatigue damage. That means below this stress or strain level the specimen can withstand an infinite number of load cycles. For instance,

Monismith et al. (1970) first proposed an endurance limit of 70 micro-strain for asphalt pavement. Plain concrete was reported to have an endurance limit of 50 to 57% of the ultimate flexural strength (Ramakrishnan et al. 1989).

However, there is very limited information regarding the definite value or existence of endurance limit for cement stabilized materials. In theory, specimens tested at a stress level below the endurance limit should withstand an infinite number of load cycles. To obtain endurance limit, it is not practical to subject specimens to an infinite number of cycles and it is very time consuming to conduct fatigue tests with a very high number of cycles. Therefore, herein the stress or strain level that corresponds to one million load cycles is considered as the condition without causing fatigue damage and provides an indication of the endurance limit.

Figure 4.37 lists the calculated stress level that corresponds to one million load cycles, which is based on the above fatigue models (stress-based) presented in Table 4.7. Moreover, the ratio of this obtained stress level to the ultimate flexural strength for all the mixtures is also shown in Figure 4.37. The result of the mixture (0.56, 159) is excluded from this analysis due to the rather low $R^2$ of its fatigue relation.

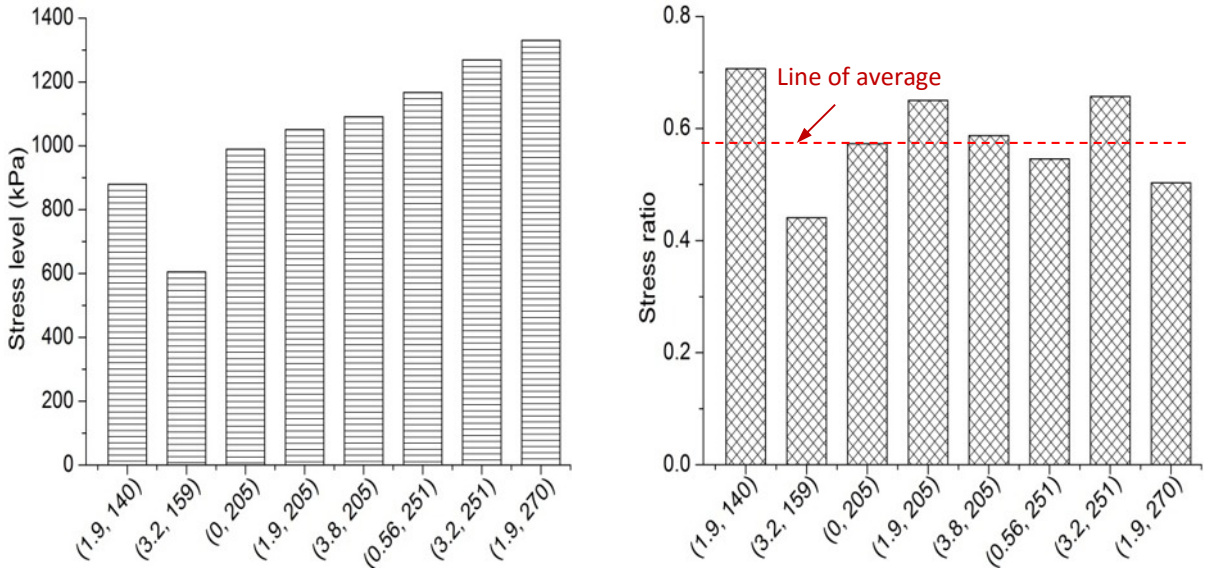


(a) Stress level (b) Stress ratio

**Figure 4.37** Stress level and stress ratio of sand-cement material corresponding to one million load cycles

As can be seen in Figure 4.37(a) the stress level is much dependent on the mix design. Generally it can be seen that a higher cement content allows a higher stress level. It means that a mixture with a higher cement content can withstand higher loading stress when one million load cycles are required. Besides, a higher Rc additive content also appears to increase the stress level.

In Figure 4.37(b) it shows that the stress ratio that corresponds to one million load cycles to failure is in a range of 0.45 to 0.70, on average around 0.58. It implies that if the stress to be applied on the sand-cement material stays below 58% of the failure strength, no fatigue damage will occur during one million load cycles.

Compared with this, Williams (1986) gave a broad conclusion that when the stress level is restricted to 50% of the failure strength a fatigue life of one million load applications can be expected. However, other studies indicated more variable values ranging from 0.18 to 0.7 (Balbo, 1996; Xuan 2012), which is based on cement treated granular materials. This means there doesn't exist one definite endurance limit value for cement stabilized materials, which is much dependent on the soil type, the variable grain size of the soil or aggregates and the mix design used in stabilization.

Similarly, the strain levels and the strain ratio (related to the strain at break) leading to $1\times10^6$ cycles are given in Figure 4.38, calculated by the strain-based fatigue relations. Figure 4.38 shows that the strain level that allows one million load cycles is on average 60 μm/m and this strain level is around 43% of the strain at break. Besides, these strain levels are not clearly related either to cement content or Rc additive content. One exception occurs in mixture (3.2, 159) which shows the lowest strain level and strain ratio. In a literature by Molenaar & Pu (2008) the strain level 50 μm/m was developed as the endurance limit for cement stabilized sand road base below which no traffic induced cracking would occur.

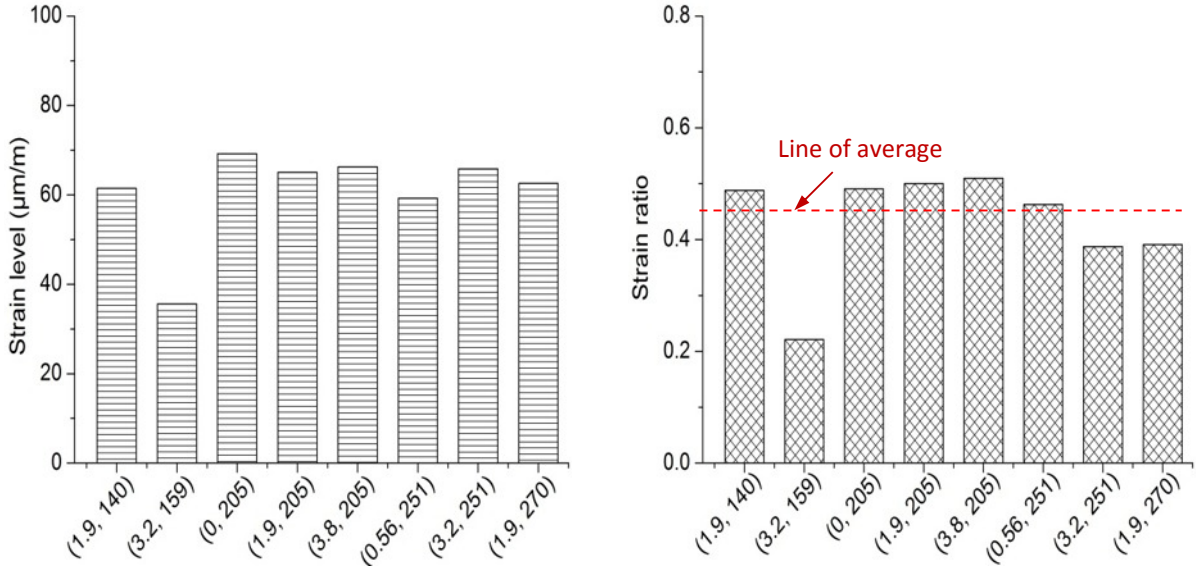


(a) Strain level (b) Strain ratio

**Figure 4.38** Strain level and strain ratio of sand-cement material corresponding to one million load cycles

## 4.6 Correlations between the mechanical properties

The unconfined compressive strength and indirect tensile strength tests, by using cylindrical specimens and compression machine, are widely used methods and easy to perform. However, in some cases obtaining beam specimens may be difficult and the corresponding flexural testing equipment may not be available everywhere. So, knowing the correlation between the mechanical properties is very useful to determine other mechanical properties from the measured ones.

### 4.6.1 Compressive strength and tensile strength

Based on the literature survey, numerous documents (TRH 13, 1986; Kersten, 1961; Babic, 1987) demonstrate linear relationships between the compressive strength and the tensile strength. In this study, Figure 4.39 gives the correlations between the indirect tensile strength or the flexural tensile strength and the compressive strength. It also includes the regressed mathematical models which can be used to predict the tensile strength at given compressive strength. All the data are based on the mean value of three tested specimens and includes 9 mixtures at all curing times.

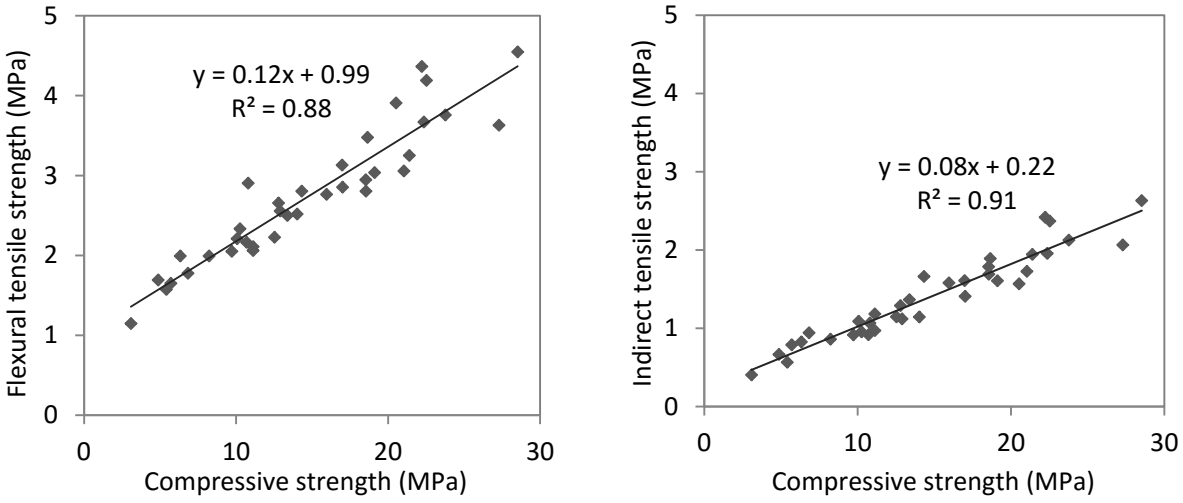


**Figure 4.39** Correlation between compressive strength and tensile strength

From Figure 4.39 it can be concluded that the indirect tensile strength and flexural tensile strength are both in linear relation with the compressive strength, independent on the curing time and mix proportions. These two linear models both exhibit satisfactory $R^2$ values and indicate a good correlation, expressed as the following equations:

$$FTS = 0.12 \cdot UCS + 0.99 \qquad R^2 = 0.88 \qquad (4\text{-}25)$$

$$ITS = 0.08 \cdot UCS + 0.22 \qquad R^2 = 0.91 \qquad (4\text{-}26)$$

Where, $UCS$ is unconfined compressive strength (MPa), $ITS$ is indirect tensile strength (MPa), $FTS$ is flexural tensile strength (MPa).

Figure 4.40 shows the ratio of tensile strength to compressive strength of all the sand-cement mixtures including all different curing times. From Figure 4.40 it can be concluded that for stabilized sand materials, the indirect tensile strength is 8% to 14% of the compressive strength, on average 10%. The ratio of flexural tensile strength to compressive strength shows much more scatter, generally ranging from 15% to 30%, and most of the data remains within 20%. The literature studies generally concluded that indirect tensile strength is about 10% to 15% of the compressive strength and the flexural strength is about 20% of the compressive strength.

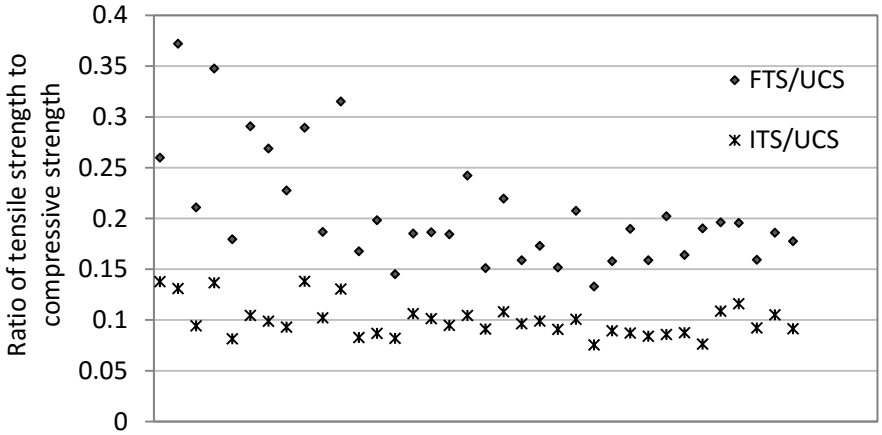


**Figure 4.40** Ratio of tensile strength to compressive strength

### 4.6.2 Indirect tensile and flexural tensile strength

The correlation between indirect tensile strength and flexural tensile strength (obtained from three-point bending test) is also established, shown in Figure 4.41.

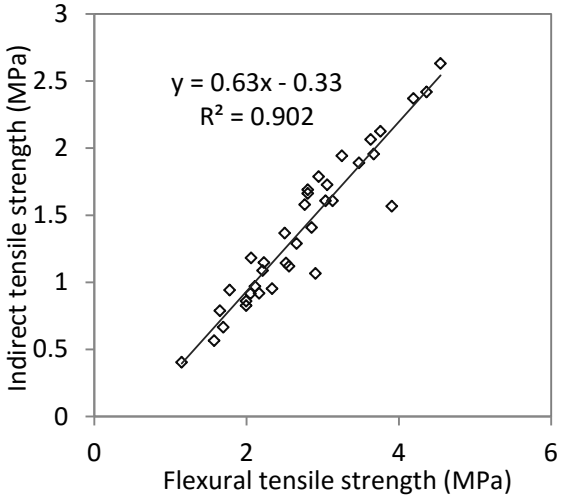


**Figure 4.41** Correlation between indirect tensile strength and flexural tensile strength

The equation in Figure 4.41 is described as follows:

$$ITS = 0.63 \cdot FTS - 0.33 \qquad R^2 = 0.902 \qquad (4\text{-}27)$$

From the above equation, it can be found that the indirect tensile strength is approximately 50% to 60% of the flexural tensile strength. This finding is in reasonable agreement with literature (Sherwood, 1968; Pretorius & Monismith, 1971) which reported that the flexural tensile strength is generally 1.5 times the indirect tensile strength (*ITS*/*FTS* is 67%).

Another finding also to be noted is that the flexural tensile strength obtained from the strain-sweep test (cyclic four-point bending) and from the monotonic three-point bending test is significantly different. Figure 4.42 compares the flexural tensile strength obtained from these two tests and includes the test data from all mixtures cured for 28 days. It can be clearly seen in Figure 4.42 that the flexural tensile strength obtained from the strain-sweep test (four-point bending) is 35% to 40% lower than the one from the three-point bending test. The reason can be attributed to the variable sizes of the specimen as well as the repeated loading in the sweep test which might contribute to some sort of fatigue and hence weakens the material. The correlation between these two flexural tensile strength values is given in Figure 4.43, which shows a low $R^2$ value.

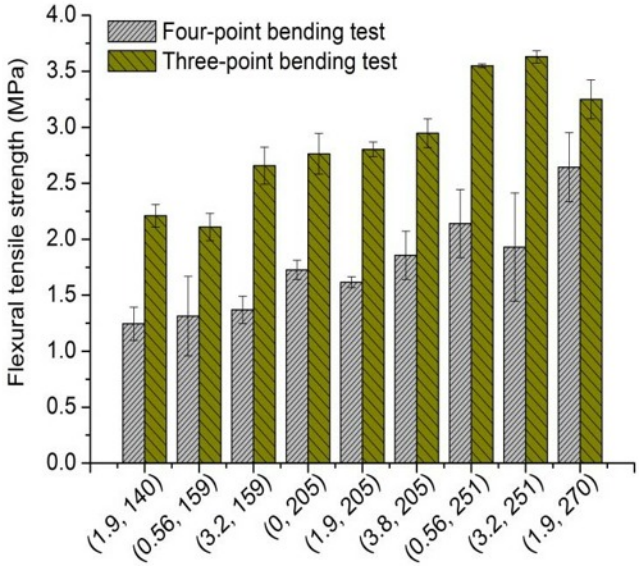


**Figure 4.42** Flexural tensile strength from three-point and four-point bending test

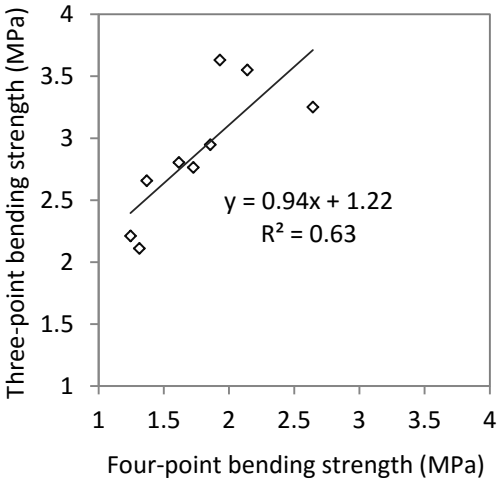


**Figure 4.43** Correlation between these two flexural strength

### 4.6.3 Mechanical strength and stiffness

On the basis of the literature study, correlations between stiffness and the mechanical strength have been documented and generally expressed as the following forms:

$$E = a(UCS) + b \quad \text{and} \quad E = a(UCS)^{b} + c \tag{4-28}$$

Where, $E$ is the stiffness modulus (MPa), $UCS$ is the unconfined compressive strength (MPa), a, b and c are experimentally determined coefficients.

In this study the correlation between stiffness and mechanical strength is also evaluated, shown in Figure 4.44. Figure 4.44 includes the correlation between stiffness modulus and compressive, indirect tensile, flexural tensile (three-point bending) and flexural strength (four-point bending). In these correlations, the linear relation in equation 4-28 is shown. The stiffness modulus discussed hereby is obtained as the stiffness at the applied strain of 50 μm/m during the strain-sweep test. Due to the fact that the stiffness was tested at the curing time of 28 days, the following figures only include the mechanical test results at 28 days. Figure 4.44 (a), (b) and (c) are based on the average value of test data from three tested specimens.

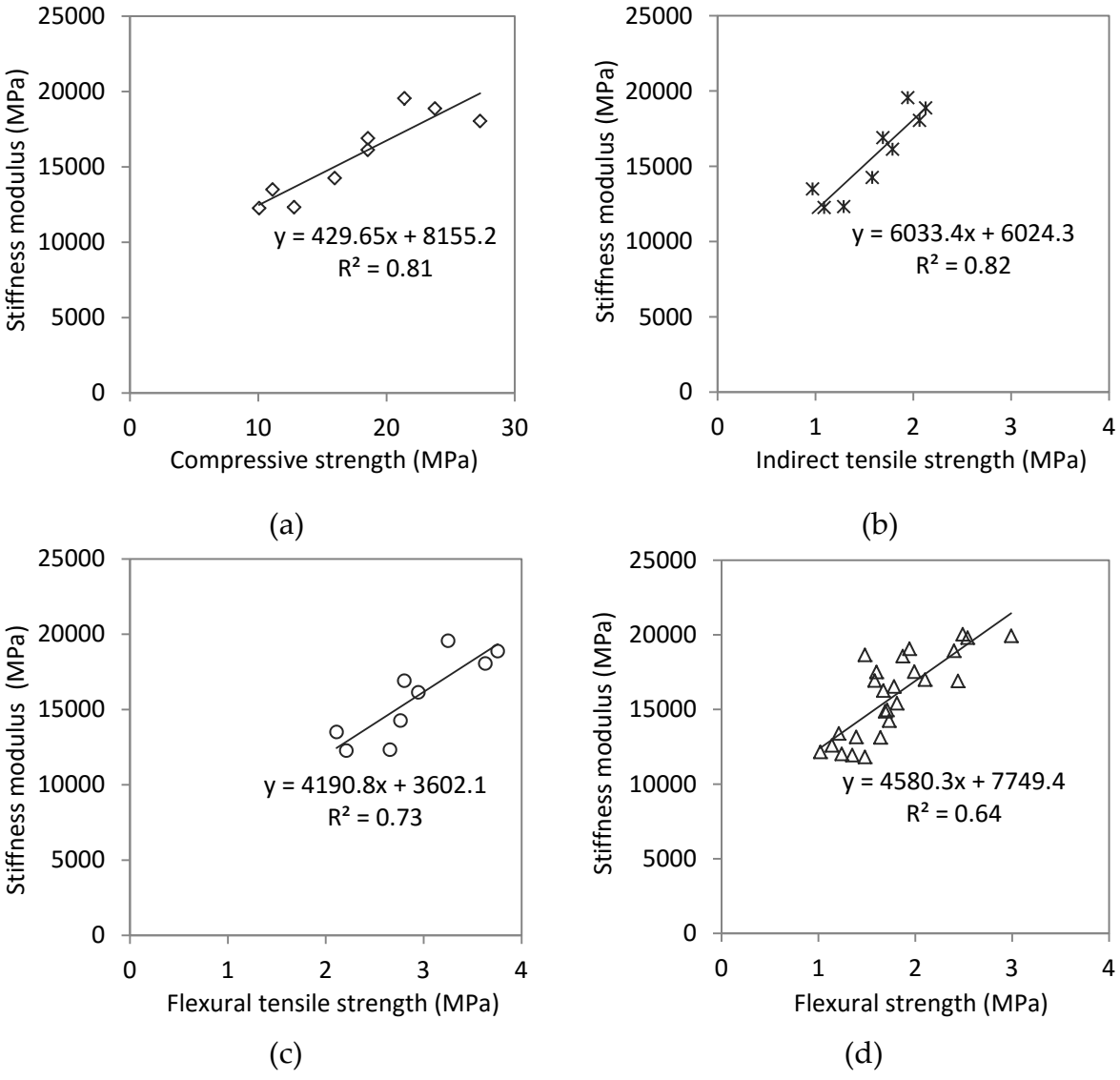


**Figure 4.44** Correlation between tensile strength and stiffness modulus

In Figure 4.44 graphs (a) (b) and (c) show that the stiffness modulus is well related to compressive strength and tensile strength, which generally indicates that a higher compressive strength or tensile strength corresponds to a higher stiffness modulus. Graph (d) indicates a rather weak correlation between stiffness and flexural strength, shown as a low $R^2$. Research (Crockford & Little, 1987) attributed the large scatter in the flexural test results to the fact that such a test is very sensitive to the quality of the beam specimen, curing environment, etc.

As discussed above, the mechanical properties of cement stabilized sand are well related and equations have been achieved to correlate between each physical parameter. Table 4.8 summarizes all the established correlations.

**Table 4.8** Correlations between mechanical properties of sand-cement

| Correlations | Curing age | Equations | $R^2$ |
|---|---|---|---|
| Compressive strength and tensile strength | Up to 91 days | $FTS = 0.12 \times UCS + 0.99$ | 0.88 |
| | | $ITS = 0.08 \times UCS + 0.22$ | 0.91 |
| Indirect and flexural tensile strength | Up to 91 days | $ITS = 0.63 \times FTS - 0.33$ | 0.90 |
| | | $FTS = 0.94 \times FTS^a + 1.22$ | 0.63 |
| Strength and stiffness modulus | At 28 days | $E = 429.7 \times (UCS) + 8155.2$ | 0.81 |
| | | $E = 6033.4 \times ITS + 6024.3$ | 0.82 |
| | | $E = 4190.8 \times FTS + 3602.1$ | 0.73 |
| | | $E = 4580.3 \times FTS^a + 7749.4$ | 0.64 |

Note: *UCS* is unconfined compressive strength (MPa); *FTS* is flexural tensile strength (MPa), obtained from monotonic three-point bending test; *ITS* is indirect tensile strength (MPa); $FTS^a$ is the flexural strength (MPa, obtained from four-point bending test); E is stiffness modulus (MPa).

## 4.7 Conclusions

Laboratory tests including compression, indirect tensile, flexural tensile and fatigue tests were carried out to investigate the effect of Rc additive on the mechanical properties of cement stabilized sand materials. For each physical parameter, variable factors consisting of cement and Rc contents and curing time were taken into account. Based on the laboratory test results, the effect of the variable factors were analyzed and estimation models for the mechanical strength were obtained. Additionally, four-point bending tests were performed to obtain the stiffness modulus and fatigue

properties of all the mixtures. The principle findings of this Chapter can be summarized as below:

- Cement and Rc additive both contribute to the compressive, indirect tensile and flexural tensile strength of cement stabilized sand materials. Addition of Rc additive leads to higher strength of cement stabilized sand. The strength improvement by adding Rc additive in sand-cement mixtures is generally in a range of 10% to 30%.
- The mechanical strength of cement stabilized sand is also closely related to the curing time. The strength increases substantially from 3 to 7 days, and then steadily increases until 28 days, but after 28 days the strength generally remains constant, which is applicable to compressive, indirect tensile and flexural tensile strength.
- Estimation models to predict the mechanical strength of cement stabilized sand materials are developed, based on the combined effect of cement and Rc contents, density of the specimen and the curing time. These estimation models exhibit a satisfactory approximation of the test data and thus can be adopted for use.
- The stiffness modulus of the cement stabilized materials is influenced by the applied strain. As the strain increases, the stiffness modulus significantly decreases until failure. Addition of a certain amount of Rc additive appears to enable the beam specimen to withstand a higher strain before failure.
- Regarding the strain at break and flexural strength obtained from four-point bending test, the Rc content has a positive influence on the strain at break but no clear influence on the flexural strength. On the contrast, the cement content increases the flexural strength but has no observed influence on the strain at break. Based on the calculation from the linear-elastic multilayer program, as the Rc content increases from 0.56 to 3.2 kg/m$^3$, the maximum bearing load of the base layer increases on average by 45%.
- At different loading frequencies the stiffness modulus of the cement stabilized sand materials remains almost constant and it means that the frequency of dynamic loading does not influence the stiffness modulus of sand-cement materials.
- Fatigue relations with the number of load cycles to failure as a function of applied stress level or the initial strain level are obtained for all the tested

mixtures. However, these fatigue relations are much dependent on the mix design. The $k_2$ value of the stress-based fatigue relations ranges from 12 to 16 indicating a large slope of fatigue lines and rather brittle behavior of cement stabilized sand materials.

- Correlations between the mechanical properties have been given, based on compressive strength and tensile strength as well as the stiffness modulus, which can be used to estimate the mechanical properties.

## References

ACI (1998). ACI Manual of concrete practice: Part 1 (No. ACI 209R-92). U.S.A., Farmington Hills: ACI committee 230.

Babic, B. (1987). Relationships between mechanical properties of cement stabilized materials. Materials and Structures 20(6): 455-460.

Crockford, W.W., & Little, D.N. (1987). Tensile fracture and fatigue of cement-stabilized soil. Journal of transportation engineering, 113(5), 520-537.

Consoli, N.C., A.V. da Fonseca, et al. (2011). Voids/Cement Ratio Controlling Tensile Strength of Cement Treated Soils." Journal of geotechnical and geo environmental engineering 1(1): 306.

Dempsey, B.J., & Thompson, M.R. (1973). Effects of freeze-thaw parameters on the durability of stabilized materials. University of Illinois.

Hudson, W.R. & Kennedy T.W. (1968). An Indirect Tensile Test for Stabilized Materials. Research Report 98-1. Center for Highway Research, University of Texas at Austin, USA.

Ghuzlan, K.A., & Carpenter, S.H. (2002). Traditional fatigue analysis of asphalt concrete mixtures. Urbana, 51, 61801.

Kersten, M.S. (1961). Soil Stabilization with Portland Cement. National Academy of Sciences National Research Council, Washington, D. C., USA.

Kolias, S.,V. Kasselouri-Rigopoulou, et al. (2005). Stabilization of clayey soils with high calcium fly ash and cement." Cement and Concrete Composites 27(2): 301-313.

Little, D.N. (2009). Recommended Practice for Stabilization of Subgrade Soils and Base Materials. NCHRP web-only document 144. Texas A&M University, Texas.

NEN-EN 12386-41. Test method for the determination of the compressive strength of hydraulically bound mixtures.

NEN-EN 12386-42. Test method for the determination of the indirect tensile strength of hydraulic bound mixtures.

EN 199-1-1. (2005). Design of concrete structures-part 1-1: General Rules and Rules for buildings. Brussels: Europe Committee for stabilization.

ENE-EN 12697-24 (2012). Test methods for hot mix asphalt-Part 24: Resistance to fatigue.

Monismith, C.L., Epps, J.A., Kasianchuk, D.A., and McLean, D.B. (1970). Asphalt Mixture Behavior in Repeated Flexure, Report No. TE 70-5, Institute of Transportation and Traffic Engineering, University of California, Berkeley.

Molenaar, A. A. A., & Pu, B. (2008). Prediction of fatigue cracking in cement treated base courses. Proceedings of 6th RILEM International Conference on Cracking in Pavements (pp. 191-199).

Neville, A.M. (1996). Properties of Concrete (4th and final ed.). Wiley, New York.

Pretorius, P.C. and Monismith, C.L. (1971). The prediction of shrinkage stresses in pavements containing soil cement bases. Paper presented at the Annual Meeting of the Highway Research Board, Washington, D.C.

Ramakrishnan, V., Wu, G. Y., and Hosalli, G. (1989). Flexural Fatigue Strength, Endurance limit, and Impact Strengths of Fiber Reinforced Concretes, Transportation Research Record No. 1226, Washington, D.C., pp. 17.

Sherwood, P.T. (1968). The properties of cement stabilized Materials. Road Research Laboratory, Crowthorne, UK.

Terrel, R.L., Epps, J.A., Barenberg, E.J., Mitchell, J.K., & Thompson, M.R. (1979). Soil stabilization in pavement structures, a User's manual-volume 1: pavement design and construction considerations (No. FHWA-IP-80-2). Washington D.C: federal Highway Administration, Department of Transportation.

TRH 13 (1986). Cementitious Stabilizers in Road Construction South Africa. Pretoria, South Africa.

Xuan, D.X. (2012). Cement Treated Recycled Crushed Concrete and Masonry Aggregates for Pavements. PhD dissertation, Delft University of Technology, Delft, the Netherlands.

Williams, R.I.T. (1986). Cement treated pavements: Materials, Design, and construction. Elsevier Applied Science Publishers, London.

# CHAPTER 5

# CEMENT STABILIZED CLAY WITH ROADCEM ADDITIVE

Serious soil problems in road engineering are often associated with fine-grained materials such as clay. The principal concerns regarding the utilization of clay soil as road material are the volumetric changes as a function of variation in moisture. If the clay soil has a high LL and a high PI, it has a high potential of swell and shrinkage. The instability of this material may result in an uneven pavement surface, rutting and increased susceptibility to deterioration of the pavement structure. The poor characteristics of clay soil can be upgraded by means of stabilization. However, high plastic clay soil is not favoured in cement stabilization mainly due to the fact that clay material generally requires more cement for satisfactory hardening and is usually more difficult to pulverize for proper mixing (ACI, 1990).

This Chapter aims to assess the effect of Rc additive on the properties of cement stabilized clay materials. The test program conducted on stabilized clay soil follows the same test methods used for stabilized sand material. The structure of this Chapter follows the same pattern as the previous Chapter, consisting of analyzing the effect of the variable factors on the mechanical properties, obtaining estimation models as well as exploring the correlation between different mechanical properties.

## 5.1 Background

### 5.1.1 Mechanisms of stabilization of clay with cement and lime

Cement and lime are considered as efficient stabilizers for clay materials in terms of reducing plasticity and improving the engineering properties. The interaction between cement or lime and clay is complex due to the presence of variable clay minerals. Many researchers have reported the mechanism of stabilization of clay with calcium-based stabilizers such as cement and lime and mainly illustrated it as the following processes in order of occurrence:

- Cation exchange
- Flocculation and agglomeration
- Cementitious hydration
- Pozzolanic reaction

These four processes are discussed in the followings, mainly referring to literature studies (Molenaar, 2010; Prusinski & Bhattacharja, 1999; Halsted, 2011; Shon, 2010)

(1) Cation exchange

There are three main groups of clay minerals commonly found in clay soil: kaolinite, illite and montmorillonite. The montmorillonite content is regarded as the main factor determining the plasticity of clay soil. This mineral is formed by one alumina octahedral layer sandwiched between two silicate tetrahedral layers. The surface of this mineral is negatively charged and it has a strong cation exchange capacity. To balance the charge deficiency, cations ($Na^+$ and $K^+$) and water molecules can enter the interlayers and become attracted to the negatively charged sites, resulting in electrical charged surfaces, commonly called as a "diffuse double layer". These adsorbed cations are exchangeable. When a calcium-based stabilizer is introduced, positively charged calcium ions ($Ca^{2+}$) are available in the solution and are able to replace cations ($Na^+$ and $K^+$) with the lower valence. The replacement of the cation generally takes place in the following order:

$$Na^+ < K^+ < Mg^{2+} < Ca^{2+} < Al^{3+} \quad (5\text{-}1)$$

Equation 5-1 means that the $Ca^{2+}$ will replace $Mg^{2+}$ which will in turn replace $Na^+$. On cation exchange, the highly charged cations tend to be held more tightly than those with less charge, and cations with smaller hydrated radius bond more tightly to the clay surface in such a way that the space between clay minerals is reduced, resulting

to reduced thickness of the diffuse double layer (Shon, 2010). Figure 5.1 indicates the mechanism of cation exchange.

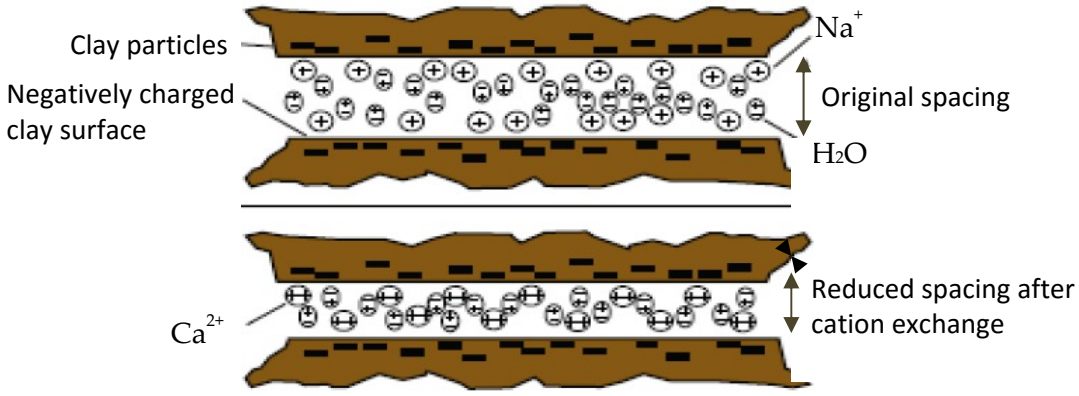


**Figure 5.1** Mechanism of cation exchange (Prusinski & Bhattacharja, 1999)

(2) Flocculation and agglomeration

Flocculation and agglomeration is known as modification of the clay texture from fine-grained soil particles into larger aggregate sizes. This process involves altering the clay particle arrangement from a flat and parallel structure to a more random orientation of the clay particles due to reduced thickness of the double layer, high electrolyte concentration and high pH environment (Prusinski & Bhattacharja, 1999). Moore and Reynolds (1989) attribute this flocculation process to van der Waals force which occurs when the particles approach one another closely and binds the particles together into composites or clumps, resulting in a granular-like material, shown in Figure 5.2.

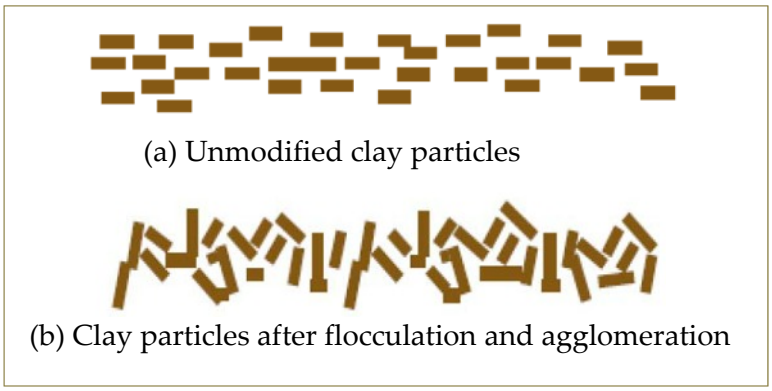


**Figure 5.2** Particle rearrangement (Prusinski & Bhattacharja, 1999)

The cation exchange as well as flocculation and agglomeration process leads to reduction in the plasticity of clay materials, increased internal friction among the modified soil texture and better workability for moulding. As with cation exchange, flocculation and agglomeration occur rapidly within several hours after mixing with cement or lime (Prusinski & Bhattacharja, 1999).

(3) Cementitious hydration

The main components of Portland cement are tricalcium silicates ($C_3S$), dicalcium silicates ($C_2S$), tricalcium aluminates ($C_3A$) and tetracalcium aluminoferrite ($C_4AF$) (where C=CaO, S=$SiO_2$, A=$Al_2O_3$ and F=$Fe_2O_3$). When Portland cement is mixed with water, hydration is initiated and produces calcium silicate hydrate (C-S-H) and calcium hydroxide ($Ca(OH)_2$). The cementitious reaction is schematically shown in Figure 5.3 (a). The hydration reaction is presented in the following equations (Prusinski & Bhattacharja, 1999).

$$2C_3S + 6H_2O \rightarrow C_3S_2H_3 + 3Ca(OH)_2 \quad (5\text{-}2)$$

$$2C_2S + 4H_2O \rightarrow C_3S_2H_3 + Ca(OH)_2 \quad (5\text{-}3)$$

The hydrate gel (C-S-H) serves as a "glue" and binds the flocculated clay particles. The cement hydrates develop a strong bond between hydrating cement and clay particles and provide the strength.

(4) Pozzolanic reaction

The high pH environment of the calcium-based system, due to the formation of $Ca(OH)_2$ in lime solution or from the cement hydration, enables silica and alumina to solubilize from the clay lattice. The solubilized soil silica and alumina may react with calcium ions which are released from $Ca(OH)_2$ and form into additional cementitious products (C-S-H and C-A-H) (Little, 2003). This process is generally referred to as pozzolanic reaction, indicated in Figure 5.3 (b) and the chemical equations are shown as below:

$$Ca(OH)_2 + SiO_2\,(clay\ silica) \rightarrow C - S - H \quad (5\text{-}4)$$

$$Ca(OH)_2 + Al_2O_3\,(clay\ alumina) \rightarrow C - A - H \quad (5\text{-}5)$$

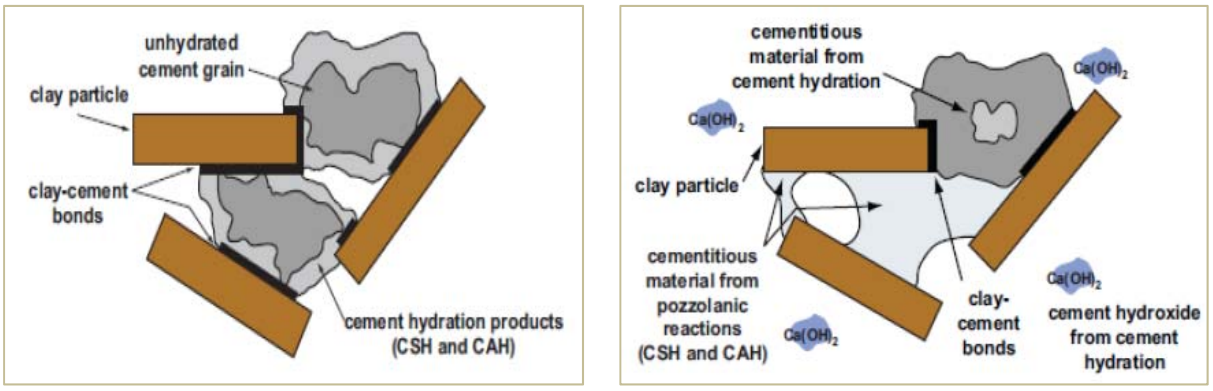


(a) Cementitious reaction (cement only) (b) Pozzolanic reaction

**Figure 5.3** Chemical reaction between clay and calcium-based stabilizer (Prusinski & Bhattacharja, 1999; Halsted, 2011)

In a cement-stabilized system, the cementitious reaction produces calcium hydroxide and creates a high pH environment, causing silica and alumina solubilized from clay particle. High pH is favoured by pozzolanic reaction because increasing pH in soil solution can increase the reactivity and dissolution of the clay minerals (Little, 2009). For cement stabilization, the cementitious reaction produces the main hydration product and provides the main strength of the structure while pozzolanic reaction is the secondary process and takes place slowly, over months and years, and it can further contribute to the strength (Prusinski & Bhattacharja, 1999, Rafalko et al., 2007). Therefore, compared with the stabilization of sandy soil, when clay soil is involved in cement treatment the resulting product can't be regarded as a simple mixture in which hydrated cement binds unaltered clay particles, but as a system in which secondary cementing reactions take place (Williams, 1986).

### 5.1.2 Engineering properties of stabilized clay with cement or lime

Lime is traditionally considered as an effective stabilizer for most cohesive soils while cement is more efficient for granular materials (Ingles, 1972). For high plastic clay soils, lime may be used as a pre-treatment to reduce plasticity and make the soil more susceptible to pulverization prior to mixing with cement (ACI, 1990), because the lime-soil reaction, which mainly involves cation exchange and short-term pozzolanic reactions, results in larger particle agglomerates and workable soils (Little, 2009). Since the strength of lime-stabilization relies on the pozzolanic reaction, Little (2009) mentioned that the level of reactivity between soil and lime depends on the type and amount of clay minerals in the soil. For example, some clay soils may not be pozzolanically reactive, and even though the application of lime initially reduces plasticity and improves workability, the desired strength gain doesn't develop due to the lack of sufficient pozzolanic reactions. Therefore, in this case the stabilizer has to be cement or combining lime with cement.

Apart from lime, fly ash is also a promising stabilizer for clay soil and it has been extensively evaluated and significant strength improvement of clay treated with fly ash was reported in many studies (Solanki, 2010; Parsons, 2003; Kolias et al., 2005). However, fly ash is a by-product from burning coal during power generation and therefore the properties of fly ash can vary significantly depending on the source of the coal and the steps followed in the coal burning process (Little, 2009).

On the basis of the literature survey, a large number of comparative studies on stabilizing clay with cement and lime (Bhattacharja & Bhatty, 2003; Achampong, 1997; Prusinski, 1999; Jauberthie, 2010) concluded that cement is as effective in reducing

plasticity of clay as lime and the compressive strength of cement-stabilized soil is generally much higher than that of lime-stabilized soil at all curing ages. One example is shown in Table 5.1 which compares the effect of cement and lime on the plasticity index, shrinkage limit and the compressive strength of treated clay.

Plasticity index is a rough measure for the swell potential and PI >25 indicates great swell potential (Molenaar, 2010). As indicated in Table 5.1, cement and lime accomplish a similar reduction in PI and increase in shrinkage limit at similar content levels. Cement generally produces a much higher strength than lime at all ages.

**Table 5.1** Average change in properties for clay soils (Christensen, 1969)

| % Stabilizer | Plasticity Index | Shrinkage Limit | Improvement of UCS with stabilizer | |
|---|---|---|---|---|
| | | | 7-day | 28-day |
| 3% Cement | -52% | 122% | 468% | 605% |
| 5% Cement | -64% | 158% | 775% | 993% |
| 3% Lime | -55% | 123% | 183% | 348% |
| 5% Lime | -64% | 151% | 266% | 481% |

Besides, another comparative study by Scullion et al (2005), on stabilizing clay (LL=45, PI=28) also supports this finding, Figure 5.4 (a). It can be seen that a cement content of about 3% or 4% (by mass) would reduce the PI sufficiently. Again, the compressive strength of cement stabilized clay is much higher than using lime regardless of the application methods of the stabilizer, Figure 5.4 (b).

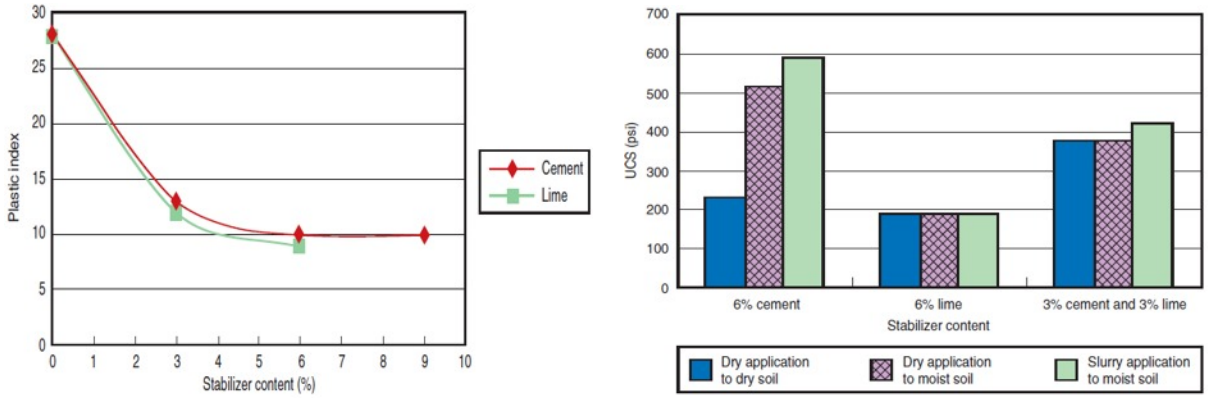


(a) (b)

**Figure 5.4** Plasticity index (PI) and 21-day compressive of clay-cement and lime-cement (Scullion et al., 2005)

This Chapter aims to investigate the effect of Rc additive on the mechanical properties of cement stabilized clay materials, with focus on the comparison of the performance of stabilized clay with variable cement and Rc contents.

## 5.2 Unconfined compressive strength

The compressive, indirect tensile and flexural tensile strength tests are performed in the same way as conducted on sand-cement materials, as illustrated in Chapter 4. Test data for all the clay-cement mixtures are presented in Appendix B. For each item three specimens were tested.

### 5.2.1 Test data and analysis with variable factors

In the mix design for the clay soil, the cement and Rc contents (by dry mass of soil) are two independent factors which mainly contribute to the properties of the stabilized material. In order to visualize the effect of these two factors on the compressive strength of clay-cement mixtures, Figure 5.5 presents the average compressive strength results for each mix design covering all curing times. Each data is the average value of three tested specimens and the highest strength at each curing time is indicated by the blue dot. The mix compositions of all the mixtures are presented together with the average strength data at 3 days, shown as (Rc content, cement content, in kg/m$^3$).

For reason of comparison with the estimated data, the compressive strength derived from the estimation model (equation 5-11), is also indicated herein by means of colors. The compressive strength increases from the color of orange to yellow and reaches the highest values marked in dark colors (black for 3 days, purple for 7 days, blue for 28 days and green for 91 days) indicating a compressive strength higher than 5, 7, 10 and 12 MPa, respectively. The estimation models for the compressive strength will be discussed in section 5.2.2.

It can be seen in Figure 5.5 that the highest compressive strength at each curing time is observed in the mixture (1.9, 270) with the Rc content 1.9 kg/m$^3$ and the highest cement content 270 kg/m$^3$, shown as the blue dot. This result is different from the compressive strength of sand-cement material which shows that the mixture exhibiting the highest compressive strength varies at different curing time. In addition to this, it has also to be noted that the relatively high values of compressive strength (indicated by the dark colors) obtained from the estimation model also tend to be in the mixture (1.9, 270) with the highest amount of cement.

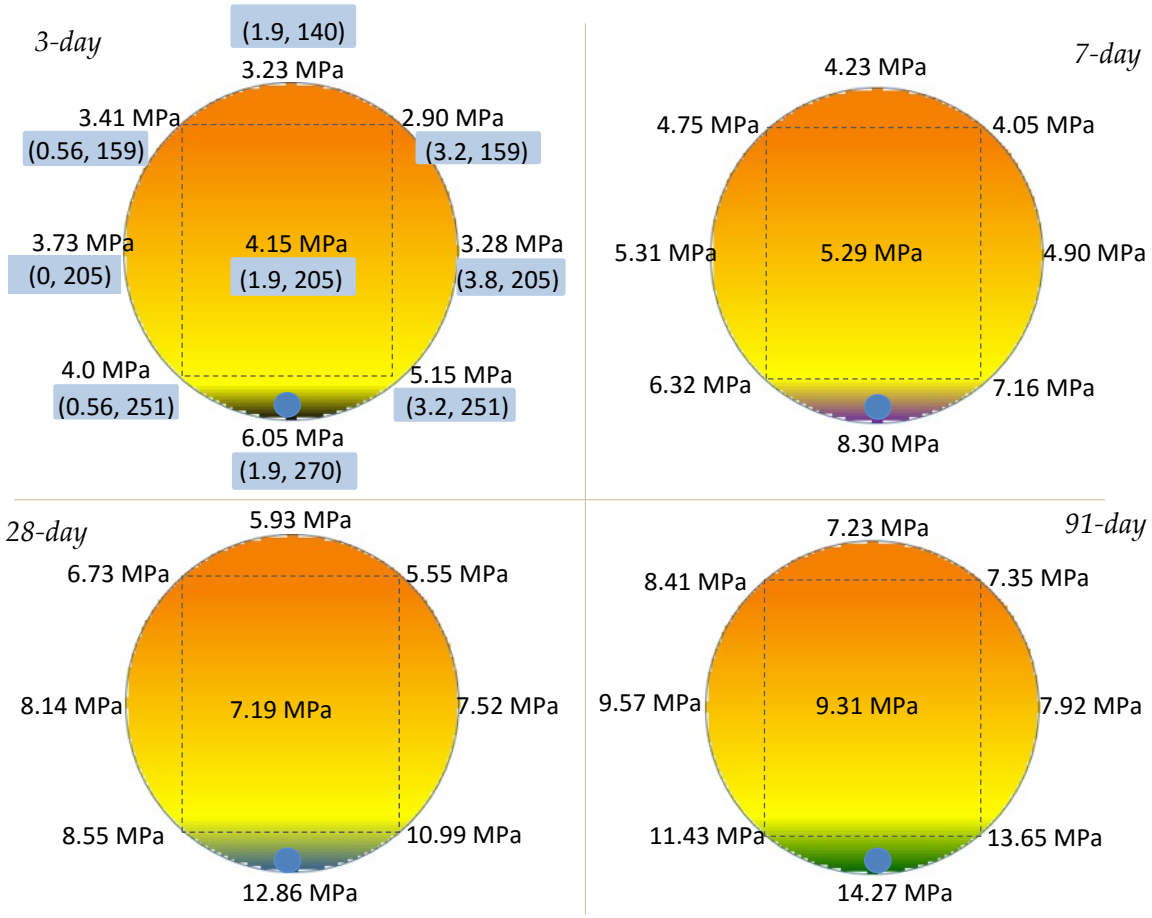


**Figure 5.5** Average compressive strength of all the clay-cement mixtures

In Figure 5.5 the influence of Rc content is variable at different cement levels. For instance, for the mixtures with cement content 159 and 205 kg/m$^3$, rise of the Rc content doesn't result in a higher compressive strength. However, when the cement content increases to 251 kg/m$^3$, more Rc in the mixture leads to a higher compressive strength by around 20% at 91 days. It is probably because that higher cement and Rc contents may react more sufficiently which can be observed in the changes of compressive strength.

Curing time is another important factor contributing to the properties of cement stabilized materials. Figure 5.6 illustrates the compressive strength of all the stabilized clay mixtures as a function of the curing time. Each value represents the average compressive strength of three tested specimens.

In Figure 5.6 it can be seen that the compressive strength keeps increasing until 91 days. This is different from the sand-cement material which exhibits a nearly constant strength after 28 days (see Figure 4.3). It is because in clay-cement material, pozzolanic reactions take place that continue to contribute to further strength development, which is caused by the reaction between the solubilized silica and

alumina from the clay soil and the calcium ions which are released from $Ca(OH)_2$, as discussed earlier.

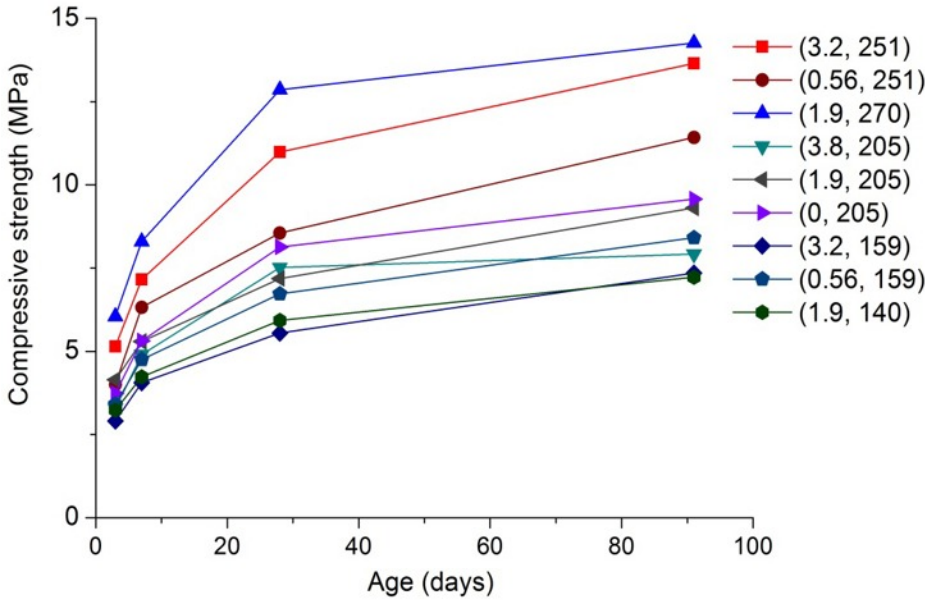


**Figure 5.6** Average compressive strength of all clay-cement mixtures at different ages

Furthermore, in Figure 5.6 the rate of increase of the compressive strength at different time intervals is variable. For instance, the increase of this strength from 3 to 7 days is in a range from 30% to 50% based on all the mixtures and the rate of increase remains nearly the same from 7 to 28 days, but after 28 days the rate is much lower which is about 20% for most of the mixtures. Besides, different mixtures exhibit variable increasing rates, for instance, the strength of the mixtures (1.9, 270) and (3.2, 251) with relatively high cement contents still increases substantially from 7 to 28 days. Additionally, the mixture (1.9, 270) with Rc 1.9 kg/m$^3$ and highest amount of cement leads to the highest compressive strength at all curing ages.

### 5.2.2 Estimation model of compressive strength (UCS)

The variable factors evaluated in this research include the cement and Rc contents, the density of the compacted specimen and the curing time. These variable factors will be taken into account into the estimation model for the compressive strength of clay-cement material. The general procedures to obtain the estimation models for stabilized clay are the same as used for stabilized sand materials (as illustrated in Chapter 4).

***(1) Influence of cement and Rc contents on the compressive strength***

Estimation models are obtained by firstly considering the effect of the mix variables at each curing time and then obtaining an overall model including the influence of

the curing time. The influence of each factor will be verified by the same statistical functions as used for the sand-cement materials, for instance, the Rc content is evaluated by two types of functions: exponential and linear relations.

Figure 5.7 shows the estimation models with combined effects of cement and Rc contents and density, which is based on all the tested mixtures at the curing period of 7 days. In this study, C, Rc and D represent the cement content, additive content and density of the specimen (kg/m$^3$), respectively.

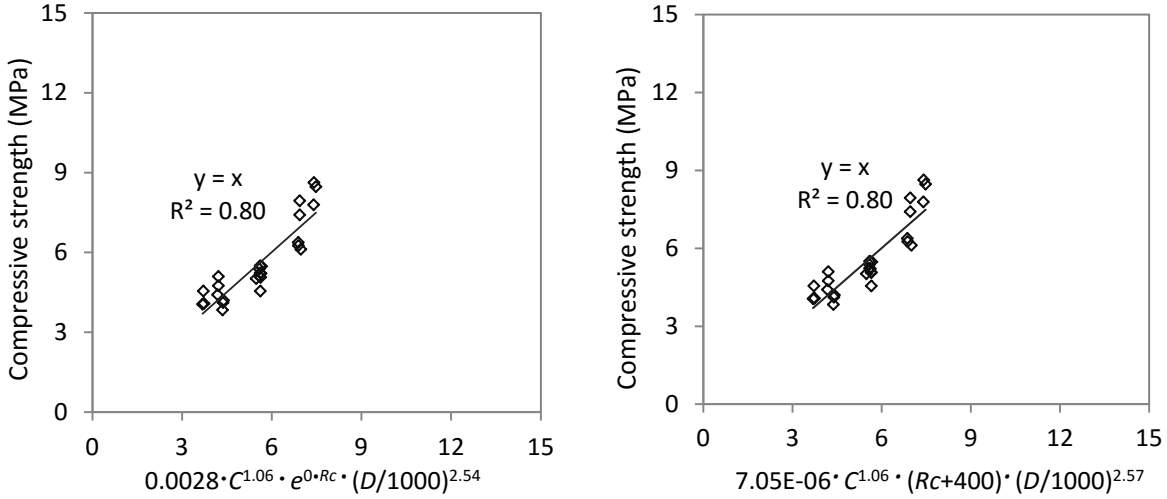


(a) Exponential function (b) Linear function

**Figure 5.7** Estimation models of compressive strength with effects of cement and Rc contents and density (t = 7 days)

In Figure 5.7 the two estimation models to predict the compressive strength at 7 days can be described as follows:

$$UCS\ (7\text{d}) = 0.0028 \cdot C^{1.06} \cdot e^{0 \cdot Rc} \cdot \left(\frac{D}{1000}\right)^{2.54} \qquad R^2=0.80 \qquad (5\text{-}6)$$

$$UCS\ (7\text{d}) = 7.05 \cdot 10^{6} \cdot C^{1.06} \cdot (Rc + 400) \cdot \left(\frac{D}{1000}\right)^{2.57} \qquad R^2=0.80 \qquad (5\text{-}7)$$

Where, $UCS$ is unconfined compressive strength (MPa); $C$ is cement content (kg/m$^3$); $Rc$ is additive content (kg/m$^3$); $D$ is density of specimen (kg/m$^3$).

It is found that in the exponential function model the Rc content doesn't show clear relation to the estimated compressive strength. Similarly, the linear function model indicates that the influence of the Rc content is very limited since the term of coefficient 400 would mask any contribution of Rc content which ranges from 0 to 3.8.

For the purpose of estimation, these two models achieve the same $R^2$ and the exponential function of Rc content is adopted for use, expressed as follows:

$$UCS = \text{a} \cdot C^{n_1} \cdot e^{n_2 \cdot Rc} \cdot \left(\frac{D}{1000}\right)^{n_3} \qquad (5\text{-}8)$$

With consideration of the curing time, the above estimation model is subsequently applied to approximate the test data at the individual curing time, shown in Figure 5.8. The parameters for each variable factor as influenced by the curing time to achieve an acceptable coefficient of determination $R^2$ are shown in Table 5.2.

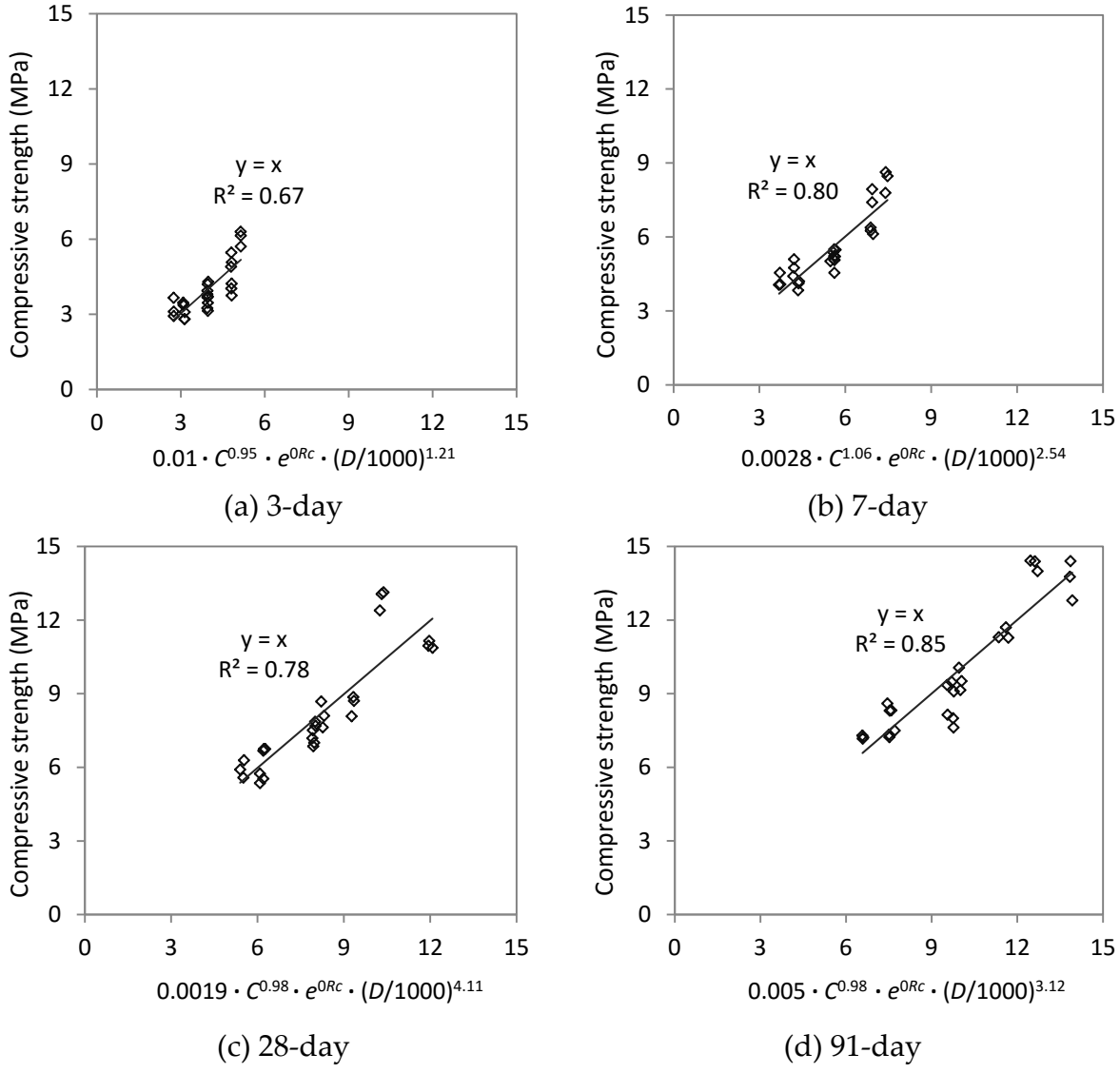


**Figure 5.8** Estimation models of compressive strength at different curing times

**Table 5.2** Coefficients for the estimation models at different curing times

| Curing time | $UCS = \mathrm{a} \cdot C^{n_1} \cdot e^{n_2 \cdot Rc} \cdot (\frac{D}{1000})^{n_3}$ | | | | |
|---|---|---|---|---|---|
| | a | $n_1$ | $n_2$ | $n_3$ | $R^2$ |
| 3-day | 0.01 | 0.95 | 0 | 1.21 | 0.67 |
| 7-day | 0.0028 | 1.06 | 0 | 2.54 | 0.80 |
| 28-day | 0.0019 | 0.98 | 0 | 4.11 | 0.78 |
| 91-day | 0.005 | 0.98 | 0 | 3.12 | 0.85 |

In Table 5.2 the coefficients for the cement and Rc contents exhibit almost constant values which is around 0.98 and 0, respectively, throughout 4 different curing times. It implies that the effects of cement and Rc contents on the estimation models of compressive strength are independent of the curing time. It has to be noted that the effect of the Rc content doesn't appear to be related to the compressive strength in these models. Therefore, the effects of cement and Rc contents on the compressive strength model can be expressed as the coefficients 0.98 and 0, respectively. In contrast, the coefficients "a" and "$n_3$" in equation (5-8) vary largely for the different curing times, and appropriate values for "a" and "$n_3$" (for density) can be obtained when incorporating the influence of the curing time.

***(2) Influence of curing time on the compressive strength***

In Chapter 4, the factor curing time for sand-cement mixtures is evaluated by four different statistical models: log-scale, exponential, ACI and power-function models and these models have generally achieved satisfactory estimation relations. Similarly, these four models are also employed to evaluate the influence of the curing time for clay-cement material. Figure 5.9 presents the estimation models with influence of curing time which is evaluated by these four functions. Each graph includes the test data of all the clay-cement mixtures at all evaluated curing times.

The estimation models shown in Figure 5.9 can be described as the following equations:

$$UCS = 0.0043 \cdot C^{0.98} \cdot e^{0 \cdot Rc} \cdot \left(\frac{D}{1000}\right)^3 \cdot \left(1 + 0.58 \cdot \log\left(\frac{t}{28}\right)\right) \qquad R^2 = 0.92 \qquad (5\text{-}9)$$

$$UCS = 0.0016 \cdot C^{0.98} \cdot e^{0 \cdot Rc} \cdot \left(\frac{D}{1000}\right)^3 \cdot \left(\frac{t}{1.43 + 0.29 \cdot t}\right) \qquad R^2 = 0.91 \qquad (5\text{-}10)$$

$$UCS = 0.0045 \cdot C^{0.98} \cdot e^{0 \cdot Rc} \cdot \left(\frac{D}{1000}\right)^3 \cdot e^{0.5 \cdot \left(1 - \left(\frac{28}{t}\right)^{0.39}\right)} \qquad R^2 = 0.92 \qquad (5\text{-}11)$$

$$UCS = 0.0018 \cdot C^{0.98} \cdot e^{0 \cdot Rc} \cdot \left(\frac{D}{1000}\right)^3 \cdot t^{0.248} \qquad R^2 = 0.90 \qquad (5\text{-}12)$$

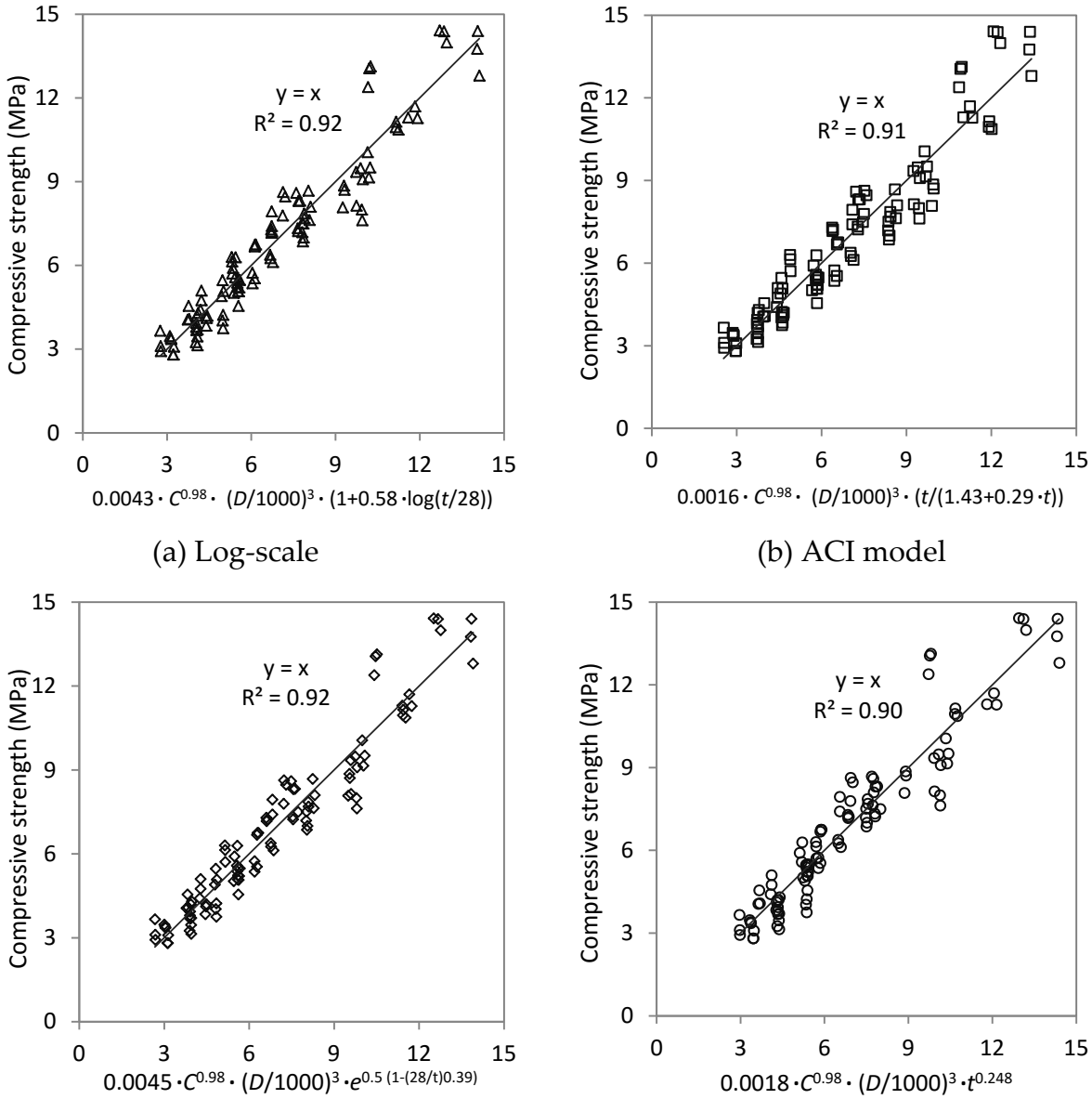


(a) Log-scale (b) ACI model

(c) Exponential model (d) Power-function model

**Figure 5.9** Estimation models of compressive strength with curing time

It can be seen that the log and exponential functions (equations 5-9 and 5-11) both exhibit a good fit to the real data with high $R^2 = 0.92$. Therefore, these two models can both be adopted to estimate the compressive strength of stabilized clay material with the combined effects of mix variables, density and curing time.

***(3) Additional analysis of the obtained models***

The statistical models in Figure 5.9 are obtained based on all the 9 mix compositions with variable cement and Rc additive contents. According to these models, the Rc additive has no effect on the compressive strength. However, in the test data it can be observed that at the high cement level 251 kg/m$^3$, an increasing Rc additive content

can increase the compressive strength by 10% to 30% at different curing times. Besides, when the cement content is lower than 251 kg/m$^3$, increasing Rc content seems to slightly reduce the strength (as shown in Figure 5.5). This means the obtained overall models seem to exhibit certain limitations in approaching the test data at variable cement contents.

Therefore, attempts are made to further evaluate the obtained overall models by incorporating the factor of Rc additive, based on different cement contents, shown in Figure 5.10. In Figure 5.10, two separate models are obtained from the test data of the mix compositions with cement contents lower than 251 kg/m$^3$ (graph a; 6 mix compositions) and cement contents at and higher than 251 kg/m$^3$ (graph b; 3 mix compositions). These two models are based on the exponential model (equation 5-11) which shows the best fit, and thus it is chosen to be evaluated herein. The factor of Rc additive is expressed in exponential function. Each model includes the test data at all the curing times. In Figure 5.10, C represents the cement content.

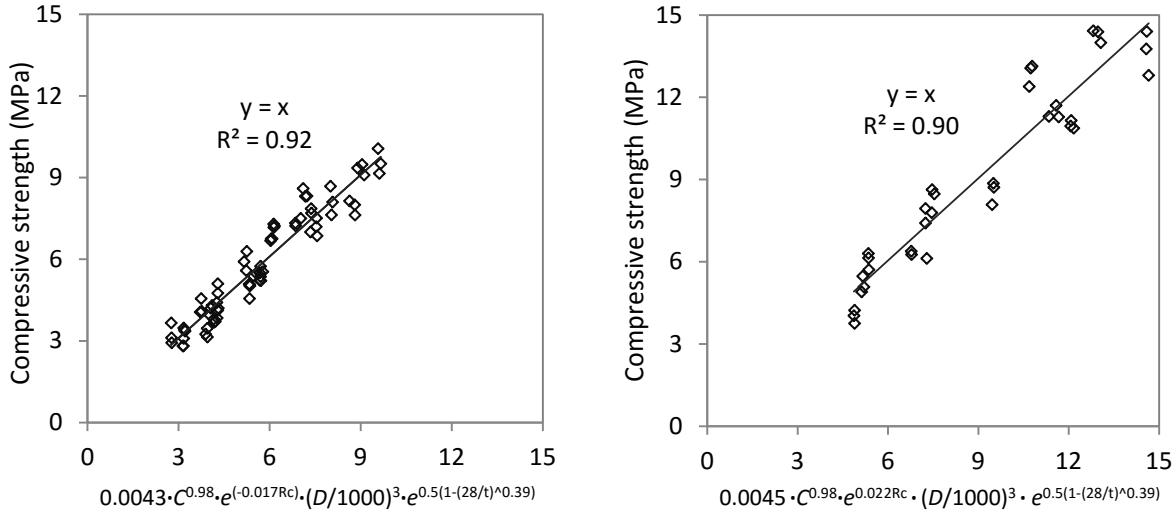


(a) 140 kg/m$^3$ ≤ C< 251 kg/m$^3$ (b) 251 kg/m$^3$ ≤ C ≤ 270 kg/m$^3$

**Figure 5.10** Estimation models of compressive strength at different cement contents

The estimation models in Figure 5.10 are shown as the following equations:

$$UCS = 0.0043 \cdot C^{0.98} \cdot e^{-0.017 \cdot Rc} \cdot \left(\frac{D}{1000}\right)^3 \cdot e^{0.5 \cdot \left(1 - \left(\frac{28}{t}\right)^{0.39}\right)} \qquad R^2 = 0.92 \qquad (5\text{-}13)$$

$$UCS = 0.0045 \cdot C^{0.98} \cdot e^{0.022 \cdot Rc} \cdot \left(\frac{D}{1000}\right)^3 \cdot e^{0.5 \cdot \left(1 - \left(\frac{28}{t}\right)^{0.39}\right)} \qquad R^2 = 0.90 \qquad (5\text{-}14)$$

As shown above, when the cement content is lower than 251 kg/m$^3$ the Rc additive content shows a slightly negative influence on the compressive strength but when the cement content is equal to and higher than 251 kg/m$^3$, the Rc additive content shows a positive influence on the compressive strength. However, the two

coefficients for the factors of Rc content are rather small, and therefore the overall estimation models in Figure 5.9 can be used.

## 5.3 Indirect tensile strength

### 5.3.1 Test data and analysis with variable factors

The indirect tensile strength test results for each mix design are presented in the design model, shown in Figure 5.11. It presents the indirect tensile strength test results for all the mixtures at different curing times and each data is the average value of three specimens. The blue dot represents the mixture which produces the highest measured indirect tensile strength at each curing time. Meanwhile, similar to the analysis of the compressive strength, the indirect tensile strength based on the estimation model (equation 5-18) (discussed later in this section) is also shown herein. The indirect tensile strength increases from the color of orange to yellow and reaches the highest values in the areas marked in dark colors (black, purple, blue and green colors representing the indirect tensile strength higher than 0.7, 1, 1.6 and 2 MPa, respectively).

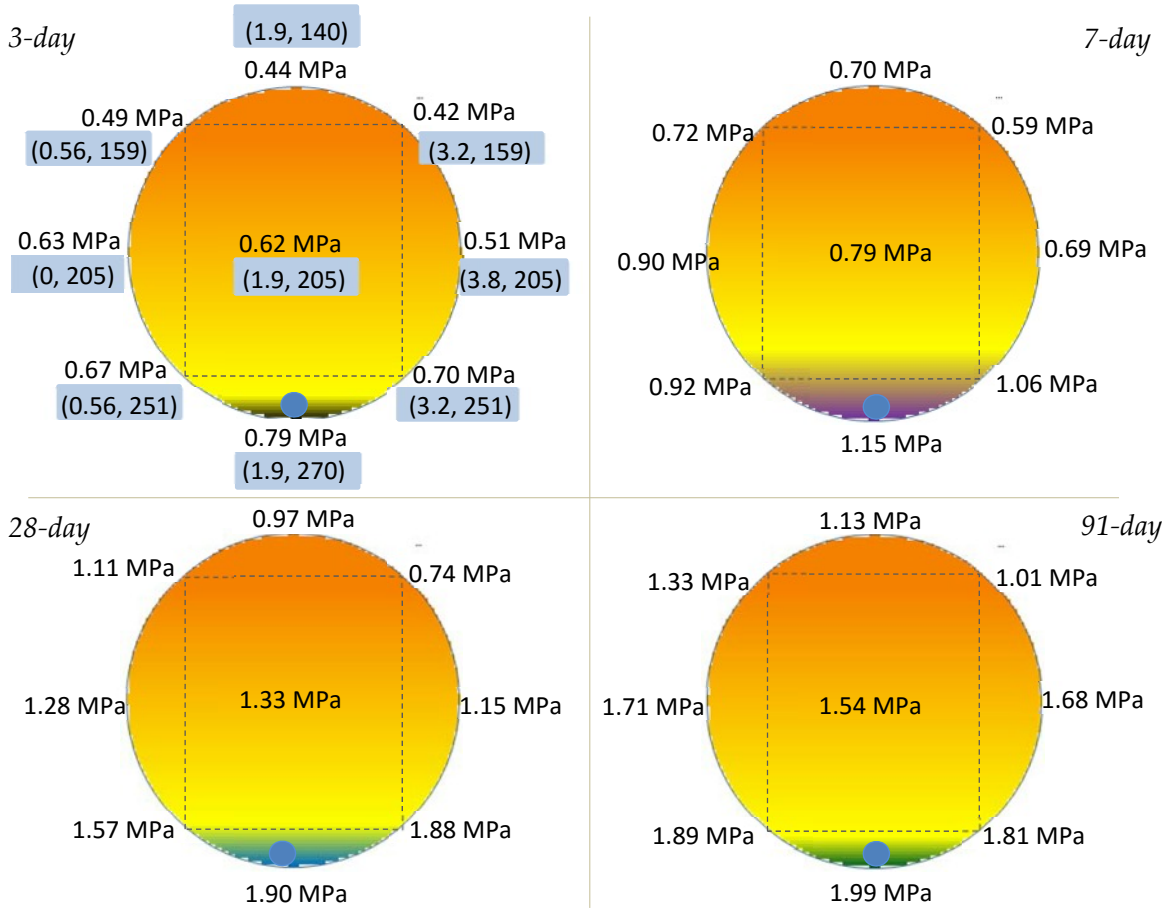


**Figure 5.11** Average indirect tensile strength of all the clay-cement mixtures

As can be seen in Figure 5.11, the indirect tensile strength of clay-cement material exhibits a similar pattern as the compressive strength which illustrates that the highest indirect tensile strength at all curing times is observed in the mixture (1.9, 270) with Rc additive 1.9 kg/m$^3$ and highest amount of cement 270 kg/m$^3$. Meanwhile, the highest values obtained from the estimation model at each curing time is also found to favour this mixture. This finding is consistent with the compressive strength.

Regarding the influence of the cement content, it is found that the higher the cement content, the higher the indirect tensile strength, which can be seen in the vertical direction showing mixtures with different cement contents. However, the indirect tensile strength of stabilized clay is generally low, especially at 3 days ranging from 0.42 to 0.79 MPa. The small range of strength values might cause difficulties in distinguishing the influences of cement or Rc content. For instance, the average 3-day strength of the mixtures (1.9, 140), (0.56, 159) and (3.2, 159) is nearly the same and hence it is not obvious to identify the contribution of either the cement or Rc contents.

Figure 5.12 gives the indirect tensile strength of all tested mixtures as a function of the curing age. Figure 5.12 includes the results of all tested mixtures at different curing times. Each data point is the mean value of three repeated test specimens.

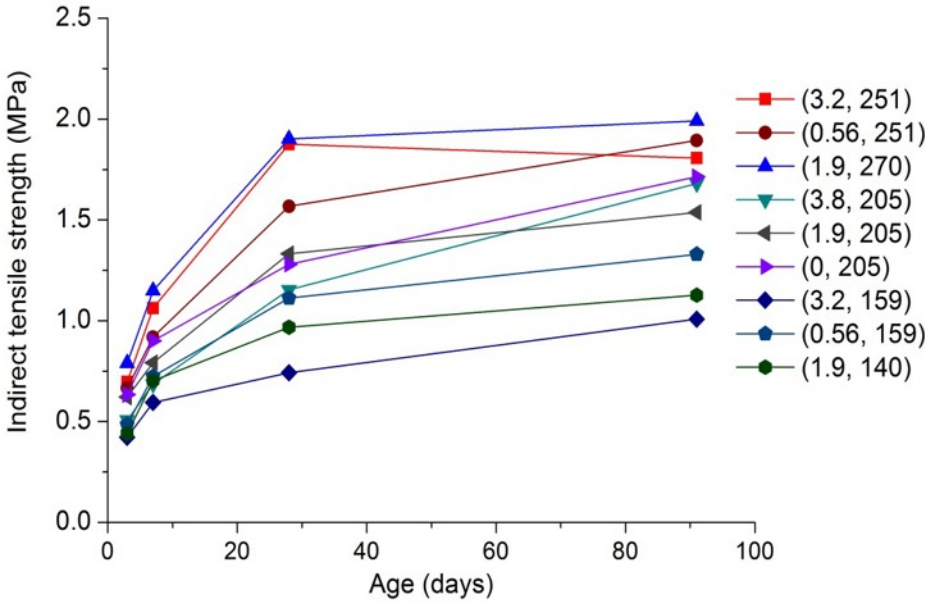


**Figure 5.12** Indirect tensile strength of all clay-cement mixtures at different ages

In Figure 5.12 it can be seen that the relation of the indirect tensile strength with the curing time is similar to that of the compressive strength. The indirect tensile strength substantially increases from 3 days to 7 days. For instance, the 7-day strength is generally 40 ~ 60% higher than the 3-day strength. When the curing time increases from 7 days to 28 days, the rate of increase stays around 60% for most of

the mixtures. But from 28 to 91 days the rate of increase is lower and remains within 20%. One exception occurs in mixture (3.2, 251) which shows a slightly lower 91-day strength.

### 5.3.2 Estimation model of indirect tensile strength (ITS)

#### *(1) Influence of cement and Rc contents on the indirect tensile strength*

To estimate the indirect tensile strength, the exponential function is also chosen to evaluate the influence of the Rc content to stay consistent with the estimation model of the compressive strength, shown as the following equation:

$$ITS = \mathrm{a} \cdot C^{n_1} \cdot e^{n_2 \cdot Rc} \cdot \left(\frac{D}{1000}\right)^{n_3} \quad (5\text{-}15)$$

Where, $ITS$ is indirect tensile strength (MPa); $C$ is cement content (kg/m$^3$); $Rc$ is additive content (kg/m$^3$); $D$ is density of specimen (kg/m$^3$).

Figure 5.13 shows the estimation models of the indirect tensile strength at different curing times by utilizing the exponential function for the Rc content. The parameters of these estimation models are summarized in Table 5.3.

**Table 5.3** Coefficients for the estimation models at different curing times

| Curing time | $ITS = \mathrm{a} \cdot C^{n_1} \cdot e^{n_2 \cdot Rc} \cdot (\frac{D}{1000})^{n_3}$ | | | | |
|---|---|---|---|---|---|
| | a | $n_1$ | $n_2$ | $n_3$ | $R^2$ |
| 3-day | 0.0019 | 0.91 | 0 | 1.12 | 0.76 |
| 7-day | 0.0024 | 0.91 | 0 | 1.22 | 0.69 |
| 28-day | 0.00038 | 1.20 | 0 | 2.28 | 0.82 |
| 91-day | 0.0079 | 0.91 | 0 | 0.59 | 0.79 |

In Table 5.3 it can be seen that the coefficient of the cement content shows an almost constant value of 0.91. One exception is that the 28-day model has a slightly higher coefficient for the cement content which is probably caused by the large variation of the 28-day results. To keep the influence of the mix variables consistent, the coefficient of the cement content "$n_1$" is fixed as 0.91 for the following estimation models. Again, the coefficient of the Rc content is not found to show obvious correlation with the estimated indirect tensile strength. On the other hand, the curing time greatly influences the coefficients of "a" and "$n_3$" (for density D) and hence these two coefficients will be optimized by incorporating the effect of curing time.

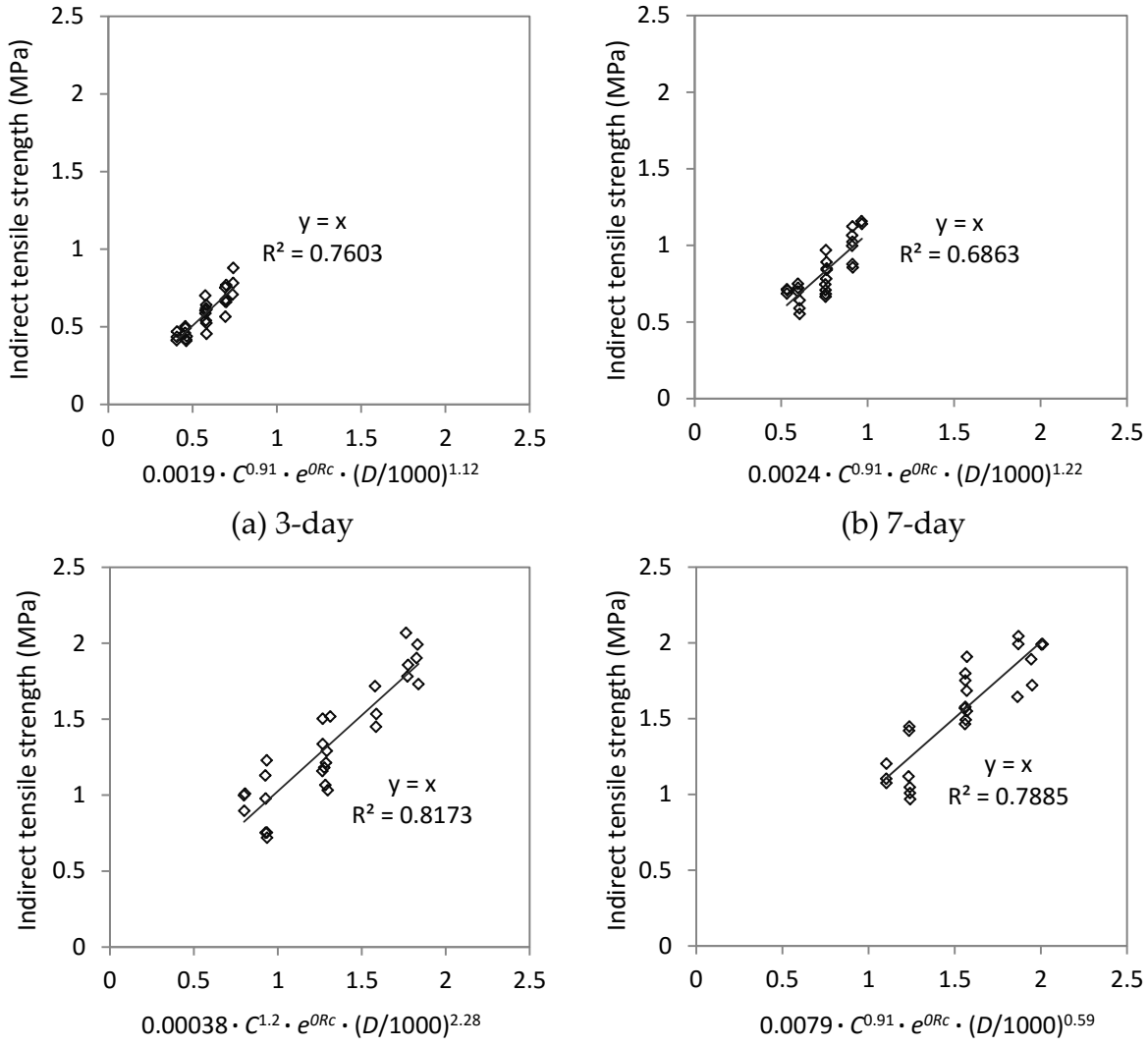


**Figure 5.13** Estimation models of indirect tensile strength at different curing times

***(2) Influence of curing time on the indirect tensile strength***

The influence of the curing time on the estimation model for the indirect tensile strength is also verified by four proposed statistical models which were used previously for estimating the compressive strength. Figure 5.14 presents the test data and the approximation models for the indirect tensile strength. The following figures are based on the experimental results of all evaluated clay-cement mixtures including all curing times.

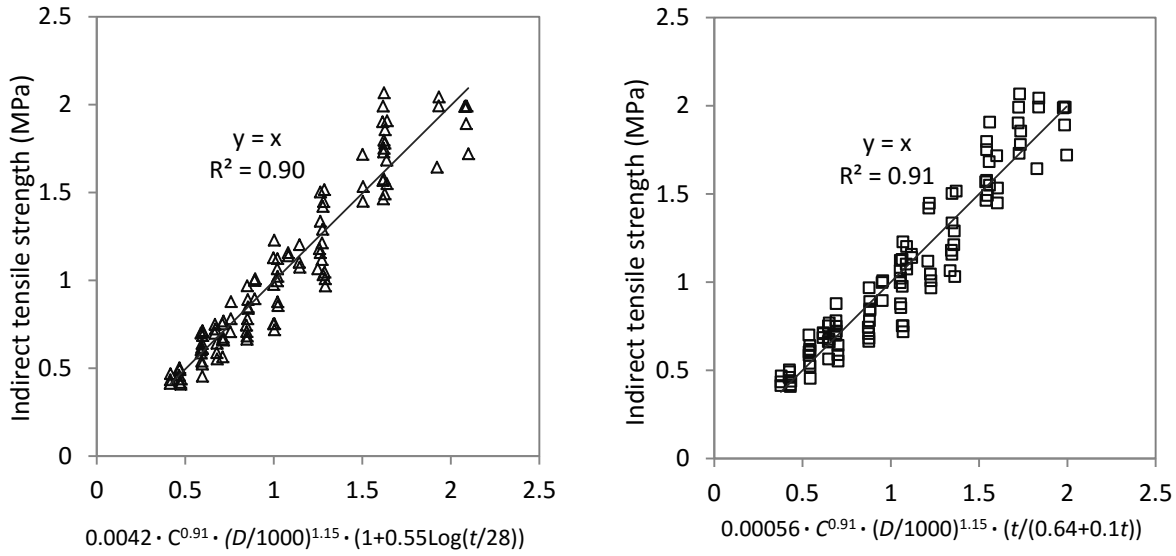


(a) Log-scale (b) ACI model

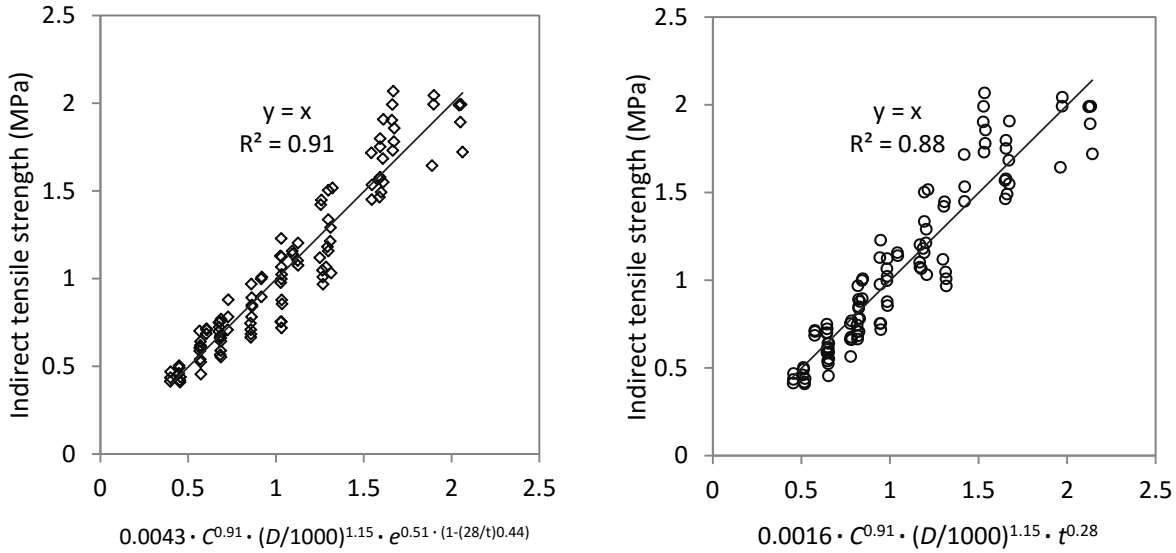


(c) Exponential model (d) Power-function model

**Figure 5.14** Estimation models of indirect tensile strength with curing time

The estimation models of indirect tensile strength shown in Figure 5.14 are described as follows:

$$ITS = 0.0042 \cdot C^{0.91} \cdot e^{0 \cdot Rc} \cdot \left(\frac{D}{1000}\right)^{1.15} \cdot \left(1 + 0.55 \cdot \log\left(\frac{t}{28}\right)\right) \quad R^2 = 0.91 \quad (5\text{-}16)$$

$$ITS = 0.00056 \cdot C^{0.91} \cdot e^{0 \cdot Rc} \cdot \left(\frac{D}{1000}\right)^{1.15} \cdot \left(\frac{t}{0.64+0.1 \cdot t}\right) \quad R^2 = 0.91 \quad (5\text{-}17)$$

$$ITS = 0.0043 \cdot C^{0.91} \cdot e^{0 \cdot Rc} \cdot \left(\frac{D}{1000}\right)^{1.15} \cdot e^{0.51 \cdot \left(1 - \left(\frac{28}{t}\right)^{0.44}\right)} \quad R^2 = 0.91 \quad (5\text{-}18)$$

$$ITS = 0.0016 \cdot C^{0.91} \cdot e^{0 \cdot Rc} \cdot \left(\frac{D}{1000}\right)^{1.15} \cdot t^{0.28} \quad R^2 = 0.89 \quad (5\text{-}19)$$

Obviously, the first three estimation models all achieve $R^2$=0.91 and indicate a good approximating trend and thus they can be utilized for prediction of the indirect tensile strength of cement stabilized clay materials. Among these four models, the power-function model exhibits a somewhat lower $R^2$ which is 0.89. It implies that for estimating the indirect tensile strength of stabilized clay, the influence of curing time can be investigated by means of the log-scale, ACI and exponential models which would achieve nearly the same approximating trend.

***(3) Additional analysis of the obtained models***

Similar to the analysis of compressive strength, the obtained estimation models in Figure 5.14 are further analyzed. Figure 5.15 shows the estimation models based on test data of the mix compositions with cement contents lower than 251 kg/m$^3$ (graph a) and the cement contents equal to and higher than 251 kg/m$^3$ (graph b), based on the equation 5-18. Test data at all the curing times are included. In Figure 5.18, C represents the cement content.

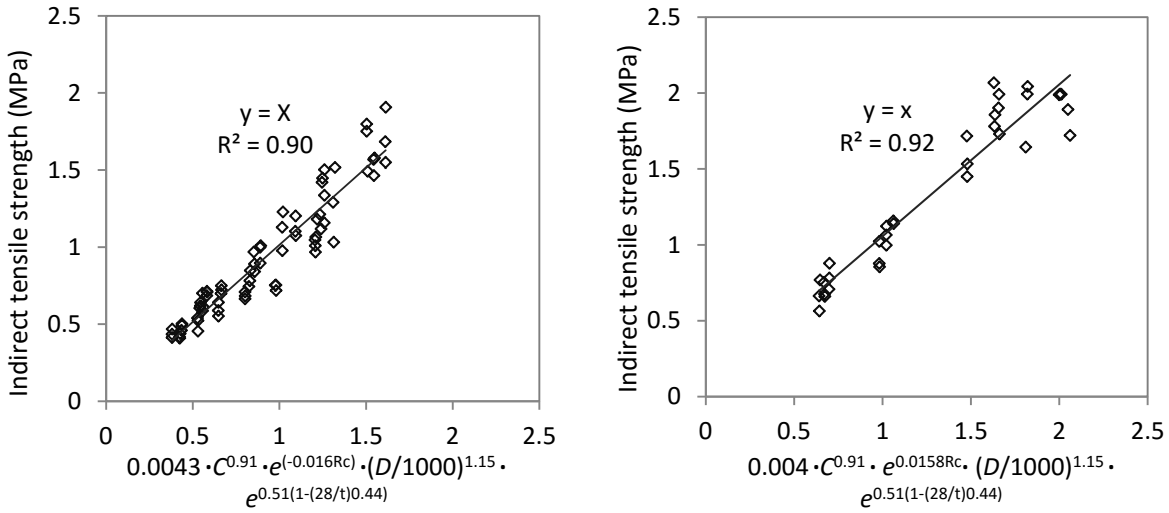


(a) 140 kg/m$^3$ ≤ C< 251 kg/m$^3$ (b) 251 kg/m$^3$ ≤ C ≤ 270 kg/m$^3$

**Figure 5.15** Estimation modelds of indirect tensile strength at different cement contents

The models in Figure 5.15 are shown as the following two equations:

$$ITS = 0.0043 \cdot C^{0.91} \cdot e^{-0.016 \cdot Rc} \cdot \left(\frac{D}{1000}\right)^{1.15} \cdot e^{0.51 \cdot (1-\left(\frac{28}{t}\right)^{0.44})} \qquad R^2 = 0.90 \qquad (5\text{-}20)$$

$$ITS = 0.004 \cdot C^{0.91} \cdot e^{0.0158 \cdot Rc} \cdot \left(\frac{D}{1000}\right)^{1.15} \cdot e^{0.51 \cdot (1-\left(\frac{28}{t}\right)^{0.44})} \qquad R^2 = 0.92 \qquad (5\text{-}21)$$

The above equations show that the Rc additive content negatively influences the indirect tensile strength of the stabilized clay when cement contents are less than 251 kg/m$^3$, but shows positive influence when the cement levels are equal to or higher

than 251 kg/m$^3$. However, the coefficients of the factors for Rc additive herein are rather small which can be negligible for estimation purposes, and thus the overall models in Figure 5.14 can be adopted for use.

## 5.4 Flexural tensile strength

### 5.4.1 Test data and analysis with variable factors

Similar to the analysis of the compressive strength and the indirect tensile strength, the results of the flexural tensile strength tests are also indicated in the mix design model, given in Figure 5.16. Each data is the average value of three tested prismatic specimens and the blue dot represents the mixture which exhibits the highest measured flexural tensile strength at each curing time. Again, the results deduced from the estimation model of flexural tensile strength (based on equation 5-24) are indicated by marked colors (black, purple, blue and green colors herein representing a flexural tensile strength higher than 2.2, 2.8, 4 and 5 MPa, respectively).

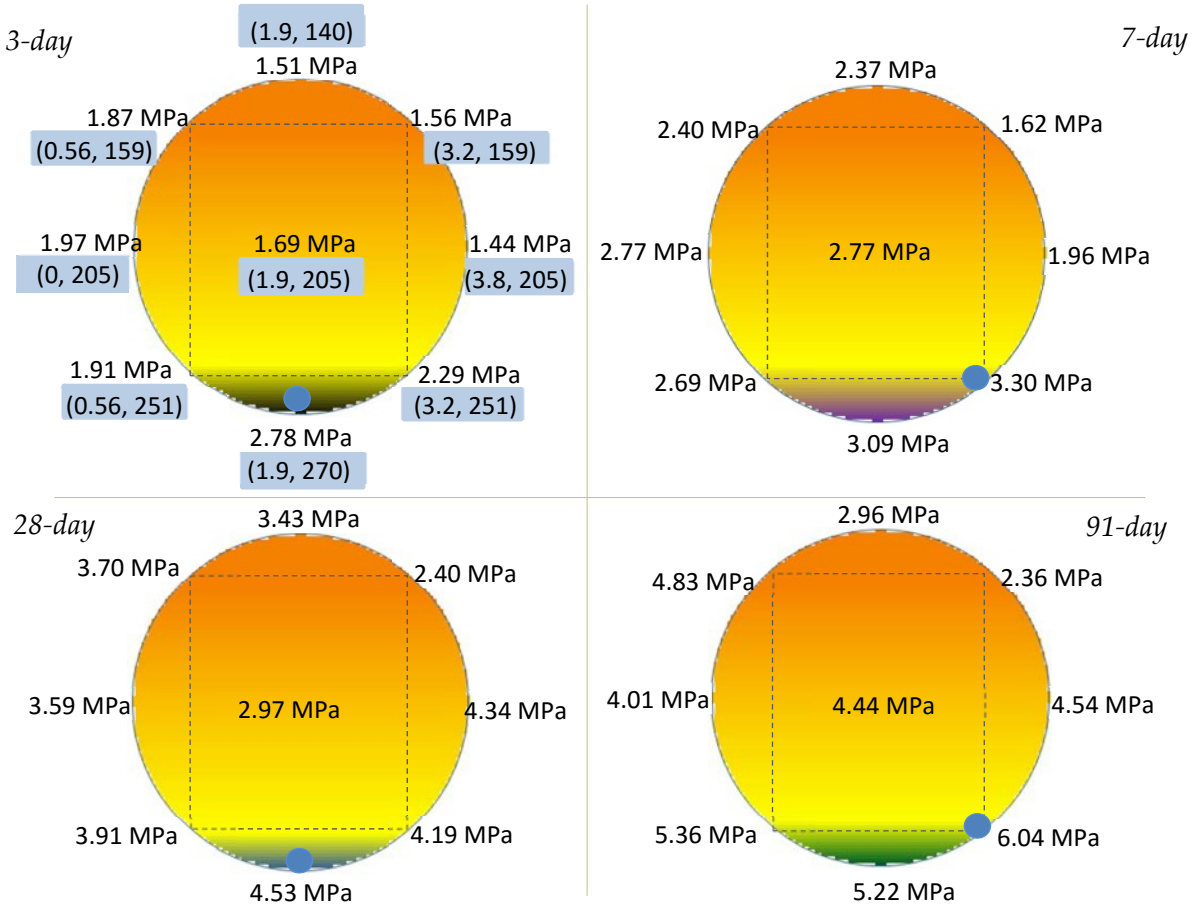


**Figure 5.16** Average flexural tensile strength of all the clay-cement mixtures

In Figure 5.16 it can be seen that the highest measured flexural tensile strength is achieved in the mixture (1.9, 270) at 3 and 28 days, and at 7 and 91 days it is found in

mixture (3.2, 251), one having the highest cement content and medium Rc content and the other one having a lower cement content but a higher Rc content. The maximum strength obtained from the estimation model is always in the mixture with the highest amount of cement.

In general, the cement content can be considered as a positive factor that contributes to the flexural tensile strength, which can be seen from comparing the results of the mixtures in the vertical direction which exhibit different cement contents. Compared with this, the influence of Rc content on the flexural tensile strength of clay-cement is not consistent. For instance, at lower cement content, such as 159 kg/m$^3$, a higher Rc content results in a lower flexural tensile strength. As the cement content increases to higher cement content, i.e. 251 kg/m$^3$, the flexural tensile strength is increased approximately by 10 to 20% at different curing times.

The flexural tensile strength of clay-cement mixtures as a function of curing time is shown in Figure 5.17. Each data is the average value of three tested specimens.

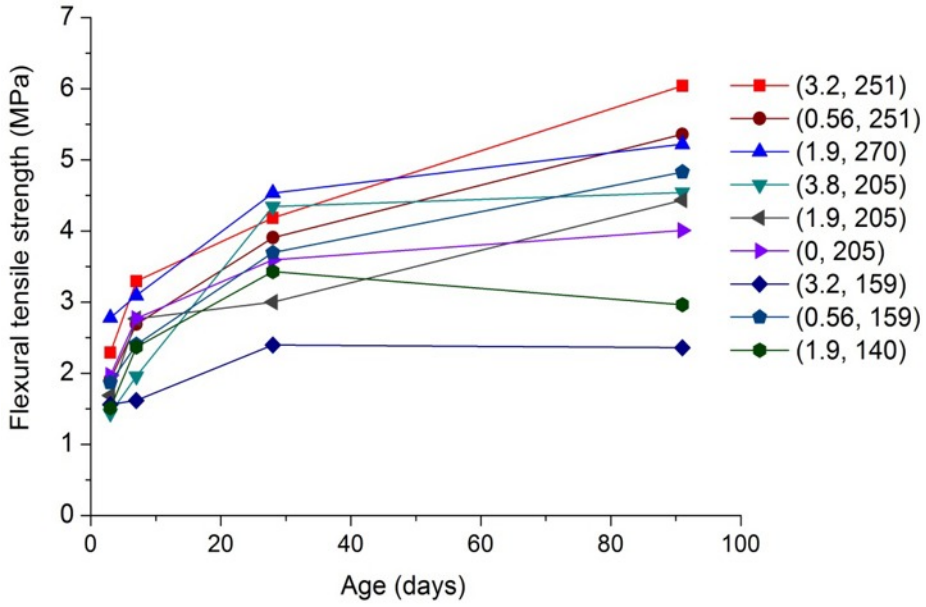


**Figure 5.17** Average flexural tensile strength of all clay-cement mixtures at different ages

In Figure 5.17 it can be seen that the flexural tensile strength of clay-cement exhibits a significant rate of increase from 3 to 7 days by 30~40% and subsequently an increase by around 50% from 7 to 28 days. After 28 days, some of the mixtures keep this increasing rate by 50% until 91 days but some mixtures exhibit a constant or even decreasing strength. However, the mixture (3.2, 159) with low cement and high Rc contents appears to have the lowest flexural tensile strength at all curing times. The

highest 91-day strength is observed in the mixture (3.2, 251), which is 16% higher than that of the mixture (1.9, 270) with the highest amount of cement.

### 5.4.2 Estimation model of flexural tensile strength (FTS)

***(1) Influence of cement and Rc contents on the flexural tensile strength***

Similar to the estimation of compressive and indirect tensile strength, the general model (equations 5-8 and 5-15) with the exponential function for the Rc content is applied to approximate the flexural tensile strength. Figure 5.18 gives the estimation models at each curing time. As expected, the coefficients for each model are different for various curing times, listed in Table 5.4.

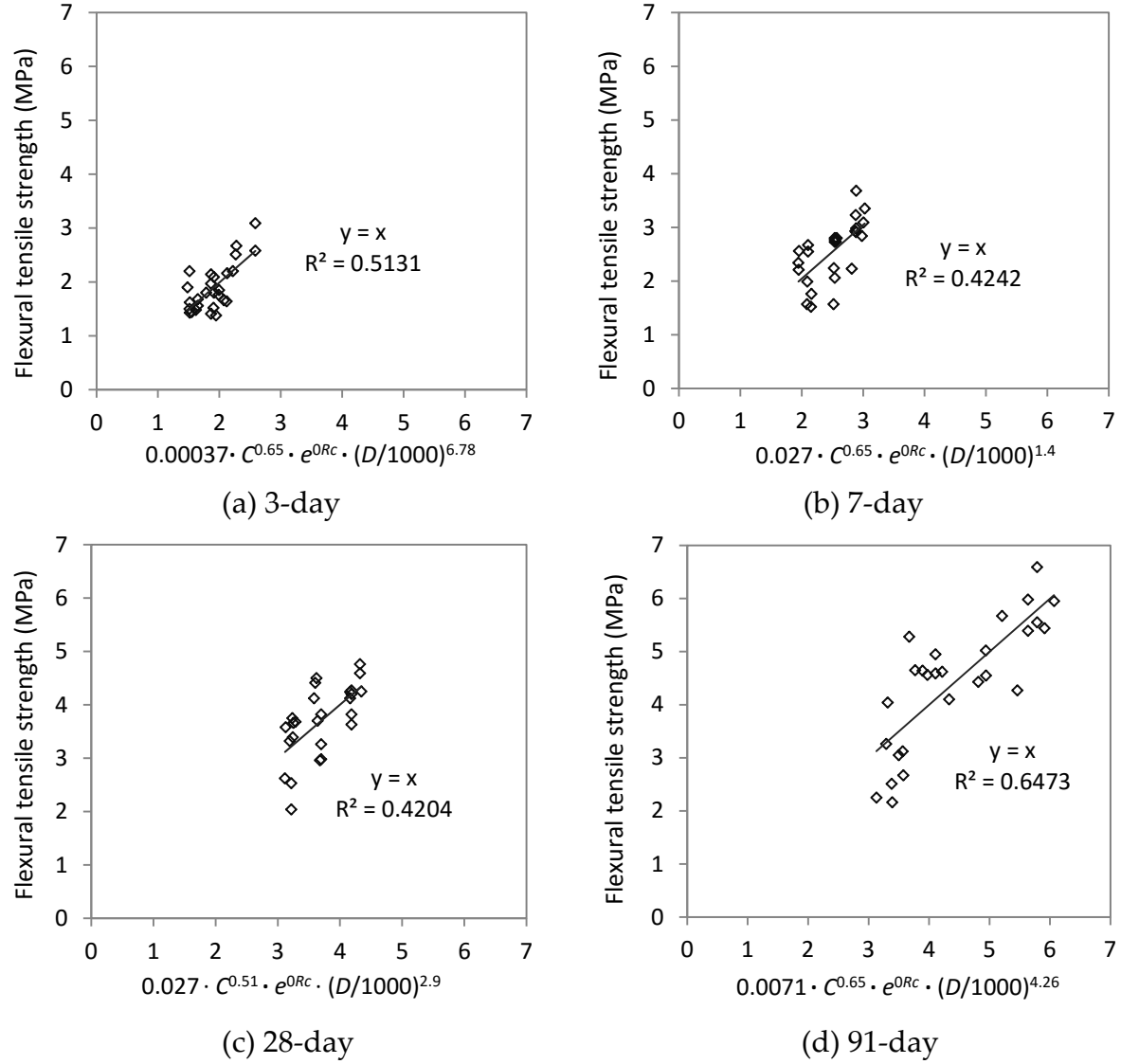


**Figure 5.18** Estimation models of flexural tensile strength at different curing times

**Table 5.4** Coefficients for the estimation models at different curing times

| Curing time | $FTS = \mathrm{a} \cdot C^{n_1} \cdot e^{n_2 \cdot Rc} \cdot (\frac{D}{1000})^{n_3}$ | | | | |
|---|---|---|---|---|---|
| | a | $n_1$ | $n_2$ | $n_3$ | $R^2$ |
| 3-day | 0.00037 | 0.65 | 0 | 6.78 | 0.513 |
| 7-day | 0.027 | 0.65 | 0 | 1.4 | 0.424 |
| 28-day | 0.027 | 0.51 | 0 | 2.9 | 0.285 |
| 91-day | 0.0071 | 0.65 | 0 | 4.26 | 0.647 |

As shown in Table 5.4, the coefficient for the cement content has the same value at different curing times with exception of the 28-day model. Besides, the $R^2$ value of the estimation models for the flexural tensile strength is rather low, below 0.7. Especially the $R^2$ value of the 28-day model is low, only 0.29. That implies that the test data of the flexural tensile strength can't be estimated well with the chosen model, compared with the results obtained from the compression and indirect tensile tests. This finding also occurred in sand-cement mixtures (Table 4.3). However, to obtain the estimation models comprising all the tested mixtures, the coefficients "$n_1$" and "$n_2$" are fixed as 0.65 and 0 at each curing time. Additionally, the coefficients of "a" and "$n_3$" are variable and will be modified based on the influence of curing time.

***(2) Influence of curing time on the flexural tensile strength***

For the estimation models of flexural tensile strength, the influence of the curing time is also evaluated by four statistical models as used for estimating the compressive strength and indirect tensile strength and shown in Figure 5.19.

As shown in Figure 5.19, the log-scale and exponential models achieved the same $R^2$ which is 0.83. The ACI model exhibits a slightly lower $R^2$. These four models are described as follows:

$$FTS = 0.0075 \cdot C^{0.65} \cdot e^{0 \cdot Rc} \cdot \left(\frac{D}{1000}\right)^{3.57} \cdot \left(1 + 0.48 \cdot \log\left(\frac{t}{28}\right)\right) \qquad R^2 = 0.83 \qquad (5\text{-}22)$$

$$FTS = 0.011 \cdot C^{0.65} \cdot e^{0 \cdot Rc} \cdot \left(\frac{D}{1000}\right)^{3.57} \cdot \left(\frac{t}{5.85 + 1.21 \cdot t}\right) \qquad R^2 = 0.80 \qquad (5\text{-}23)$$

$$FTS = 0.0075 \cdot C^{0.65} \cdot e^{0 \cdot Rc} \cdot \left(\frac{D}{1000}\right)^{3.57} \cdot e^{1.02 \cdot \left(1 - \left(\frac{28}{t}\right)^{0.21}\right)} \qquad R^2 = 0.83 \qquad (5\text{-}24)$$

$$FTS = 0.0033 \cdot C^{0.65} \cdot e^{0 \cdot Rc} \cdot \left(\frac{D}{1000}\right)^{3.57} \cdot t^{0.234} \qquad R^2 = 0.82 \qquad (5\text{-}25)$$

Compared with the estimation models of compressive strength and indirect tensile strength, the $R^2$ value of flexural tensile strength is lower, which also occurred in the

sand-cement mixtures. However, the $R^2$ obtained from the estimation models of sand-cement (around 0.85) is a bit higher than the $R^2$ for the clay-cement mixtures.

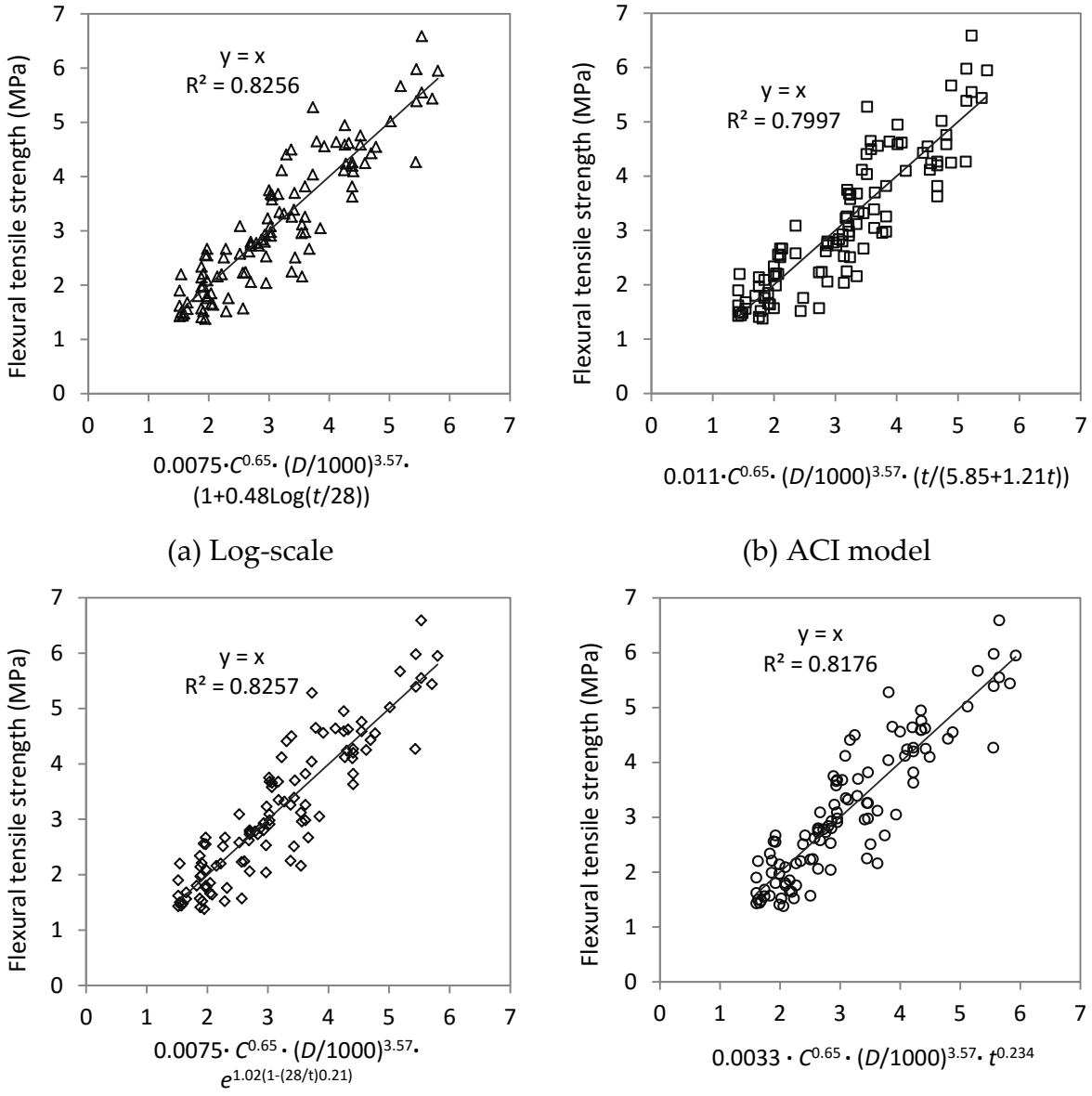


**Figure 5.19** Estimation models of flexural tensile strength with curing time

### *(3) Additional analysis of the obtained models*

Analysis herein is performed to further evaluate the obtained overall model (equation 5-24) by incorporating the factor of Rc additive, by approximating test data at different cement contents, shown in Figure 5.20.

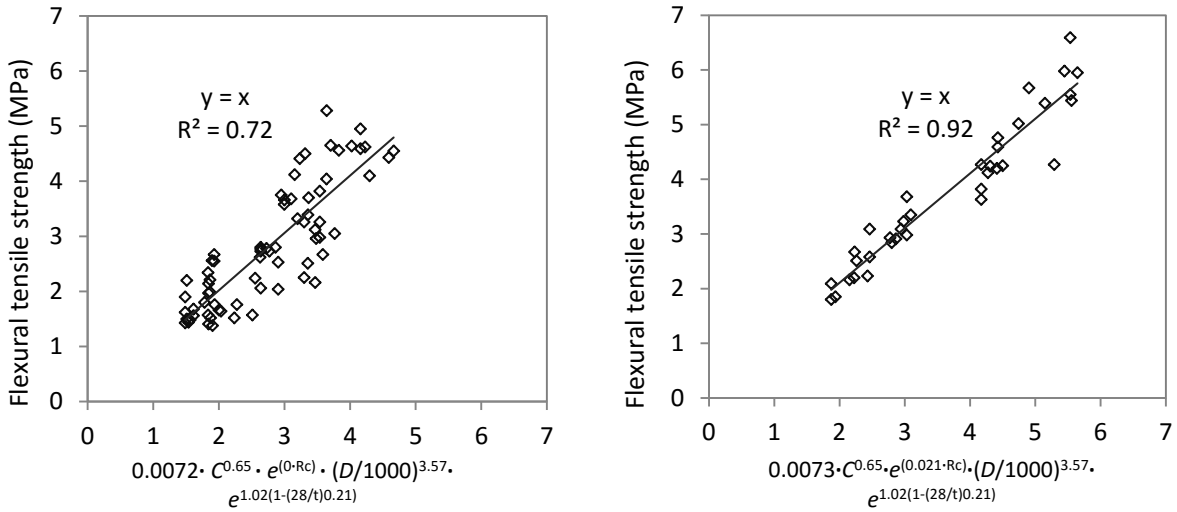


(a) 140 kg/m$^3$ ≤ C< 251 kg/m$^3$ (b) 251 kg/m$^3$ ≤ C ≤ 270 kg/m$^3$

**Figure 5.20** Estimation models of flexural tensile strength at different cement contents

In Figure 5.20, graph a includes the test data of the mix compositions with cement contents lower than 251 kg/m$^3$ and graph b includes the test data based on the cement contents equal to and higher than 251 kg/m$^3$. The estimation models in Figure 5.20 are shown in the following two equations:

$$FTS = 0.0072 \cdot C^{0.65} \cdot e^{0 \cdot Rc} \cdot \left(\frac{D}{1000}\right)^{3.57} \cdot e^{1.02 \cdot \left(1 - \left(\frac{28}{t}\right)^{0.21}\right)} \qquad R^2 = 0.72 \qquad (5\text{-}26)$$

$$FTS = 0.0073 \cdot C^{0.65} \cdot e^{0.021 \cdot Rc} \cdot \left(\frac{D}{1000}\right)^{3.57} \cdot e^{1.02 \cdot \left(1 - \left(\frac{28}{t}\right)^{0.21}\right)} \qquad R^2 = 0.92 \qquad (5\text{-}27)$$

It can be observed that test data of the mix compositions with cement contents lower than 251 kg/m$^3$ shows large scatter and the $R^2$ is rather low. When the cement content is equal to or higher than 251kg/m$^3$ the model shows good fit and also shows that increasing the Rc content increases the flexural tensile strength of stabilized clay (in graph b). However, the coefficients of Rc additive herein are low and therefore the estimation models in Figure 5.19 can be used.

## 5.5 Stiffness modulus in four-point bending test

The stiffness modulus of clay-cement material is investigated by means of the cyclic four-point bending test by applying various strain and frequency levels, described as strain-sweep and frequency-sweep tests. The test methods are the same as used for the sand-cement material, i.e. the prismatic specimen (400×50×50 mm) is subjected to cyclic loading in a four-point bending fatigue machine with controlled environmental chamber (Figure 4.23).

### 5.5.1 Strain-sweep test data and analysis of results

The strain sweep test was performed by applying an increasing strain level from 50, 60 until 400 μm/m at a fixed frequency of 10 Hz. During each sweep stage, 200 load cycles were applied and the stiffness modulus was taken as the average value during the last 10 cycles. In both sweep tests, all the beam specimens were cured for 28 days and tested at controlled temperature of 20°C. Due to the fact that large variation in strain-sweep test results may occur, 5 prismatic specimens were tested for each mixture to increase the reliability of the test results.

**(1) Strain-sweep test data**

In a strain-sweep test, the stiffness of the clay-cement material in flexure is evaluated under various strain levels. In addition to the stiffness development, the correlation between tensile stress and the applied strain is also obtained from this test. As an example, Figure 5.21 presents the strain-sweep results, including the curves of stiffness and tensile stress as a function of applied strain, for mixture (1.9, 205), i.e. cement 205 kg/m$^3$ and Rc 1.9 kg/m$^3$. Analysis of strain-sweep test results was conducted on 5 test repetitions excluding the results exceeding 20% of the average value, which applies to three parameters, namely initial stiffness, flexural strength and strain at break. The initial stiffness modulus is the value obtained in the first stage (at strain level of 50 μm/m) and is used to evaluate the magnitude of the stiffness under the influence of variable factors. The strain at break is defined as the strain level where the peak tensile stress occurs. The peak tensile stress is described as flexural strength in order to distinguish with the flexural tensile strength obtained from three-point bending test.

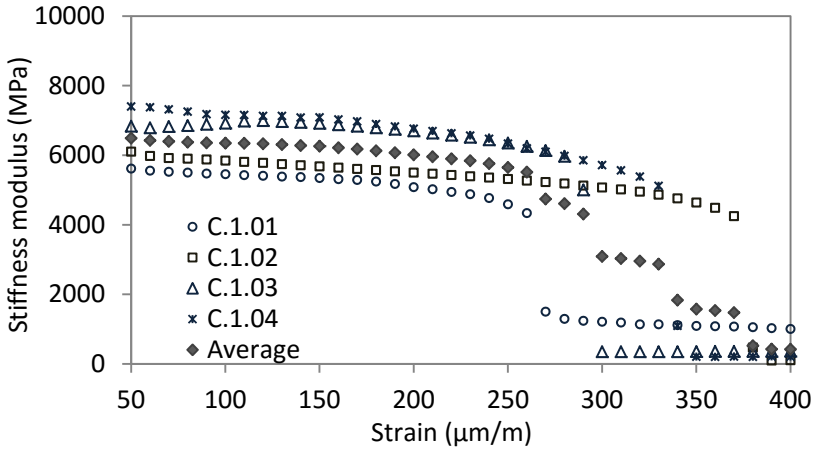


(a) Stiffness versus strain

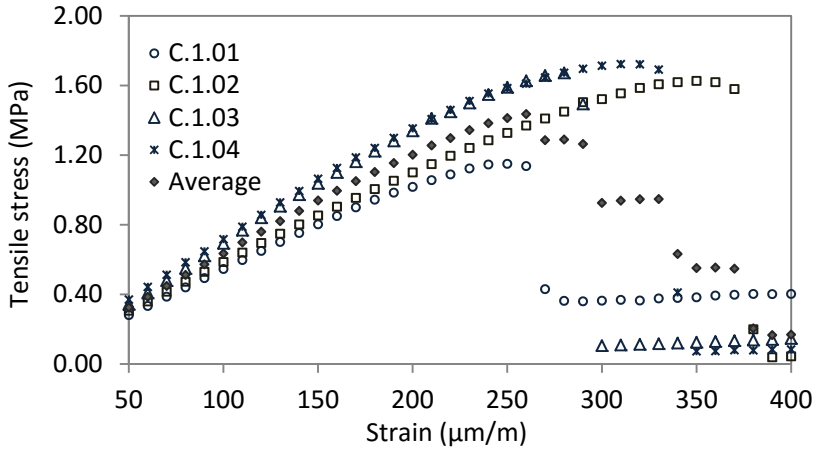


(b) Tensile stress versus strain

**Figure 5.21** Strain-sweep test results for mixture (1.9, 205)

In Figure 5.21 (a) it can be seen that the stiffness of clay-cement material gradually decreases when subjected to increased strain levels. In the strain-stress correlation, shown in Figure 5.21 (b), the flexural strength of this mixture is on average around 1.50 MPa. The strain at break ranges from 250 to 350 µm/m which indicates a large variation in the test results. Compared with the sand-cement material the strain at break of clay-cement is nearly two times higher at the same mix design.

Table 5.5 summarizes the test data from the strain-sweep tests consisting of the initial stiffness modulus, flexural strength as well as the strain at break. All the test results presented in Table 5.5 are based on 5 tested specimens for each mixture excluding the results exceeding the deviation of 20%, and thereby all these evaluated clay-cement mixtures include at least 3 test repetitions.

**Table 5.5** Strain-sweep test data

| Specimen code | Mix design | | Stiffness modulus at strain 50 μm/m | Flexural Strength | Strain at break |
|---|---|---|---|---|---|
| | Rc | Cement | | | |
| | kg/m³ | kg/m³ | MPa | MPa | μm/m |
| $Rc_0C_0$-1 | 1.9 | 205 | 5615 | 1.17 | 260 |
| $Rc_0C_0$-2 | 1.9 | 205 | 6104 | 1.64 | 350 |
| $Rc_0C_0$-3 | 1.9 | 205 | 6835 | 1.68 | 281 |
| $Rc_0C_0$-4 | 1.9 | 205 | 7400 | 1.73 | 320 |
| $Rc_0C_{-a}$-1 | 1.9 | 140 | 5072 | 1.33 | 341 |
| $Rc_0C_{-a}$-2 | 1.9 | 140 | 5733 | 1.75 | 380 |
| $Rc_0C_{-a}$-3 | 1.9 | 140 | 5980 | 1.73 | 328 |
| $Rc_0C_{-a}$-4 | 1.9 | 140 | 5785 | 1.75 | 351 |
| $Rc_1C_{-1}$-1 | 3.2 | 159 | 6690 | 0.71 | 121 |
| $Rc_1C_{-1}$-2 | 3.2 | 159 | 7226 | 0.77 | 121 |
| $Rc_1C_{-1}$-3 | 3.2 | 159 | 7121 | 0.82 | 141 |
| $Rc_1C_{-1}$-4 | 3.2 | 159 | 6871 | 0.81 | 151 |
| $Rc_aC_0$ -1 | 3.8 | 205 | 7390 | 1.27 | 201 |
| $Rc_aC_0$ -2 | 3.8 | 205 | 7603 | 1.04 | 201 |
| $Rc_aC_0$ -3 | 3.8 | 205 | 7081 | 0.81 | 141 |
| $Rc_aC_0$ -4 | 3.8 | 205 | 7335 | 0.79 | 110 |
| $Rc_1C_1$-1 | 3.2 | 251 | 8543 | 1.98 | 263 |
| $Rc_1C_1$-2 | 3.2 | 251 | 9240 | 2.22 | 290 |
| $Rc_1C_1$-3 | 3.2 | 251 | 9471 | 2.31 | 300 |
| $Rc_0C_a$-1 | 1.9 | 270 | 9232 | 2.46 | 279 |
| $Rc_0C_a$-2 | 1.9 | 270 | 8420 | 2.32 | 289 |
| $Rc_0C_a$-3 | 1.9 | 270 | 9659 | 2.49 | 270 |
| $Rc_0C_a$-4 | 1.9 | 270 | 10323 | 2.14 | 221 |
| $Rc_{-1}C_1$-1 | 0.56 | 251 | 6662 | 1.80 | 290 |
| $Rc_{-1}C_1$-2 | 0.56 | 251 | 6882 | 1.48 | 240 |
| $Rc_{-1}C_1$-3 | 0.56 | 251 | 6871 | 1.99 | 310 |
| $Rc_{-a}C_0$ -1 | 0 | 205 | 7018 | 2.50 | 402 |
| $Rc_{-a}C_0$ -2 | 0 | 205 | 7401 | 2.11 | 310 |
| $Rc_{-a}C_0$ -3 | 0 | 205 | 6634 | 1.32 | 250 |
| $Rc_{-1}C_{-1}$-1 | 0.56 | 159 | 5967 | 1.12 | 200 |
| $Rc_{-1}C_{-1}$-2 | 0.56 | 159 | 6485 | 1.28 | 220 |
| $Rc_{-1}C_{-1}$-3 | 0.56 | 159 | 5542 | 1.43 | 280 |

**(2) Analysis of results from strain-sweep test**

***a) Stiffness modulus in the strain-sweep test***

Figure 5.22 presents the stiffness modulus of clay stabilized with variable Rc contents, as a function of the applied strain level. Each curve is the average result of 4 or 3 test repetitions.

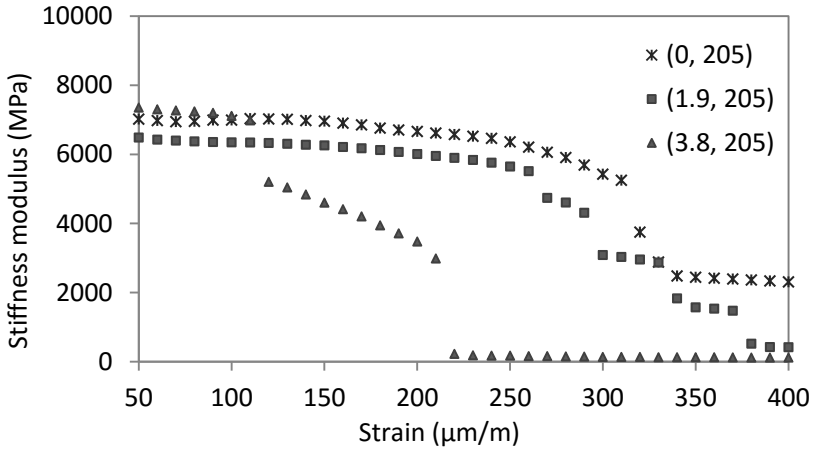


(a)

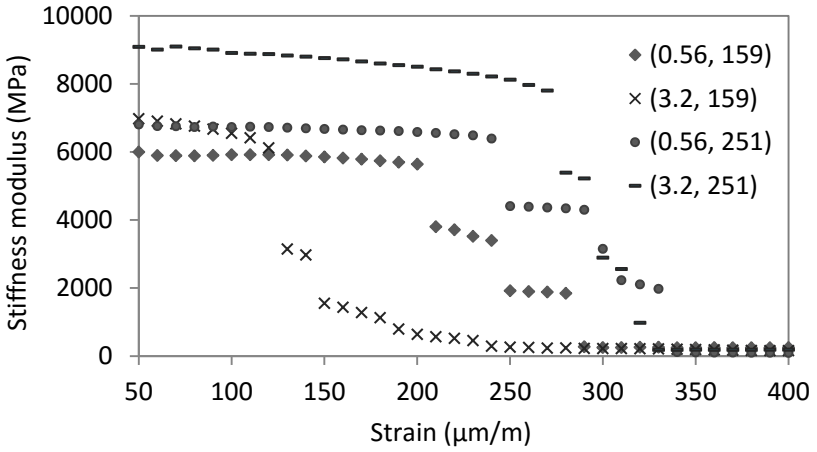


(b)

**Figure 5.22** Influence of Rc additive content on the stiffness modulus

In Figure 5.22 it can be seen that the stiffness modulus of cement stabilized clay materials is strongly influenced by the applied strain. As the strain increases, the stiffness modulus slightly decreases until failure. In comparison, the sand-cement materials showed a dramatic decrease under increased strain level and suddenly broke at strain levels mostly smaller than 150 μm/m, while the clay-cement materials showed very slight decrease in stiffness and most of the mixtures are able to withstand much higher strain levels before breaking.

By comparing the curves with different Rc content, it can be seen that the stiffness-strain relation is variable in different Rc contents. In Figure 5.22 (a) the mixture without Rc is observed to withstand a strain level which is 320 μm/m, while mixture (3.8, 205) with the highest amount of Rc breaks at lower strain 120 μm/m. It also occurred in mixtures with cement content of 159 kg/m$^3$, shown in Figure 5.22 (b), which shows that as the Rc content increases from 0.56 to 3.2 kg/m$^3$, the strain level at failure is reduced from 200 to 130 μm/m. However, mixtures with cement content of

251 kg/m$^3$ exhibit the opposite trend that an increasing Rc content results in a slightly increased strain level at failure. Based on the above results, it implies that a high Rc content may lead to failure of the beam at a rather low strain level when a low cement content is used. In contrast, if the cement content is relatively high, a higher Rc content may have a positive influence which makes the mixture break at a higher strain level.

Regarding the influence of the cement content, Figure 5.23 shows the stiffness modulus of three mixtures with different cement contents and the same Rc content 1.9 kg/m$^3$.

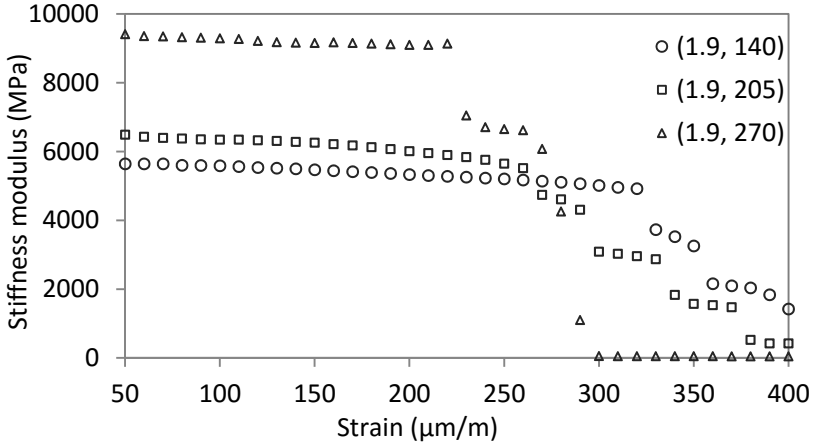


**Figure 5.23** Influence of cement content on the stiffness modulus

It can be seen from Figure 5.23 that the higher the cement content, the more brittle the clay-cement material. For instance, the mixture (1.9, 270) with the highest cement content breaks at strain level 230 μm/m, while the mixture (1.9, 140) with the lowest cement content could withstand the much higher strain level 330 μm/m before failure. It means that a higher cement content will lead to failure of the beam at a lower strain level. Conversely, the results from Figure 5.22(b) exhibit the opposite trend, i.e. when the cement content increases from 159 to 251 kg/m$^3$, the beam specimens withstood a higher strain level at failure. It implies that there seems to be an optimum cement content which can increase the flexibility of clay-cement materials and enable the material to withstand a higher strain level till failure.

Apart from the analysis of the development of stiffness under increased strain levels, the magnitude of the stiffness when subjected to the same strain level is also compared for all the tested mixtures, see Figure 5.24. Since the stiffness decreases under increased strain levels, and will experience micro-cracking, the initial stiffness obtained at a strain level of 50 μm/m (illustrated in Table 5.5) is used to identify the influence of the cement and Rc contents on this property.

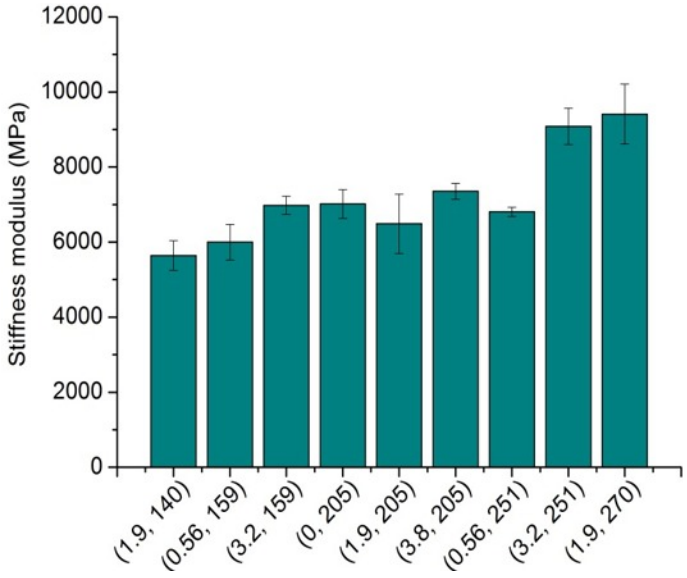


**Figure 5.24** Initial stiffness modulus of all the tested clay-cement mixtures

In Figure 5.24 it can be seen that the three mixtures with cement content 205 kg/m$^3$ have nearly the same stiffness value. In contrast, the Rc content seems to increase the stiffness in the mixtures with cement contents of 159 and 251 kg/m$^3$: if the Rc content increases from 0.56 to 3.2 kg/m$^3$, the stiffness increases on average by 17% and 30%, respectively. Moreover, the cement content is also observed to contribute to the increased stiffness.

In order to quantify the effect of cement and Rc contents on the stiffness modulus, estimation models are developed for the initial stiffness modulus of cement-clay material, shown in Figure 5.25. Figure 5.25 includes the test data of initial stiffness of all the tested clay mixtures cured for 28 days.

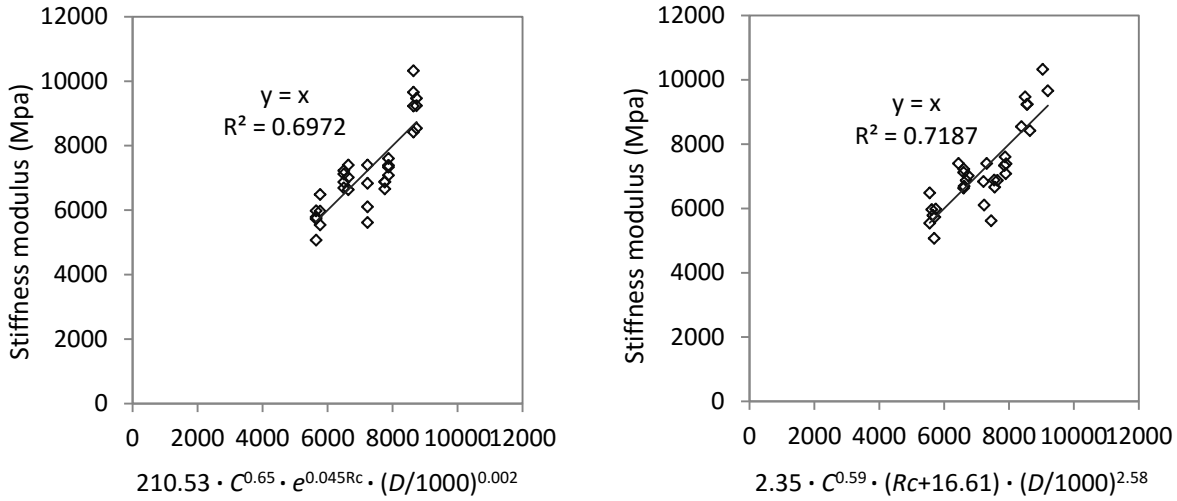


(a) Exponential function (b) Linear function

**Figure 5.25** Estimation models of initial stiffness modulus

In Figure 5.25 linear and exponential functions are applied for the effect of the Rc content and the model with the linear function for the Rc content shows a slightly higher $R^2$. From the estimation models it can be seen that the stiffness modulus at the applied strain 50 μm/m is positively related to the cement content, the Rc content and the density of the specimen. These two models shown above can be described as follows:

$$E = 210.53 \cdot C^{0.65} \cdot e^{0.045Rc} \cdot \left(\frac{D}{1000}\right)^{0.002} \qquad R^2 = 0.70 \qquad (5\text{-}28)$$

$$E = 2.35 \cdot C^{0.59} \cdot (Rc + 16.61) \cdot \left(\frac{D}{1000}\right)^{2.58} \qquad R^2 = 0.72 \qquad (5\text{-}29)$$

Where, $E$ is the stiffness modulus of the clay-cement material cured for 28 days, MPa.

In order to visualize the contribution of the cement and Rc contents to the estimation model of the stiffness modulus of clay-cement material, the response surface and contour plot are developed on the basis of the estimation model (equation 5-28), shown in Figure 5.26. As can been seen from Figure 5.26 both the cement content and the Rc content can increase the stiffness of the clay-cement materials.

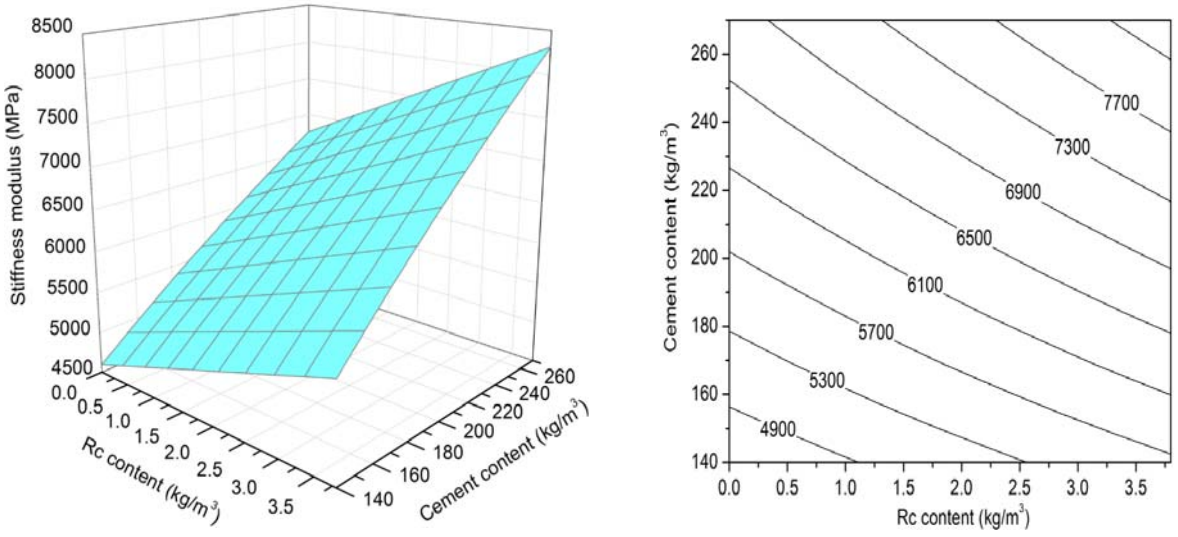


(a) Response surface (b) Contour plot

**Figure 5.26** Influence of cement and Rc contents on the stiffness modulus

***b) Strain at break and flexural strength in the strain-sweep test***

Figure 5.27 shows the strain at break obtained from all the clay-cement mixtures. An error bar is given to indicate the variation of the repeated test results. Strain at break is obtained from the stress-strain curve (example shown in Figure 5.21) where the maximum flexural stress is observed.

It can be observed in Figure 5.27 that the strain at break and flexural strength are influenced by the Rc content. In the mixtures with cement content 159 and 205 kg/m$^3$, when the Rc content increases, both the strain at break and the flexural strength decrease. For the two mixtures with cement content 251 kg/m$^3$, a higher Rc content leads to a higher flexural strength but doesn't seem to influence the strain at break. The cement content doesn't show a clear influence on these two properties.

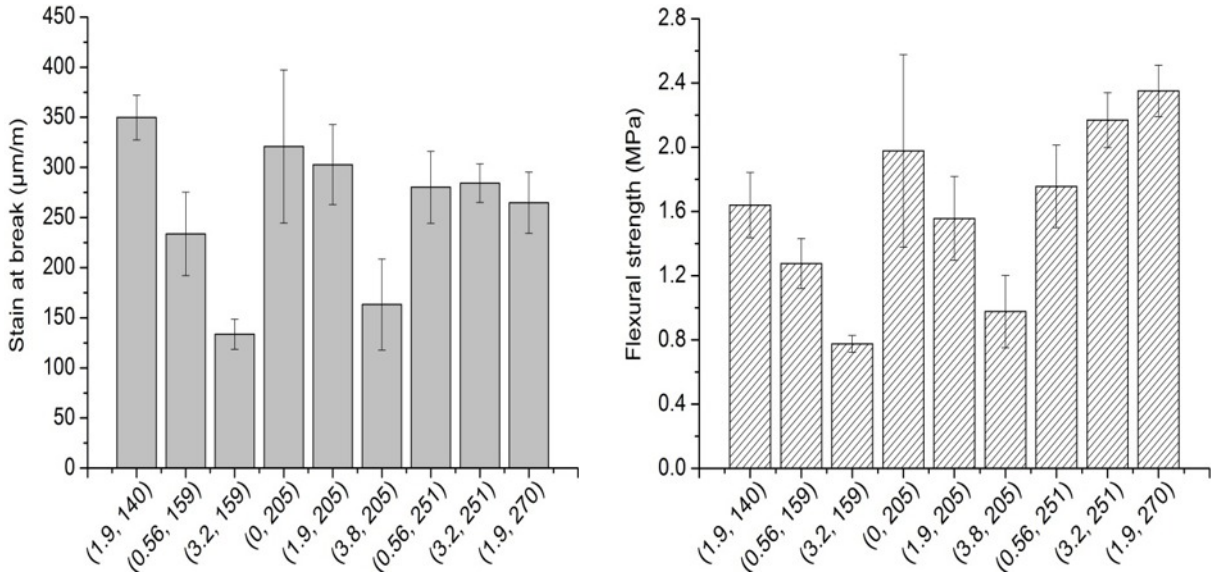


(a) Strain at break (b) Flexural strength

**Figure 5.27** Strain at break and flexural strength in the cyclic bending test

Regression models have also been developed to estimate the flexural strength and strain at break of cement stabilized clay materials, shown in Figure 5.28. Figure 5.28 presents the flexural strength and the strain at break for all tested mixtures. An exponential function for the effect of Rc content is applied in the estimation models.

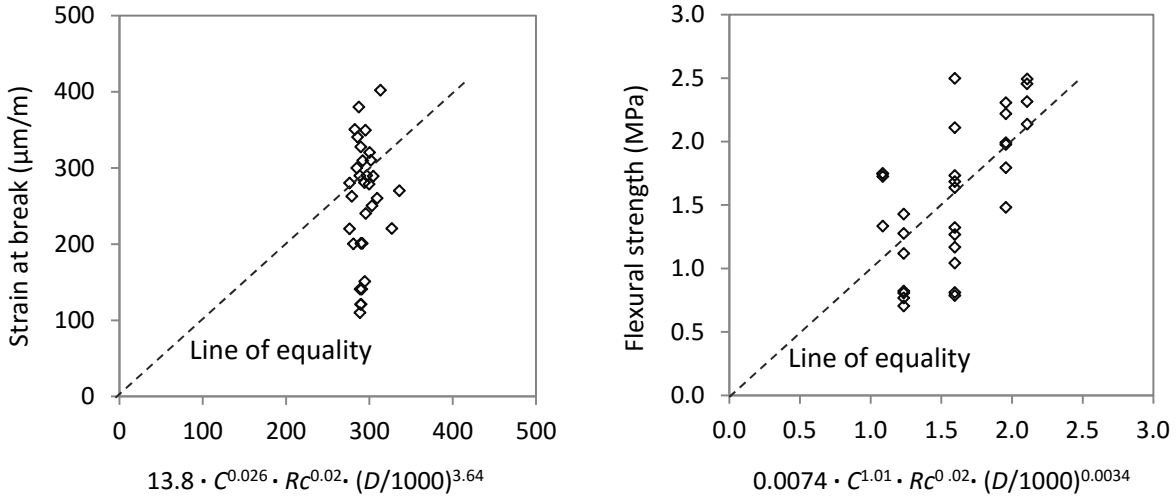


(a) Strain at break (b) Flexural strength

**Figure 5.28** Estimation models of strain at break and flexural strength

Figure 5.28 demonstrates that both estimation models can't be employed to approximate the real strain at break and real flexural strength, indicated by the large deviation from the line of equality.

### *c) Maximum wheel load from linear-elastic multilayer calculation*

Based on the obtained strain at break, the linear-elastic multilayer program BISAR is used to back-calculate the traffic wheel load under which this strain at break will occur at the bottom of the cement stabilized layer, illustrated in Table 5.6. This wheel load indicates the maximum heavy traffic which may cause immediate cracking of the base. This BISAR calculation is done for a assumed two-layer pavement structure. The input parameters for each layer, e.g. stiffness modulus and the expected strain at break, are referring to the results for each mixture (shown in Table 5.5) and the average value of three test data is used.

**Table 5.6** Input parameters for BISAR calculation

| Pavement Structure | Materials | Input parameters | | | | | Calculated result |
|---|---|---|---|---|---|---|---|
| | | Thickness | Poisson's ratio | Stiffness modulus | Tire pressure | Wheel load | Strain at break |
| | | m | – | MPa | MPa | kN | µm/m |
| Base layer | Cement-clay | 0.25 | 0.25 | Table 5.5 | 1 | Target | Table 5.5 |
| Subgrade | Subsoil clay | – | 0.35 | 35 | – | – | – |

The obtained maximum wheel load for each mixture is indicated in the mix design and shown in Figure 5.29.

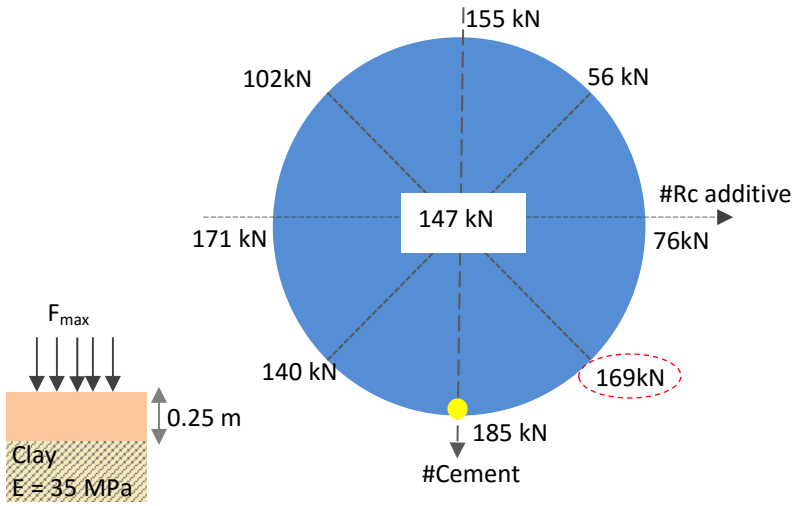


**Figure 5.29** Maximum wheel load of stabilized clay base layer before breaking

In Figure 5.29 it can be seen that the highest wheel load before cracking can be

applied to the mixture with the highest amount of cement, shown as the yellow dot. In contrast, the influence of the Rc content shows a large variation. For instance, when the cement content is low, an increasing Rc content leads to a reduced wheel load. However, when the mixtures have a relatively high amount of cement, adding more Rc yields a higher wheel load, marked in the red circle. The large variation of this parameter is mainly caused by the variation in the results of strain at break.

### 5.5.2 Frequency-sweep test data and analysis of the results

As for the frequency sweep test, frequencies with a range from 0.4 to 20 Hz were subsequently applied at a constant strain of 100 μm/m, which is approximately 30% of the strain at break for the clay-cement materials. During each sweep stage, 200 load cycles were applied and the stiffness modulus was taken as the average value of the last 10 cycles. In sweep tests, all the beam specimens are cured for 28 days and tested at controlled temperature of 20°C. For the frequency-sweep test, 3 specimens were tested for each mixture composition. Figure 5.30 gives an example of the test data from a frequency-sweep test on individual clay-cement specimens (mix design with cement 205 kg/m$^3$ and Rc 1.9 kg/m$^3$). As shown in Figure 5.30 the frequency of cyclic loading doesn't influence the stiffness of clay-cement materials. Besides, the variation of the three specimens is relatively small.

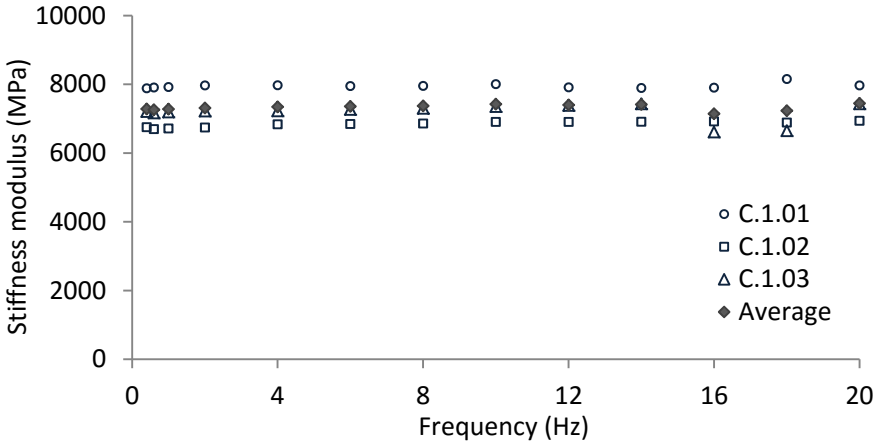


**Figure 5.30** Frequency-sweep test results from 3 test repetitions

The influence of the frequency of dynamic loading on the stiffness modulus of cement stabilized clay is evaluated on all the mixtures, shown in Figure 5.31. In Figure 5.31, each curve is the average value of three tested specimens.

As can be seen in Figure 5.31, the stiffness modulus of all tested cement stabilized clay materials remains almost constant at different frequency levels. This finding is consistent with that of sand-cement material (see Figure 4.32). Therefore it can be concluded that the frequency of dynamic loading doesn't have clear influence on the

stiffness modulus of cement stabilized materials. Figure 5.31 again shows that a higher cement content generally yields a higher stiffness at all frequency levels.

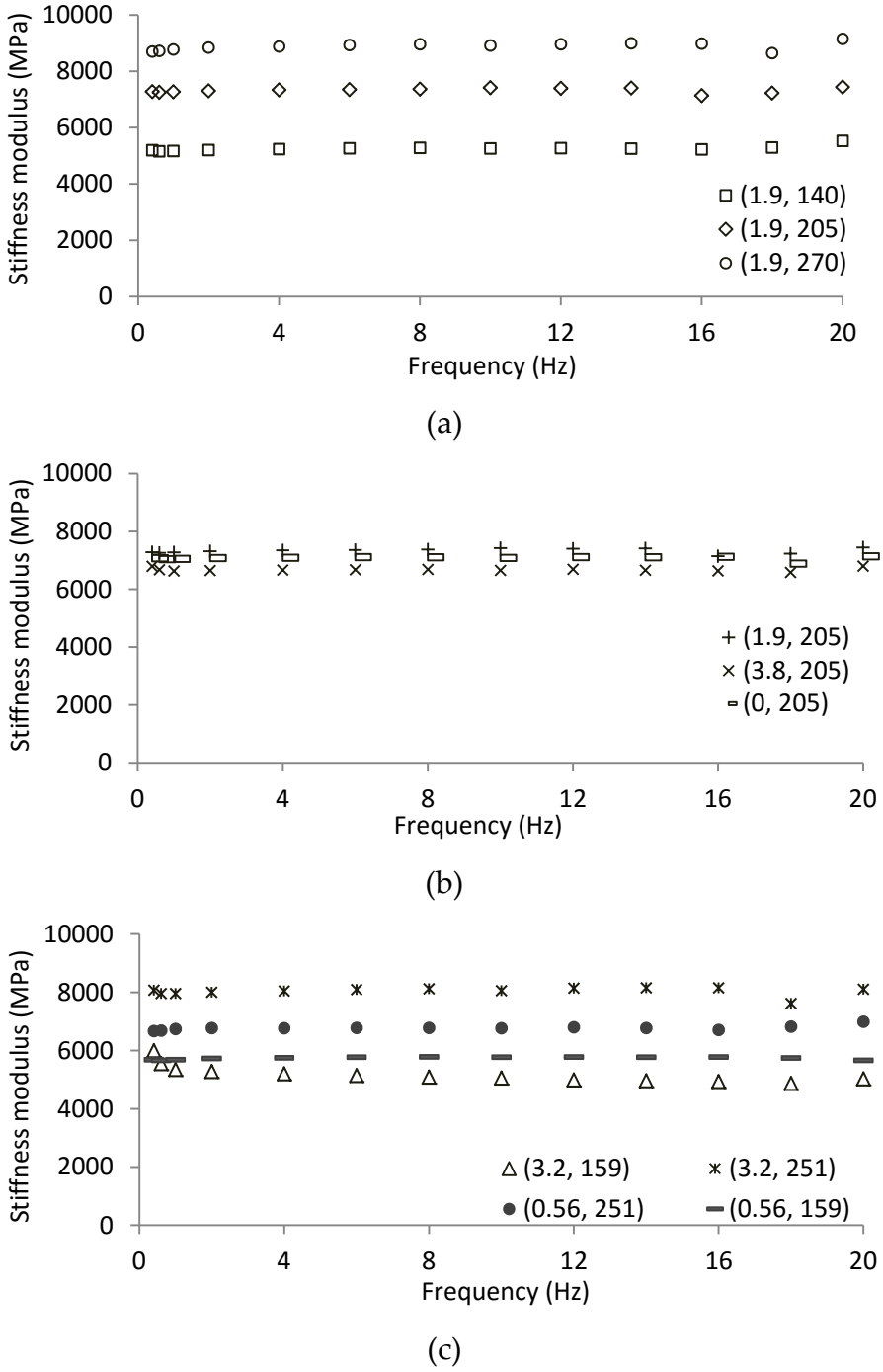


**Figure 5.31** Influence of load frequency on the stiffness modulus of clay-cement

## 5.6 Fatigue property

### 5.6.1 Fatigue test condition

The fatigue property of clay-cement material is determined by subjecting the beam specimen to various stress levels. The four-point bending test machine was used (see

Figure 4.23). The stress-controlled loading mode is applied at each stress level and hence the amplitude of the applied load is held constant during testing. The stress level to be applied is less than the flexural strength obtained from the four-point bending test for individual mixture. The test conditions for the fatigue test on clay-cement mixtures, which are the same as used for the sand-cement mixtures, are given in Table 4.6.

Figure 5.32 gives an example of fatigue test results by applying different stress levels which shows a typical plot of stiffness modulus ratio (defined as the ratio of the occurring stiffness modulus to the initial value) versus the number of load repetitions. The initial stiffness modulus is obtained as the average value during the 90$^{th}$ to 100$^{th}$ load application.

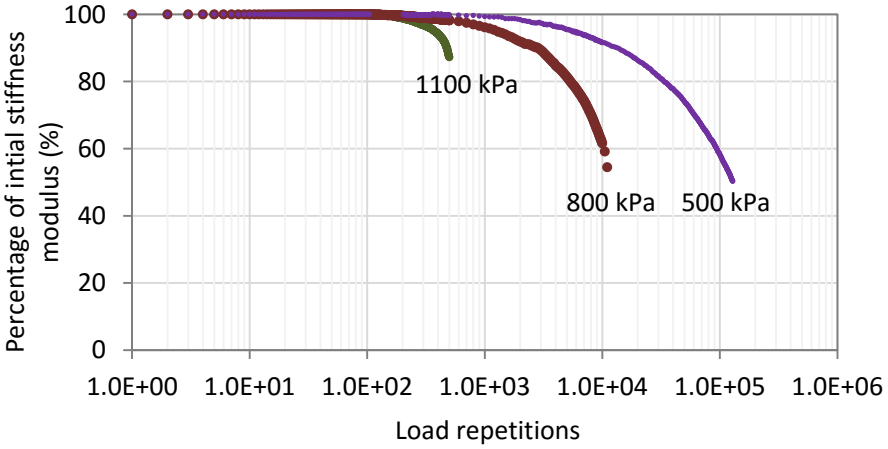


**Figure 5.32** Stiffness ratio versus number of load repetitions of mixture (1.9, 205)

It can be seen in Figure 5.32 that under repeated loading the stiffness modulus ratio decreases gradually while at the end of the test the stiffness modulus decreases rapidly until fracture occurs.

### 5.6.2 Fatigue relation of all the tested mixtures

In this study, the fatigue line is plotted as a function of the applied stress level against the corresponding number of load repetitions to failure. However, in Standard NEN-EN 12697-24 the fatigue life in relation to the initial strain (strain amplitude at 100$^{th}$ cycle) is suggested. Therefore, these two types of fatigue models are both evaluated, described as follows:

$$N = k_1 \cdot \sigma^{-k_2} \text{ or } N = k_1 \cdot \varepsilon^{-k_2} \quad (5\text{-}30)$$

Where, N is the number of load cycles at each applied stress level; $\varepsilon$ is the initial strain (μm/m); $\sigma$ is the applied stress (kPa); $k_1$ and $k_2$ are experimentally determined coefficients.

As an example, Figure 5.33 shows the two fatigue models for mixture (1.9, 205). In Figure 5.33 the number of load cycles N and applied stress level σ and initial strain ε are all presented by a log-log plot, aiming to provide straight fatigue lines and illustrate the slope $k_2$. As demonstrated in Figure 5.33, the correlation between the number of load cycles at failure and the applied stress level and the fatigue correlation with the initial strain show similar $R^2$ values.

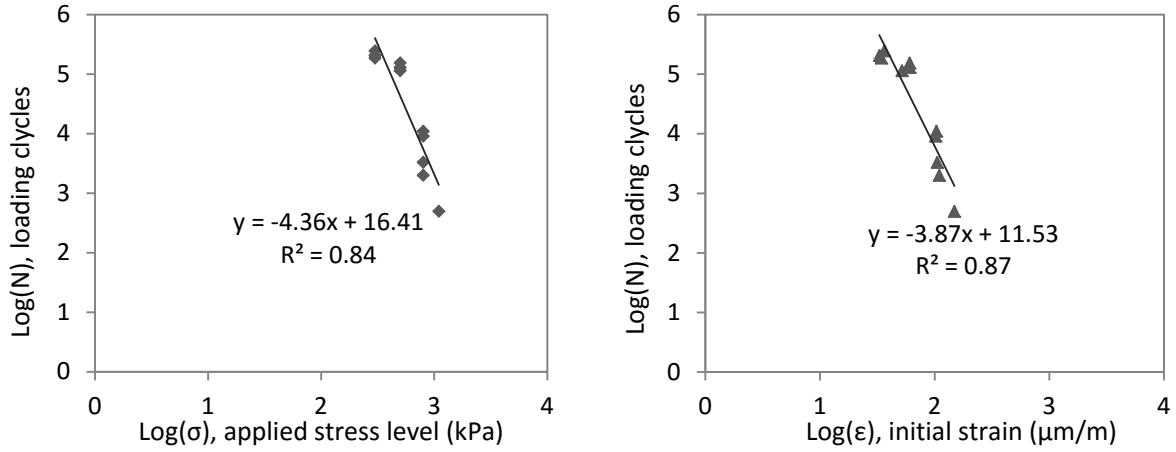


(a) Stress-based fatigue relation (b) Strain-based fatigue relation

**Figure 5.33** Fatigue relation of the tested mixture (1.9, 205)

By using these two models the fatigue relations for all the clay-cement mixtures are given in Table 5.7, presented by the coefficients of log ($k_1$) and $k_2$.

**Table 5.7** Parameters for fatigue relations of all the clay-cement mixtures

| Mix code | Mix design | | Fatigue life, log(N) | | | | | |
|---|---|---|---|---|---|---|---|---|
| | | | Stress-based relation | | | Strain-based relation | | |
| | Rc | Cement | log($k_1$) | $k_2$ | $R^2$ | log($k_1$) | $k_2$ | $R^2$ |
| | (kg/m³) | (kg/m³) | (-) | (-) | | (-) | (-) | |
| $Rc_0C_0$ | 1.9 | 205 | 16.41 | 4.36 | 0.84 | 11.53 | 3.87 | 0.87 |
| $Rc_0C_{-a}$ | 1.9 | 140 | 12.06 | 2.59 | 0.36 | 10.67 | 2.85 | 0.49 |
| $Rc_{+1}C_{-1}$ | 3.2 | 159 | 11.69 | 3.14 | 0.28 | 9.94 | 3.46 | 0.74 |
| $Rc_{+a}C_0$ | 3.8 | 205 | 16.20 | 3.93 | 0.39 | 10.08 | 2.43 | 0.89 |
| $Rc_{+1}C_{+1}$ | 3.2 | 251 | 18.81 | 4.57 | 0.61 | 14.46 | 4.50 | 0.52 |
| $Rc_0C_{+a}$ | 1.9 | 270 | 24.47 | 6.34 | 0.28 | 9.25 | 1.88 | 0.29 |
| $Rc_{-1}C_{+1}$ | 0.56 | 251 | 11.17 | 1.93 | 0.41 | 10.90 | 2.51 | 0.46 |
| $Rc_{-a}C_0$ | 0 | 205 | 11.91 | 2.45 | 0.84 | 9.14 | 2.18 | 0.93 |
| $Rc_{-1}C_{-1}$ | 0.56 | 159 | 4.73 | 0.25 | 0.00 | 8.11 | 1.23 | 0.03 |

In Table 5.7 it can be observed that $k_1$ and $k_2$ values are quite variable between different mixtures in both types of relations. In the stress-based relations, the $k_2$ value ranges from 2 to 6, which is similar to that of asphalt concrete mixtures, reported as

from 3 to 6 (Ghuzlan & Carpenter, 2002). Compared with this, sand-cement material exhibits much higher $k_2$ values ranging from 12 to 16 (shown in Table 4.7), which implies that sand-cement material is more brittle. However, the $R^2$ value of the fatigue relations of clay-cement is generally rather low and indicate very low accuracy. Especially the $R^2$ value obtained for some mixtures marked in red are around 0.3. This considerable scatter of the test data leading to the low $R^2$ is also mentioned in research by Croney (1977) and he attributed it to the reason of the variation in the quality of the test specimens. Extremely, $R^2$ of the fatigue models of mixture (0.56, 159) is nearly 0 and this mixture is therefore excluded from the following discussions on the fatigue property.

Figure 5.34 presents the fatigue lines of all the clay-cement mixtures, expressed in log-log scale (log of load cycles at failure versus log of applied stress/initial strain).

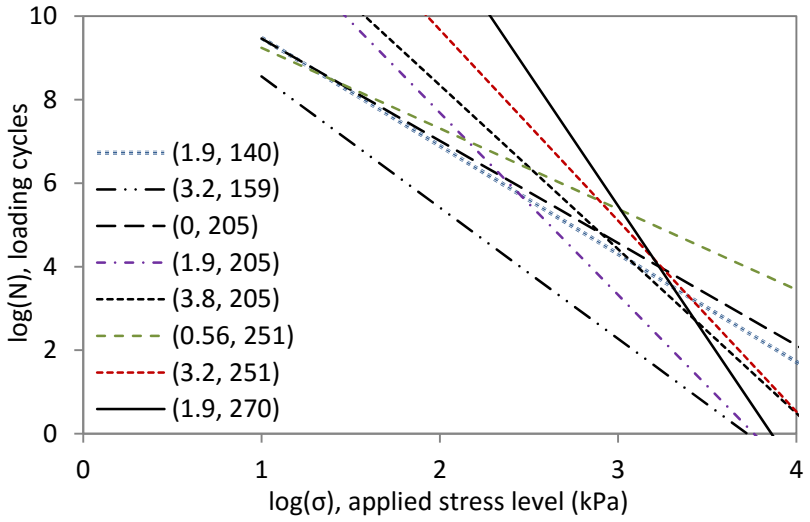


(a) Stress-based fatigue relations

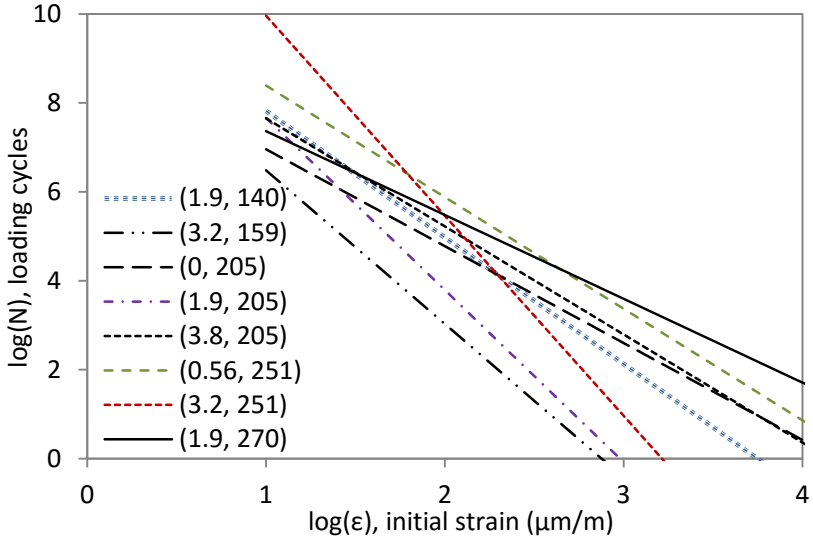


(b) Strain-based fatigue relations

**Figure 5.34** Fatigue lines for all the tested clay-cement mixtures

In Figure 5.34 it can be observed that fatigue lines exhibit a large scatter both in stress-based and strain-based relations and these two types of models indicate the similar trend among all the clay-cement mixtures. It can be noted that the mixture (3.2, 159) exhibits the lowest fatigue life at given stress or strain levels of all the investigated mixtures.

The $k_1$ and $k_2$ values are found to be correlated, shown in Figure 5.35. Figure 5.35 includes all the $k_1$ and $k_2$ values in the fatigue models of all the mixtures and $k_1$ is indicated by its log. Although different mixtures alter the values of $k_1$ and $k_2$, the relation between $k_1$ and $k_2$ is consistent. The correlations indicated in Figure 5.35 are described as the following equations:

$$k_2 = 0.30 \cdot \log(k_1) - 0.96 \qquad R^2=0.95 \qquad \text{stress-based fatigue relation} \qquad (5\text{-}31)$$

$$k_2 = 0.45 \cdot \log(k_1) - 1.89 \qquad R^2=0.73 \qquad \text{strain-based fatigues relation} \qquad (5\text{-}32)$$

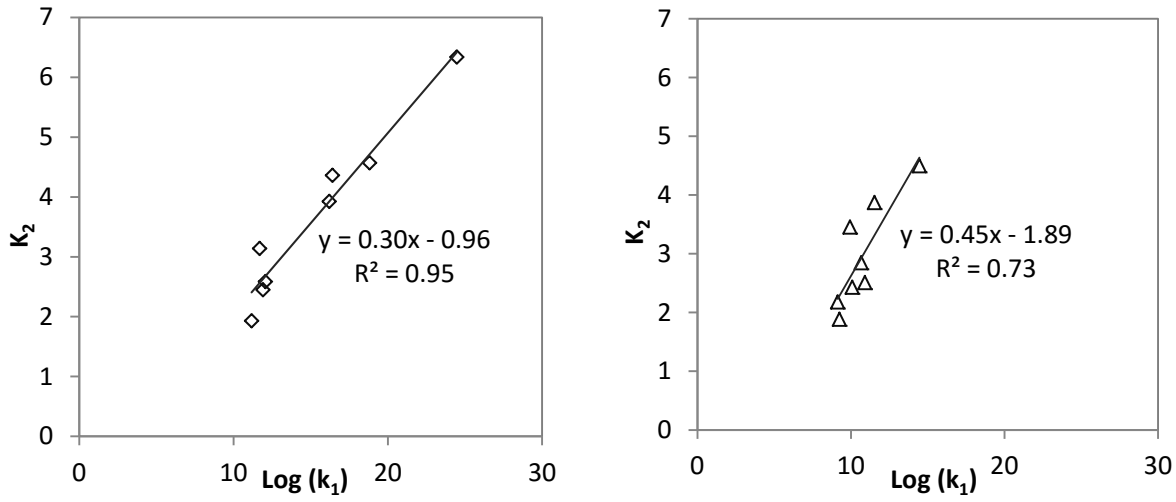


(a) Stress-based fatigue relation (b) Strain-based fatigue relation

**Figure 5.35** Correlation between $k_1$ and $k_2$

Similar to the analysis of the sand-cement materials, the stress and strain levels that allow one million load cycles are discussed herein. Figure 5.36 lists the calculated stress (obtained from stress-based fatigue relations) and stress ratio (the obtained stress level related to the ultimate flexural strength) of clay-cement materials based on one million load cycles.

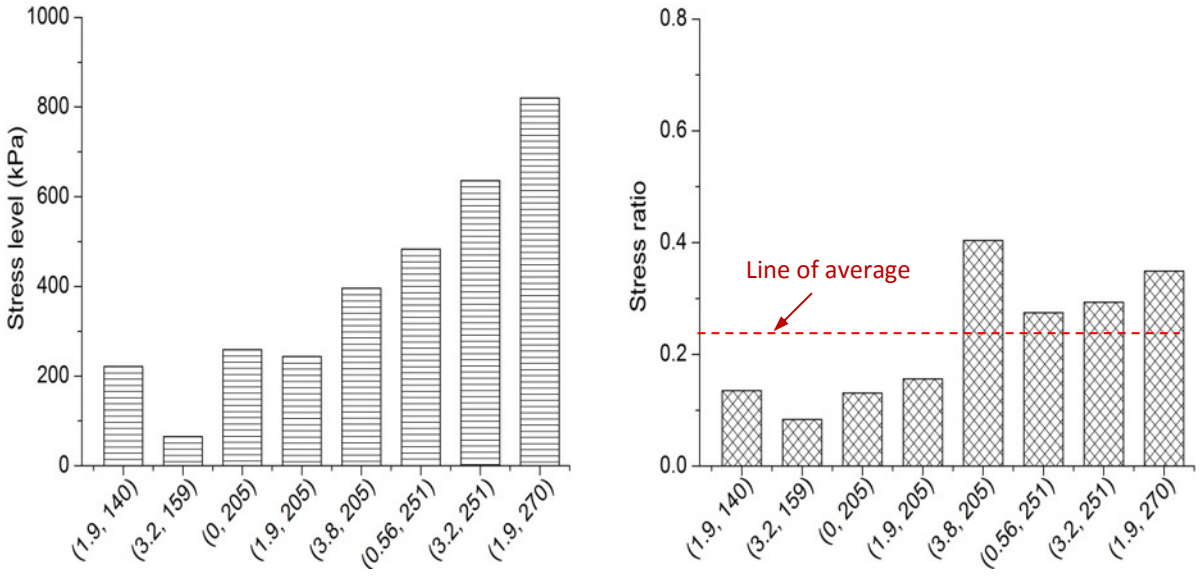


(a) Stress level (b) Stress ratio

**Figure 5.36** Stress level and stress ratio of clay-cement material corresponding to one million load cycles

In Figure 5.36 it can be seen that the stress level is quite variable, dependent on the mix design. Generally a higher cement content generates a higher stress level. That means that a mixture with a higher cement content can withstand a higher stress level when the same fatigue lifetime is required. Also a higher Rc content appears to increase the loading stress level. For instance, when comparing the mixtures (0.56, 251) and (3.2, 251), the mixture with the higher Rc content can withstand a 32% higher stress. The mixture (3.2, 159) exhibits the lowest loading stress.

Figure 5.36 (b) shows the stress ratio that corresponds to one million load cycles is in a range of 0.08 to 0.40, and generally the higher the cement content, the higher the stress ratio, with exception of mixture (3.8, 205). That means there is no definite value of stress ratio that can be used for the clay-cement materials which can result in one million load cycles at failure (indicating no fatigue damage). Compared with this, for sand-cement materials the stress ratio is on average 0.58 (58% of the flexural strength), with much smaller variation between mixtures. Besides, the stress level for sand-cement is generally three times higher than that for clay-cement material.

Figure 5.37 gives the similar analysis based on the strain levels and strain ratio (strain related to the strain at break), for clay-cement mixtures. As can be seen in Figure 5.37, the strain levels and strain ratio exhibit a large scatter between mixtures and no consistent and clear correlation with either cement or Rc content can be drawn.

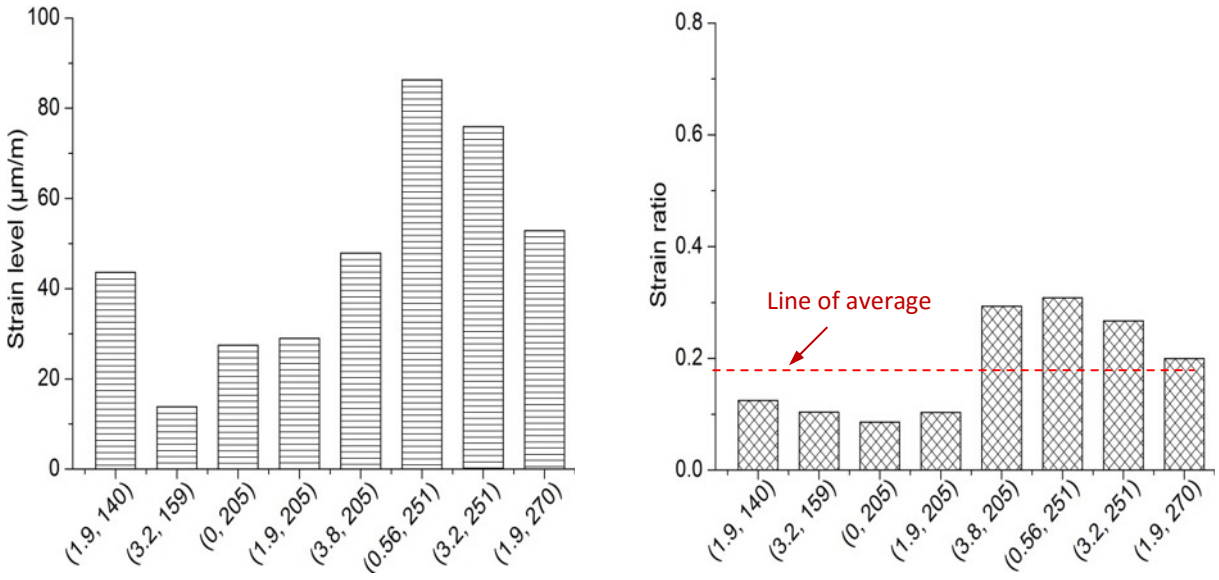


(a) Strain level (b) Strain ratio

**Figure 5.37** Strain level and strain ratio of clay-cement material corresponding to one million load cycles

## 5.7 Correlations between the mechanical properties

The unconfined compressive strength and indirect tensile strength tests, by using cylindrical specimens and compression machine, are widely used methods and easy to perform, but in some cases obtaining beam specimens may be difficult and the corresponding flexural testing equipment may not be available everywhere. So, knowing the correlation between the mechanical properties is very useful to determine other mechanical properties from the measured ones.

### 5.7.1 Compressive strength and tensile strength

Figure 5.38 gives the correlations between on one hand the indirect tensile strength or the flexural tensile strength and on the other hand the compressive strength. It also includes the regressed mathematical models which can be used to predict the tensile strength at given compressive strength. All the data are based on the mean value of three tested specimens and includes all tested mixtures at all curing times. From Figure 5.38 it can be concluded that the indirect tensile strength and flexural tensile strength are both in linear relation with the compressive strength, independent on the curing time and mix proportions. These two linear models both exhibit satisfactory $R^2$ values and indicate a good correlation, expressed as the following equations:

$$ITS = 0.153 \cdot UCS + 0.022 \qquad R^2 = 0.91 \qquad (5\text{-}33)$$

$$FTS = 0.376 \cdot UCS + 0.536 \qquad R^2 = 0.84 \qquad (5\text{-}34)$$

Where, $UCS$ is unconfined compressive strength (MPa), $ITS$ is indirect tensile strength (MPa), $FTS$ is flexural tensile strength (MPa).

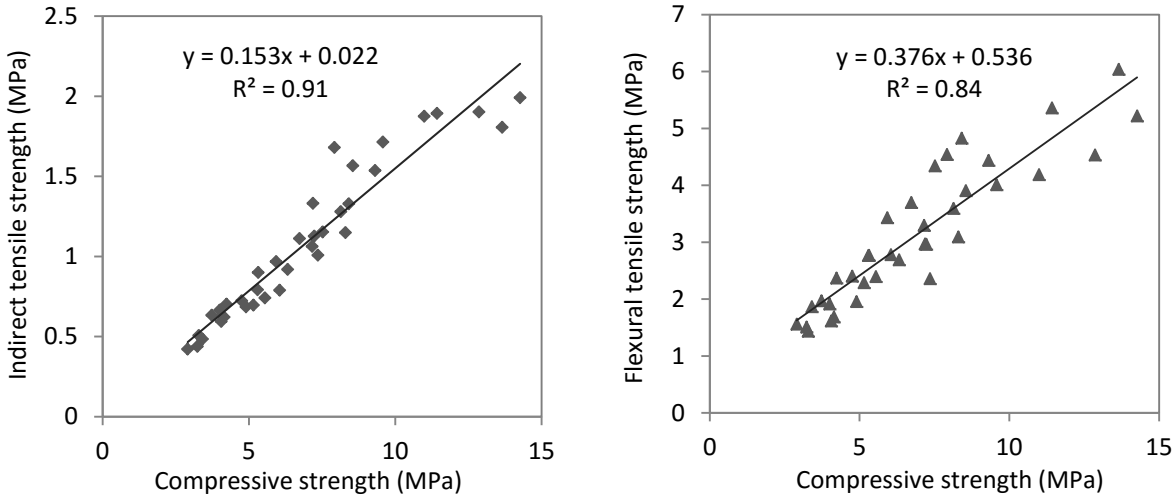


**Figure 5.38** Correlation between compressive strength and tensile strength

Figure 5.39 shows the ratio of tensile strength to compressive strength of all the clay-cement mixtures including all different curing times. In Figure 5.39 it can be observed that the indirect tensile strength is around 15% of the compressive strength for clay-cement material and this ratio is about constant for all the mixtures. In contrast, the ratio of flexural tensile strength to compressive strength shows much more scatter, ranging from 0.3 to 0.6.

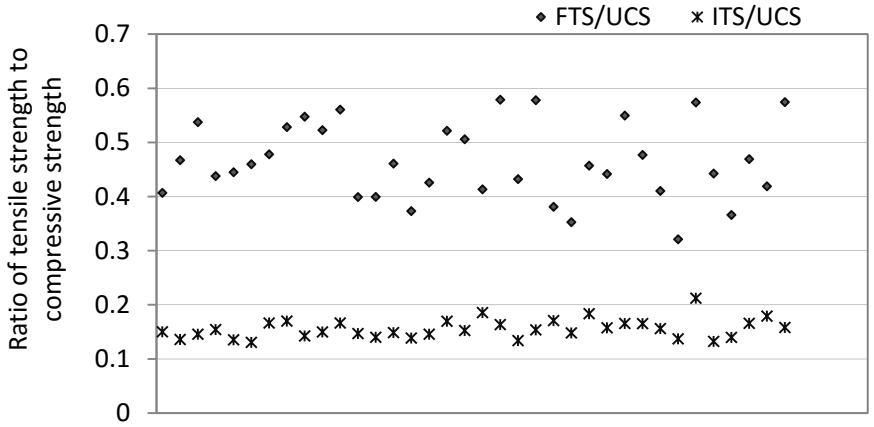


**Figure 5.39** Ratio of tensile strength to compressive strength

Table 5.8 summarizes the ratio of tensile strength and compressive strength for both sand-cement and clay-cement materials in this study, as well as the findings obtained from literature studies.

**Table 5.8** Ratio of tensile strength to compressive strength of cement stabilized materials

| Ratio | Sand-cement | Clay-cement | Literature studies | |
|---|---|---|---|---|
| ITS/UCS | 0.10 | 0.15 | 0.1~0.13 | (Sherwood, 1968; Little, 1995; Thompson, 1996) |
| FTS/UCS | 0.15~0.30 | 0.3~0.6 | 0.2~0.33 | (TRH 13, 1986) |

As shown in Table 5.8, the ratio of tensile to compressive strength for clay-cement material is higher than the ratio for sand-cement material, especially FTS/UCS. It means that clay-cement material has a much higher flexural tensile strength related to compressive strength than sand-cement which indicates a higher flexibility of clay-cement material compared to sand-cement material. Compared with the literature studies, the ratio of FTS to UCS obtained on clay-cement in this study is much higher, which means that this ratio is strongly related to the soil type.

### 5.7.2 Indirect tensile and flexural tensile strength

Indirect tensile and flexural tensile strength are commonly used to characterize the tensile strength of stabilized materials. The correlation between these two properties is shown in Figure 5.40. As presented in Chapter 4, the ratio of ITS to FTS is approximately 50% to 60% for sand-cement mixture (equation 4-27). Compared with this, for clay-cement material, the ratio of ITS to FTS is nearly 36%.

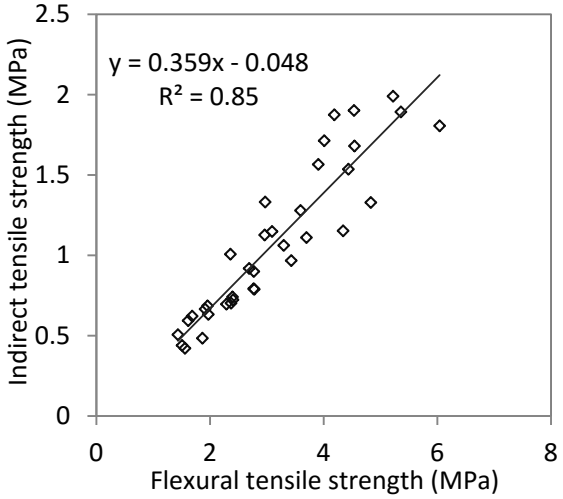


**Figure 5.40** Correlation between indirect tensile strength and flexural tensile strength

The equation shown in Figure 5.40 is described as follows:

$$ITS = 0.359 \cdot FTS - 0.048 \qquad R^2 = 0.85 \qquad (5\text{-}35)$$

Another finding also to be noted is that the flexural tensile strength obtained from the strain-sweep test (four-point bending) and from the monotonic three-point bending test is significantly different. Figure 5.41 compares the flexural tensile strength obtained from these two tests and includes the test data of all tested mixtures cured for 28 days.

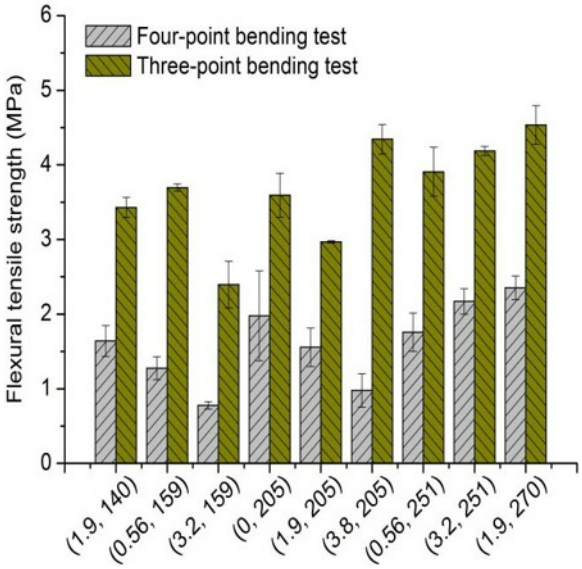


**Figure 5.41** Flexural tensile strength from three-point and four-point bending test

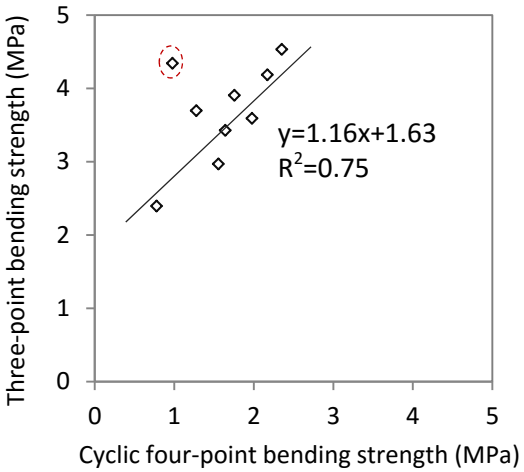


**Figure 5.42** Correlation between these two flexural strength

It can be clearly seen in Figure 5.41 that the flexural strength obtained from the strain-sweep test under cyclic loading is considerably lower than the one from the monotonic three-point bending test, on average 50% lower. This can be explained by the fact that the repeated loading in the sweep test might contribute to some sort of fatigue and hence weakens the material. The correlation between these two flexural tensile strength values is given in Figure 5.42 which indicates a relation model excluding a largely deviating data (as marked).

### 5.7.3 Mechanical strength and stiffness

Correlations between strength $f$ (*UCS, ITS* and *FTS*) and stiffness modulus $E$ have been developed for sand-cement material using either linear or non-linear models (as discussed in section 4.6.3), shown as follows:

$$E = a(f) + b \quad \text{and} \quad E = a(f)^b + c \tag{4-28}$$

Similarly, attempts are made to correlate the stiffness modulus with the mechanical strength of clay-cement material, shown in Figure 5.43. Figure 5.43 includes the correlation between stiffness modulus and the mechanical strength. The stiffness modulus discussed hereby is obtained as the stiffness at the applied strain of 50

μm/m during the strain-sweep test. Due to the fact that the stiffness was tested at the curing time of 28 days, all the data used here are obtained at the curing period of 28 days. Figure 5.43 (a), (b) and (c) are based on the average values of three tested specimens.

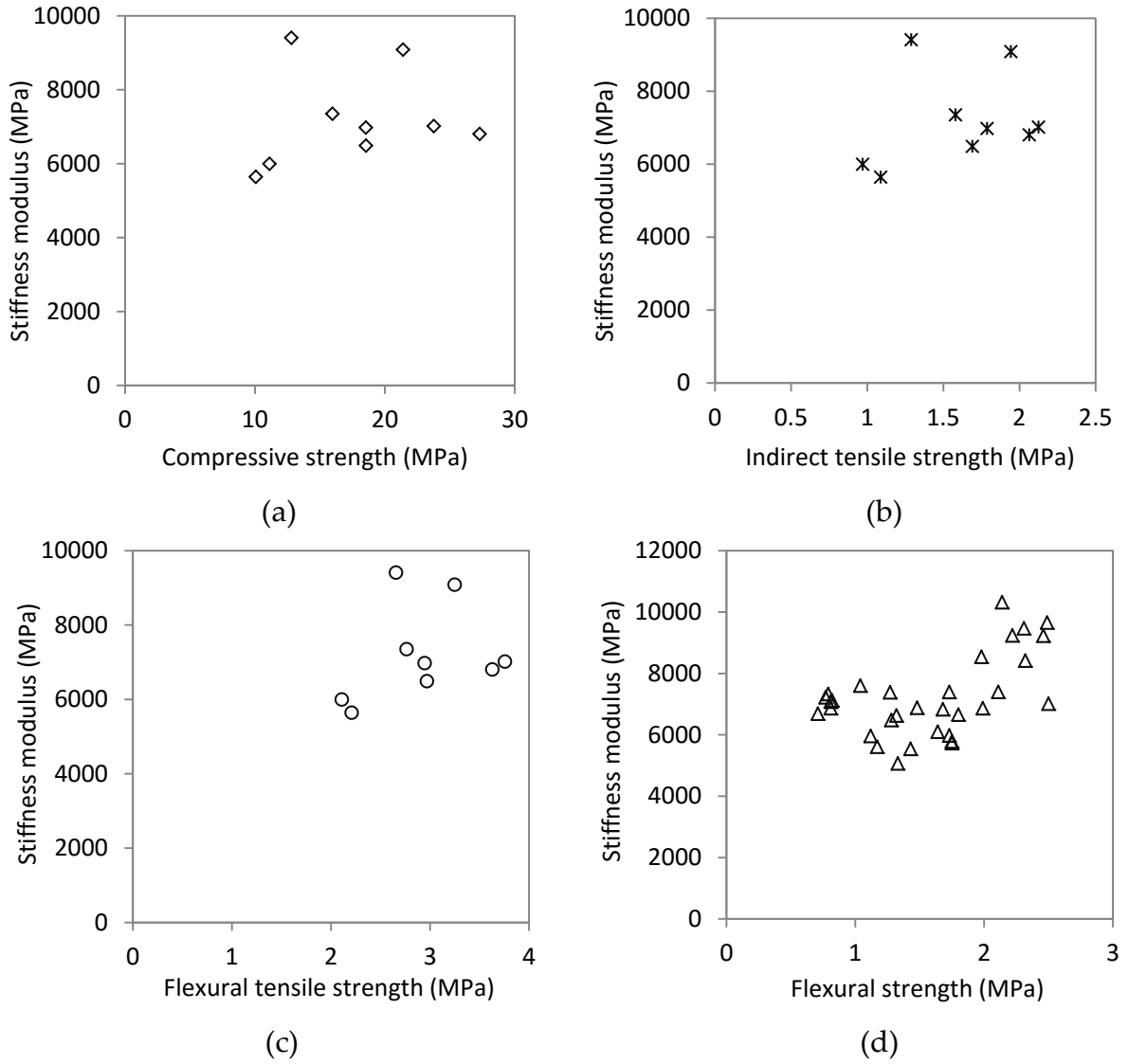


**Figure 5.43** Correlation between mechanical strength and stiffness modulus for clay-cement materials

In Figure 5.43 it can be observed that no clear correlation between stiffness modulus with any of the strength properties can be established due to the large scatter of the test data. So, the stiffness modulus of the clay-cement is not well related to the strength, either compressive or tensile strength. Compared with this, the results of sand-cement revealed reasonable correlations (discussed in section 4.6.3) and the higher strength generally corresponds to the higher stiffness modulus. So it implies that the stiffness modulus and the strength of cement stabilized materials are not uniquely related and much dependent on the soil type.

### 5.7.4 Strain at break and stiffness

Figure 5.44 presents the strain at break and stiffness obtained from the strain-sweep test (data illustrated in Tables 4.4 and 5.5).

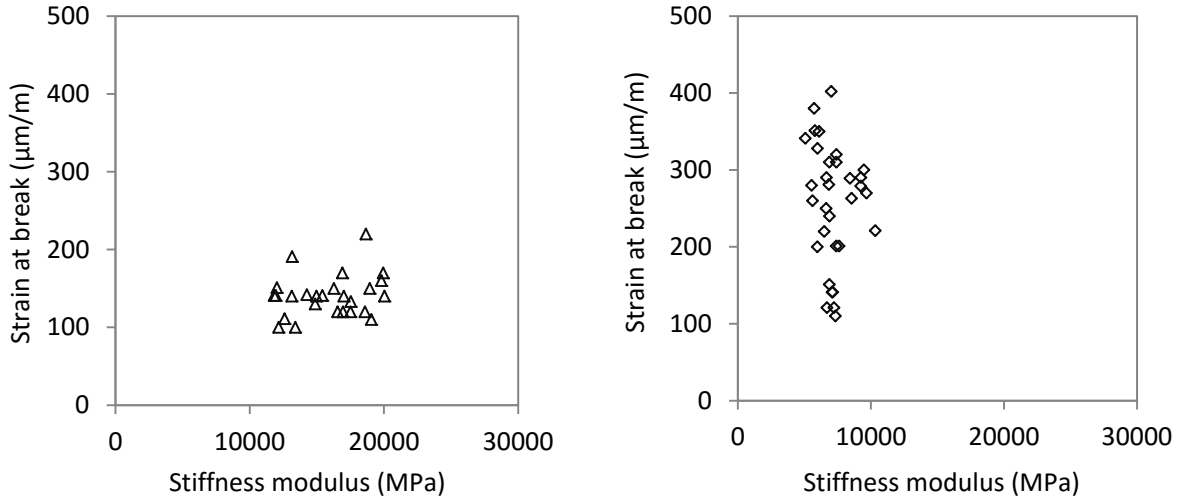


(a) Sand-cement (b) Clay-cement

**Figure 5.44** Correlation between strain at break and stiffness modulus

As can be observed in Figure 5.44, no obvious correlations between these two properties can be obtained which implies that the stiffness modulus doesn't influence the strain at break. On the basis of literature review, limited information regarding the correlation between strain at break and stiffness in flexure has been reported mainly due to the large variation of test results. One example from literature based on flexural tests is shown in Figure 5.45. Figure 5.45 demonstrates the similar trend that the strain at break is not well related to the stiffness modulus due to the large variation in these two properties.

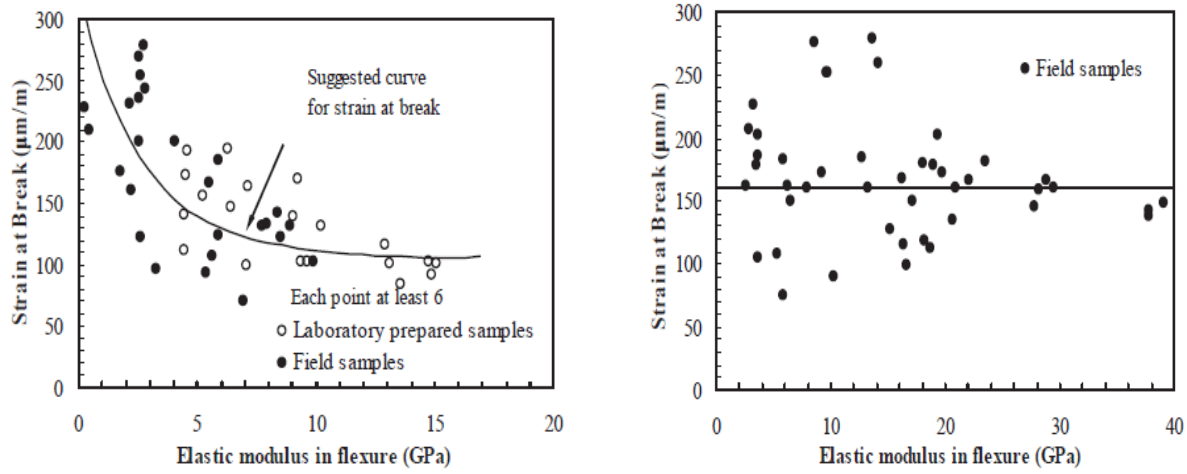


(a) Natural weathered gravel (b) Crushed rock material

**Figure 5.45** Correlation between strain at break and stiffness in flexural test (Walker et al., 1977)

However, as shown in Figure 5.44, sand-cement and clay-cement exhibit quite different values for stiffness modulus and strain at break, compared in Table 5.9.

**Table 5.9** Strain at break and stiffness of cement-sand and cement-clay materials

| Materials | Strain at break (μm/m) | Stiffness modulus (MPa) |
|---|---|---|
| Sand-cement | 100~200 | 12000~20000 |
| Clay-cement | 100~400 (mostly >200) | 6000~10000 |

It can be seen from Table 5.9 that the strain at break of clay-cement material is approximately two times higher than that of sand-cement material. In contrast, the stiffness modulus of clay-cement material is two times lower than that of sand-cement.

As discussed above in this section, it can be concluded that compressive strength, indirect tensile and flexural tensile strength are well correlated, whereas their relations with the stiffness modulus could not be achieved. Table 5.10 summarizes the established correlations, based on the curing period of up to 91 days. Flexural tensile strength is obtained from three-point bending test.

**Table 5.10** Equations for correlations between mechanical properties of clay-cement

| Correlations | Equations | $R^2$ |
|---|---|---|
| Compressive and indirect tensile strength | $ITS = 0.153 \cdot UCS + 0.022$ | 0.91 |
| Compressive and flexural tensile strength | $FTS = 0.376 \cdot UCS + 0.536$ | 0.84 |
| Flexural and indirect tensile strength | $ITS = 0.359 \cdot FTS - 0.048$ | 0.85 |

## 5.8 Conclusions

This Chapter focused on the properties of a specific cement stabilized clay. The test methods consisted of compression, indirect tensile and flexural tensile tests, as well as four-point bending fatigue tests. Based on the test results, the effects of cement and Rc contents on these properties were analyzed and estimation models were developed to predict the compressive and tensile strength. The principle findings of this Chapter can be summarized below:

- In the investigated cement stabilized clay, the cement content is found to be the main factor controlling the compressive, indirect tensile and flexural tensile strength. A higher cement content generally yields a higher strength.

Increasing Rc additive content shows a moderate strength improvement on the stabilized clay with high cement content 251 kg/m$^3$.

- The compressive and tensile strength of the investigated cement stabilized clay keeps increasing as the curing time continues. That is because after the cementitious reaction, the pozzolanic reaction takes place and continues to contribute to further strength development.
- Similar to the sand-cement material, estimation models for the mechanical properties of the cement stabilized clay were also formulated with the influencing factors of cement content, density of the specimen and the curing time, based on all the tested mixtures. The Rc additive content doesn't show influence on these general estimation models.
- Further analysis of these models at different cement contents shows that Rc content has a negative influence on the strength of mixtures with lower cement content contents (less than 251 kg/m$^3$), and positively influences the strength when higher cement content is used.
- The stiffness modulus of the investigated cement stabilized clay is influenced by the applied strain, which shows that the stiffness decreases until failure under increased strain. Compared with sand-cement material, the rate of decrease is lower and most of the clay-cement mixtures are able to withstand a much higher strain level before breaking.
- The estimation model of the initial stiffness modulus of cement stabilized clay shows a positive influence of the cement and Rc contents. In contrast, the results of strain at break and flexural strength show much variation and no consistent correlation with either the cement or Rc content was found.
- Fatigue relations have been obtained for all the clay-cement mixtures. However, these relations show a large scatter between mixtures and most of the mixtures exhibit low $R^2$ for the fatigue relations. No consistent correlation with either cement or Rc content could be drawn.

## References

ACI. (1990). American Concrete Institute Committee 230. State-of-the-Art Report on Soil Cement. ACI Materials Journal, Vol. 87, No. 4, pp. 395–417.

Achampong, F., Usmen, M., & Kagawa, T. (1997). Evaluation of Resilient Modulus for Lime-and Cement-Stabilized Synthetic Cohesive Soils. Transportation Research Record: Journal of the Transportation Research Board, 1589(1), 70-75.

Adaska, W.S. and D.R. Luhr. (2004). Control of reflective cracking in cement stabilized pavements, RILEM Publications.

Aydogmus, T., Alexiew, D., & Klapperich, H. (2004). Investigation of interaction behaviour of cement-stabilized cohesive soil and PVA geogrids. In Geotechnical engineering with geosynthetics, Proceedings of the third European Geosynthetics Conference, Munich, Germany. p (Vol. 3).

Balbo, J.T., & Cintra, J.P. (1996). Fatigue verification criteria for semi-rigid pavements. In National Meeting on Asphalt Mixture and Pavements, available online at: http://www, ptr. usp. br.

Bhattacharja, S. and J.I. Bhatty. (2003). Comparative performance of Portland cement and lime stabilization of moderate to high plasticity clay soils. Research and Development Bulletin RD 125. PCA Skokie, USA.

Christensen, A.P. (1969). Cement modification of clay soils. Research and development Bulletin RD002.01S, Portland Cement Association, Skokie, Illinois, USA.

Ghuzlan, K.A., & Carpenter, S.H. (2002). Traditional fatigue analysis of asphalt concrete mixtures. Urbana, 51, 61801.

Halsted, G. (2011). Cement-Modified Soil for Long Lasting Pavements. Annual conference of the transportation association of Canada Edmonton, Albert.

Ingles, O.G., Metcalf, J.B. (1972). Soil Stabilization Butterworths, Sydney.

Jauberthie, R., Rendell, F., Rangeard, D., & Molez, L. (2010). Stabilisation of estuarine silt with lime and/or cement. Applied Clay Science, 50(3), 395-400.

Kolias, S., Kasselouri-Rigopoulou, V., & Karahalios, A. (2005). Stabilisation of clayey soils with high calcium fly ash and cement. Cement and Concrete Composites, 27(2), 301-313.

Little, D.N. (1995). Handbook for stabilization of pavement subgrades and base courses with time, Dubuque: Kendall/hunt.

Little, D.N. (2009). Recommended Practice for Stabilization of Subgrade Soils and Base Materials. NCHRP web-only document 144. Texas A&M University, Texas.

Molenaar, A.A.A. (2010). Road Paving Materials Part 1 Cohesive and non-cohesive soils and unbound granular materials for bases and sub-bases in roads. Lecture notes CT 4880, Delft University of Technology, Netherlands.

Moore, D.M., & Reynolds, R. C. (1989). X-ray Diffraction and the Identification and Analysis of Clay Minerals (Vol. 378). Oxford: Oxford university press. pp. 120-121.

Prusinski, J.R., & Bhattacharja, S. (1999). Effectiveness of Portland cement and lime in stabilizing clay soils. Transportation Research Record: Journal of the Transportation Research Board, 1652(1), 215-227.

Rafalko, S.D., Filz, G.M., Brandon, T.L., & Mitchell, J.K. (2007). Rapid chemical stabilization of soft clay soils. Transportation Research Record: Journal of the Transportation Research Board, 2026(1), 39-46.

Scullion.T, Sebesta. S., Harris, J.P., and Syed, I., (2005). Evaluating the Performance of Soil-Cement and Cement-Modified Soil for Pavements: A Laboratory Investigation, RD120, Portland Cement Association, Skokie, Illinois, USA.

Shon, C.S., Saylak, D., & Mishra, S.K. (2010). Combined use of calcium chloride and fly ash in road base stabilization. Transportation Research Record: Journal of the Transportation Research Board, 2186(1), 120-129.

Sherwood, P.T. (1968). The properties of cement stabilized Materials. London: Road Research laboratory.

Solanki, P., Zaman, M. M., & Dean, J. (2010). Resilient modulus of clay subgrades stabilized with lime, class C fly ash, and cement kiln dust for pavement design. Transportation Research Record: Journal of the Transportation Research Board, 2186(1), 101-110.

Thompson, M.R. (1996). The Split-Tensile Strength of Lime-Stabilized Soils, Record 92, Highway Research Board.

TRH 13 (1986). Cementitious Stabilizers in Road Construction South Africa. Pretoria, South Africa.

Tingle, J.S., Newman, J.K., Larson, S.L., Weiss, C.A., & Rushing, J.F. (2007). Stabilization mechanisms of nontraditional additives. Transportation Research Record: Journal of the Transportation Research Board, 1989(1), 59-67.

Walker, R.N., Paterson, W.D.O., Freeme, R.N., & Marais, C.P. (1977). The South African Mechanistic Design Procedure. The 4th International Conference Structural Design of Asphalt Pavements, Michigan.

Williams, R.I.T. (1986). Cement-treated pavements: Materials, Design and Construction, London: Elsevier Applied Science Publishers LTD.

# CHAPTER 6

# MICROSTRUCTURE AND MINERALOGICAL CHARACTERIZATION OF CEMENT STABILIZED SOIL WITH ROADCEM ADDITIVE

Use of Rc additive in cement stabilized sand and clay materials has been observed to result in changes in mechanical properties, which was mainly discussed in Chapters 4 and 5. In order to explain the observed behavior of the property changes caused by using Rc additive, this Chapter focuses on the properties of stabilized materials in the microscale. In this Chapter, laboratory test methods consisting of X-ray diffraction analysis (XRD) and scanning electron microscopy (SEM) were performed on the cement based materials with and without use of Rc additive.

Use of X-ray diffraction patterns will aid in the analysis of the chemical changes in hydration products as a result of using the Rc additive. SEM images provide comparison of the morphology of the microstructure with and without addition of the Rc additive.

## 6.1 Background

Traditional stabilizers, such as cement and lime, have been intensively researched and the fundamental stabilization mechanisms have been identified (Little, 2009; ACI, 1990). However, due to the diverse chemical composition of non-traditional additives, limited information of their mechanism in the stabilization system is reported. In this study, Rc additive in cement stabilization is evaluated, and the mechanical properties have been presented in the previous Chapters which generally show that use of this Rc additive can cause changes in mechanical properties, such as strength improvement in cement stabilized sand materials. The results generally give an indication that the Rc additive may influence the cementitious hydration process. Therefore, this Chapter focuses on the analysis of the microstructure of the cementitious materials which can provide a better understanding of the interaction of the Rc-cement-soil system.

It appeared from the literature that scanning electron microscopy (SEM) and X-ray diffraction analysis (XRD) are often employed for the analysis of cement stabilized materials in the microscale (Katz et al., 2001; Tingle et al., 2007; Kamon & Nontananandh, 1991). A SEM image provides a useful tool for visual characterization of the microstructure. Figure 6.1 shows some SEM images which illustrate the changes of cement stabilized clay at different curing times.

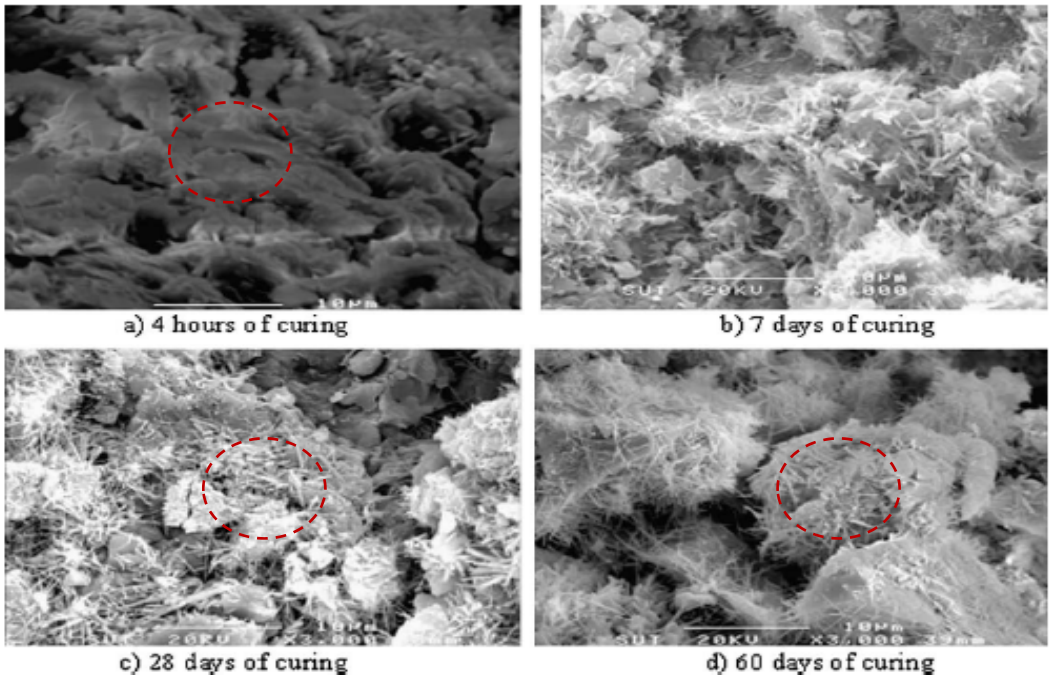


**Figure 6.1** SEM images of clay stabilized with 10% cement at different curing times (Horpibulsuk et al., 2010)

It can be seen from Figure 6.1 that after 4 hours of curing, the soil clusters and the pores are covered and filled by the cement gel (hydrated cement) (graph a). Over time, as the cement hydration proceeds, more hydration products are formed, binding the clay particles together and the soil–cement clusters tend to be larger (graph d).

Powder XRD technique uses the scattering of X rays from a crystal to produce a characteristic interference pattern (a diffractogram) that can be compared with standard diffractograms for different minerals. XRD diffraction pattern is a direct method to identify the crystalline phase present in the cementitious materials and aid in the assessment of the change in mineralogy. For instance, the XRD technique was used in a study by Mutaz et al (2011) to detect the presence of the smectite group of clay mineral which is primarily responsible for the high swelling potential of clay soil. A typical study on stabilizing clay with a liquid ionic stabilizer conducted by Katz et al (2001) well documented the comparative XRD results of using different amounts of this stabilizer, shown in Figure 6.2. Figure 6.2 compares the X-ray diffraction patterns of the treated and untreated clay specimens with an ionic stabilizer to assess the changes in mineralogy of clay soil. The clay soil used in the study is classified as fat clay (CH), mainly consisting of montmorillonite mineral.

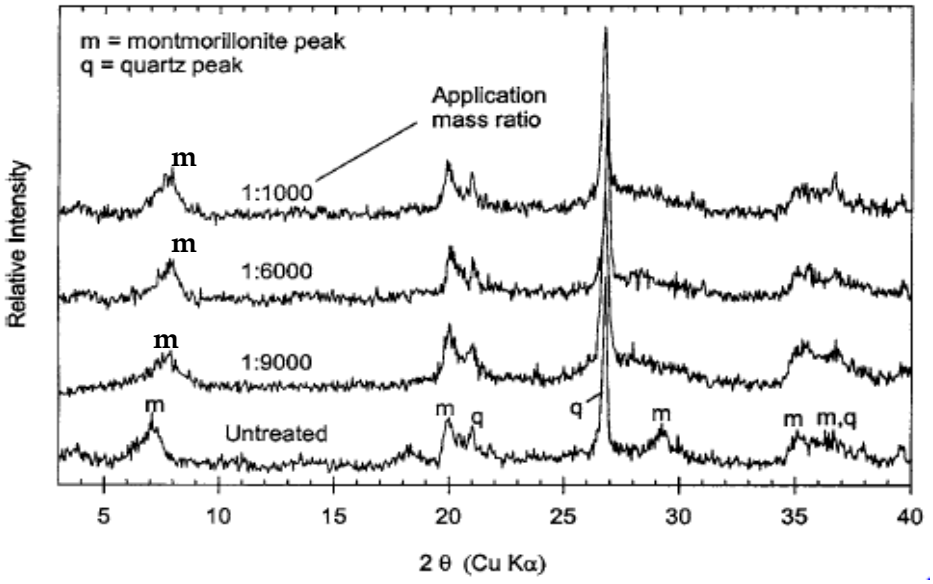


**Figure 6.2** X-ray diffraction patterns for the composite clay sample when treated with different amounts of a liquid ionic stabilizer (Katz et al, 2001)

Figure 6.2 reveals a noticeable change in the montmorillonite spectra, the peak at $2\theta=29^{o}$ diminished when treated with the ionic stabilizer. However, the mineralogy after treatment was still consistent with the untreated clay.

Based on the use of these two test methods, this Chapter aims to investigate the properties of cement stabilized soil in the micro-scale. The basic idea is to identify the changes of using the Rc additive in cement based materials by evaluating the morphology in microstructure and the chemical analysis of the hydration products.

## 6.2 Materials and test method

### 6.2.1 Materials and mix design

To continue with the research of the Chapters 4 and 5, cement stabilized clay and sand with Rc additive are chosen to be further investigated. The test program only concentrates on the influence of the Rc additive on the properties of cementitious materials, without considering the factor of cement content. Thus, two mix compositions with the same amount of cement 251 kg/m$^3$ with use of Rc 3.2 kg/m$^3$ and without Rc are evaluated. The chosen amounts of cement and Rc additive are relatively high, which may maximize the chemical changes and morphology of the cemented structure for observation.

In addition to this, in order to indicate the pure reaction between cement and Rc additive, cement paste is also chosen to be assessed, excluding the influence of the soil materials. Three different amounts of Rc additive were applied in the cement paste, i.e. 0, 1.27% and 2.55% (by mass of the cement content). Especially the high amount of Rc 2.55% was chosen to increase the likelihood of observing changes. Water-cement ratio 0.35 was used for preparing cement paste specimens.

Table 6.1 illustrates the mix design used for this test program. Two curing times were considered, 3 and 28 days.

**Table 6.1** Mix design and test method

| Materials | Mix design | Test method | Age (days) |
|---|---|---|---|
| Cement paste | Rc 0% | XRD plus SEM | 3, 28 |
| Cement paste with Rc | Rc 1.27% | XRD plus SEM | 3, 28 |
| Cement paste with Rc | Rc 2.55% | XRD plus SEM | 3, 28 |
| Cement stabilized clay | (0, 251) | XRD plus SEM | 3, 28 |
| Cement stabilized clay with Rc | (3.2, 251) | XRD plus SEM | 3, 28 |
| Cement stabilized sand | (0, 251) | SEM | 3, 28 |
| Cement stabilized sand with Rc | (3.2, 251) | SEM | 3, 28 |

In order to avoid the influence of blast furnace slag (contained in CEM III) on the observation of cement hydration products, Portland cement CEM I 42.5N was used to prepare specimens for SEM and XRD tests. XRD analysis was not conducted on cement stabilized sand material due to the fact that the quartz mineral in sand particles have a strong scattering pattern which might influence the observation of the scattering pattern of the cement hydration product.

### 6.2.2 Sample preparation and test method

Cement stabilized sand and clay specimens were prepared by moulding prismatic specimens 160×40×40 mm and cement paste was shaped into cubes 50×50×50 mm. After cured in the climate chamber (temperature 20°C and relative humidity 90%) for 3 or 28 days, the specimens were broken into portions and immersed into liquid nitrogen to stop hydration, and subsequently freeze-dried before testing. For the XRD tests the samples were prepared by grinding a small portion of the material by a mortar into very fine powder, examined by a Bruker D5005 diffractometer equipped with Huber incident-beam monochromator and Braun PSD detector using Cu Ka radiation at incident angle 2θ between 5° and 90°, see Figure 6.3 (a).

For the SEM test, the cement paste and cement stabilized sand and clay samples were all examined. Samples for the SEM test were prepared by fracturing the specimen after freeze-dried to expose clean fresh surfaces. Afterwards, the exposed fractured surfaces were coated with carbon and then examined by an Environmental Scanning Electron Microscope (ESEM, Philips XL30 Series) equipped with an Energy Dispersive X-ray element analyzing system, see Figure 6.3 (b). SEM images in this research were all taken in the secondary electron detection mode. Energy Dispersive X-ray Spectroscopy (EDS) patterns were obtained at the points of interest.

(a) X-ray diffractometer

(b) Scanning electron microscope

**Figure 6.3** Test equipment

## 6.3 Analysis of the results

### 6.3.1 X-Ray Diffraction

X-ray diffraction is used to identify the crystalline phases present in cement based materials. The following section discusses the XRD results of the cement paste and cement-stabilized clay materials with and without Rc additive.

**(1) Cement paste**

The major crystalline phases to be detected in XRD patterns of cement paste include the cement hydration products portlandite $Ca(OH)_2$ (CH) and ettringite (AFt), as well as the un-hydrated Tricalcium silicate ($C_3S$), Dicalcium silicate ($C_2S$) and Tetracalcium alumino ferrite ($C_4AF$) (where C=Ca, S=$SiO_2$, A=$Al_2O_3$, F=$Fe_2O_3$ and t=tri). The main cement hydration product C-S-H gel is not considered herein due to its poor crystalline nature. Figure 6.4 presents the XRD pattern of cement paste cured for 3 days which illustrates a sum of the diffraction patterns of each individual phase. Three cement paste mixtures with different amounts of Rc additive are compared.

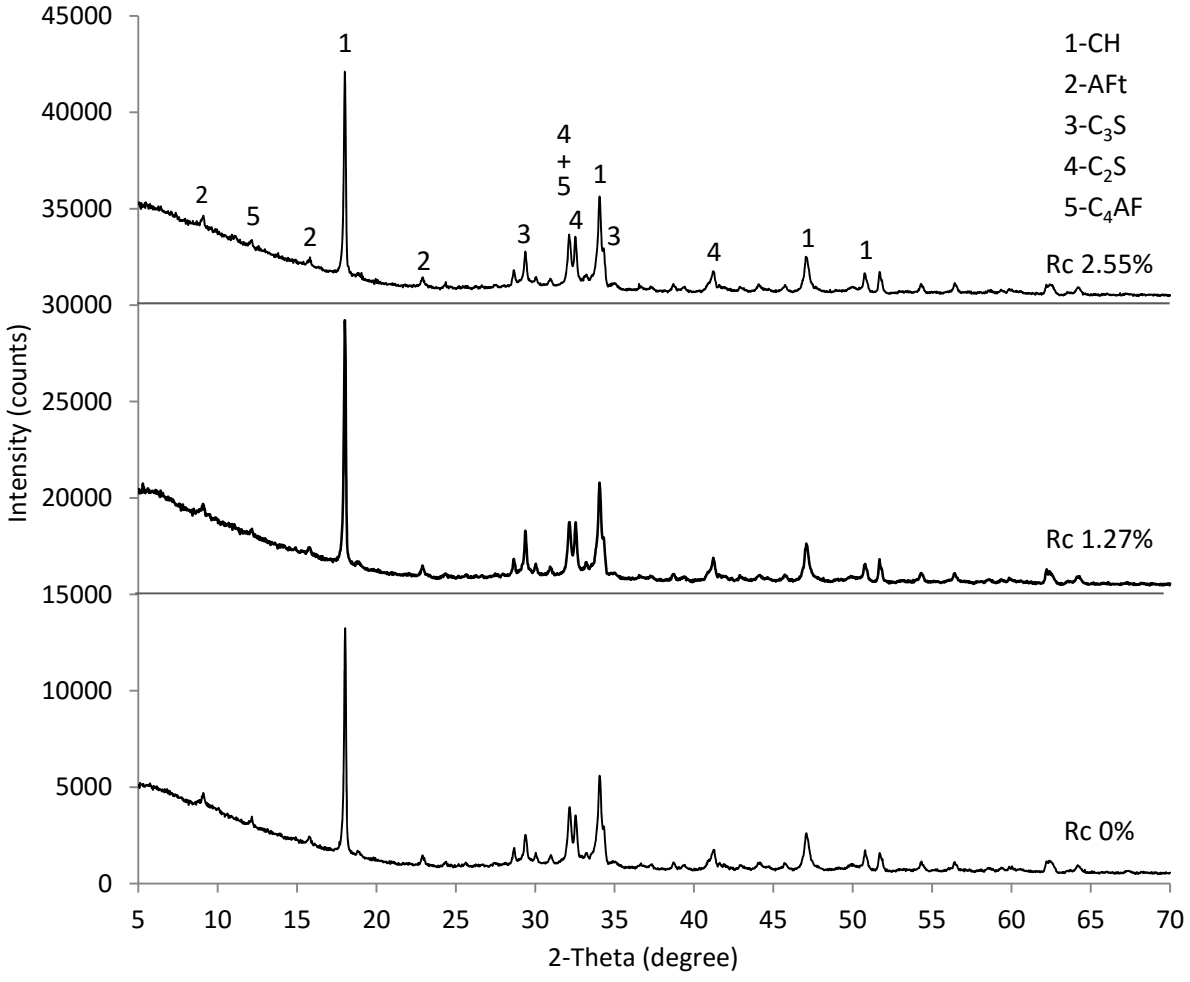


**Figure 6.4** X-ray diffraction pattern of cement paste at 3 days

As shown in Figure 6.4, portlandite ($Ca(OH)_2$) was the major crystalline phases which dominated in the XRD pattern of cement paste. These three mixtures exhibit very similar XRD patterns, including the peak position and width and shape of each diffraction peak. However, it can be noted that the intensity of portlandite peak in the mixture with Rc 1.27% is slightly higher than the mixtures without Rc and with higher Rc content, which might give an estimate of higher amount of portlandite resulted in the hydration products.

Similarly, the XRD results of the cement paste cured for 28 days are given in Figure 6.5. In Figure 6.5 it can be observed that the 28-day XRD patterns exhibit the same crystalline phases as detected in the 3-day patterns. The similar XRD patterns are observed for these three mixtures and again the diffraction peak of the portlandite of the mixture with Rc 1.27% shows the highest intensity. The diffraction peak intensity doesn't give precise quantitative assessment of the cement hydration products, therefore, the quantitative influence of the Rc additive on the cement hydration needs to be further verified.

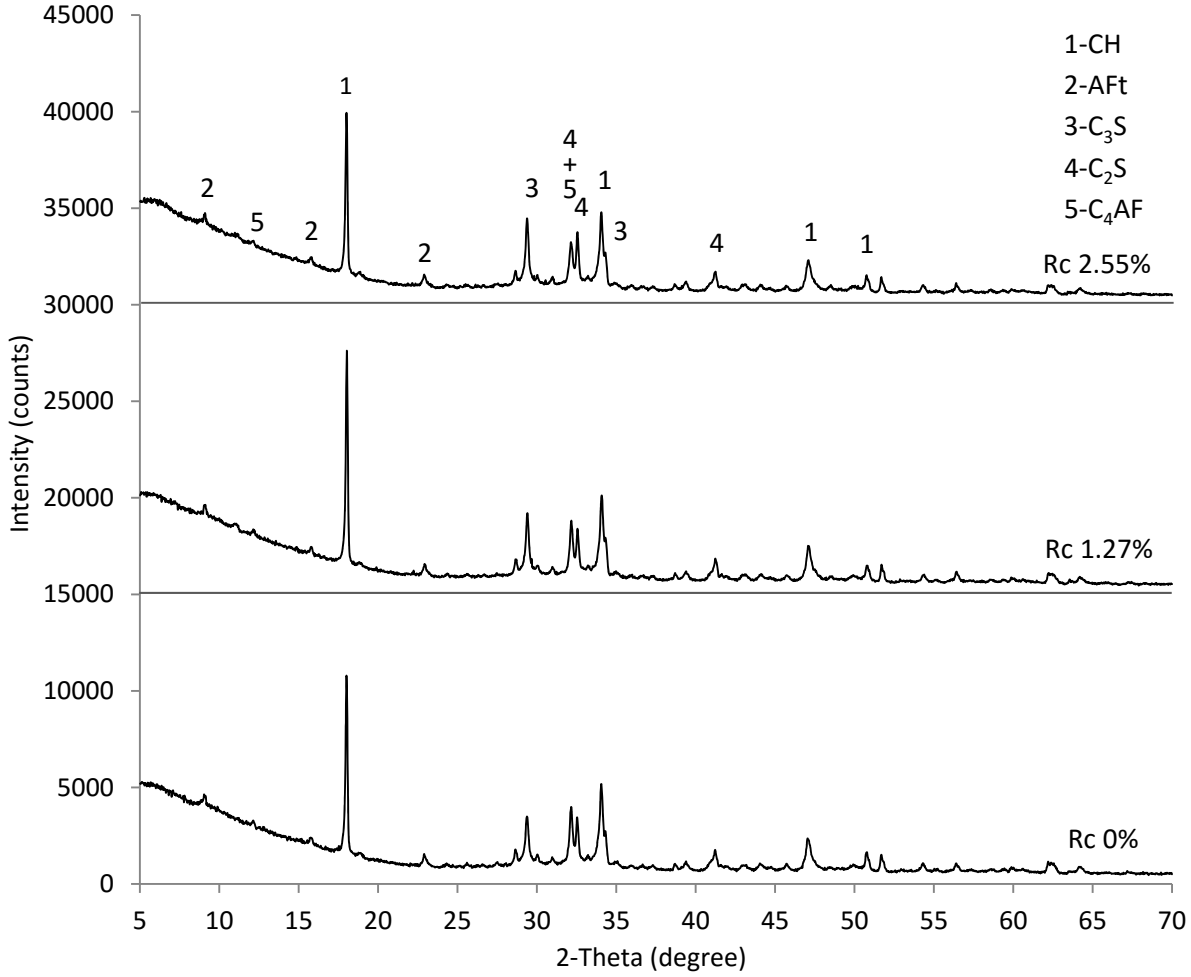


**Figure 6.5** X-ray diffraction pattern of cement paste at 28 days

**(2) Cement stabilized clay**

Comparison of the XRD patterns of the cement stabilized clay samples with and without Rc additive (cured for 3 days) is shown in Figure 6.6. Except for quartz (Q), the clay minerals including kaolinite (K), illite (I) and montmorillonite (M) are identified in both samples. However, the cement hydration products, such as CH and ettringite can't be obviously observed in the XRD patterns mainly due to the fact that the clay minerals, especially quartz, has a strong X-ray scatter and thus exhibits a much higher intensity than the cement hydration products.

Figure 6.7 presents the XRD patterns of cement stabilized clay with and without Rc additive cured for 28 days, which also shows the similar XRD patterns of the clay minerals in these three mixtures. It might be caused by the high intensity of quartz peak influences the observation of other mineral peaks as well as the cement hydration products.

Besides, observation of the mineralogy of the stabilized clay soil can also be influenced by the complex constituents of the clay minerals. Since the natural clay soil encountered in the filed typically contains a mixture of many different minerals, Katz (2001) advised to evaluate the "pure" clay with one type of mineral, which can increase the likelihood of observing the physical-chemical changes induced by the stabilizer.

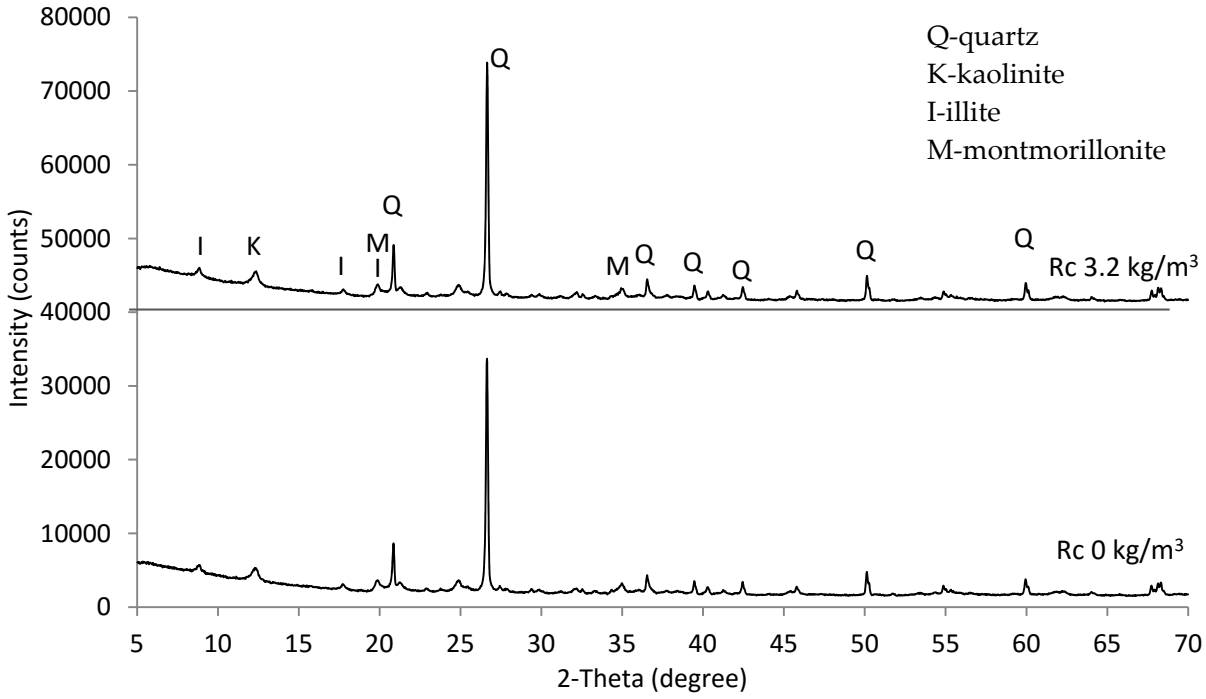


**Figure 6.6** X-ray diffraction pattern of cement stabilized clay at 3 days

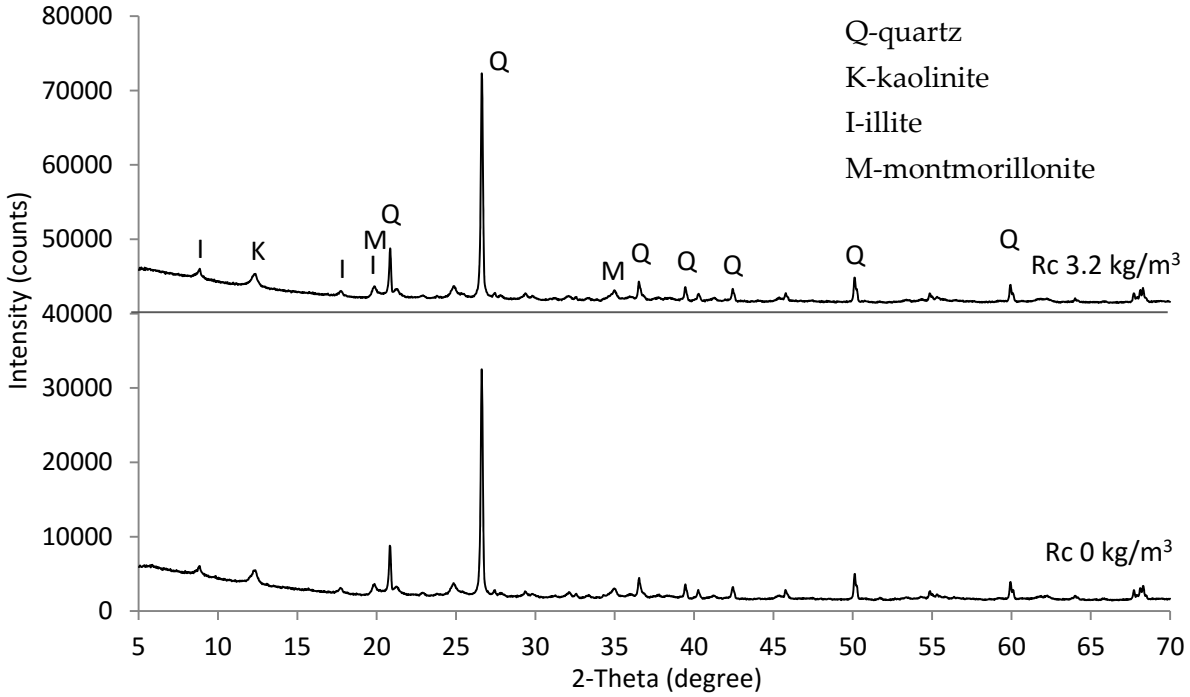


**Figure 6.7** X-ray diffraction pattern of cement stabilized clay at 28 days

### 6.3.2 SEM analysis

The SEM micrograph of cement paste, cement stabilized sand and cement stabilized clay are presented in the following figures. Mixtures with different Rc additive contents are evaluated and two curing ages are considered. For each sample three locations were examined and at each location images with different magnifications were taken. For each mixture, only one location which shows typical micrographs is presented.

**(1) Cement paste**

The SEM images with three magnifications of 500, 3000 and 5000 times for cement paste with different amounts of the Rc additive cured for 3 and 28 days are shown in Figure 6.8 and Figure 6.10, respectively. The EDS patterns were collected from two locations (marked as 1 and 2), shown in Figure 6.9.

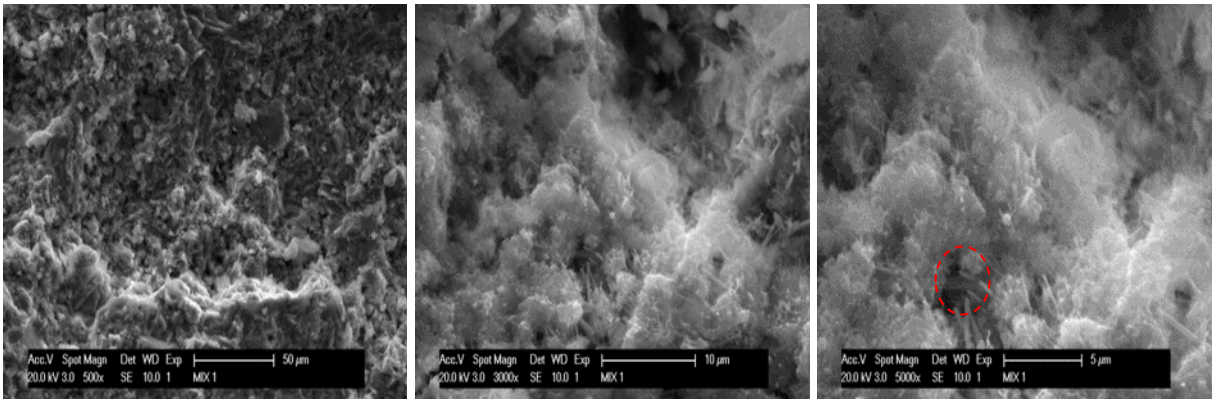

(a) Cement paste without Rc additive 0%

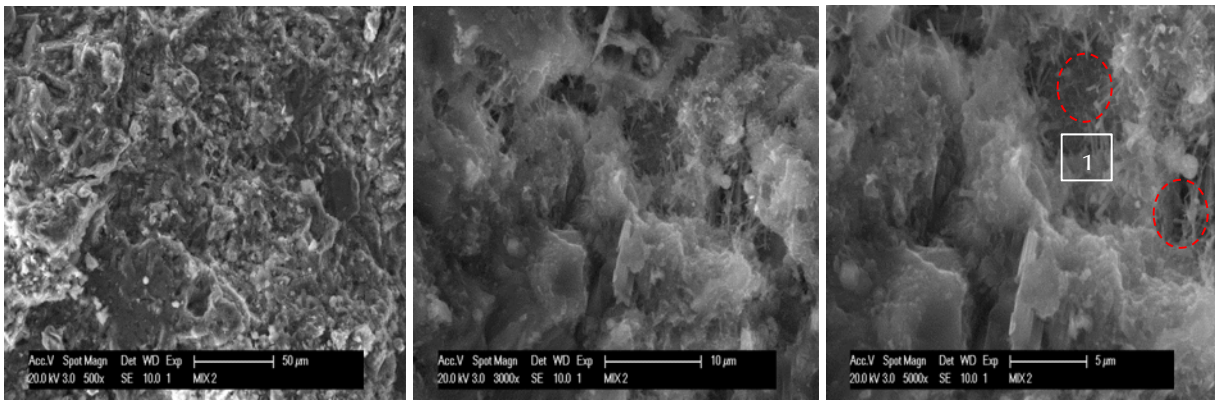


(b) Cement paste with Rc additive 1.27%

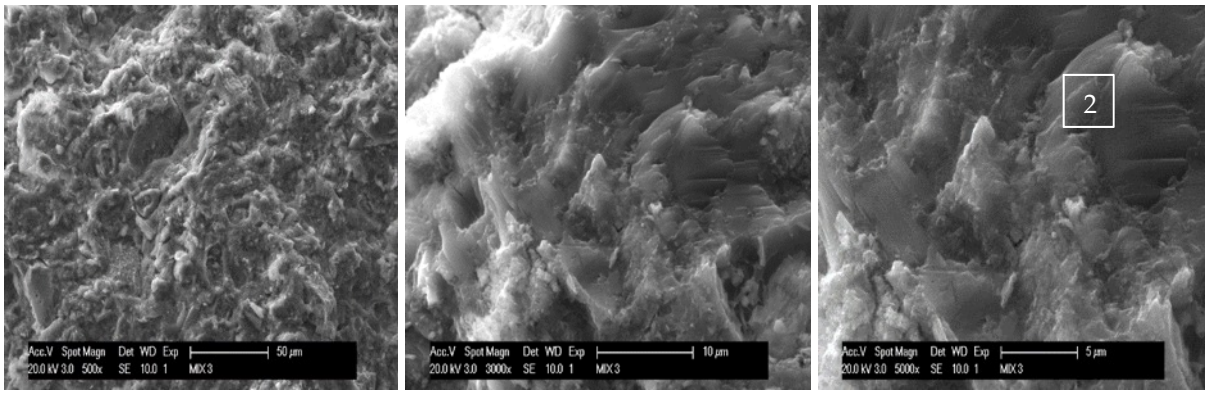


(c) Cement paste with Rc additive 2.55%

**Figure 6.8** SEM images of cement paste with different Rc contents at 3 days

In Figure 6.8 the SEM images at a magnification of 500 times show a similar morphology in these three mixtures. When zooming into higher magnifications (3000× and 5000×), needle-like minerals are visible in the mixtures with Rc 1.27% and without Rc (as marked), where the needle-like minerals are abundantly present and distributed throughout the entire area.

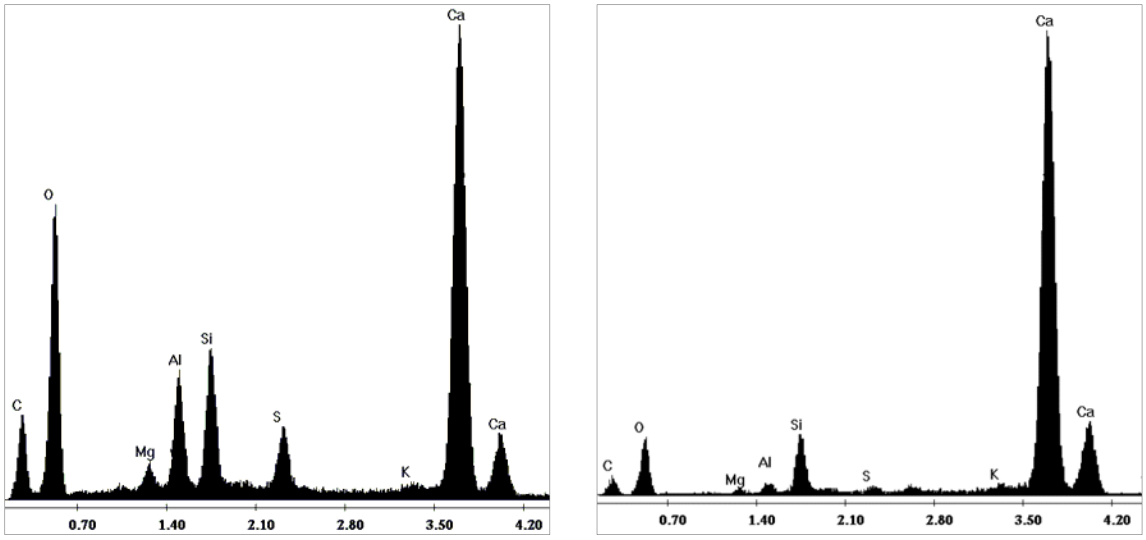


(a) Location 1 (b) Location 2

**Figure 6.9** EDS patterns of the cement paste

The EDS spectrum in Figure 6.9 (a), collected from the needle-like minerals shows Ca-S-Al peaks which indicate the presence of ettringite minerals. These ettringite mineral, which is the result of the reaction of calcium aluminate with calcium sulfate in the presence of water. This finding is consistent with the XRD results of cement paste which showed the formation of ettringite (Figure 6.4). EDS pattern in Figure 6.9 (b) shows the main component calcium which might indicate the calcium hydroxide.

It can also be clearly noted that the mixture without Rc exhibits much voids. Whereas, in the mixture with the highest Rc content, the microstructure seems more dense and shows fewer voids, which might indicate that more cement hydration products are formed filling the voids.

Similarly, the SEM images of cement paste cured for 28 days are presented in Figure 6.10. Figure 6.10 shows a more dense microstructure and fewer voids resulting from the 28-day cement hydration process. One has to note that the mixture without Rc shows visible cracks which can be caused by the shrinkage during cement hydration. Again, the mixtures with addition of Rc additive show dense micro-structure at 28 days which may lead to a higher strength in mechanical properties.

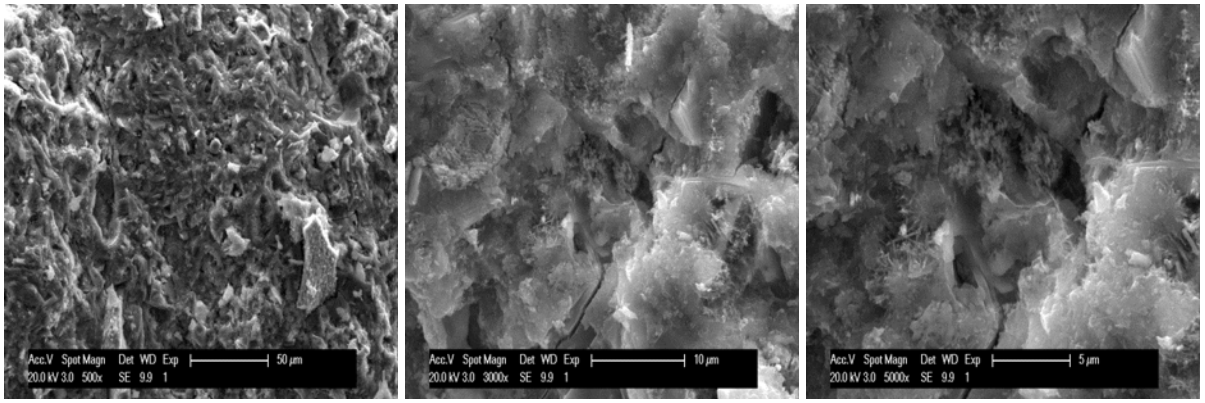


(a) Cement paste without Rc additive 0%

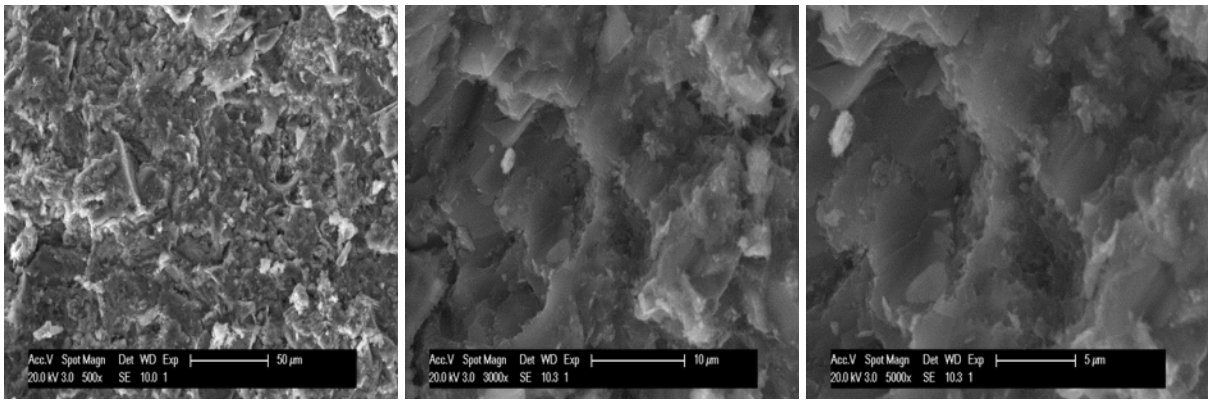


(b) Cement paste with Rc additive 1.27%

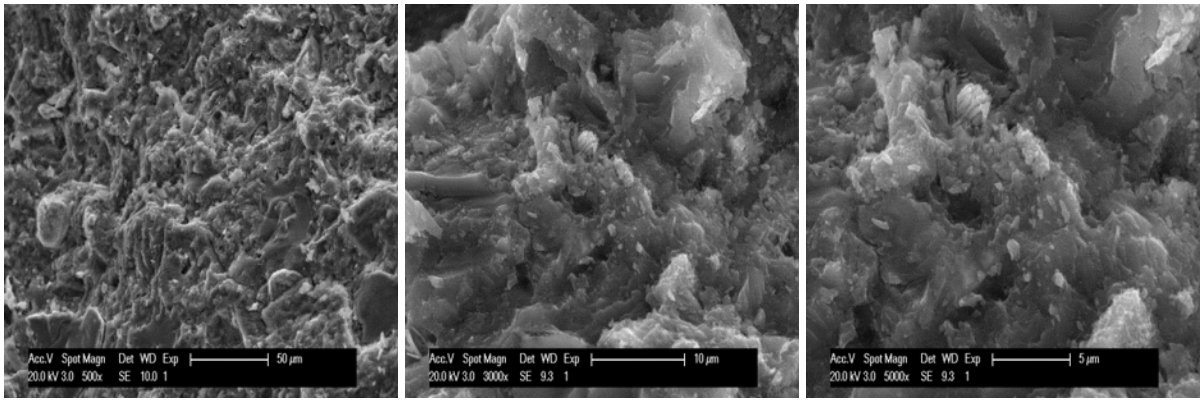


(c) Cement paste with Rc additive 2.55%

**Figure 6.10** SEM images of cement paste with different Rc contents at 28 days

**(2) Cement stabilized clay**

Figure 6.11 shows the SEM images of cement stabilized clay with and without Rc additive cured for 3 and 28 days. For each sample, SEM images with three magnifications, 500, 3000 and 5000 times are given.

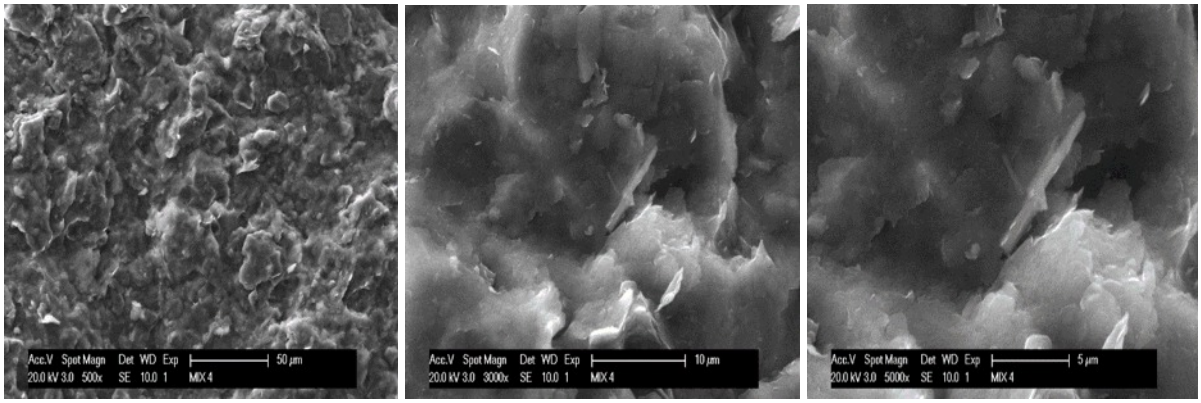

(a) Cement stabilized clay without Rc additive (0, 251) at 3 days

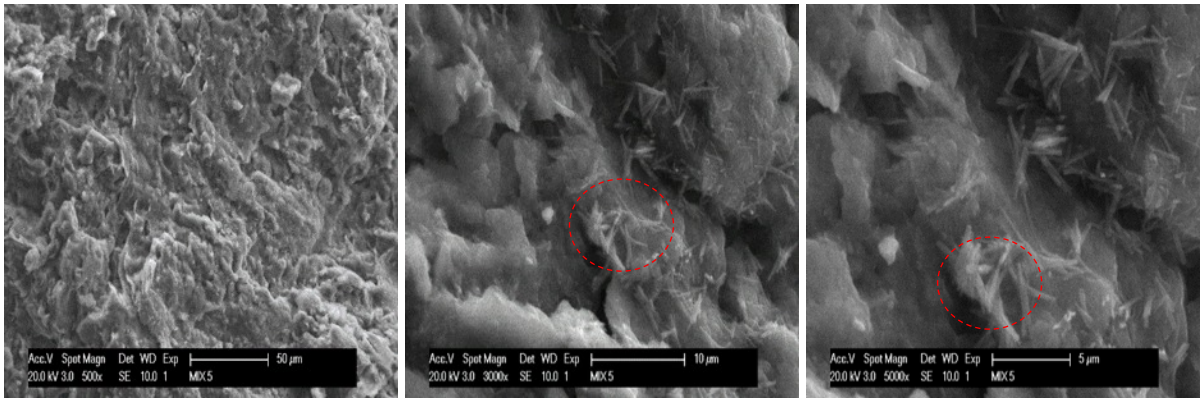

(b) Cement stabilized clay with Rc additive (3.2, 251) at 3 days

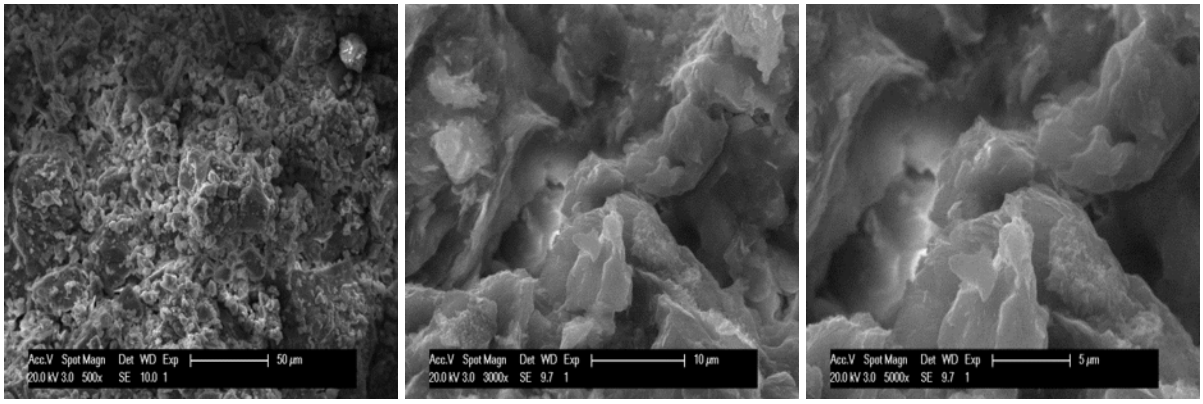

(c) Cement stabilized clay without Rc additive (0, 251) at 28 days

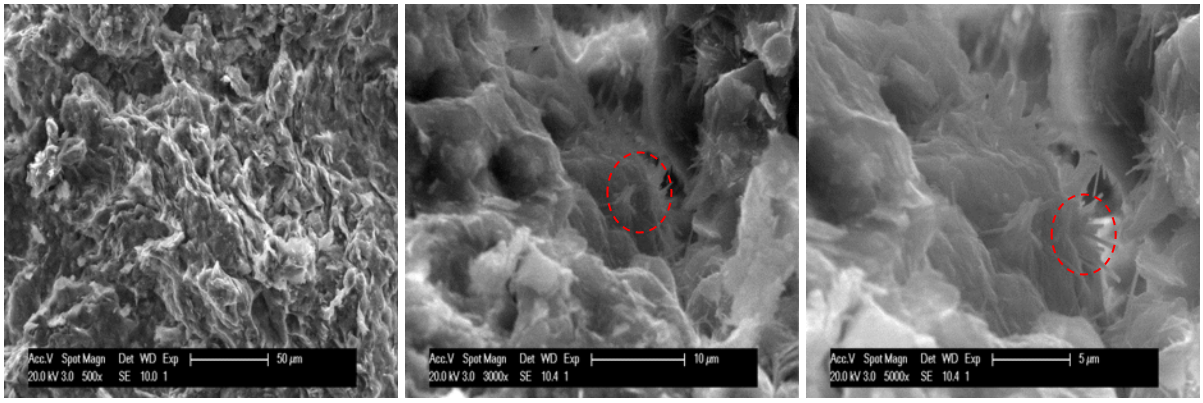

(d) Cement stabilized clay with Rc additive (3.2, 251) at 28 days

**Figure 6.11** SEM images of cement stabilized clay with and without Rc additive

Figure 6.11 compares the microstructure of cement stabilized clay with and without Rc additive at curing periods of 3 and 28 days. The needle-like mineral ettringite is observed in the mixture with Rc additive at 3 days and 28 days (as marked). These needle-like crystals are scattered throughout the scanning area, whereas these ettringite needles are not observed in the mixture without Rc additive.

When treating the clay soil with sulfate content by calcium-based stabilizer, the ettringite crystals are often formed because of the reaction of calcium with sulfates and alumina present in the soil (Katz et al, 2001; Little, 2009). The significant amounts of ettringite crystals can cause the pavement distress such as the volume expansion (Hunter, 1988; Wang et al, 2003). In the case of this study, when this type of clay (without sulfate content) stabilized with cement and Rc additive, the ettringite crystals could be resulted from the reaction of clay-cement with the compounds in Rc additive. Such expansion damage has not been reported in the road projects with use of Rc additive. To some extent, it may be hypothesized that the formed expansive crystals could compensate the volume shrinkage due to the moisture loss during cement hydration. However, cement stabilized soil materials with use of Rc additive is involved with complex chemical reaction, which needs further investigation.

As shown in the SEM images of the mixtures at age of 3 days, the hydrated clay-cement shows a homogeneous fabric and the components are indistinguishable. But at the age of 28 days, the SEM images show aggregated arrangement due to the modification by cement. During this modification process, cation exchange and flocculation occur. Afterwards, cement hydration and pozzolanic reactions would take place, producing the hydration products which bind the flocculated clay particles together.

Figure 6.12 gives the EDS results collected from the small portion of the clay-cement area covering the needle-like minerals. The EDS results show majority of silicon (Si) and aluminum (Al) minerals which are mainly from the clay soil. Besides, the EDS pattern of the location in the mixture with Rc additive shows weak trace of Ca-S-Al peaks which is in agreement with the presence of ettringite mineral as observed in Figure 6.11.

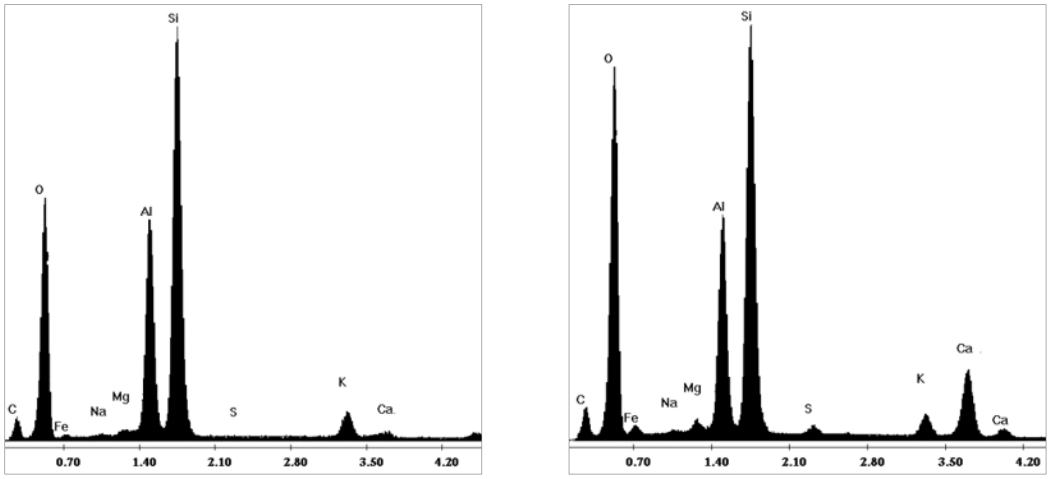


(a) Mixture without Rc (0, 251) (b) Mixture with Rc (3.2, 251)

**Figure 6.12** EDS pattern of cement stabilized clay at 3 days

**(3) Cement stabilized sand**

Similarly, the SEM images of cement stabilized sand are also obtained and shown in Figure 6.13, including the curing ages of 3 and 28 days. For each sample, SEM images with three magnifications of 100, 500 and 5000 times are given.

In Figure 6.13 from the images at a low magnification (100×), it can be seen that the sand particles were bonded together by the cement hydrates. The voids between sand particles are not fully filled with the hydration products and exhibit a very porous structure. However, it can be observed that the SEM image of the mixture with Rc at 28 days seems to exhibit more cement hydration products filling the voids which might explain the increased mechanical strength caused by adding Rc additive, as discussed in Chapter 4.

When zooming to 500× magnification, the interface between soil particle and cement paste is visible which shows that the bonding between the sand particles at 28 days is much stronger than at 3 days because of further cement hydration. The images at magnification 5000 were taken from the area of cement paste which showed the hydrated cementitious structure. It can be noticed that at 28 days there seems to exhibit more hexagonal plate-shaped crystals (calcium hydroxide) in the mixture with Rc additive compared to the mixture without Rc.

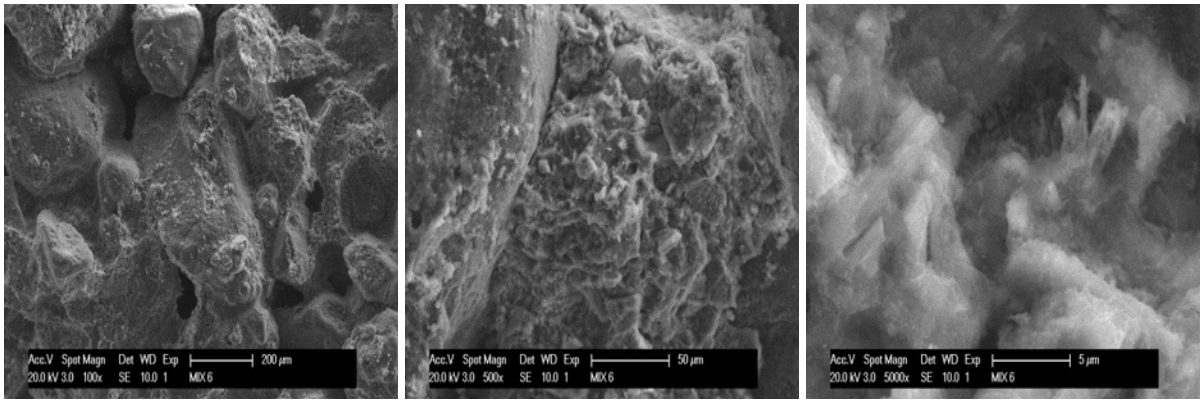


(a) Cement stabilized sand without Rc additive (0, 251) at 3 days

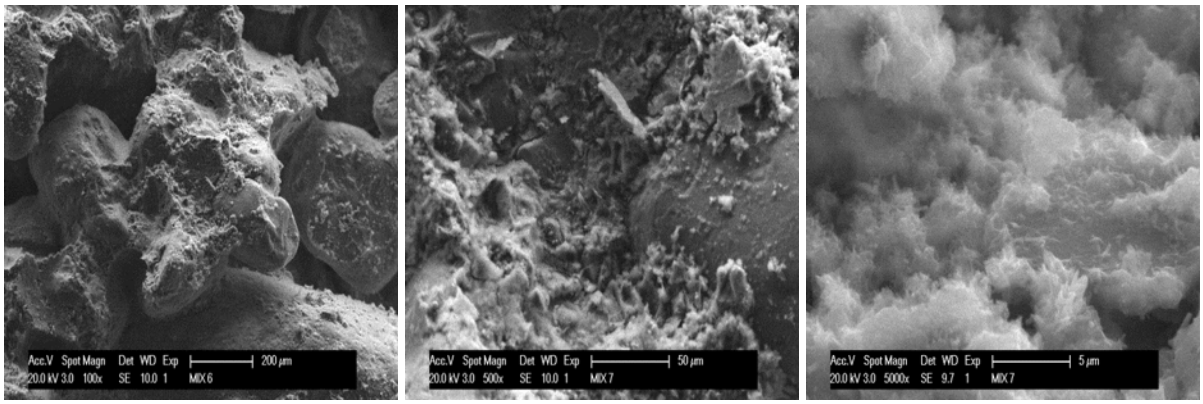


(b) Cement stabilized sand with Rc additive (3.2, 251) at 3 days

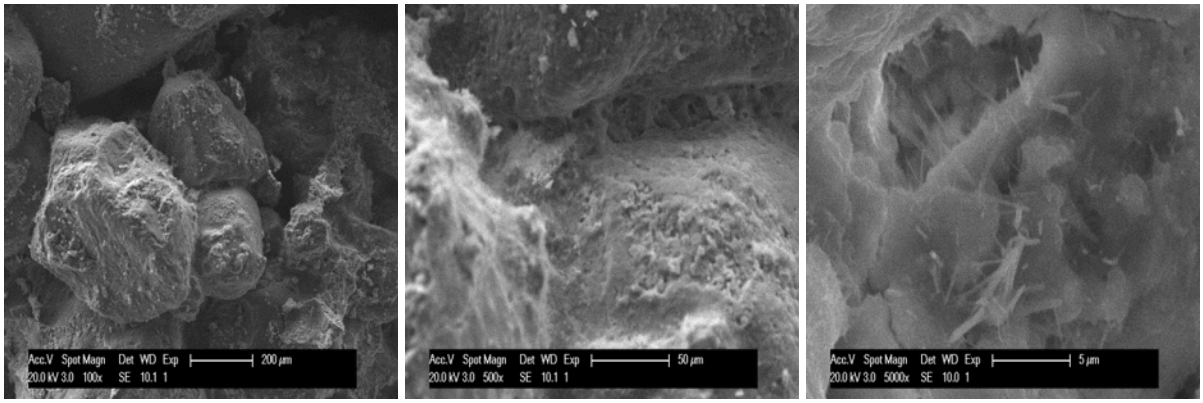


(c) Cement stabilized sand without Rc additive (0, 251) at 28 days

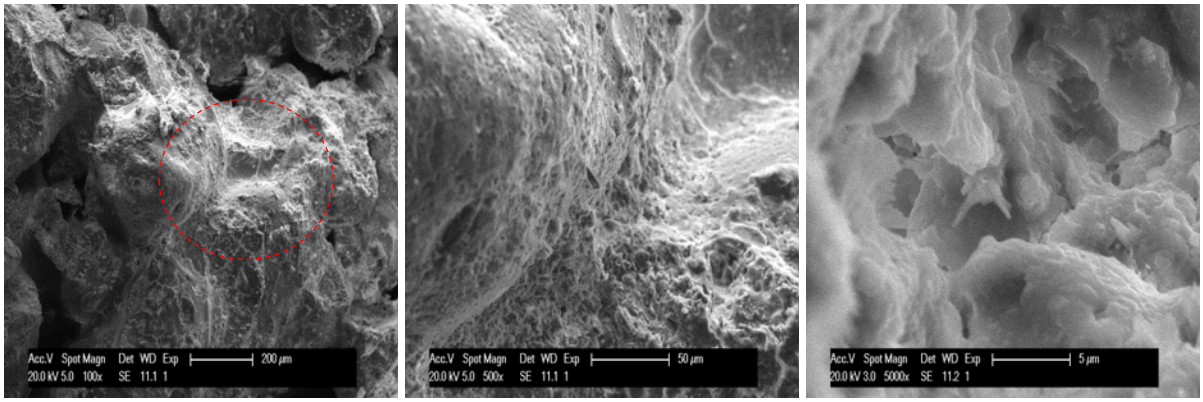


(d) Cement stabilized sand with Rc additive (3.2, 251) at 28 days

**Figure 6.13** SEM images of cement stabilized sand with and without Rc additive

## 6.4 Conclusions and recommendations

In this Chapter X-ray diffraction (XRD) and scanning electron microscopy (SEM) analysis were conducted to evaluate the effect of Rc additive on cement based materials in the microscale. The principal findings in this Chapter can be concluded as follows:

- The mixtures of cement paste and clay-cement with different amounts of Rc additive exhibit similar XRD patterns such as the peak position, the width and shape of each diffraction peak. Whereas, the portlandite peak of the cement paste mixtures with moderate amount of Rc additive exhibits slightly higher intensity which might indicate a higher amount of portlandite formed.
- The SEM images of cement paste showed that the mixture with Rc additive exhibits a more dense microstructure and fewer voids at 3 and 28 days. Similarly, the SEM images of cement stabilized sand showed that the mixture with Rc at 28 days seems to exhibit more cement hydration products filling the voids which might explain the increased mechanical strength caused by adding Rc additive.
- The SEM images of cement stabilized clay showed different morphology of the two mixtures with and without Rc additive. The ettringite crystals are observed in the samples with Rc additive at 3 and 28 days, but the samples without Rc additive were not observed to show the trace of ettringite crystals.

In this study, the XRD test was limited to the identification of the crystalline phases that are present in the cementitious materials without providing a quantitative measure of different crystal phases. Therefore, further research needs to be performed for the precise quantitative assessment of the cement hydration products with and without adding Rc additive, which can provide insight into the influence of Rc additive on the degree of cement hydration. Besides, the SEM images indicate the cement paste and sand-cement mixtures seem to exhibit a more dense microstructure by using Rc additive, so it is recommended to evaluate the porosity of the cementitious microstructure with and without Rc additive in further research.

## References

ACI. (1990). American Concrete Institute Committee 230. State-of-the-Art Report on Soil Cement. ACI Materials Journal, Vol. 87, No. 4, pp. 395–417.

Bakharev, T., Sanjayan, J.G., & Cheng, Y.B. (2003). Resistance of alkali-activated slag concrete to acid attack. Cement and Concrete Research, 33(10), 1607-1611.

Horpibulsuk, S., Rachan, R., Chinkulkijniwat, A., Raksachon, Y., & Suddeepong, A. (2010). Analysis of strength development in cement-stabilized silty clay from microstructural considerations. Construction and Building Materials, 24(10), 2011-2021.

Hunter, D. (1988). Lime-induced heave in sulfate-bearing clay soils. Journal of geotechnical engineering, 114(2), 150-167.

Kamon, M. & Nontananandh, S. (1991). Combining industrial wastes with lime for soil stabilization. Journal of Geotechnical Engineering, 117(1), 1-17.

Katz, L. E., Rauch, A. F., Liljestrand, H. M., Harmon, J. S., Shaw, K. S., & Albers, H. (2001). Mechanisms of soil stabilization with liquid ionic stabilizer. Transportation Research Record: Journal of the Transportation Research Board, 1757(1), 50-57.

Little, D.N. (2009). Recommended Practice for Stabilization of Subgrade Soils and Base Materials. NCHRP web-only document 144. Texas A&M University, Texas.

Mutaz, E., Shamrani, M.A., Puppala, A. J., & Dafalla, M.A. (2011). Evaluation of chemical stabilization of a highly expansive clayey soil. Transportation Research Record: Journal of the Transportation Research Board, 2204(1), 148-157.

Solanki, P., & Zaman, M. (2012). Microstructural and mineralogical characterization of clay stabilized using calcium-based stabilizers. Scanning electron microscopy. Intech, Rijeka, 771-798.

Tingle, J.S., Newman, J. K., Larson, S.L., Weiss, C.A., & Rushing, J. F. (2007). Stabilization mechanisms of nontraditional additives. Transportation Research Record: Journal of the Transportation Research Board, 1989(1), 59-67.

Wang, L., Roy, A., Seals, R.K., & Metcalf, J.B. (2003). Stabilization of sulfate-containing soil by cementitious mixtures mechanical properties. Transportation Research Record: Journal of the Transportation Research Board, 1837(1), 12-19.

# CHAPTER 7

# FIELD EVALUATION OF CEMENT STABILIZED MATERIALS WITH ROADCEM ADDITIVE

Previous Chapters are only focused on the laboratory investigation into the properties of cement stabilized materials with Rc additive. However, the results obtained in the laboratory tests are not directly correlated to the field performance due to the variable factors encountered in the field condition. For instance, in a laboratory the mixing and compaction process can be closely controlled as well as the curing condition for specimens, whereas the field conditions, including local circumstances (e.g. type of soil, the groundwater level and weather conditions) and construction procedures (mixing and compaction techniques) are quite variable. These field factors can have a major influence on the properties of cementitious materials and therefore the field performance can significantly differ from the properties obtained in the laboratory.

On the basis of literature, tremendous studies are conducted through laboratory testing (Shihata & Baghdadi, 2001; Kolias et al., 2005; Park, 2010; Consoli et al., 2011; Xuan, 2012). Only a few field studies have been undertaken which primarily investigated the field strength as well as the deformation characteristics of cement stabilized layers (Guthrie et al., 2009; Gaspard, 2002; Vorobieff, 1998; Jonathon & Tingle, 2009; Chai et al., 2005). However, due to the large variety of soil types, equipment type and climate conditions, it proves to be difficult to generalize conclusions derived from a particular field study. Therefore, in order to obtain a better understanding of the field properties of cement stabilized materials, a wide

range of soil types are employed to be stabilized and the field performance and the lab-properties are evaluated in this Chapter.

In this field study, teste sections of the cement stabilized road base were constructed by utilizing 6 types of materials (in-situ sand, imported sand, sandy clay, clay, crushed gravel, reclaimed asphalt). In-situ sand is the subsoil underneath the existing asphalt pavement layer and reclaimed asphalt is obtained by pulverizing the existing asphalt surface. Acquiring appropriate soil materials for stabilization in practice is often difficult due to the lack of good quality soil materials in some areas and long distance for hauling the required materials. Therefore, stabilizing existing in-situ materials not only considerably reduces the construction costs, but also saves the landfill space of the excavated materials and hence it leads to beneficial environmental issues and sustainable development (Vorobieff, 1998; Guthrie, 2005).

The main objective of this Chapter is to evaluate the field performance of cement stabilized materials with and without use of Rc additive and to identify the difference between laboratory test results and field performance. The evaluation program was performed by establishing different test sections by stabilizing a wide range of soil types and applying variable mix proportions (cement and Rc contents). After construction and cured for specified ages, field cores were extracted from each test section and subjected to compression and indirect tensile strength tests in the laboratory. Based on the field results, estimation models were developed for the mechanical strength of cement stabilized materials in the field. The field test results were also compared with those obtained from laboratory-prepared specimens. This Chapter illustrates the specific construction procedures with use of Rc additive, collection of specimens and data analysis on the field cores and the laboratory-prepared specimens.

## 7.1 Background

Environmental factors and the construction techniques are important variables influencing the field performance of cement stabilized materials. Relevant construction factors, such as the quality of mixing, time between mixing and compaction, the way of applying stabilizers, and moisture content are evaluated in various documents (Guthrie & Rogers, 2010; Dixon et al., 2012; George, 2002a). The quality of mixing, compaction and curing at a given location governs the uniformity of the base layer with depth and the degree of cement hydration that occurs (Guthrie & Rogers, 2010). In the study by Dixon et al. (2012) some construction-related variables, including the way of spreading cement and the in-place mixing time, were

evaluated. It was found that increasing the mixing time gives higher 7-day strength by 15 to 22 percent. Besides, many studies reported that the characteristics determined on field cores are much less than the characteristics of the same material when mixed in the laboratory. An example is given in Table 7.1, which shows the ratio between the characteristics obtained on the field cores and the laboratory-prepared specimens.

**Table 7.1** Comparison of the field and laboratory strength (field/lab ratio) (Wang & Mitchell, 1971)

| Cement content | Compressive strength | Flexural strength |
|---|---|---|
| 3% | 0.33-0.45 | 0.25-0.63 |
| 6% | 0.55-0.6 | 0.13-0.54 |

Similar research was done in a field trial by George (2002a) comparing the compressive strength of laboratory-prepared specimens with field-mixed specimens (compacted by Proctor), shown in Figure 7.1. Figure 7.1 covers different test sections by using different stabilizing agents and variable construction techniques. As expected the field-mixed material strengths are 30 to 50% lower than those of laboratory-mixed specimens. Non-uniform distribution of the stabilizing agent as well as compaction delay of one to two hours are identified as the main causes of the different results (George, 2002a). Based on the huge difference between the field and lab strength, Molenaar (2006) suggested to take 50% of the laboratory determined values as input for design.

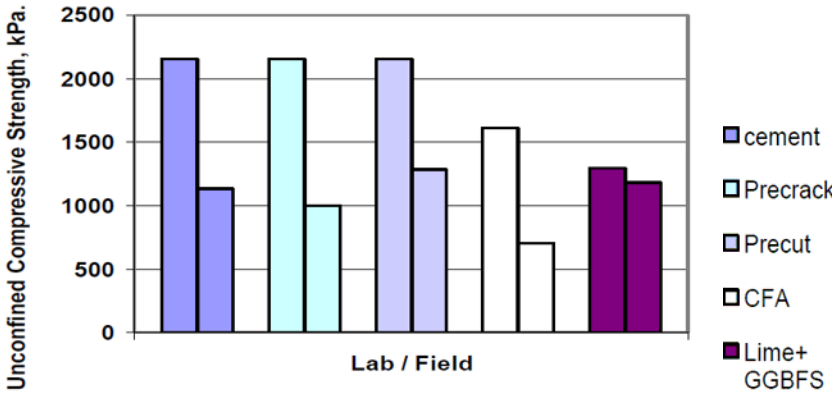


**Figure 7.1** Compressive strengths of lab prepared (left bar) and field mixed Proctor specimens (right bar) (George, 2002a)

Besides, large variations in density and moisture content were also recorded, attributed to inherent difficulties in in-place mixing and compaction, shown in Figure 7.2 (George, 2002a).

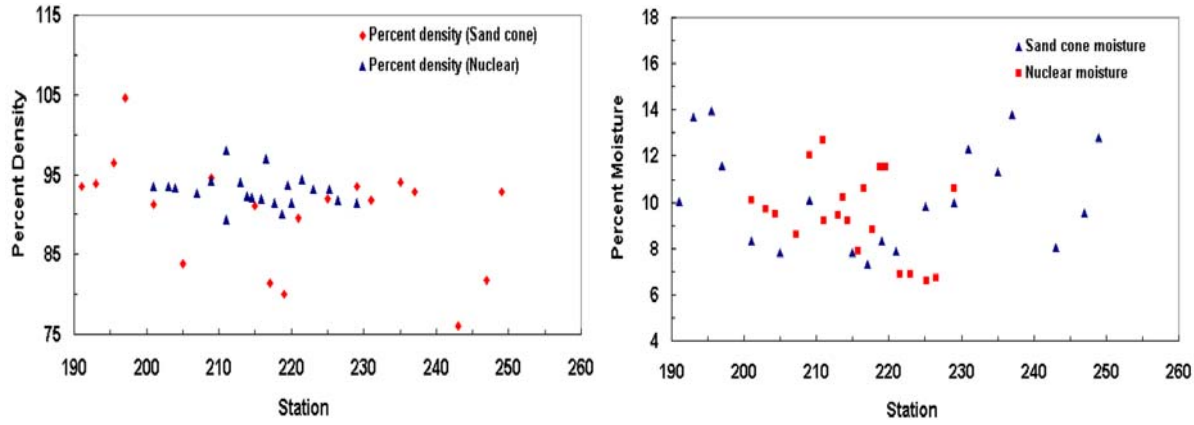


**Figure 7.2** Density and moisture content determined by Nuclear density devices

Compaction is of significant importance in the field construction and it is known that a cement stabilized mixture should be compacted as soon as the mixing procedure is accomplished. Delayed compaction will result in reduced strength and performance of the cement stabilized material, because cement begins hydrating as soon as it comes into contact with water and hydration products bond the soil particles together (Guthrie et al., 2009; TRH13, 1986). Delayed compaction can destroy the early-formed cementitious bonds (Guthrie et al., 2009; Guthrie & Rogers, 2010). In practice, immediate compaction is not always practical. Therefore, an allowable compaction time of 2 hours after mixing is widely adopted.

In soil-cement materials, the rate at which the cementitious product calcium silicate hydrate (C-S-H) forms at a given cement content depends on environmental factors such as wind speed, air temperature and relative humidity, because these factors affect the rate of water evaporation from the soil-cement layer and alter the rate of cement hydration (Guthrie et al., 2009; Mindess et al., 2003).

The effects of the environmental factors on the relative compressive strength were quantified in research by Guthrie (2009) which indicates that a higher wind speed, higher air temperature, lower relative humidity and higher compaction delay time generally result in lower relative strength (high temperature normally leads to higher compressive strength, but in this study probably due to the high evaporation, the opposite was found), presented in Figure 7.3. Conversely, in another field study (George, 2002a) it was found that hot summer weather (about 40°C) during and after construction contributed to a substantial increase in modulus and strength gain in stabilized materials.

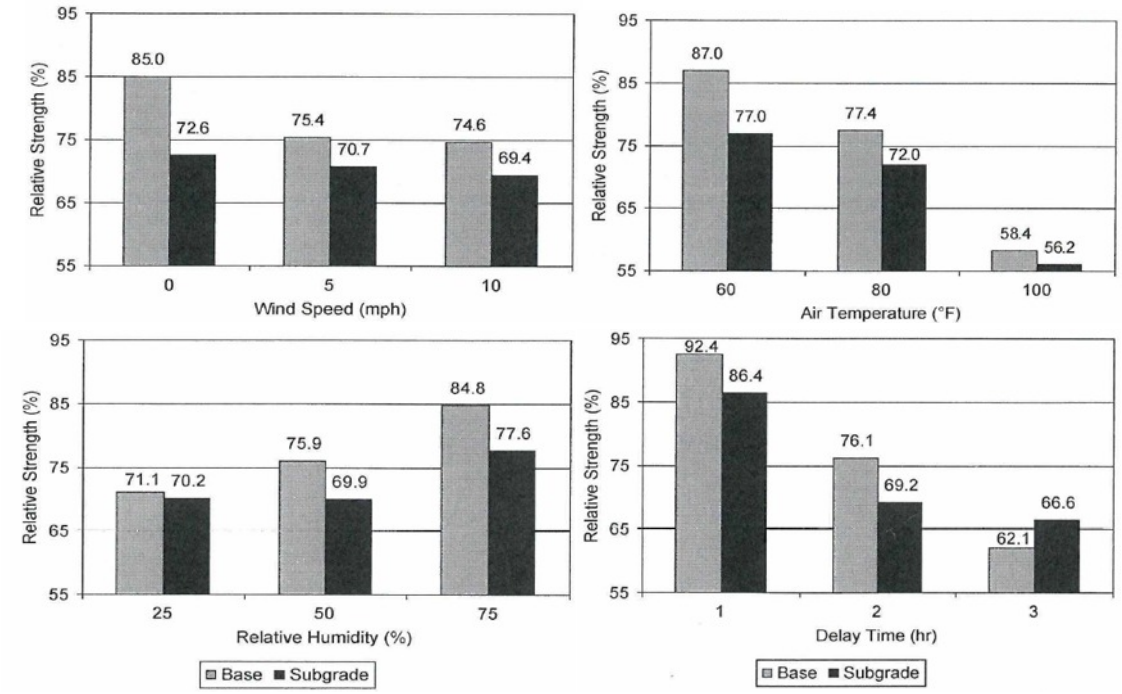


**Figure 7.3** Main effects on the relative compressive strength (Guthrie et al., 2009)

## 7.2 Field evaluation methodology

In this field program, test sections of cement stabilized road base were constructed by utilizing various soil materials. During stabilization, three different mix compositions with varying cement and Rc additive contents were applied for each type of soil material. Thus, the road base is divided into distinct test sections. After construction and cured at specified ages of 7, 14 and 28 days, cores were drilled from each test section and subjected to compression and indirect tensile strength tests in the laboratory. Meanwhile, specimens with the same mix design were prepared in the laboratory to compare the properties of the laboratory-prepared specimens with the field cores.

The variable factors in this field study include soil type, cement content, Rc content and curing time. Based on the test results, the effect of these factors on the properties in the field and lab conditions were analysed and prediction models for the field performance were developed based on the results obtained from the field cores. Besides, the environmental and construction issues were also taken into account in the analysis of the results. Figure 7.4 gives the overall review of this field evaluation program.

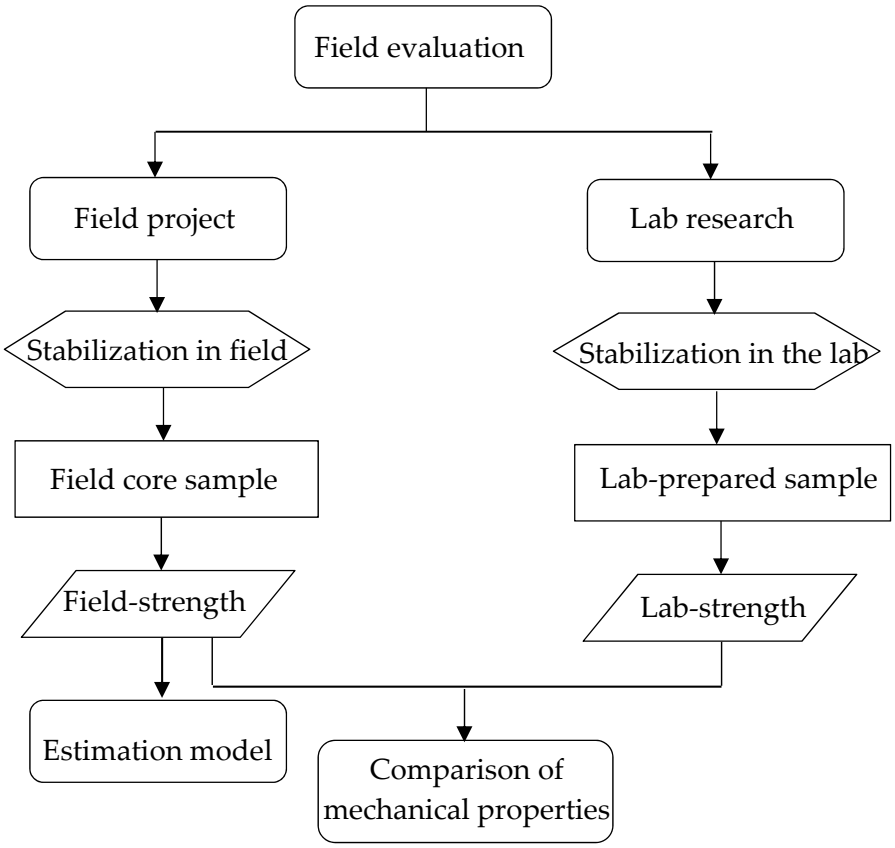


**Figure 7.4** Research methodology of field evaluation

## 7.3 Field project and construction materials

### 7.3.1 Existing pavement

The project site is located on a rural road in Lunteren, the Netherlands. Figure 7.5 shows the existing pavement with severe damage. As can be seen in Figure 7.5, this asphalt pavement was seriously damaged and tremendous cracking was observed, which considerably reduced the load bearing capacity and increased the susceptibility to moisture. During rainfall moisture penetrated into the underlying layer and hence accelerated the failure of the pavement. A new cement stabilized road base was constructed.

**Figure 7.5** Observed distress in the existing asphalt pavement

### 7.3.2 Mix design and test sections

The new road base is constructed over a length 600 m, width 4.7 m and thickness 300 mm. It consists of 8 main sections, based on 8 types of soil materials. Each main section is subdivided into three sub-sections by utilizing different mix compositions.

Figure 7.6 gives the layout of the pavement sections and Table 7.2 lists the mix design for each test sub-section. The mix compositions listed in Table 7.2 are based on the mass of soil which contains optimum moisture content. Sections A150, A200 and A250 refer to different proportions of crushed asphalt and in-situ sand. Crushed gravel is obtained from crushing concrete and brick materials, generally referred to as crushed granular materials, and sand is the same type of material evaluated in Chapter 4. The clay used herein is different from the type used in Chapter 5.

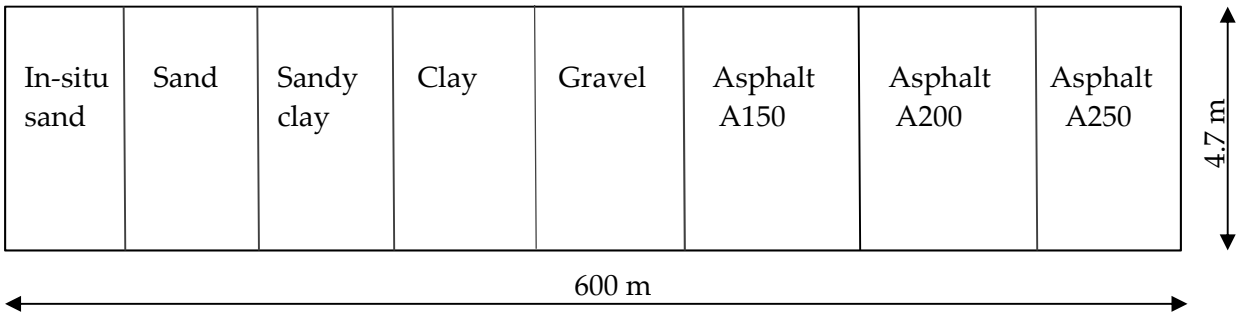


**Figure 7.6** Outline of the field sections

**Table 7.2** Mix composition for each field section

| Material type | Main section | Section | Length (m) | Mix composition (kg/m$^3$) | |
|---|---|---|---|---|---|
| | | | | Rc | Cement |
| In-situ sand | S0 | S0-1 | 20 | 0 | 205 |
| | | S0-2 | 15 | 1.9 | 205 |
| | | S0-3 | 16 | 3.8 | 270 |
| Sand | S | S-1 | 18 | 3.8 | 270 |
| | | S-2 | 17 | 1.9 | 205 |
| | | S-3 | 25 | 0 | 205 |
| Sandy clay | SC | SC-1 | 12 | 0 | 205 |
| | | SC-2 | 12 | 1.9 | 205 |
| | | SC-3 | 12 | 3.8 | 270 |
| Clay | C | C-1 | 15 | 3.8 | 270 |
| | | C-2 | 15 | 1.9 | 205 |
| | | C-3 | 20 | 0 | 205 |
| Crushed gravel | G | G-1 | 15 | 0 | 205 |
| | | G-2 | 15 | 1.9 | 205 |
| | | G-1 | 16 | 1.8 | 160 |
| Mixture of 150 mm crushed asphalt plus 150 mm in-situ sand | A150 | A150-1 | 135 | 1.8 | 160 |
| | | A150-2 | 17.5 | 1.9 | 205 |
| | | A150-3 | 17.5 | 0 | 205 |
| Mixture of 200 mm crushed asphalt plus 100 mm in-situ sand | A200 | A200-1 | 17.5 | 0 | 205 |
| | | A200-2 | 17.5 | 1.9 | 205 |
| | | A200-3 | 100 | 1.8 | 160 |
| Mixture of 250 mm crushed asphalt plus 50 mm in-situ sand | A250 | A250-1 | 17 | 1.8 | 160 |
| | | A250-2 | 17 | 1.9 | 205 |
| | | A250-3 | 17 | 0 | 205 |

### 7.3.3 Material characterization

This field study evaluates 8 types of materials for stabilization. Among these 8 types of materials, in-situ sand (the subsoil underneath the existing asphalt layer), crushed gravel (by crushing concrete and brick materials) and reclaimed asphalt (by pulverizing the existing asphalt layer) are the common in-situ materials for

stabilization, shown in Figure 7.7. Currently, more and more deteriorated pavements require maintenance or rehabilitation. Therefore, recycling the deteriorated pavement materials with addition of cement to create a new stabilized base is a cost effective alternative. In this study, reclaimed asphalt was processed by milling the existing asphalt layer and placing it on the site and then mixing with the in-situ sand. This process is different from the traditional full-depth reclamation (FDR) which pulverizes and mills the existing asphalt and underlying base materials in the field.

(a) In-situ sand (b) Crushed gravel (c) Pulverized asphalt

**Figure 7.7** In-situ materials used in this study

Characterization of the soil materials mainly includes particle size distribution. For coarse grained materials, dry sieving was performed according to ASTM C 136, while the grain size distribution of clay and sandy clay was determined by a sedimentation process using a hydrometer. The cumulative percentage passing through each sieve size is plotted to obtain the particle size distribution curve. The average grain size distribution of all types of soils are summarized in Figure 7.8.

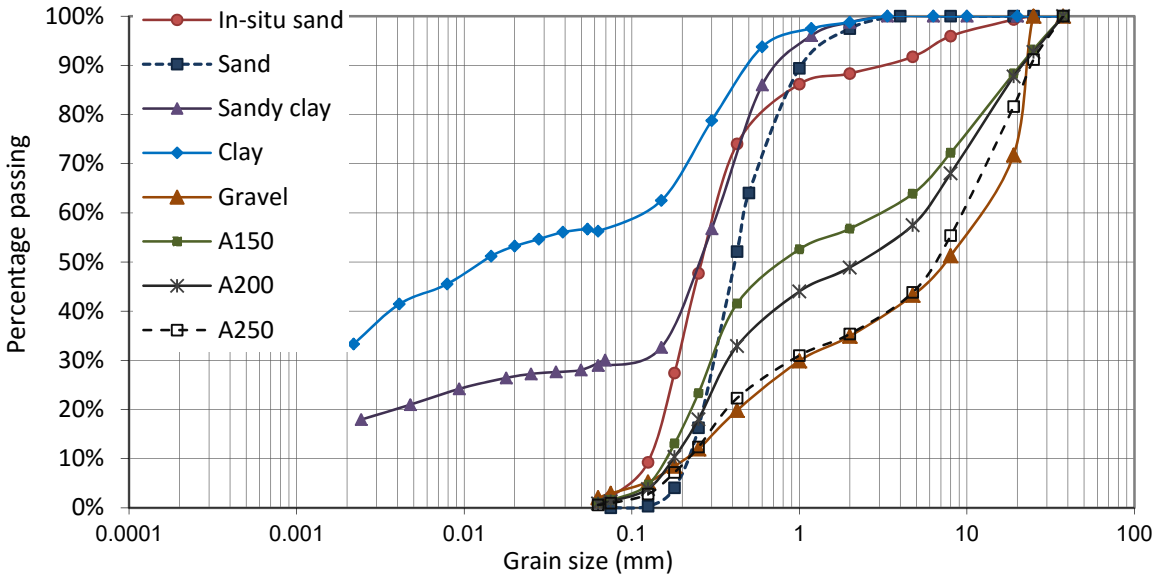


**Figure 7.8** Grain size distribution of all types of soil materials

In addition to the particle size distribution, Atterberg limits including liquid limit and plastic limit were obtained for the clay soil, according to standard ASTM D 4318. Additionally, as for the natural occurring in-situ soil as well as clay, the organic content is an important factor that needs to be determined, because the presence of organic matter can have a negative effect on the cement hydration. The organic content of in-situ sand and clay were determined by the loss of the dry mass under the oven drying at 500˚C for 5 hours. The general properties of all these materials are summarized in Table 7.3.

**Table 7.3** Properties of the materials

| Material properties | In-situ sand | Sand | Sandy clay | Clay | Gravel | A150 | A200 | A250 |
|---|---|---|---|---|---|---|---|---|
| Organic content (%) | 2 | _ | _ | 3.1 | _ | _ | _ | _ |
| Coefficient of uniformity ($C_u$) | 1.1 | 3.3 | _ | _ | 12.5 | 10 | 15.7 | 10.5 |
| Curvature index ($C_c$) | 1.4 | 0.96 | _ | _ | 0.38 | 0.19 | 0.12 | 0.41 |
| LL (Liquid limit) | _ | _ | _ | 36.1 | _ | _ | _ | _ |
| PI (Plasticity index) | _ | _ | _ | 16 | _ | _ | _ | _ |
| Classification (USCS) | SP | SP | SC | CL | GW | SP* | SP* | GW |

Note: crushed asphalt is not included in the USCS classification, but considering it for classification purpose, it is classified based on the grain size of the coarse-grained material. SP-poorly graded sand; SC-clayey sand; CL-sandy lean clay; SP*-Poorly graded sand with gravel; GW-Well graded gravel with sand.

Portland blast furnace slag cement (CEM III/B 42.5 N LH, contains 70% blast-furnace slag and 30% Portland Clinker) is the used cement type.

## 7.4 Field construction procedures

The general construction process started with adding and blending the additives, followed by leveling the base course, compaction and finally polishing the surface. In this stabilization process, addition of the Rc additive took place one day before applying cement. An in-place mixer was used to pulverize and blend the base materials. The detailed procedures are described hereafter:

**Step 1: Profile soil material layer**

After the removal of the asphalt surface and leveling the subsoil, all the soil materials were brought to the specified locations and placed in the profile, shown in Figure 7.9.

(a) In-situ sand (b) Sand (c) Sandy clay

(d) Clay (e) Gravel (f) Asphalt plus in-situ sand

**Figure 7.9** Preparation of the layers of soil materials

**Step 2: Spreading and mixing the Rc additive**

Initially the specified amount of Rc additive was distributed on the soil layer manually due to the test sections with limited length. In the asphalt sections, it was however done by a spreader. Subsequently, additive and soil materials were mixed by an in-place mixer through the depth of 2/3 of the thickness. After completion of the incorporation of Rc, the mixtures were slightly compacted to prevent the infiltration of rain water and then remained overnight in order to ensure that Rc was thoroughly distributed amongst the soil particles. Figure 7.10 illustrates these construction procedures.

(a) Rc additive (b) Distribute by a spreader (c) Mixing Rc and in-situ sand

(d) Rc on the sand layer (e) Rc on the gravel layer (f) Rc on the asphalt layer

**Figure 7.10** Distribution of Rc and mixing with soil materials

**Step 3: Adding cement and water and thorough mixing**

Because of the high cement contents as designed to evaluate the cracking performance of the cement stabilized base, application of cement was done in two stages. The initial half amount of the specified cement content was applied by the spreader. After the cement was distributed evenly over the surface, cement was incorporated into the soil materials by using the in-place mixer (Figure 7.11).

**Figure 7.11** Applying cement and dry mixing

Subsequent to the first dry mixing of the cement into the soil materials, water was added by means of a water truck. After addition of water, wet mixing with the cement and soil materials was accomplished by the same mixer (Figure 7.12). Subsequently, the other equal amount of cement was distributed over the wet mixture, followed by thorough mixing with the same equipment.

**Figure 7.12** Adding water and wet mixing

**Step 4: Levelling, compaction and surface polishing**

After the mixing process, the mixture was levelled by a grader to obtain the even base surface (Figure 7.13). Once levelling was finished, the base course was compacted by a steel-wheel roller compactor. For cohesive soil clay, the sheep foot roller compactor is generally preferred before the steel wheel roller compactor does the final compaction. After completion of the compaction, the surface of the cement stabilized base was polished smooth to achieve a dense and impermeable surface. During the polishing process (Figure 7.13), water was spread on the surface for the operation and it also contributed to the cement hydration during curing. The completed base course was closed for traffic for 7 days to prevent early damage.

**Figure 7.13** Levelling, compaction and polishing surface

## 7.5 Visual observation after construction

Cement stabilized materials are prone to shrinkage cracking mainly due to the moisture loss during cement hydration or the temperature variation. Accumulated cracks may cause accelerated pavement damage, erosion and susceptibility to deterioration and hence reduce the strength and durability of the base layer. Shrinkage cracking is a natural characteristic of all cement-based materials, however, appropriate construction techniques and mix design methods can minimize these adverse effects. A number of research studies (Cho et al., 2006; FM 5-410, 2012; George, 2002b) present various methods to minimize shrinkage cracking, which include altering the mix design, proper construction process and techniques, the use of "pre-cracking" and adding additives. These methods were also evaluated in some field studies (Gaspard, 2002; Bryan & Guthrie, 2011; George, 2002a). This field trial aims to investigate the effect of Rc additive on the cracking behavior.

In this field study, visual inspection was undertaken in the first week after completion of the base course. In order to observe the cracking, the asphalt wearing course was not overlaid. Figure 7.14 shows the base course surfaces at 5 days.

(a) In-situ sand (b) Sand (c) Sandy clay

(d) Clay (e) Crushed gravel (d) Crushed asphalt

**Figure 7.14** Cement stabilized base surfaces at 5 days after construction

Hairline transverse cracking was observed in the stabilized sand section S-1 which was stabilized with 270 kg/m$^3$ cement and 3.8 kg/m$^3$ Rc, shown in Figure 7.15.

**Figure 7.15** Observed cracks in stabilized sand section S-1

As can be seen in Figure 7.15, the length of crack is around 1.1 m and the crack width is approximately 1 mm. This transversal crack might be caused by the high amount of cement used in this mix design. In other test sections no cracks were observed in the first 7 days. In the following 20 days, continuous snowy weather had posed huge difficulties on observing cracks.

## 7.6 Laboratory testing method

### 7.6.1 Core samples collected from the field

At the ages of 7, 14 and 28 days a large number of cores were extracted from the road sections. Cores were drilled two days before the specified curing ages. For each test section at each curing time three representative cores were collected to ensure the reliability of the testing results. A drilling machine with a 150 mm diameter tube was used. The field cores were drilled in the middle of the sections to avoid the edge area where weak spots may exist. After labeling the drilled cores were transported to the laboratory. Figure 7.16 shows the drilling process.

**Figure 7.16** Drilling operation

At the age of 7 days, the sections of clay and sandy clay were not strong enough to extract cores, and thus field cores from these two main sections were only collected at the age of 14 and 28 days. Figure 7.17 shows the core specimens drilled at the age of 5 days (clay and sandy clay at 12 days).

(a) In-situ sand (b) Sand (c) Sandy clay

(d) Clay (e) Crushed gravel (f) Crushed asphalt

**Figure 7.17** Field cores

One should note that at the age of 5 days field cores from the sand sections achieved 300 mm in length equal to the designed thickness, but the length of other field cores ranges from 200 to 250 mm. All the field cores were sawn into the required dimension with height 120 mm and diameter 150 mm. Due to the excessive water used in the drilling and sawing process, all the field cores were dried at the room temperature before testing.

### 7.6.2 Specimen preparation in the laboratory

To enable a comparison with the strength of field cores, specimens by stabilizing the same types of soil materials were prepared in the laboratory. Steel moulds with diameter of 101.6 mm and height of 116.4 mm were used to prepare specimens and representative mix designs are chosen, presented in Table 7.4. The cement and Rc additive contents are based on the dry mass of soil. Two mix compositions were evaluated, with and without Rc additive. Moisture contents used for preparing the specimens in the laboratory are approximately similar as used in the field stabilization.

**Table 7.4** Mix design for the laboratory-prepared specimens

| Material type | Corresponding field Section | Mix composition (kg/m$^3$) | |
|---|---|---|---|
| | | Rc | Cement |
| In-situ sand | S0-1 | 0 | 205 |
| | S0-2 | 1.9 | 205 |
| Sand | S-3 | 0 | 205 |
| | S-2 | 1.9 | 205 |
| Clay | C-3 | 0 | 205 |
| | C-2 | 1.9 | 205 |
| Sandy clay | SC-1 | 0 | 205 |
| | SC-2 | 1.9 | 205 |
| Gravel | G-2 | 1.9 | 205 |
| 200 mm asphalt plus 100 mm in-situ sand | A200-1 | 0 | 205 |
| | A200-2 | 1.9 | 205 |

An electronic vibrating hammer (Hilti TE1000-AVR) was used for compaction. All the laboratory-prepared specimens were cured in a climate chamber with a temperature of 20°C and a relative humidity of 90% for specified periods of 7, 14 and 28 days. Figure 7.18 shows the field cores after sawing and the laboratory-prepared specimens.

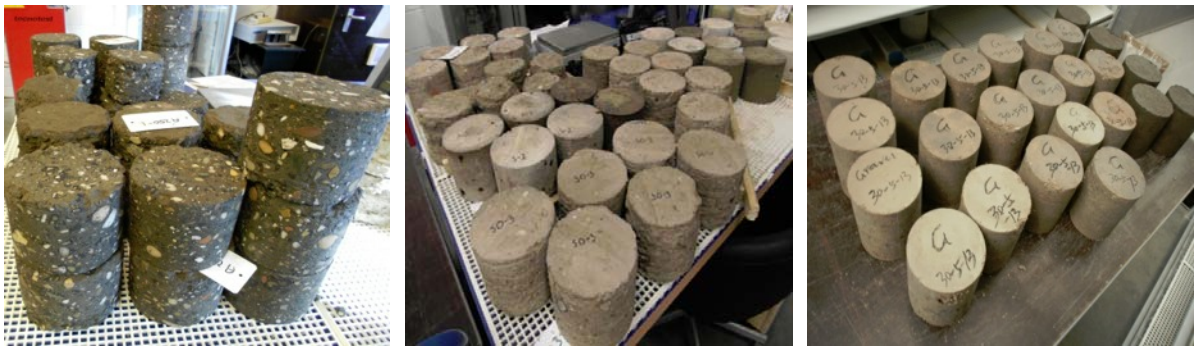

**Figure 7.18** Field cores (left and center) and laboratory-prepared specimens (right)

### 7.6.3 Mechanical testing methods

At the specified ages, the field cores and the laboratory-prepared specimens were subjected to compression and indirect tensile strength tests, which are widely used to characterize the mechanical properties of cement stabilized materials. The specimens were loaded at a constant loading rate until failure. Figure 7.19 shows the compression and indirect tensile tests and the specimens after failure.

**Figure 7.19** Compression and indirect tensile strength tests

## 7.7 Comparison of field and laboratory strength

Due to the different size of the field cores and the laboratory-prepared specimens, a conversion factor 1.3 is used to obtain equivalent results according to preliminary research (Wu et al., 2013), which is also adopted in a study by George (2002a). All the tested data obtained from the field cores and the laboratory-prepared specimens are presented in the figures shown in Appendix C. In the following discussion, the analysis of the test results only concentrates on the mix design with cement content 205 kg/m$^3$, and with and without Rc additive.

### 7.7.1 Methodology of comparing the field results with the laboratory results

The local conditions, including construction techniques and weather conditions during and after construction, may have a strong influence on the field performance of cement stabilized materials. Under the appropriate curing regime the cementitious materials gain strength as the curing continues. Especially in the early curing period substantial increase of strength can be achieved due to the rapid cement hydration. However, cold winter weather occurred in this field trial which probably had adversely affected the strength development. Figure 7.20 indicates the local air temperature during the period of 28 days and the snowy weather condition which occurred in the period from 14 to 28 days after construction. It implies that the freezing ambient temperature due to the snowfall might have had a detrimental influence on the chemical reaction in the cement stabilized materials. That means the progress of the cement hydration in the field is significantly different from that in the laboratory (a constant temperature of 20˚C).

Therefore, in order to include the considerable influence of the hardening environment and enable a reasonable comparison of the field-strength and the laboratory designed-strength, the material performance is compared based on the

same progress of cement hydration which is measured by the Maturity method (commonly known as Nurse-Saul maturity function).

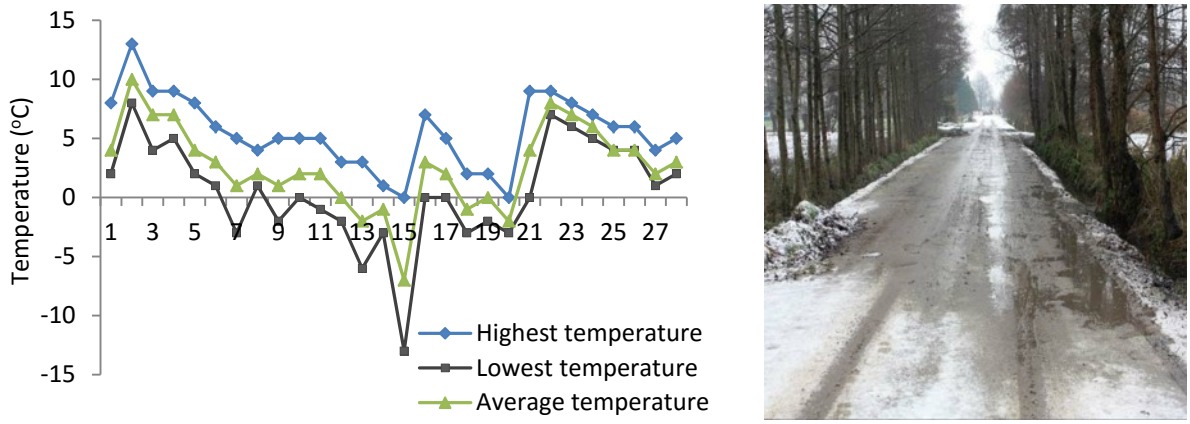


**Figure 7.20** Air temperatures in this field during the first 28 days after construction

The maturity method is a measure of concrete strength gain based on how long the concrete cured and at what temperature, and it is widely adopted to estimate the in-place concrete strength (Carino, 1984; Naik, 1980; ASTM C 1074). In this study it is assumed that the maturity method also applies to the cement stabilized materials (whether or not with the Rc additive under consideration). The maturity method is expressed as the following equation:

$$\text{Maturity index} \quad M(t) = \sum(T_a - T_o)\Delta t \tag{7-1}$$

Where, $T_a$ is the average concrete temperature (°C) during the time interval $\Delta t$; $T_o$ is the datum temperature (°C) below which cement hydration is assumed to cease; $\Delta t$ is the time interval (days).

The maturity index is given as a time-temperature factor. The datum temperature depends on the admixture type or water-cement ratio (Naik, 1980; ASTM C 1074) and in this study it is suggested to be 0°C (Saul, 1951). One limitation of this equation is that the rate of strength development is assumed to be a linear function of the temperature. In most cases it follows more an exponential than a linear relationship, but a linear relationship is considered adequate in most applications (Wade, 2006; Wilde, 2013). In this study, the maturity index for the field condition is calculated based on the average air temperature at each age (see Figure 7.20), i.e. it is assumed that in the winter conditions the average daily temperature of the stabilized base layer is equal to the average daily air temperature. The laboratory maturity index is obtained in terms of summation of the constant curing temperature of 20°C. The maturity index for the field and lab conditions are shown in Table 7.5.

**Table 7.5** Maturity index for field and laboratory conditions

| Age | $M=\sum(T_a - T_o)\Delta t$ | |
|---|---|---|
| | Laboratory (°C·day) | Field (°C·day) |
| 7 days | 140 | 72 |
| 14 days | 280 | 83 |
| 28 days | 560 | 121 |

As shown in Table 7.5, the maturity index of the field condition is much lower than that of the lab at the same age because of the cold winter temperature in the field indicating different progress of cement hydration. Therefore, it is essential to compare the strength at the equivalent maturity index. The following sections will compare and analyse the results by developing the maturity and strength relationship.

### 7.7.2 Compressive strength of field cores and the laboratory-prepared specimens

Figure 7.21 presents the maturity and strength correlation comparing the two mixtures with 205 kg/m$^3$ cement content, with and without Rc additive. This maturity and strength relationship is established by plotting compressive strength as a function of the corresponding maturity index, based on the test data from the field cores and the laboratory-prepared specimens at specified ages of 7, 14 and 28 days. The logarithmic model obtained from the laboratory maturity-strength relationship is used to estimate the laboratory designed-strength at the equivalent maturity index of the field strength.

For example, in Figure 7.21 (in-situ sand) the laboratory strength at the maturity index of 72, 83 and 121$^o$C·day is estimated from the reference laboratory maturity-strength curve and compared with the field strength at the same maturity level, as marked. The field strength of stabilized clay and sandy clay at 7 days were not measured and the 3-day compressive strength of stabilized sand is included in the sand curves.

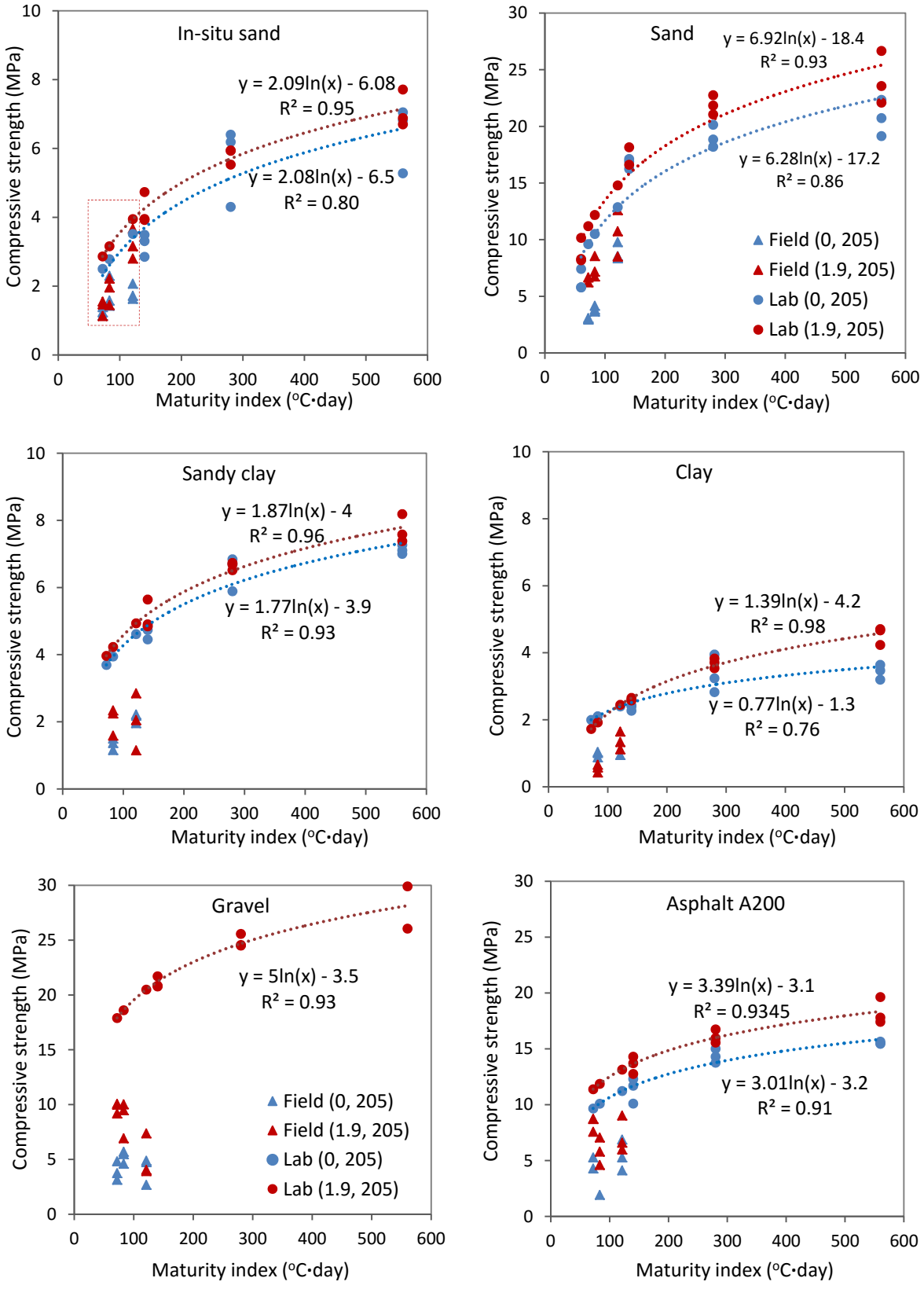


**Figure 7.21** Maturity and compressive strength correlation of cement stabilized materials in the field and lab conditions

Note: (0, 205) indicates mixture with cement 205 kg/m$^3$ and Rc 0 kg/m$^3$; (1.9, 205) indicates mixture wth cement 205 kg/m$^3$ and Rc 1.9 kg/m$^3$.

In Figure 7.21 it is found that the compressive strength obtained from the field cores is much lower than the laboratory designed strength at the same maturity index. Based on these 6 types of stabilized soil materials, the achieved compressive strength in the field approximately ranges from 30% to 70% of the laboratory strength.

Additionally, it can be clearly noted that use of Rc can increase the compressive strength of cement stabilized materials which is found in both the field cores and the laboratory-prepared specimens. For instance, addition of Rc gives rise to higher compressive strength of laboratory-prepared specimens for stabilized sand and in-situ sand materials at all ages, while the field strength of these two materials is also observed to increase with the addition of the Rc. As for stabilized clay materials, the initial compressive strength in the lab condition is slightly lower in the mixture with Rc but later the strength of this mixture exceeds that without Rc after the age of 3 days. The field cores also exhibits the similar strength development.

With respect to the difference between field strength and the laboratory strength, Figure 7.22 lists the average compressive strength obtained from the field cores and the laboratory-strength which is estimated from the maturity-strength curve at the same maturity index. As can be seen from Figure 7.22, the compressive strength from the field cores is generally much lower than that obtained from the laboratory-prepared specimens which is found in all evaluated stabilized mixtures. The difference between field strength and the laboratory strength (estimated from the maturity curve) varies significantly in different soil materials and at different maturity index. For instance, the field strength of stabilized in-situ sand mixture (1.9, 205) at M 72 and 83 °C·day are both about 50% of the lab strength, but later reached almost 80% of the lab strength at M 121°C·day. Besides, it has to note that the field strength of the gravel-cement mixture with Rc 1.9 kg/m$^3$ is only 25% of the lab strength. It can be attributed to the low density of these three gravel field cores. The low density may be caused by construction issues such as the insufficient compaction.

In summary, the ratio of the field compressive strength to the laboratory-compressive strength is observed to be in a general range of 0.3 to 0.7 at the same maturity index. Similarly, previous studies (Gaspard, 2002; Vorobieff, 1998; George, 2002a; Melancon & Shah, 1973) revealed that soil-cement base courses achieved 50~75 percent of the laboratory strength. The huge difference between the field strength and the strength obtained in the laboratory condition is mainly caused by the construction techniques. It is due to the fact that uniform mixing and adequate compaction can be achieved in the laboratory, but in-place mixing and compaction

have unavoidable inherent difficulties, which is also addressed in research (George, 2002a).

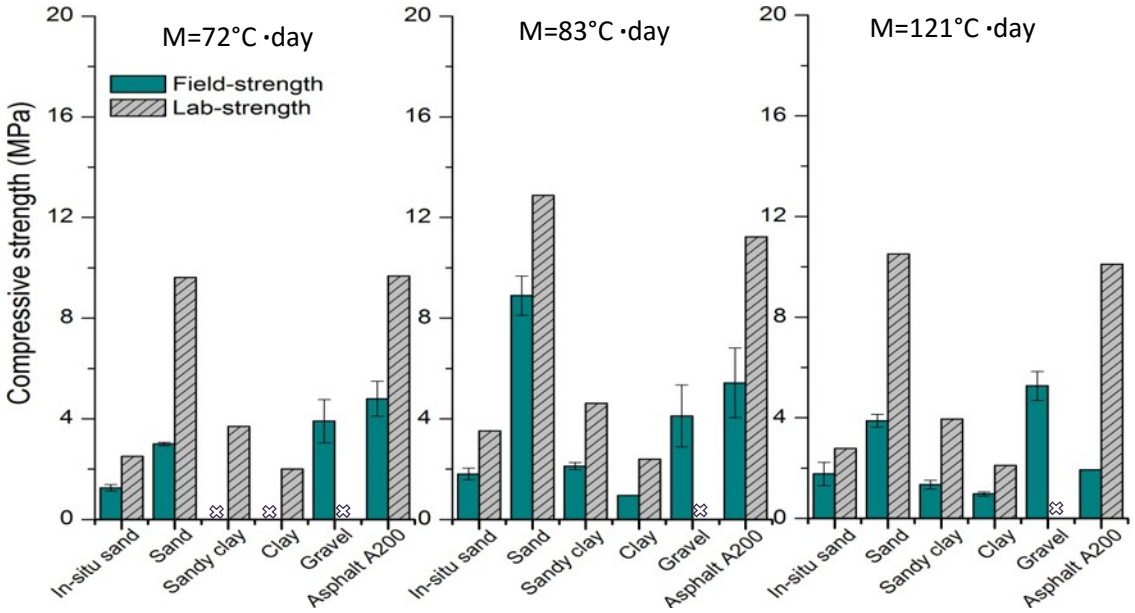


(a) Mixture (0, 205) without Rc additive

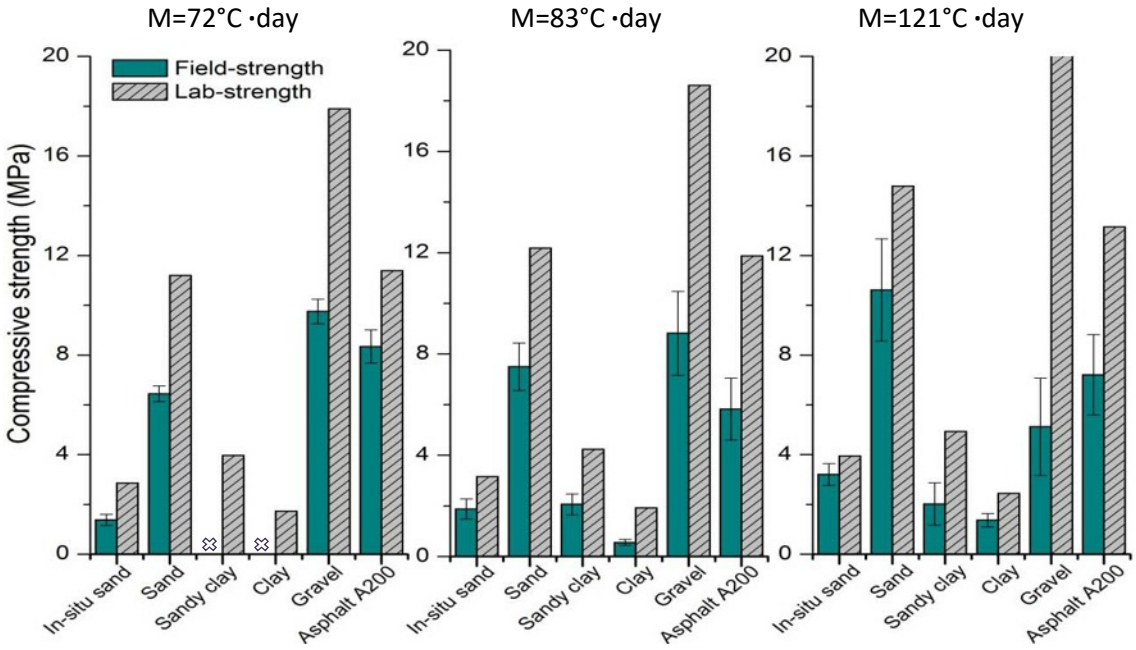


(b) Mixture (1.9, 205) with Rc additive 1.9 kg/m$^3$

**Figure 7.22** Difference between field compressive strength and lab-compressive strength

Note: M 72, 83 and 121°C·day correspond to the age of 7, 14 and 28 days in the field condition, respectively. Compressive strength of clay and sandy clay at M 72°C·day (7-day) and the gravel-mixture (0, 205) are not included.

Moreover, as seen in Figure 7.22 the age is also an influential factor for compressive strength. Figure 7.23 illustrates the compressive strength of the field cores and the laboratory-prepared specimens at different ages (also represented by the maturity index), obtained from mixture with 205 kg/m$^3$ cement and 1.9 kg/m$^3$ Rc.

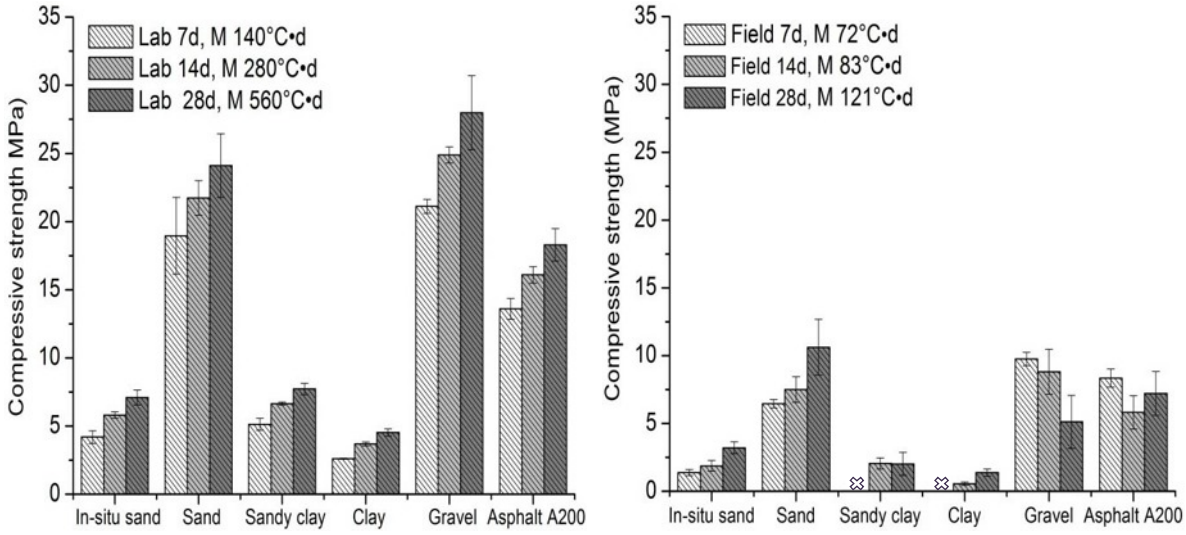


**Figure 7.23** Compressive strength development in the laboratory and in the field

In Figure 7.23 it can be seen that the compressive strength obtained from the laboratory curing regime shows a steady increase as the age continues from 7 to 28 days in all stabilized mixtures. In the field condition, the in-situ sand, sand and clay sections also exhibit the same increasing trend. Whereas the field strength doesn't always increase as the maturity index rises, especially the gravel-section shows a decreasing field strength and the asphalt section exhibits an almost constant field strength. The delayed strength development might be caused by the variation in the field density or may also indicate the frost damage occurred in the base layer.

### 7.7.3 Indirect tensile strength of field cores and the laboratory-prepared specimens

Similar to the analysis of the compressive strength, the indirect tensile strength obtained from the field cores and the laboratory-prepared specimens at equivalent maturity index are given in Figure 7.24. The indirect tensile strength of stabilized clay field cores is not included in the data analysis due to the fact that during testing the deformation under splitting loading exceeded the range of the testing machine. That is because the clay specimens were exposed to excessive water during the drilling and sawing process, which resulted in significant loss of strength.

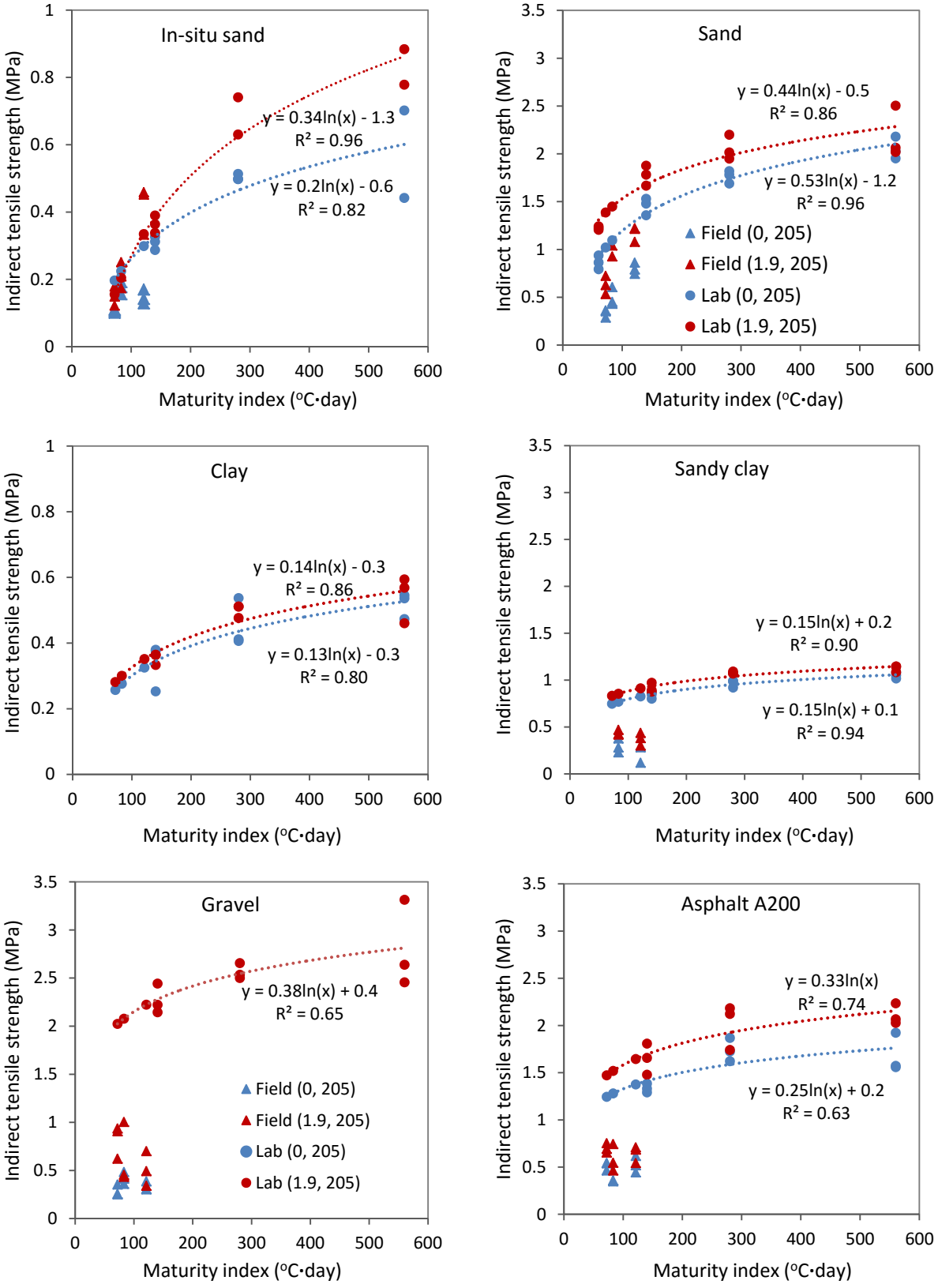


**Figure 7.24** Maturity and the indirect tensile strength correlation of cement stabilized materials in the field and lab conditions

Note: (0, 205) indicates mixture with cement 205 kg/m$^3$ and Rc 0 kg/m$^3$; (1.9, 205) indicates mixture wth cement 205 kg/m$^3$ and Rc 1.9 kg/m$^3$.

In Figure 7.24, it can be observed that using Rc additive yields a higher indirect tensile strength which occurs in all the soil types and also in both field cores and lab-prepared specimens. For instance, for asphalt material A200 at the age of 28 days, the indirect tensile strength of laboratory-prepared specimens increases by 30% with use of Rc additive. Again, the field indirect tensile strength exhibit large variations and the field strength is considerably lower than the laboratory strength.

Figure 7.25 summarizes the comparison of the indirect tensile strength obtained from the field cores and the laboratory-prepared specimens which is estimated from the maturity-strength curve.

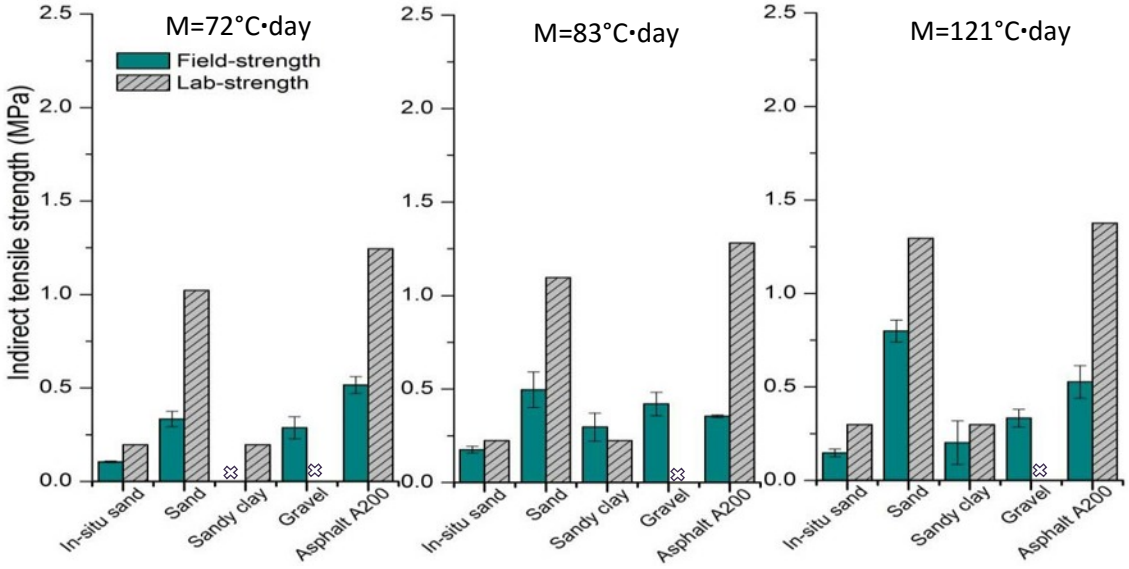


(a) Mixture (0, 205) without Rc additive

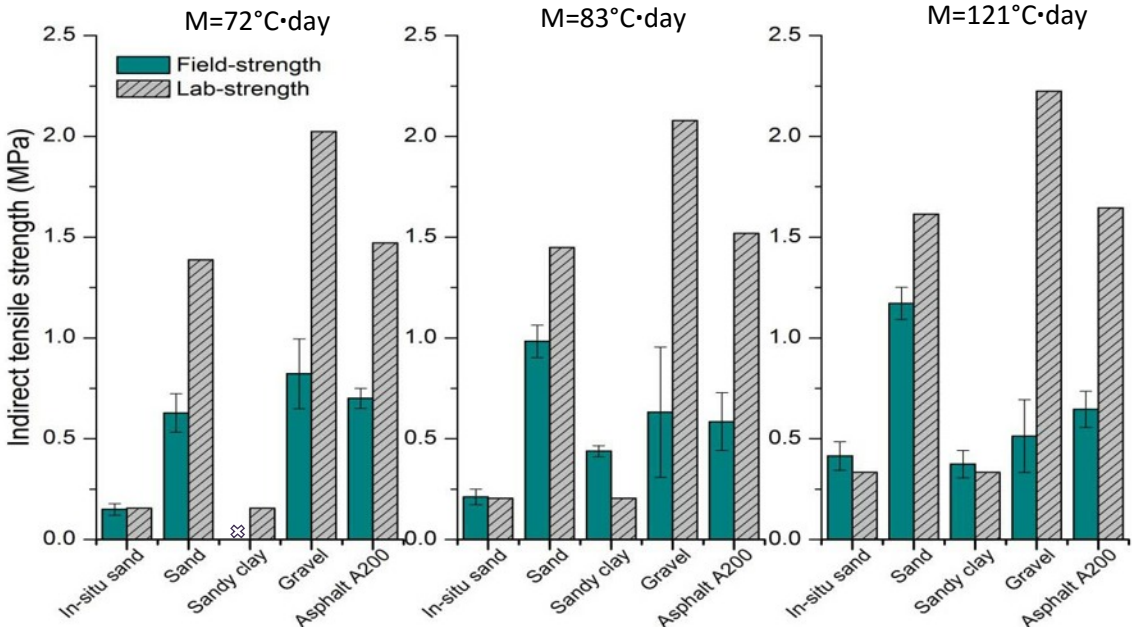


(b) Mixture (1.9, 205) with Rc additive 1.9 kg/m$^3$

**Figure 7.25** Difference between field and lab-indirect tensile strength

As can be seen in Figure 7.25, the indirect tensile strength of the field cores is generally lower than that of the laboratory-prepared specimens. However, the difference between field strength and the laboratory strength largely depends on the type of soil materials and the mix compositions. For instance, at M 121°C·day, the field indirect tensile strength of the in-situ sand mixture without Rc is about 50% lower than the lab-strength, while for the in-situ sand mixture with Rc the field indirect tensile strength is even 15% higher. Similarly, the field strength of stabilized sand with Rc reaches 75% of the lab-strength while the mixture without Rc only gets 60%. The field sections of cement stabilized gravel and asphalt A200 both show a significantly lower strength, which is approximately 35% and 45% of that of the laboratory-prepared specimens, respectively.

Furthermore, the indirect tensile strength is also observed to show different development trends in the field and in the laboratory, presented in Figure 7.26. Figure 7.26 covers the indirect tensile strength of the field cores and the laboratory-prepared specimens at different ages, obtained from mixture with 205 kg/m$^3$ cement and 1.9 kg/m$^3$ Rc.

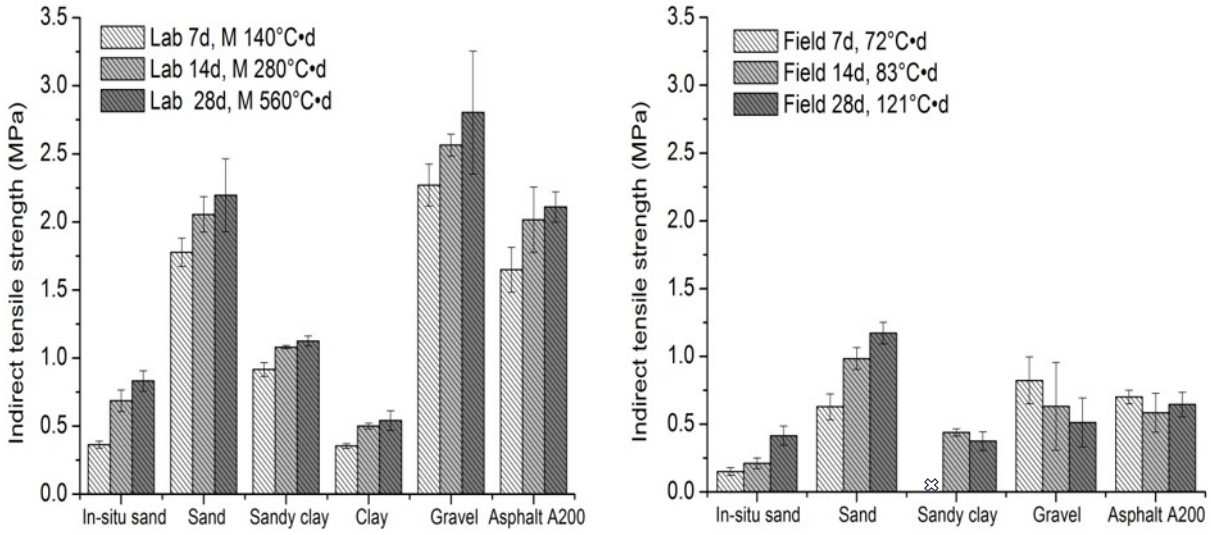


**Figure 7.26** Development of indirect tensile strength in the laboratory and in the field

In Figure 7.26, the indirect tensile strength shows the same development trend as the compressive strength. For the specimens prepared and cured in the laboratory, the indirect tensile strength increases as the age increases. In the field condition only test sections of in-situ sand and sand appear to be positively influenced by the age, but the field strength of other stabilized soil materials showed either a decreasing or constant strength with time.

### 7.7.4 Influence of Rc additive

Based on the above analysis of compressive strength and indirect tensile strength obtained from the field cores and the laboratory-prepared specimens, it can be generally concluded that addition of Rc in cement stabilization yields a higher compressive strength and indirect tensile strength. Figure 7.27 and 7.28 summarize the comparison of the strength of cement stabilized materials with and without using Rc, which is based on the field cores and laboratory-prepared specimens at age of 28 days in the field, i.e. maturity index 121°C·day.

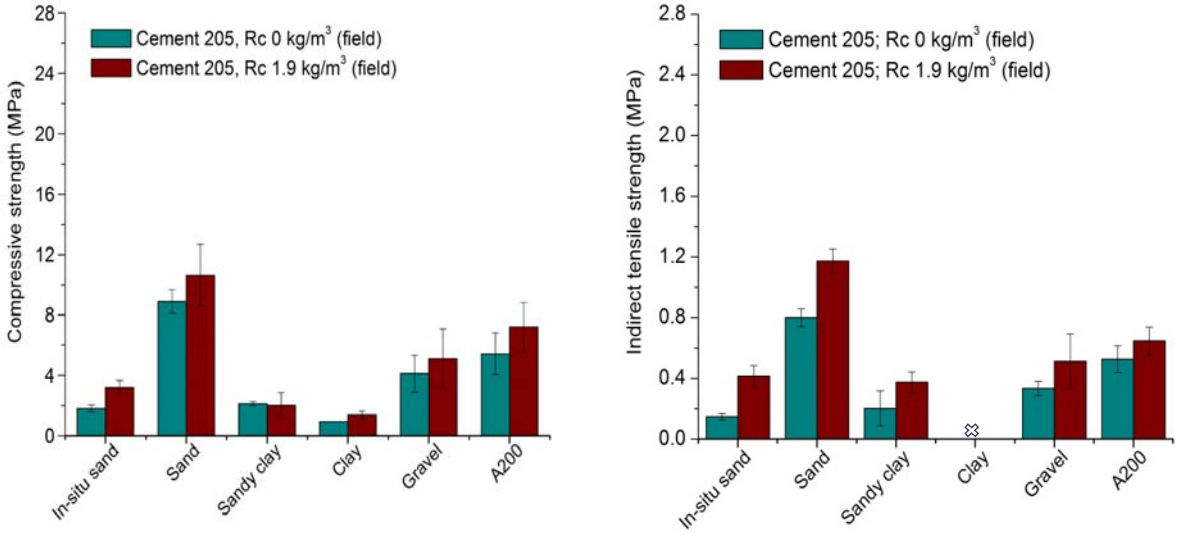


**Figure 7.27** Comparison of the field strength with and without using Rc

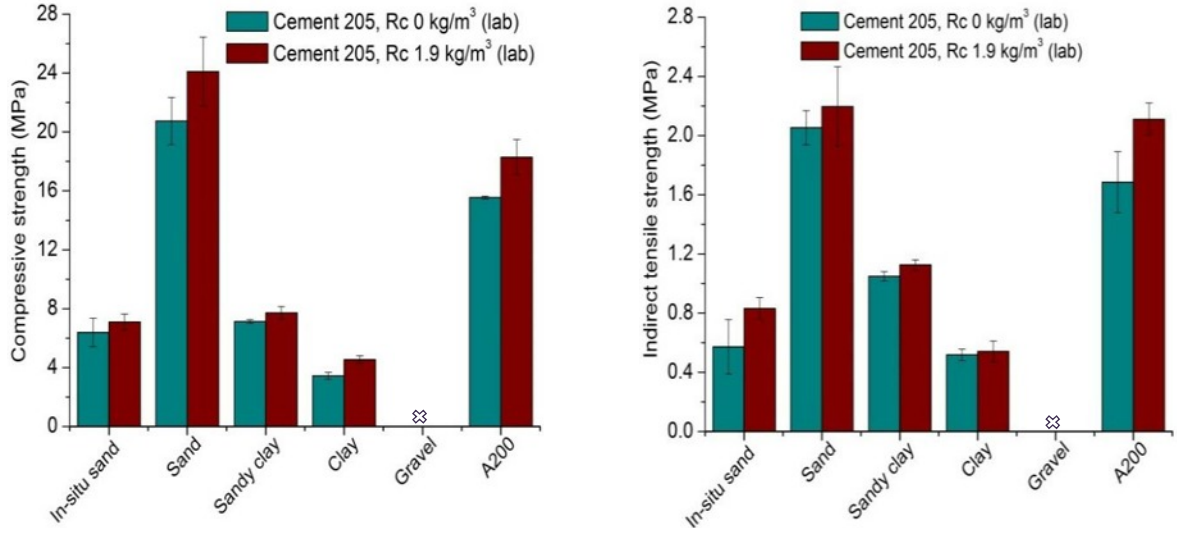


**Figure 7.28** Comparison of the laboratory-strength with and without using Rc

It appears from Figure 7.27 and 7.28 that the mixtures with use of Rc can achieve higher compressive strength and indirect tensile strength which is observed in all

these evaluated soil types and in both laboratory and field conditions. The extent of the improvement depends on the type of soil material.

Besides, it has also to be noted that the influence of Rc additive on the properties of cement stabilization is also related to the local conditions. Figure 7.29 demonstrates the ratio of the strength obtained from the mixtures with use of Rc (1.9, 205) to that of the mixture without Rc (0, 205) in the field and laboratory conditions.

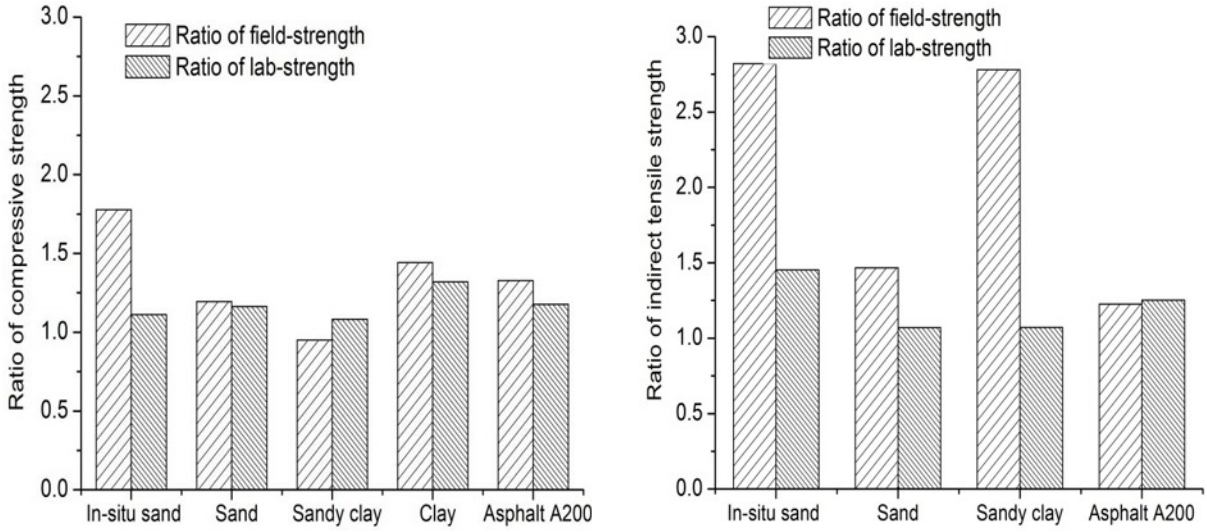


**Figure 7.29** Ratio of strength of the mixtures with Rc and without Rc (M=121°C·day)

As can be seen in Figure 7.29, the ratio of the strength of mixtures with Rc to that of mixtures without Rc is generally higher than 1, which means using Rc improves the strength. Besides, the ratio of the field strength is observed to be higher than the laboratory-ratio, especially for the indirect tensile strength, which gives an indication that using Rc additive might have a larger effect in the field base than in the laboratory-prepared specimens. This could be because during the cold winter time, the hydration rate of blast furnace slag cement is rather low, while in the mixtures with Rc additive, the compounds of this additive can accelerate the cement hydration rate and gain higher strength.

Besides, it can be noted that in stabilizing the in-situ sand soil which contains 2% organic materials, addition of Rc additive seems to give promising results. Figure 7.30 shows the field cores of stabilized in-situ sand sections.


(a) (0; 205) 160 mm (b) (1.9; 205) 240 mm (c) (3.8; 270) 270 mm

**Figure 7.30** Field cores of stabilized in-situ sand at 28 days (M=121°C·day)

In Figure 7.30 it can be clearly seen that the field core stabilized only with cement exhibits 160 mm in length as well as a rough surface. Compared with this, the field cores with addition of Rc exhibit at least 240 mm in length and a more smooth core surface, and hence it corresponds to the higher strength which is observed earlier. In organic soils, the cement reaction is adversely affected by the presence of humic substances, resulting in considerably lower strength (Robbins & Mueller, 1960). Figure 7.30 might indicate that using Rc in cement stabilization has the potential for stabilizing the in-situ organic soils.

### 7.7.5 Density of field cores and the laboratory-prepared specimens

Density is another important parameter controlling the properties of cement stabilized materials. In this field study a large variation in the field density is observed in all test sections. To observe the variation of three test repetitions, one example is shown in Figure 7.31 which compares the field density obtained from the field cores with the laboratory density obtained from the laboratory-prepared specimens, based on the in-situ sand mixture (1.9, 205) at ages of 7, 14 and 28 days.

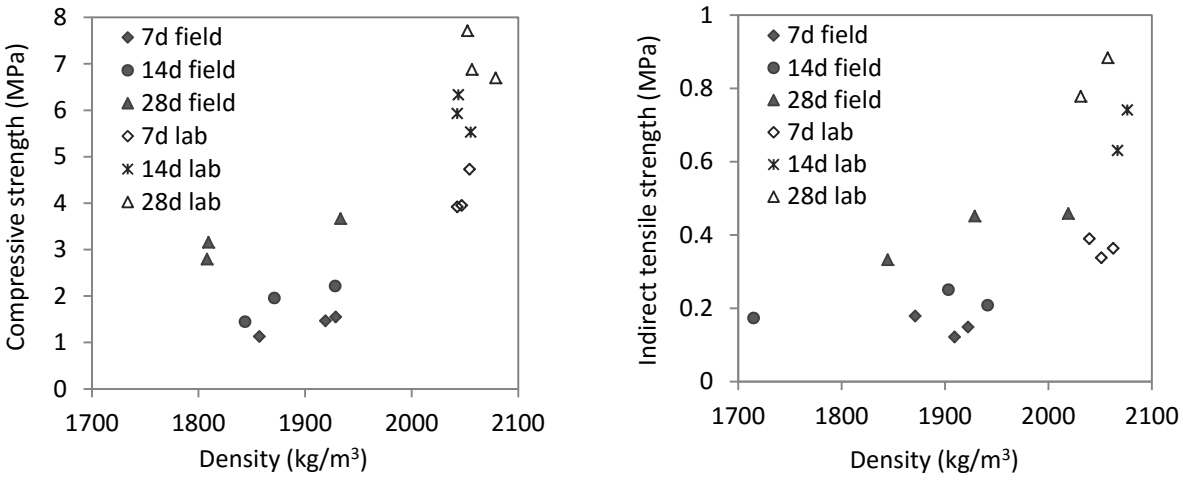


**Figure 7.31** Field density and laboratory designed density of the in-situ sand (1.9, 205)

In Figure 7.31 it can be observed that a large variation occurred in density and strength of the field cores. The density of the field cores of in-situ sand ranges from 88%~97% of the laboratory designed density caused by the inadequate compaction or non-uniform mixing.

Figure 7.32 summarizes the comparison of field density and the laboratory designed density of all the soil types, which is obtained from the field cores and the laboratory-prepared specimens at age of 28 days.

As shown in Figure 7.32, the density of the field cores is generally much lower than that of the specimens compacted in the laboratory. The lower density is one important reason which leads to the lower field strength. Additionally, the density of the field cores exhibits a quite large variation and it occurs in all test sections. The large variation in the density of the field cores also contributes to the large variation in the field strength. The large variation in field density can be caused by the non-uniform mixing and compaction during stabilization, and also could be from the variable density of the unbound gravel material before stabilization.

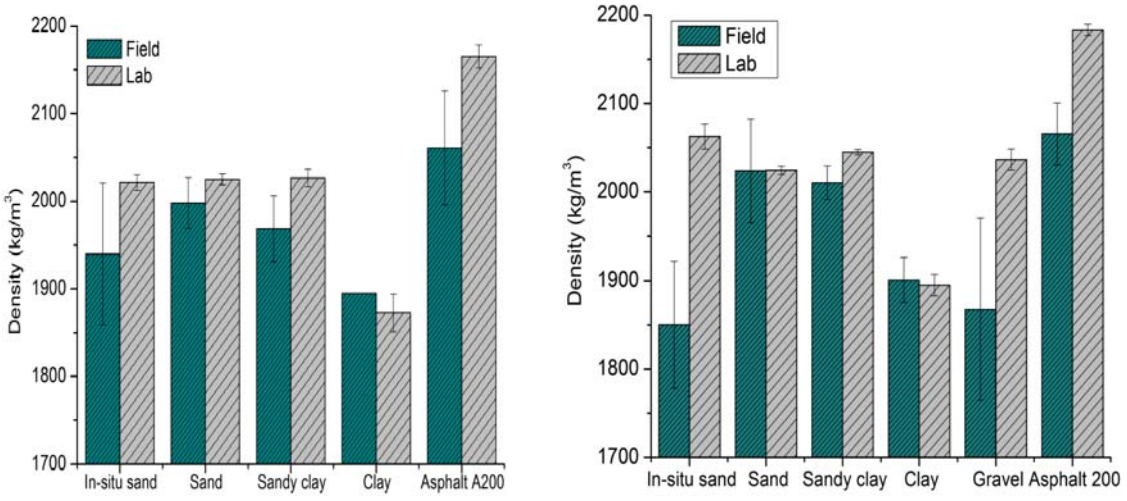


(a) Mixture (0, 205) (b) Mixture (1.9, 205)

**Figure 7.32** Comparison of the field density with the laboratory-designed density

Besides, some additional field cores were extracted from the edge of the road project, shown in Figure 7.33.

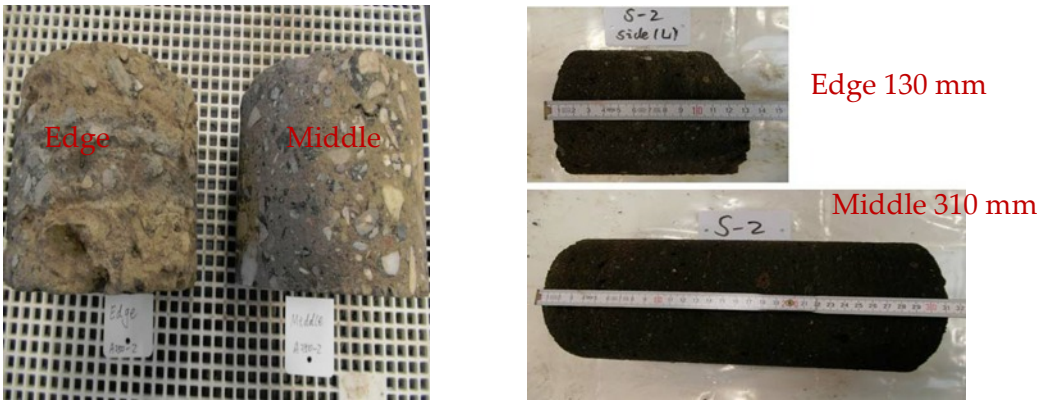


(a) Asphalt A200-2 section (b) Sand S-2 section

**Figure 7.33** Field cores extracted from the edge and middle of the road base

As observed in Figure 7.33, the field core of stabilized asphalt obtained from the edge exhibits a rough surface and some portion got broken during the drilling process. Similarly, the length of the sand core from the edge only reached 130 mm in comparison with the middle core sample with length 310 mm. It means that a much lower load bearing capacity can be expected on the edge of the base.

It can be concluded that the differences of the laboratory-preparation methods and the field construction techniques contribute to the huge difference between the lab-designed properties and the field properties which are shown as the lower field strength and variation of the field strength in this study. Molenaar (2006) attributed the aspects of the construction techniques to the pulverization of the existing soil, homogeneity of spreading, homogeneity of mixing, homogeneity in moisture content and compaction. Therefore, to achieve a satisfactory field performance, it is very essential that the stabilized mixture is uniformly blended and well compacted for the full depth and width during construction.

## 7.8 Estimation of the field strength

In order to quantify the field performance of cement stabilized materials, estimation models are established combining the effects of cement and Rc contents, field density and maturity index. These regression models are based on the strength of the field cores from all test sections including ages from 7 to 28 days which represent a maturity index from 72 to 121°C·day. As discussed earlier, in this particular study, the time alone doesn't actually reflect the field strength development due to the low ambient temperature in the field. The maturity index, accumulation of the temperature at all the time intervals, is more appropriate to indicate the hydration progress and thus is taken into account in the estimation models. A general

estimation model for compressive strength and indirect tensile strength is expressed by the following equation:

$$f = \mathrm{a} \cdot C^{n_1} \cdot e^{n_2 \cdot Rc} \cdot \left(\frac{D}{1000}\right)^{n_3} \cdot \left(\frac{M}{100}\right)^{n_4} \quad (7\text{-}2)$$

Where, f is compressive strength or indirect tensile strength, MPa;

C is the cement content, kg/m$^3$; Rc is Rc additive content, kg/m$^3$;

D is the field density, kg/m$^3$; M is the Maturity index, °C·day;

a, $n_1$, $n_2$, $n_3$ and $n_4$ are the coefficients, depending on the type of soil and the type of strength.

The chosen functions for each variable factor are based on the estimation models obtained in Chapter 4 and 5 which showed good fit for the test data.

### 7.8.1 Estimation models of compressive strength

Figure 7.34 shows the estimation models of the compressive strength obtained from the field cores. For each type of material, the field results include three different mix designs, see Table 7.2 and three different ages (i.e. maturity index 72, 83 and 121°C·day).

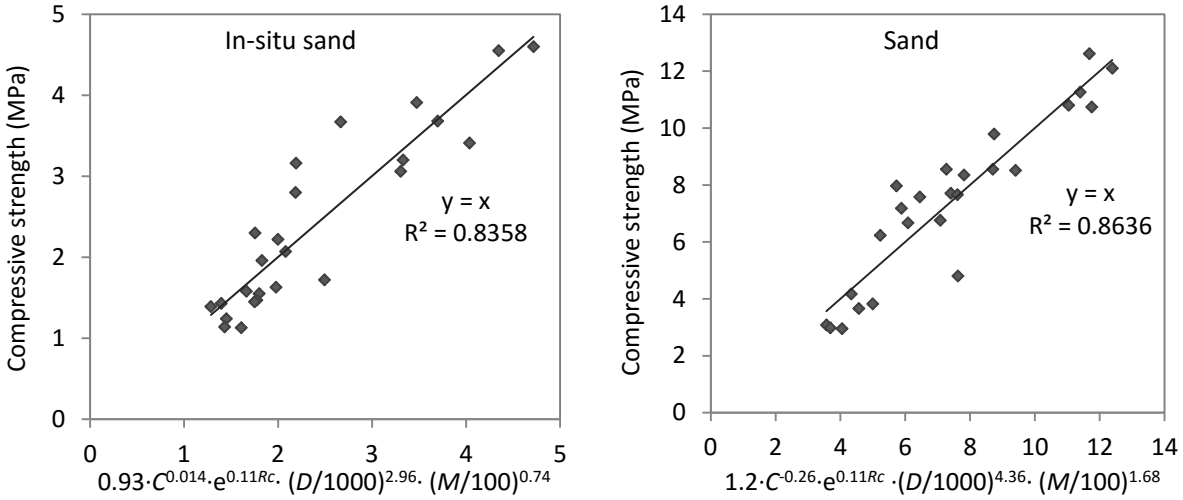

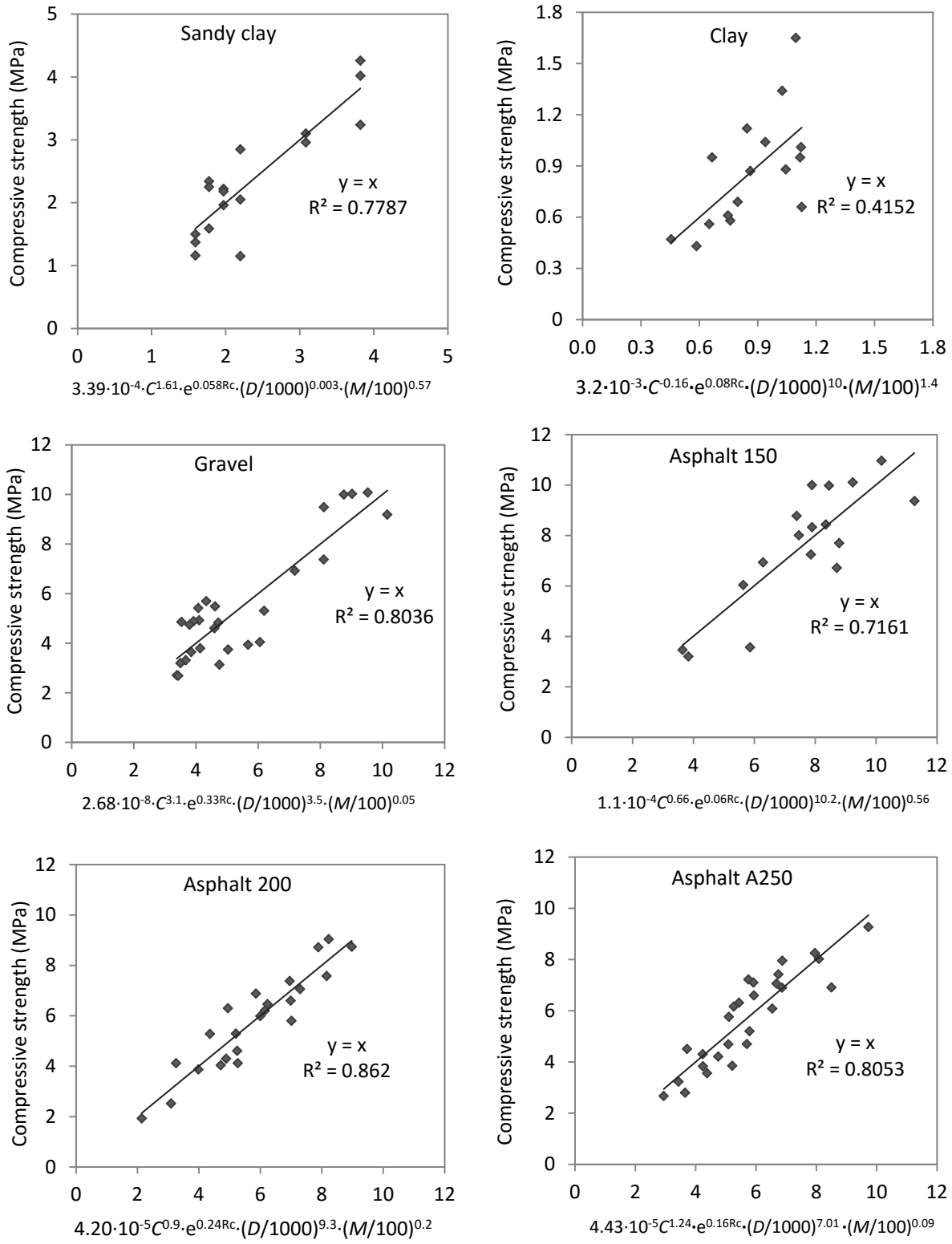


Note: C is the cement content, kg/m$^3$; Rc is the Rc additive content, kg/m$^3$, D is the field density, kg/m$^3$; M is the maturity index, °C·day.

**Figure 7.34** Estimation model of compressive strength in the field condition

Figure 7.34 gives the statistical models to predict the field compressive strength with combined effects of cement and Rc contents, field density and maturity index. In

general, it can be seen that the compressive strength of cement stabilized materials is positively correlated to these factors. Among these models, exceptions occur on the stabilized clay and sand sections which correlate the field compressive strength with the negative influence of the cement content. It is well known that the compressive strength of cement stabilized materials increases with increasing cement content which is documented in a great number of studies (TRH 13, 1986; Yoon & Abu-Farsakh, 2009; Park, 2010). Therefore, the estimation models for the clay and sand sections based on the field data are probably influenced by the construction factors. For instance, non-uniform mixing during construction might not result into the designed mixture.

Additionally, it can be noticed that the soil type influences the reliability of the estimation equation. The largest $R^2$ values are obtained for the gravel, asphalt A200 and A250 as well as for the in-situ sand, while the lowest $R^2$ value is found in the fine-grained clay soil section. This proves that stabilizing fine-grained soil has the issue of proper mixing, which may give rise to quite variable properties.

### 7.8.2 Estimation models of indirect tensile strength

Similarly, the estimation models for the field indirect tensile strength are shown in Figure 7.35. Figure 7.35 includes the field data of the indirect tensile strength of all the field cores.

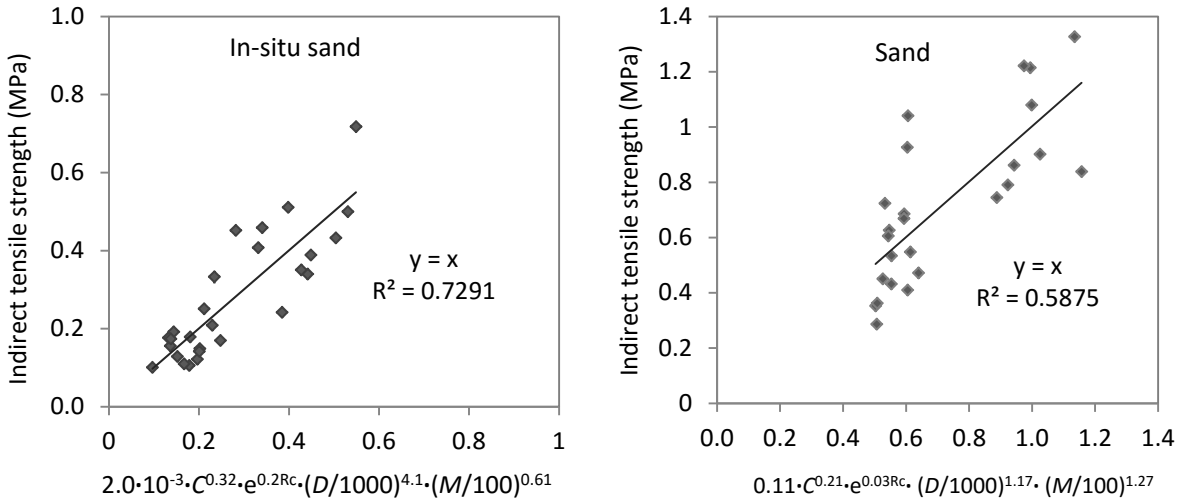

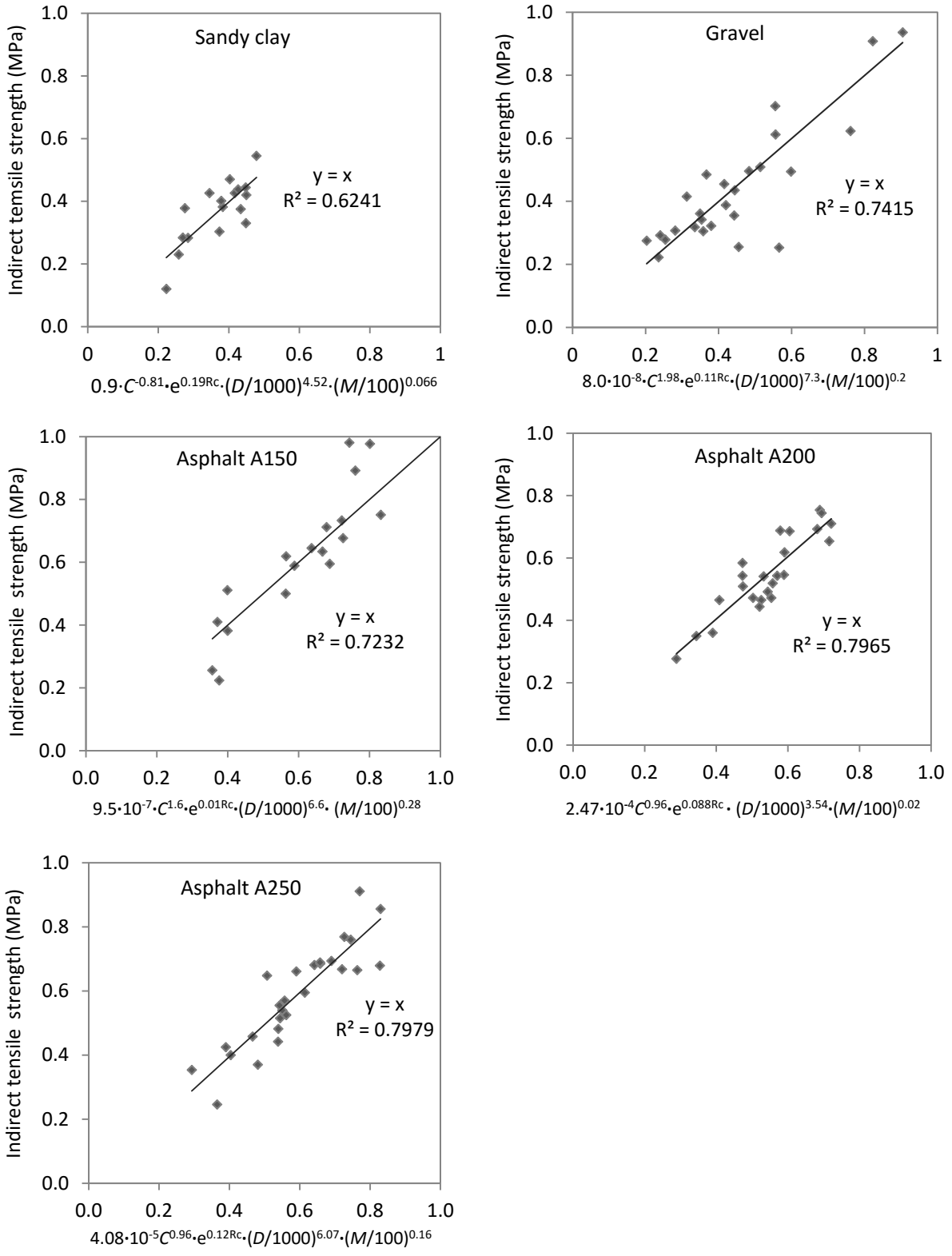


Note: C is the cement content, kg/m$^3$; R is the Rc content, kg/m$^3$, D is the field density, kg/m$^3$; M is the maturity index, °C·day.

**Figure 7.35** Estimation models of the indirect tensile strength in the field condition

As shown in Figure 7.35, similar estimation models are developed for the indirect tensile strength. It also shows that the indirect tensile strength of field cores is

positively influenced by cement and Rc contents, field density and the maturity index.

Compared with the compressive strength models, the $R^2$ values of the indirect tensile strength equations are relatively lower, which is mainly below 0.80. Similarly, the larger the grain size of the soil, the better the estimation equations of indirect tensile strength approximate the field data.

Table 7.6 summarizes the coefficients of all the estimation models shown in Figure 7.35 and 7.36.

**Table 7.6** Coefficients of the estimation models for the field strength

$$f = a \cdot C^{n_1} \cdot e^{n_2 \cdot Rc} \cdot \left(\frac{D}{1000}\right)^{n_3} \cdot \left(\frac{M}{100}\right)^{n_4}$$

| | Compressive strength | | | | | | Indirect tensile strength | | | | | |
|---|---|---|---|---|---|---|---|---|---|---|---|---|
| | a | $n_1$ | $n_2$ | $n_3$ | $n_4$ | $R^2$ | a | $n_1$ | $n_2$ | $n_3$ | $n_4$ | $R^2$ |
| In-situ sand | 0.93 | 0.014 | 0.11 | 2.96 | 0.74 | 0.84 | $2.0 \cdot 10^{-3}$ | 0.32 | 0.2 | 4.1 | 0.61 | 0.73 |
| Sand | 1.2 | -0.26 | 0.11 | 4.36 | 1.68 | 0.86 | 0.11 | 0.21 | 0.03 | 4.17 | 1.27 | 0.59 |
| Sandy clay | $3.39 \cdot 10^{-4}$ | 1.61 | 0.06 | 0.003 | 0.57 | 0.78 | 0.9 | -0.81 | 0.19 | 4.52 | 0.07 | 0.62 |
| Clay | $3.2 \cdot 10^{-3}$ | -0.16 | 0.08 | 10 | 1.40 | 0.42 | — | — | — | — | — | — |
| Gravel | $2.68 \cdot 10^{-8}$ | 3.10 | 0.33 | 3.5 | 0.05 | 0.80 | $8 \cdot 10^{-8}$ | 1.98 | 0.11 | 7.30 | 0.20 | 0.74 |
| A150 | $1.1 \cdot 10^{-4}$ | 0.66 | 0.06 | 10.2 | 0.56 | 0.72 | $9.5 \cdot 10^{-7}$ | 1.60 | 0.01 | 6.6 | 0.28 | 0.72 |
| A200 | $4.2 \cdot 10^{-5}$ | 0.90 | 0.24 | 9.3 | 0.20 | 0.86 | $2.47 \cdot 10^{-4}$ | 0.96 | 0.09 | 3.54 | 0.02 | 0.80 |
| A250 | $4.43 \cdot 10^{-5}$ | 1.24 | 0.16 | 7.01 | 0.09 | 0.81 | $4.08 \cdot 10^{-5}$ | 0.96 | 0.12 | 6.07 | 0.16 | 0.80 |

Note: Coefficients $n_1$, $n_2$, $n_3$ and $n_4$ correspond to the variable factor of cement content, Rc content, density of the sample and the maturity index, respectively.

As shown in Table 7.6, the estimation models of in-situ sand, crushed gravel and crushed asphalt materials generally approximate the field data quite well, which is indicated by the acceptable $R^2$ values. However, the models obtained for the fine-grained materials clay and sandy clay exhibit a rather low accuracy and also some factors even showed a negative influence of the cement content because of a large variation in the field results. Therefore, only the estimation models obtained with $R^2$ above 0.8 are recommended for use. However, one should keep in mind that these models are based on the specific field construction and environmental conditions under consideration and also strongly depend on the properties of the soil materials.

## 7.9 Conclusions and recommendations

This Chapter focused on the field evaluation of cement stabilized materials with and without Rc additive, comprising a wide range of materials. A cement stabilized road base was constructed by creating different test sections. Two independent variables of cement and Rc contents were evaluated. Based on the field results, the field strength was compared with the strength of the laboratory-prepared specimens under the same maturity index and estimation models were developed for the field compressive and indirect tensile strength. The principle findings of this Chapter can be concluded as follows:

1) Addition of Rc additive in cement stabilization generally yields higher compressive strength and indirect tensile strength for cement stabilized materials in the field study, in both field and laboratory conditions. The improvement of the strength is dependent on the soil type.

2) The field properties and the lab properties are compared for the same maturity index due to the huge difference of cement hydration progress in these two conditions. The compressive strength and indirect tensile strength of the field cores generally reach 30% to 70% of the strength obtained for the laboratory-prepared specimens. Besides, large variations of density and strength are found in all field sections which could be mainly caused by the un-uniform mixing and compaction during construction.

3) Curing periods of 7, 14 and 28 days don't have a clear influence on the strength development of the field cores, whereas the strength obtained from the laboratory-prepared specimens showed a steady increase within 28 days. Because of the low temperatures in the field condition, the corresponding maturity index of the field cores is in a small range.

4) Based on the field results, estimation models have been developed to predict the compressive strength and the indirect tensile strength of cement stabilized materials in the field condition. These models are based on the effects of the cement and Rc contents, field density and maturity index. The coefficients of these regression models are strongly influenced by the type of soil material.

In this study a huge difference occurred between the field temperature shortly after construction and the curing temperature in the laboratory. In order to exclude the influence of the environmental factors, the maturity method was adopted to compare the field strength and the lab-designed strength. However, some limitations might

exist. For instance, the maturity method is usually used to predict the strength of in-place concrete, herein it is assumed that it also applies to cement stabilized materials with and without using Rc additive. Another disadvantage is that the maturity was created based on the ambient temperature without recording the temperature of the laboratory-prepared specimen itself or placing the temperature sensors in the base layer. Therefore, in order to have precise information, further research is advised to be conducted to investigate the influence of the curing temperature on the properties of cement stabilized materials.

## References

ASTM C 1074. Standard Practice for Estimating Concrete Strength by the Maturity Method.

Bryan T. and W. Spencer Guthrie. (2011). Strength and performance characteristics of cement-treated reclaimed pavement with a chip seal. Journal of the Transportation Research Board, No. 2212, pp. 100-109.

Consoli, N.C., da Fonseca, A.V., Cruz, R.C., and Silva, S.R. (2011). Voids/cement ratio controlling tensile strength of cement-treated soils. Journal of geotechnical and geoenvironmental engineering, 137(11), 1126-1131.

Carino N.J. (1984). The maturity method: theory and application. Cement, Concrete, and Aggregates, 6(2): 61-73.

Chai, G.W.K., Oh, E. Y.N., and Balasubramaniam, A. S. (2005). In-Situ Stabilization of Road Base Using Cement-A Case Study in Malaysia. In The Fifteenth International Offshore and Polar Engineering Conference. International Society of Offshore and Polar Engineers.

Cho, Y.H., K.W. Lee, et al. (2006). Development of cement-treated base material for reducing shrinkage cracks. Transportation Research Record: Journal of the Transportation Research Board 1952(-1): 134-143.

Dixon, P. A., Guthrie, W.S., and Eggett, D.L. (2012). Factors Affecting Strength of Road Base Stabilized with Cement Slurry or Dry Cement in Conjunction with Full-Depth Reclamation. Transportation ReseaRch Record: Journal of the Transportation ReseaRch Board, 2310(1), 113-120.

FM 5-410. (2012). Soil Stabilization for Roads and Airfields. http://www.itc.nl/~rossiter/Docs/FM5-410/FM5-410_Ch9.pdf.

Guthrie, W., Tyler B. Young, Brandon J. Blankenagel, and Dane A. Cooley. (2005). Early-strength assessment of cement-treated base material. Journal of the Transportation Research board No. 1936, pp. 12-19.

Guthrie, W., and Rogers, M.A. (2010). Variability in Construction of Cement-Treated Base Layers: Material Properties and Contractor Performance. Transportation Research Record, No. 2186, pp. 78-89.

Guthrie, W., Jone E. Michener, Bryan T. Wison, and Dennis L. Eggett. (2009). Effects of environmental factors on construction of soil-cement pavement layers. Journal of the Transportation Research Board, No. 2014 pp. 71-79.

Gaspard, K. (2002). In-place Cement Stabilized Base Reconstruction Techniques. Interim Report: Construction and Two Year Evaluation. Louisiana Transportation Research center.

George, K.P. (2002a). Soil stabilization field trial. University of Mississippi.

George, K.P. (2002b). Minimizing cracking in cement-treated materials for improved performance, PCA Portland Cement Association, Skokie, USA.

Jonathon, R. Griffin and Jeb S. Tingle. (2009). In situ evaluation of unsurfaced Portland cement stabilized soil airfields. ERDC/GSL TR-09-20.

Kolias, S., Kasselouri-Rigopoulou, V., and Karahalios, A. (2005). Stabilisation of clayey soils with high calcium fly ash and cement. Cement and Concrete Composites, 27(2), 301-313.

Melancon, J. and Shah, S. (1973). Soil cement study. Research report number 68-95. Louisiana Department of Highways.

Molenaar. A.A.A (2006). Structural Design of Pavement, Design of Flexible Pavement. Lecture Notes CT 4860, Delft University of Technology, the Netherlands.

Mindess, S., J.F. Young, and D. Darwin. (2003). Concrete, 2nd ed. Prentice Hall, Upper Saddle River, N.J., USA.

Naik, T.R. (1980). Concrete strength prediction by the maturity method. Journal of the Engineering Mechanics Division, 106(3), 465-480.

Park, S. S. (2010). Effect of Wetting on Unconfined Compressive Strength of Cemented Sands. Journal of geotechnical and geoenvironmental engineering, Vol. 136(12) , pp. 1713-1720.

PCA (2005). Full-depth reclamation: Recycling roads saves money and natural resources. Portland cement association, Skokie, Illinois, USA.

P. Wu, L.J.M. Houben and C.E.G. Egyed (2013). Study of the variables in laboratory testing of cement stabilized materials. International Journal of Pavements, São Paulo, Brazil.

Park, S.S. (2010). Effect of Wetting on Unconfined Compressive Strength of Cemented Sands. Journal of geotechnical and geoenvironmental engineering 136(12): 1713-1720.

Robbins, E.G., and Mueller, P.E. (1960). Development of a Test for Identifying Poorly Reacting Sandy Soils Encountered in Soil-Cement Construction, Bulletin No. 267, Highway Research Board, Washington, D.C., pp. 46-50.

Ramachandran, V.S. (1996). Concrete admixtures handbook: properties, science and technology. Cambridge University Press.

Shihata, S.A. and Z.A. Baghdadi (2001). Long-term strength and durability of soil cement. Journal of materials in civil engineering, Vol. 13, pp.161.

Saul, A.G.A. (1951). Principles Underlying the Steam Curing of Concrete at Atmospheric Pressure. Magazine of Concrete Research, Mar. pp. 127-140.

TRH 13. (1986). Cementitious Stabilizers in Road Construction South Africa. Pretoria, South Africa.

Vorobieff, G. (1998). Performance and Design of In-situ Stabilised Local Government Roads. Australian Stabilisation Industry Association.

Wang, M.Ch and Mitchell, J.K. (1971). Stress deformation prediction in cement treated soil pavements. Highway Research Record No. 351.
Wilde, W.J. (2013). Development of a Concrete Maturity Test Protocol (No. MN/RC 2013-10). Center for Transportation Research and Implementation, Minnesota State University, Mankato.

Wade, S. (2006). Evaluation of the maturity method to estimate concrete strength. Highway Research Center and Department of Civil Engineering at Auburn University, research report, ALDOT Research Project 930-590.

Xuan, D.X. (2012). Cement treated recycled crushed concrete and masonry aggregates for pavements. PhD dissertation, Delft University of Technology, the Netherlands.

Yoon, S. and M. Abu-Farsakh. (2009). Laboratory investigation on the strength characteristics of cement-sand as base material. KSCE Journal of Civil Engineering 13(1): 15-22.

# CHAPTER 8

# TRANSVERSE CRACKING BEHAVIOR OF CEMENT STABILIZED MATERIALS WITH ROADCEM ADDITIVE

A cement stabilized material is susceptible to shrinkage caused by the moisture loss during hydration or a temperature decrease. As the stabilized base layer shrinks, due to the friction with the underlying layers, internal tensile stress will be induced in the base layer. As the tensile stress exceeds the tensile strength of the base material, cracks may occur. Shrinkage cracks that develop in the road base may reflect through the top surface layer, resulting in visible transverse cracks. Bofinger (1978) attributed the degree of shrinkage cracking to the following factors:

1) Moisture variation as the cement hydrates;
2) The contraction of the material as the ambient temperature falls;
3) The restraint imposed on the road base by the sub-base or subgrade;
4) The tensile properties of the hardening soil-cement material.

This Chapter evaluates the transverse cracking behavior of cement stabilized sand and clay base layers. The crack pattern of the cement stabilized sand and clay base layers are estimated by a mechanical method by means of considering the development of the tensile stress due to internal and environmental factors and the development of the tensile strength of the material. The times of occurrence of the transverse cracks, the spacing between the cracks and the development of the width of the cracks are estimated and analysed in relation to the factors of Rc additive content, curing method, stress relaxation, construction time, coefficient of friction and the amplitude of the daily temperature variation.

## 8.1. Shrinkage behaviour

Cement stabilized materials are subjected to drying shrinkage caused by moisture loss during cement hydration. Cement stabilized fine-grained soils (e.g. clay) are normally considered to exhibit more shrinkage than cement stabilized granular materials because fine-grained soils require higher water and cement contents (George, 1968; Nakayama, 1965; Adaska & Luhr, 2004). Therefore, the shrinkage characteristics are of great importance in the case of clay-cement material. The reason for shrinkage is generally believed to follow the capillary tension theory, i.e. when water is consumed for hydration or evaporates, the capillary tension force will develop in the pores, causing the overall volume shrinkage of the soil-cement structure.

The shrinkage tests in this study focus on the effect of Rc additive, therefore, the shrinkage measurements were conducted on the mixtures with variable Rc contents and constant cement content. Three mixtures (0, 205), (1.9, 205) and (3.8, 205) are evaluated, i.e. Rc additive 0, 1.9 and 3.8 kg/m$^3$, by dry mass of soil.

In addition to the mixture variables, the influence of the curing regime is also evaluated in the shrinkage tests. Under ideal conditions, in which no moisture escapes into the surrounding environment, the shrinkage caused by the cement hydration is called "autogenous shrinkage". When the cemented material is exposed to a dry environment, moisture can evaporate freely from the soil-cement which results in drying shrinkage (Bofinger, 1978). The loss of moisture due to evaporation in the dry environment is generally greater than the amount of water required for cement hydration, and therefore evaporation drying will contribute much more to shrinkage than self-desiccation (Bofinger, 1978).

In practice, it is difficult to achieve ideal curing conditions, but moisture loss due to evaporation from the soil-cement surface layer can be reduced by appropriate curing and thus reducing the likelihood of cracking. In this study, two different types of curing regimes are considered for the shrinkage tests:

- Regime 1. Initial moist curing for 3 days and afterwards exposure to dry environment (relative humidity 90% and temperature 20°C).
- Regime 2. Moist curing for 28 days.

Moist curing was performed by covering the specimen with a moist tissue and sprinkling with water, to simulate the field curing method. In this study, the specimen was not sealed, i.e. not sealed with foil and so the drying shrinkage was measured.

### 8.1.1 Specimen preparation and test method

Most researchers in the past investigated the shrinkage characteristics of cement stabilized materials by measuring the axial deformation of cylindrical specimens. However, Bofinger (1978) mentioned that specimens prepared and monitored in this way only reflect the vertical shrinkage of the road base, causing a reduction of the thickness of the layer, and therefore they don't simulate the critical horizontal shrinkage experienced in practical road bases. Therefore, in this study prismatic specimens (160×40×40mm) were prepared and the deformation change was measured horizontally. During the preparation of the specimens, two gauge studs were placed through the holes of the steel moulds and inserted to the end of the specimen during moulding, shown in Figure 8.1. The gauge studs were used to facilitate the connection of specimen to the shrinkage measuring frame. After hardening in the mould for 24 hours, the specimens were demoulded and cured according to the specified curing method. Afterwards, the change of the specimen length was measured at different time intervals. The device used for the shrinkage measurements was equipped with a dial gauge capable of measuring to the nearest 0.01 mm, Figure 8.1.

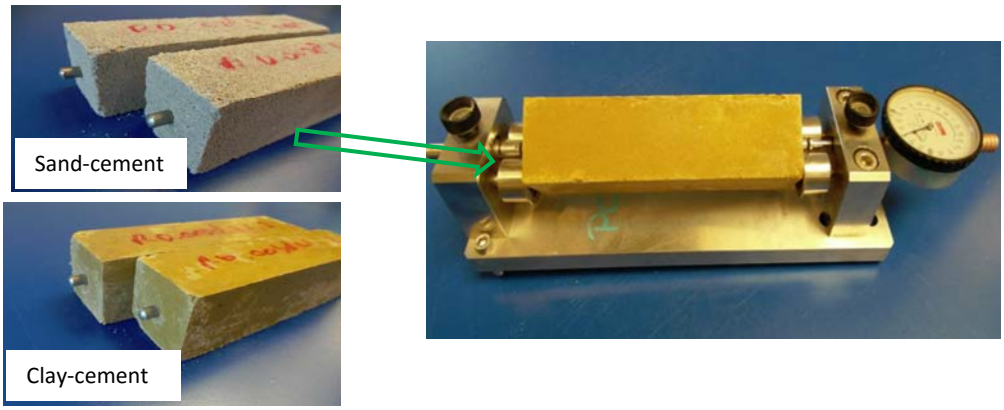


**Figure 8.1** Prismatic specimen and measurement device

The initial dial gauge reading on the specimen was recorded as $I_0$. The measurement was taken at increasing time intervals over a period of 28 days. The measurement of the specimen at each time interval was recorded as $I_i$. The length change (in percentage) of a specimen at any time interval is calculated by the following equation:

$$\text{Shrinkage} = \frac{\Delta L}{L} \cdot 100\% = \frac{I_0 - I_i}{L} \cdot 100\% \quad (8\text{-}1)$$

where, L is the original length of the specimen immediately after compaction, mm; $I_0$ is the initial reading, mm; $I_i$ is the reading taken at the following time intervals, mm; shrinkage strain is positive.

There is a gap between the specimen and the base plate, so no restraints result from the friction. This test method for shrinkage was also adopted in a study by Chakrabarti (2003).

### 8.1.2 Analysis of shrinkage test results

#### 8.1.2.1 Shrinkage test results of the sand-cement materials

Figure 8.2 shows an example of the measured shrinkage results of three replicate specimens, obtained from the sand-cement mixture (1.9, 205), i.e. cement content 205 kg/m$^3$ and Rc 1.9 kg/m$^3$.

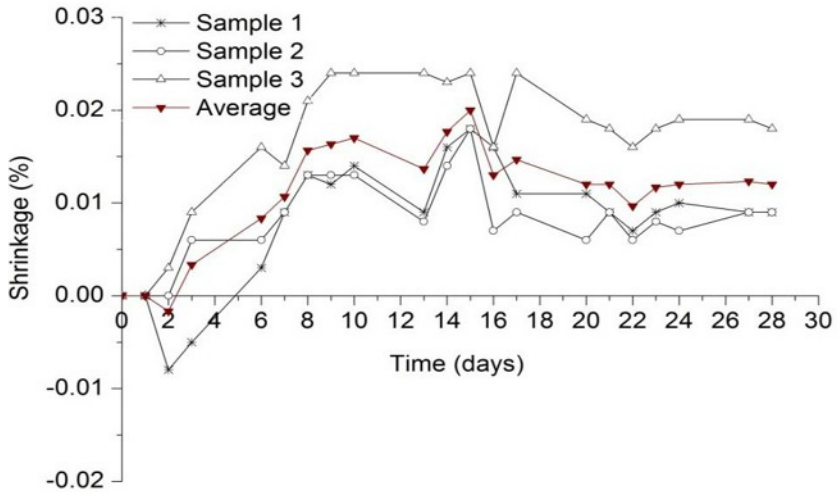


(a) Moist cured for 3 days

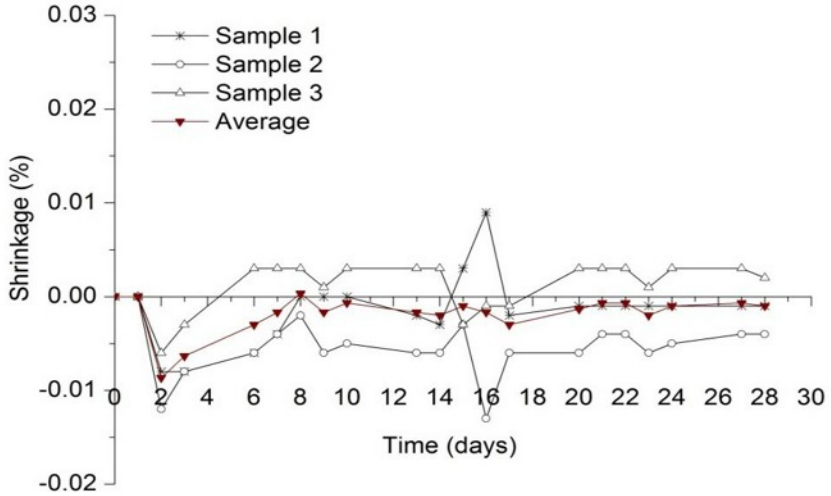


(b) Moist cured for 28 days

**Figure 8.2** Shrinkage measurement of three replicate specimens of sand-cement mixture (1.9, 205)

As can be seen from Figure 8.2, the shrinkage curves show a time-dependent pattern and are significantly influenced by the curing method. In graph (a) the specimens which were moist cured for 3 days, expanded in the first curing day and

subsequently started to shrink with a significant rate until 7 days. Afterwards, the shrinkage generally stayed stable. The specimens which were moist cured for 28 days expanded even more in the first curing day but then started to shrink until the average value reached about 0 at 7 days. The measured values of the expansion during the first curing day is different in these two curing method, which is mainly caused by the unavoidable variation in measurement procedures, such as calibrating the dial gauge and placing the beam specimen in the frame for each reading.

When specimens are moist cured for 28 days, the shrinkage almost doesn't occur. In contrast, moist curing of specimens for 3 days leads to shrinkage of approximately 0.0125% ($125\times10^{-6}$) after 7 days. It indicates that the humidity in the curing period has a great impact on the shrinkage of cement-sand materials. Neville (1996) reported that the shrinkage level of concrete may change from $-100\times10^{-6}$ to $1000\times10^{-6}$ when the relatively humidity in the curing period changes from 100% to 50%.

Figure 8.3 compares the shrinkage of three mixtures with different amounts of Rc additive and cured in two conditions. Each shrinkage curve is the mean value of three replicate specimens.

In Figure 8.3 it can be clearly seen that the use of Rc additive greatly influences the shrinkage of sand-cement materials. In graph (a), the total shrinkage after 28 days of the mixture with Rc 1.9 kg/m$^3$ is 50% less than the shrinkage of the mixture without Rc. When the Rc content increases, the total shrinkage shows an increase but is still 32% less than that of the mixture without Rc. However, during the initial 14 curing days, the measured values of the shrinkage showed much fluctuation in the three mixtures.

In graph (b), when moist cured for 28 days, it can be found that the mixture with the highest amount of Rc generally shows a slightly higher shrinkage than the mixture without Rc over 28 days. The mixture with moderate Rc content doesn't exhibit shrinkage.

In addition, in Figure 8.3 it should be noted that the two mixtures with Rc additive expanded in the first curing day. Bofinger (1973) also observed this finding on sand-cement which was measured on sealed specimens. The reason is that the mixtures are composed of volumetrically stable sand particles and surrounded by the cement hydrate gel. When cement hydrates, the cemented gel expands, and thus the overall volume could show expansion Bofinger (1973). However, the mixture without Rc additive doesn't show such expansion which is possibly because the volume shrinkage dominates in this mixture.

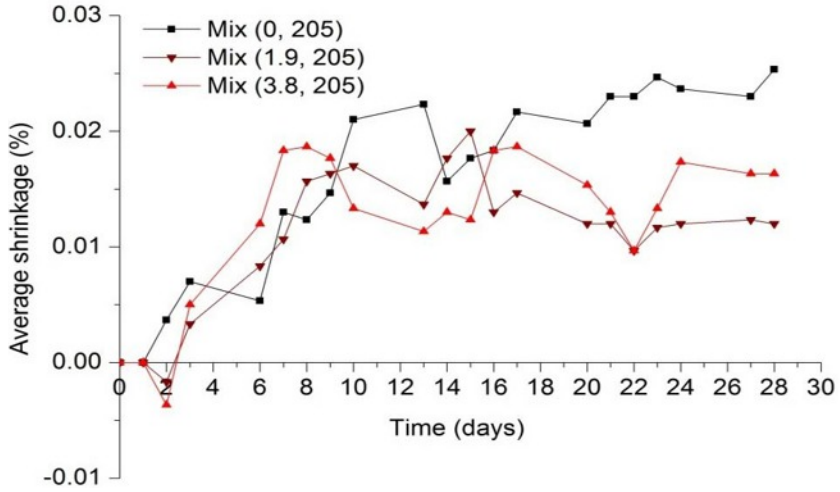


(a) Moist cured for 3 days

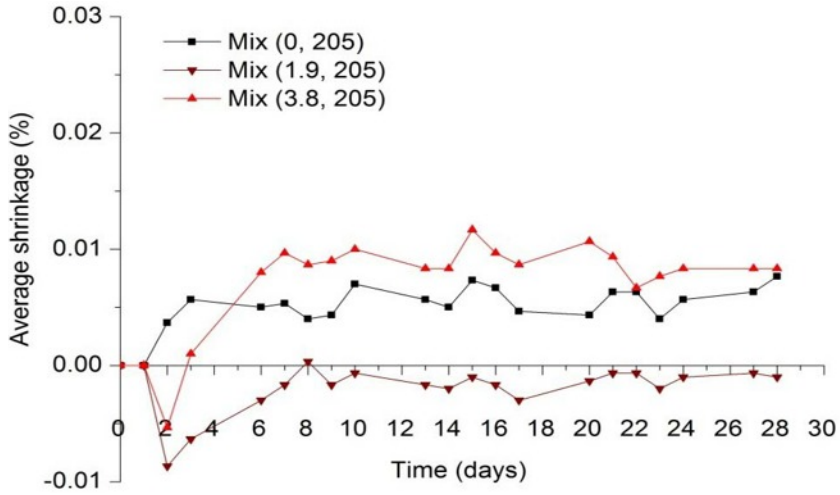


(b) Moist cured for 28 days

**Figure 8.3** Average shrinkage of three sand-cement mixtures

Regarding the influence of the curing method, it is clear that the shrinkage obtained from the specimens moist cured for 3 days showed a rapid increase when exposed to the dry environment, while 28-day moist curing leads to a stable shrinkage over 28 days and much lower final shrinkage. That is mainly because a longer moist curing period prevents large moisture loss due to evaporation. Besides, a longer period of moist curing leads to more cement hydration resulting in stiffer bonds between the sand particles, thereby also decreasing the total volume change. Especially, the mixture with 1.9 kg/m$^3$ Rc shows no shrinkage during the moist curing period of 28 days. It gives an indication that this Rc content could be an optimal amount to get minimum shrinkage.

The above findings indicate that a longer period of moist curing can significantly reduce the total final shrinkage. Therefore, in the field a longer period of moist

curing for a soil-cement base before allowing to dry out is beneficial in reducing the chance of cracks.

#### 8.1.2.2 Shrinkage test results of the clay-cement materials

Figure 8.4 shows the measured shrinkage results of three replicate specimens of the clay-cement mixture (1.9, 205), i.e. cement content 205 kg/m$^3$ and Rc content 1.9 kg/m$^3$ as a function of time in two different curing conditions.

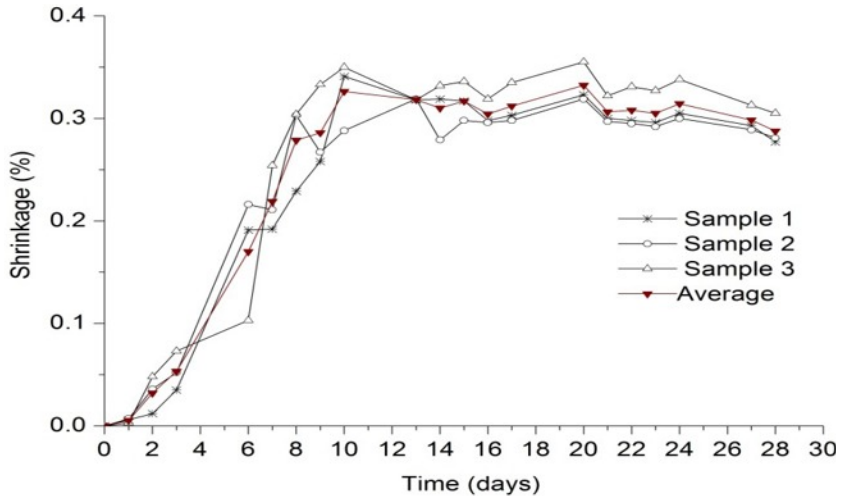


(a) Moist cured for 3 days

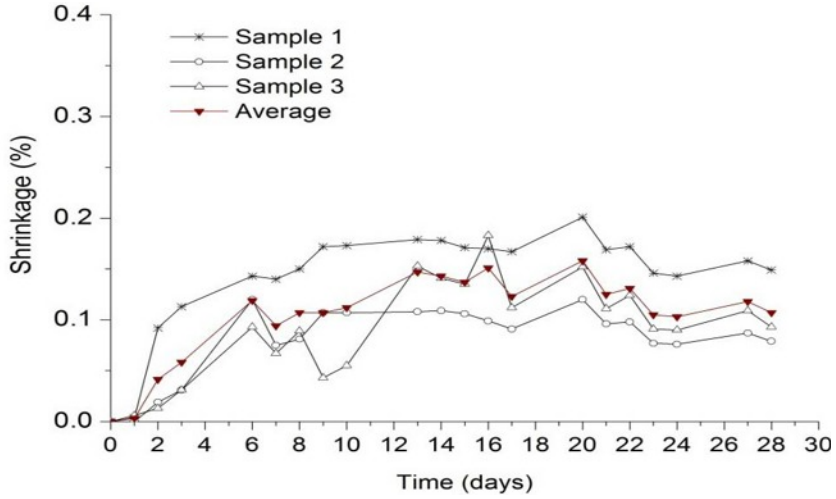


(b) Moist cured for 28 days

**Figure 8.4** Shrinkage measurement of three replicate specimens of clay-cement mixture (1.9, 205)

In Figure 8.4 it can be seen that the curing condition greatly affects the total shrinkage and the time-dependent pattern. In both conditions, during the initial moist curing period of 3 days, the shrinkage progressively increased, which is mainly from the volume change caused by the cement hydration. Bofinger (1978) explained that as hydration proceeds and the water for hydration is drawn from the moist clay,

the amount of the absorbed water in clay will steadily decrease, increasing thus the suction in the pores and consequently the intergranular stress.

When the specimens were exposed to drying and the hydration continued, shrinkage rapidly increased until 10 days and afterwards the length of the specimen remained approximately constant. Whereas, for the specimens moist cured until 28 days, the shrinkage seemed to stop after 6 days and the total shrinkage was substantially less than that of the specimens moist cured for 3 days. This means increasing the period of the moist curing can significantly reduce the magnitude of shrinkage of clay-cement materials.

Figure 8.5 compares the shrinkage of three mixtures with different amounts of Rc additive and cured in two conditions. Each shrinkage curve is plotted based on the mean value of three replicate specimens.

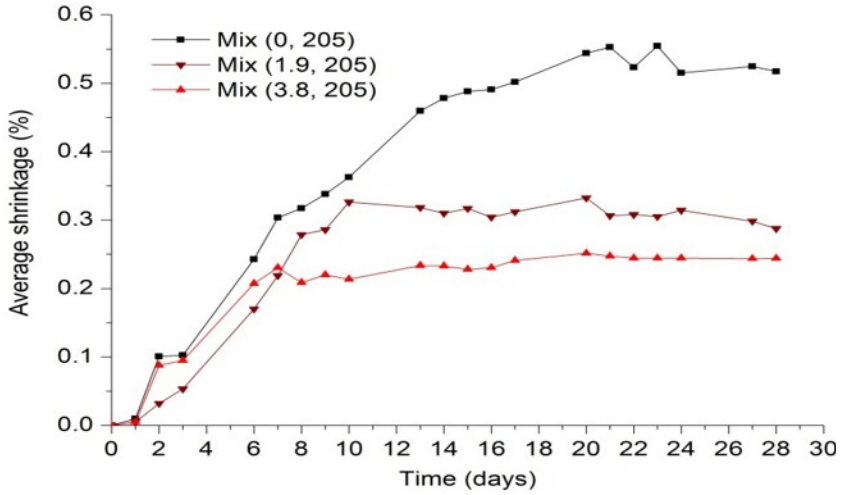


(a) Moist cured for 3 days

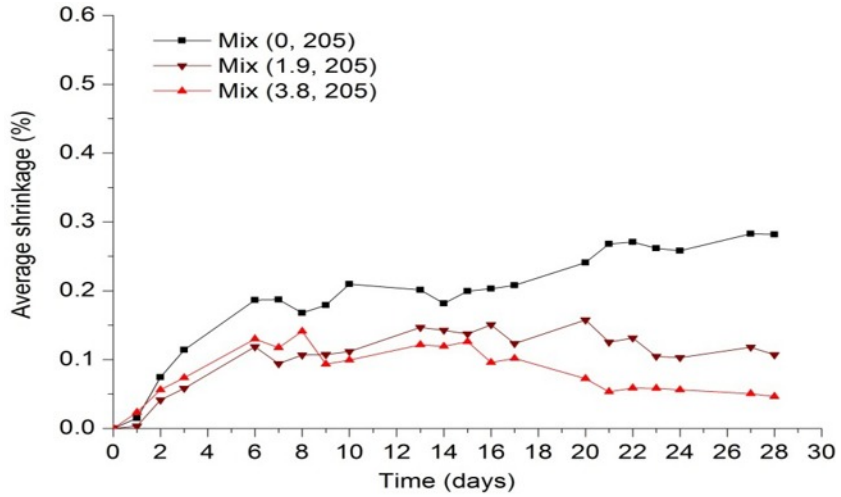


(b) Moist cured for 28 days

**Figure 8.5** Average shrinkage of three clay-cement mixtures

In Figure 8.5 it can be observed that adding Rc in clay-cement significantly reduces the shrinkage and the higher the Rc content, the less shrinkage is measured, regardless of the curing condition. For instance, for specimens moist cured for 3 days, the total shrinkage at 28 days of the mixture with Rc 3.8 kg/m$^3$ was 0.25% which is two times less than that of the mixture without Rc, i.e. 0.5%. As the number of moist curing days increased to 28 days, it can be observed that the total shrinkage of the two mixtures with Rc started to slightly decrease after 20 days. Besides, the sand-cement mixtures initially showed expansion and started to shrink after a curing period of 2 days (in Figure 8.3). In contrast, the clay-cement materials exhibited shrinkage immediately after compaction.

Table 8.1 summarizes the average total shrinkage at 28 days, based on three mixtures with different Rc contents, i.e. 0, 1.9 and 3.8 kg/m$^3$.

**Table 8.1** Average total shrinkage (%) of three mixtures at 28 days

| Materials | Moist cured for 3 days | | | Moist cured for 28 days | | |
|---|---|---|---|---|---|---|
| | (0, 205) | (1.9, 205) | (3.8, 205) | (0, 205) | (1.9, 205) | (3.8, 205) |
| Clay-cement | 0.52 | 0.29 | 0.24 | 0.28 | 0.11 | 0.046 |
| Sand-cement | 0.03 | 0.01 | 0.02 | 0.01 | 0.00 | 0.01 |

From Table 8.1 it can be seen that increasing Rc content reduces the total shrinkage of clay-cement materials while addition of a moderate Rc content achieves the minimal shrinkage for sand-cement material. Additionally, it is clear that the shrinkage of clay-cement is much higher than that of the sand-cement materials, which is in agreement with the literatures. Although clay-cement develops more shrinkage, it is found that the cracks observed in clay-cement base courses are typically finer and more closely spaced while cracks in a cement stabilized granular bases are wider and longer spaced (George, 2002).

### 8.1.3 Modelling of the shrinkage

Tensile stress induced from the drying shrinkage is critical for the cracking behaviour. Mathematical models are employed herein to estimate the shrinkage deformation as a function of the time. The correlation between shrinkage and time can be used to estimate the transverse cracking behaviour of the road base. In the initial curing period of 7 days the shrinkage of the cement stabilized materials is rapid and subsequently the rate of shrinkage tends to decrease, therefore the following exponential function is chosen, shown as equation 8-2.

$$S(t) = a \cdot e^{-b \cdot t} + c \quad (8\text{-}2)$$

Where, S(t) is the shrinkage as a function of time, %;

t is the time as shrinkage starts, day;

a, b and c are the experimentally determined coefficients.

As an example, by using the above model the estimated shrinkage curves are compared with the measured data of the shrinkage test, shown in Figure 8.6, based on the mixture (0, 205).

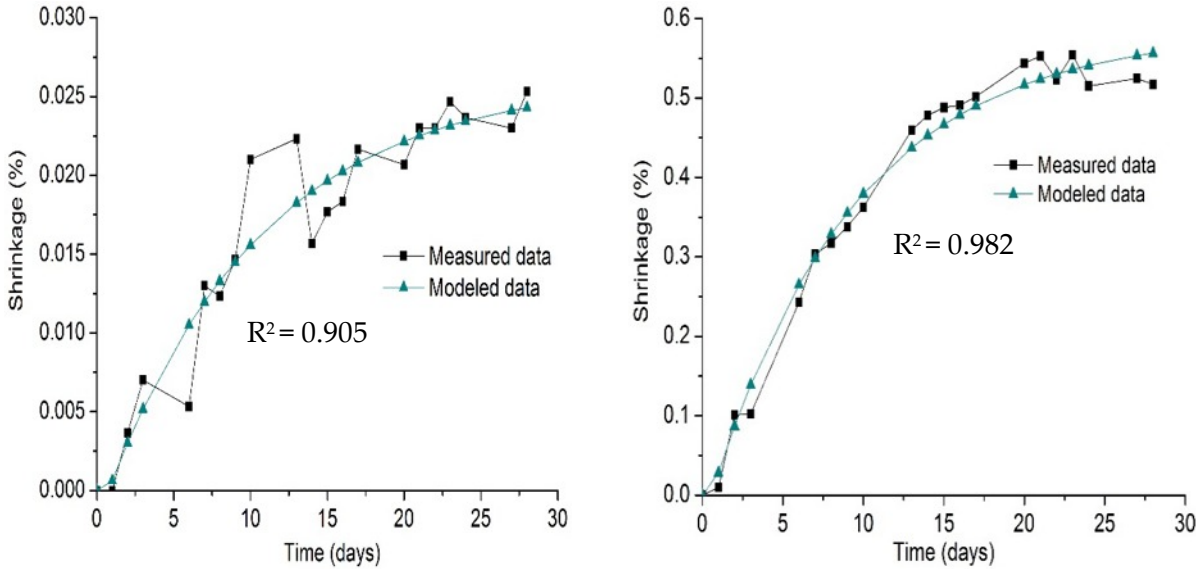


(a) Sand –cement (b) Clay-cement

**Figure 8.6** Example of modelled shrinkage curves on mixture (0, 205)

As can be seen in Figure 8.6, the shrinkage model shows a good fit with the measured data and thus is employed to be used for the other mixtures. Table 8.2 lists the coefficients a, b and c of the shrinkage model for the various cement stabilized sand and clay materials in two curing conditions.

**Table 8.2** Coefficients for the shrinkage models

| Materials | Mix design, kg/m³ | | Curing regime | $S(t) = a \cdot e^{-b \cdot t} + c$ | | | |
|---|---|---|---|---|---|---|---|
| | Rc | Cement | | a | b | c | $R^2$ |
| Sand-cement | 0 | 205 | CR 1 | -0.0281 | 0.0982 | 0.0261 | 0.905 |
| | 1.9 | 205 | CR 1 | -0.0429 | 0.4971 | 0.0137 | 0.697 |
| | 3.8 | 205 | CR 1 | -0.0849 | 0.7475 | 0.0151 | 0.745 |
| Sand-cement | 0 | 205 | CR 2 | -0.0177 | 1.1580 | 0.0056 | 0.591 |
| | 1.9 | 205 | CR 2 | -0.0545 | 0.6603 | 0.0090 | 0.913 |
| | 3.8 | 205 | CR 2 | -0.02101 | 0.5031 | -0.00124 | 0.867 |
| Clay-cement | 0 | 205 | CR 1 | -0.6212 | 0.1109 | 0.5843 | 0.982 |
| | 1.9 | 205 | CR 1 | -0.376 | 0.1908 | 0.3242 | 0.933 |
| | 3.8 | 205 | CR 1 | -0.2529 | 0.2488 | 0.2448 | 0.975 |
| Clay-cement | 0 | 205 | CR 2 | -0.2589 | 0.1217 | 0.2704 | 0.923 |
| | 1.9 | 205 | CR 2 | -0.1423 | 0.2573 | 0.1289 | 0.864 |
| | 3.8 | 205 | CR 2 | -0.09811 | 0.629 | 0.090 | 0.399 |

Note: CR 1 refers to initial moist curing for 3 days; CR 2 refers to moist curing for 28 days; Shrinkage strain $\varepsilon_S(t)$ is $S(t)/100$.

## 8.2. Coefficient of thermal expansion

Decrease or increase of temperature may cause a material to contract or to expand. Coefficient of Thermal Expansion (CTE) is a measure of the deformation change of materials caused by the temperature variation. The CTE of conventional concrete ranges from about 8 to $12\times10^{-6}/^{o}C$ (FHWA, 2011; Jahangirnejad et al, 2009) which is mainly influenced by the aggregate type. This section evaluates the influence of Rc additive content on the CTE of cement stabilized materials.

### 8.2.1 Materials and test method

Three mixtures with different amounts of Rc additive were evaluated, i.e. (0, 205), (1.9, 205) and (3.8, 205). For this test, beam specimens of cement stabilized sand materials with size of 500×100×100 mm were prepared. The specimen preparation method followed the same procedure as described in Chapter 3. The age of the tested specimens was 180 days. For clay-cement materials, it was difficult to obtain sufficient compaction for the heavy clay specimens with such large size (500×100×100 mm), so the CTE of clay-cement was not determined in this study.

The coefficient of thermal expansion (CTE) of cement stabilized sand was determined by measuring the change of the length of the specimen over the temperature range

from -20 to 20°C. The specimen was cured in the cooling chamber at -20°C for 12 hours and then placed in another environmental chamber with temperature 20°C. Three linear variable differential transformer (LVDT) were installed on the top surface of the specimen. Subsequently, the change of the length of the specimen with time was recorded. Figure 8.7 shows the measurement of the deformation change in the chamber at 20°C. The CTE, expressed as $\alpha$ , is calculated by the following equation:

$$\alpha = \frac{\Delta L}{L_0 \cdot \Delta T} \tag{8-3}$$

Where, $\Delta L$ = length change of specimen, mm;

$L_0$ = initial length of specimen, mm;

$\Delta T$ = temperature change, °C.


**Figure 8.7** Measurement of the deformation change in the environmental chamber

### 8.2.2 Analysis of the results

Figure 8.8 shows the deformation change of the specimen exposed to temperature 20°C after cured at -20°C for 12 hours. The test results are based on cement stabilized sand mixtures with different amounts of Rc additive. For each mixture, two replicate specimens were tested.

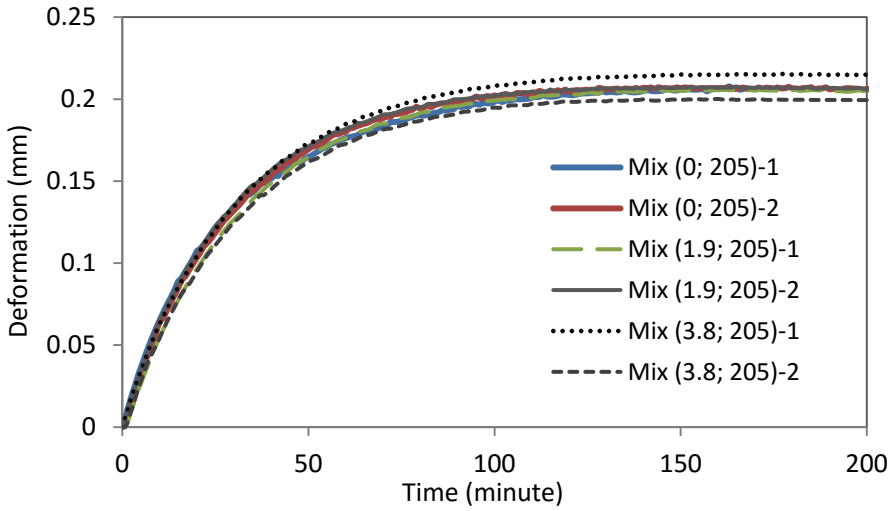


**Figure 8.8** Deformation change of the sand-cement specimens

In Figure 8.8 it can be seen that when exposed to the increased temperature in the chamber, the specimen showed rapid expansion. After about 3 hours, the temperature of the specimen remained stable and no further change of the length occurred. Besides, these three mixtures seemed to yield nearly the same deformation curves as a function of time. This means the Rc additive has no clear influence on the thermal expansion of cement stabilized sand materials, based on the cement content 205 kg/m$^3$. The average CTE of cement stabilized sand is thus calculated as $10\times10^{-6}$/$^o$C, which is in the range of the values for conventional concrete.

## 8.3. Estimation of transverse crack pattern

When a cement stabilized base layer shrinks, due to the friction with the surrounding layers, internal tensile stress will develop in the base layer. When the induced tensile stress exceeds the tensile strength of the base materials, a transverse crack will occur in the base layer, which can be described by:

$$\sigma(t) > f_t(t) \tag{8-4}$$

Where, σ(t) is the induced tensile stress due to restraint deformation at time t in hours; $f_t(t)$ is the direct tensile strength of the cement stabilized base material at time t in hours.

The following section illustrates the calculation of the development of the occurring tensile stress which results from the seasonal and daily temperature change as well as the drying shrinkage, without considering the external traffic loads.

### 8.3.1 Tensile stress development in the stabilized base layer

8.3.1.1 Deformation due to the temperature variation (thermal deformation)

Based on the climate data in the Netherlands, the following seasonal variation of the temperature of the road base layer is used for the calculations:

a) The daily temperature is on average 14°C and it occurs on May 1 and November 1;
b) The amplitude of the seasonal temperature variation is 8°C;
c) Thus the average daily temperature is minimum 6°C (on February 1) and the maximum daily temperature is 22°C (on August 1).

Thus, the average daily temperature $T_1$ at the day of construction of the base layer is:

$$T_1 = 14 + 8 \cdot \sin(t_1) \tag{8-5}$$

Where, $t_1$ = day of construction (number of days after May 1).

Besides, the variation of the daily temperature of the road base layer is also taken into account:

a) The daily temperature is average at 10:00 am and 10:00 pm. The maximum temperature occurs at 4:00 pm and minimum is at 4:00 am;
b) The amplitude of the daily temperature variation is 4°C.

Thus, the actual temperature $T_2$ at the hour of construction of the base layer is calculated by:

$$T_2 = T_1 + 4 \cdot (a + \sin(15 \cdot (t_2 - 10))) \tag{8-6}$$

Where, $t_2$ = clock hour of the construction on the construction day, from 0 to 24 hours;

a=1, when $t_2$ = 4 am; a= -1, when $t_2$ =4 pm; a=0, when $t_2$ =10 am and 10 pm.

So the climate dependent temperature $T_3$ of the base layer is the summation of the daily temperature at construction and the seasonal and daily temperature variation:

$$T_3 = T_2 + 8 \cdot \sin\left[\left(\frac{t}{24}\right) + t_1\right] - 8 \cdot \sin(t_1) + 4 \cdot (a + \sin(15 \cdot (t - 10 + t_2))) \tag{8-7}$$

Where, $t$ = time (number of hours) after construction.

In addition to the climate influence, the hydration heat that occurs after construction is also taken into account, which results in temporal temperature increase. This hydration temperature $T_4$ is calculated by the following equation (Houben, 2010):

$$T_4 = c_1 \cdot f_1 \cdot f_2 \tag{8-8}$$

Where, $f_1 = t^{c2}$; c2= 2; $f_2 = e^{-c3 \cdot t}$, c3 = 0.27; $c_1$ = 0.55.

Therefore, the actual temperature $T_5$ of the road base layer is the sum of the climate temperature and the hydration temperature:

$$T_5 = T_3 + T_4 \tag{8-9}$$

Hence the thermal deformation $\varepsilon_T(t)$ is equal to:

$$\varepsilon_T(t) = -\alpha \cdot \Delta T \tag{8-10}$$

Where, $\Delta T$, difference in temperature between time t and time of construction of road base layer, $^oC$.

The coefficient of thermal expansion $\alpha$ is taken dependent on the modulus of elasticity $E(t)$ according to the following equation (Houben, 2010):

$$\alpha = b \cdot E(t) \tag{8-11}$$

Where, coefficient b is obtained based on the measured CTE at 180 days. With this equation, the value of b for sand-cement mixture with Rc 0, 1.9 and 3.8 kg/m$^3$ is $4.94\times10^{-10}$, $4.43\times10^{-10}$ and $3.97\times10^{-10}$, respectively.

8.3.1.2 Deformation from drying shrinkage

The shrinkage deformation of cement stabilized sand and clay materials at two different curing conditions has been given in Figure 8.3 and 8.5. The time-dependent shrinkage deformation is estimated by using the mathematical model 8-2 for the evaluated mixtures. Thus these obtained estimation models for shrinkage, listed in Table 8.2, are used in the following calculations of the deformation $\varepsilon_S(t)$ due to the drying shrinkage.

8.3.1.3 Total deformation

The total deformation $\varepsilon(t)$ of the road base layer is equal to the sum of the drying shrinkage and the thermal shrinkage:

$$\varepsilon(t) = \varepsilon_T(t) + \varepsilon_S(t) \tag{8-12}$$

Where, $\varepsilon_T(t)$ = deformation from the temperature change,
$\varepsilon_S(t)$ = deformation from the drying shrinkage.

8.3.1.4 Tensile stress development in the road base layer

The stress $\sigma(t)$, occurring in the road base layer due to the strain $\varepsilon(t)$, follows from Hooke's law. Due to the fact that the stabilized base layer is subjected to the restrained shrinkage for a long period and it is only partly elastic, relaxation of the induced stress as a function of time is also taken into account, leading to the following equation (8-13).

$$\sigma(t) = R(t) \cdot E(t) \cdot \varepsilon(t) \tag{8-13}$$

Where, $R(t)$= stress relaxation at time t;

$E(t)$ = elastic modulus of the stabilized base at time t;

$\varepsilon(t)$ = total deformation of stabilized base at time t;

t = time in hours after construction.

There is a lack of research documenting the stress relaxation of cement stabilized materials and thus herein it is proposed by the following equation, referring to the literature (Xuan, 2012):

$$R(t) = m \cdot t^{-n} \tag{8-14}$$

Where, m and n are dependent on the material.

Based on the above model, three types of relaxation parameters are chosen, referred to as higher, medium and lower stress relaxation with $m$-values of 2.59, 2.22 and 1.89 and $n$-values of 0.30, 0.25 and 0.20, respectively, indicated in Figure 8.9. These stress relaxation models were proposed for cement stabilized crushed concrete and masonry.

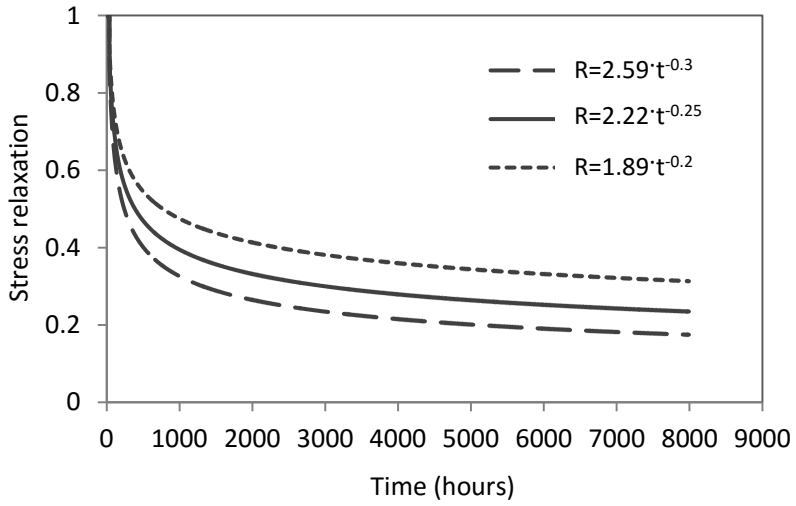


**Figure 8.9** Proposed stress relaxation of cement stabilized materials (Xuan, 2012)

### 8.3.2 Tensile strength of materials

To compare with the occurring tensile stress, the direct tensile strength of the materials is needed. In this study, the direct tensile strength $f_t$ is considered as 80% of the indirect tensile strength $ITS$, according to the standard NEN-EN 14227-1:

$$f_t = 0.8 \cdot ITS \tag{8-15}$$

The indirect tensile strength $ITS$ of cement stabilized sand and clay materials as a function of curing time can be obtained according to the estimation models, i.e. equations 4-13 and 5-18 in Chapter 4 and 5.

The modulus of elasticity used in the following calculations is derived based on the literature (Thompson, 1998), shown as below:

For cement stabilized sand material:

$$E = 1200 \cdot UCS \tag{8-16}$$

For cement stabilized clay material:

$$E = 440 \cdot UCS + 40.6 \cdot (UCS)^2 \tag{8-17}$$

Where, $E$ = the modulus of elasticity, MPa; $UCS$ = compressive strength, based on the estimation models (equations 4-6 and 5-11), MPa.

### 8.3.3 Calculation of transverse crack pattern

In this section, the crack pattern characteristics of the cement stabilized materials, including the occurrence time of cracking, the width of the cracks and the spacing of the cracks, will be determined by using the mechanical estimation model developed by Houben (2010). The starting point is that at the moment that the occurring tensile stress in the road base layer exceeds the tensile strength for the first time, a transverse crack will appear, referred to as the primary crack. The width of the primary crack $w_1$ and the spacing between the primary cracks $L_1$ are calculated by the following equations:

$$w_1 = 1000000 \cdot E(t) \cdot \varepsilon(t)^2/(\gamma \cdot \rho) \tag{8-18}$$

$$L_1 = 1000 \cdot 2 \cdot E(t) \cdot \varepsilon(t)/(\gamma \cdot \rho) \tag{8-19}$$

Where, $E(t)$ = the elastic modulus of base layer at moment of primary cracks, MPa;

$\varepsilon(t)$ = the maximum total shrinkage deformation (tensile strain) of the base layer at the moment of the primary cracks;

$\gamma$ = the volume weight of the base layer, kN/m$^3$;

$\rho$ = the coefficient of friction between the base and the surrounding layers.

Because of the initial cracks, a reduction $\Delta\sigma_1$ of the maximum tensile stress occurs that is equal to:

$$\Delta\sigma_1 = 0.5 \cdot \sigma(t) \tag{8-20}$$

Where, $t$ = time of occurrence of primary cracks;

$\sigma(t)$ = the maximum tensile stress in the road base layer at the time of occurrence of the primary cracks.

After the occurrence of the primary cracks the maximum tensile stress $\sigma_1(t)$ keeps on developing according to:

$$\sigma_1(t) = \sigma(t) - \Delta\sigma_1 \quad (8\text{-}21)$$

Where, $\sigma(t)$ = maximum tensile stress without occurrence of the primary cracks, MPa;
$\Delta\sigma_1$ = reduction of the maximum tensile stress at the time of occurrence of the primary cracks.

Accordingly, the maximum tensile strain $\varepsilon_1(t)$ in the base layer is:

$$\varepsilon_1(t) = \sigma_1(t)/E(t) \quad (8\text{-}22)$$

Where, $\sigma_1(t)$ = maximum tensile stress in the layer, MPa;
$E(t)$ = modulus of elasticity of the road base, MPa.

Therefore, the change of the width of the primary cracks is equal to:

$$\Delta w_1(t) = 1000000 \cdot E(t) \cdot \varepsilon_1(t)^2/(\rho \cdot \gamma) \quad (8\text{-}23)$$

The development of the width $w_1(t)$ of the primary cracks after the occurrence of the primary cracks follows:

$$w_1(t) = w_1 + \Delta w_1(t) \quad (8\text{-}24)$$

After the occurrence of the primary cracks, due to the increased shrinkage deformation and temperature change, the tensile stress $\sigma_1(t)$ keeps on developing and may exceed the tensile strength again, thus new series of cracks may occur, resulting in secondary or subsequently tertiary cracks. The width of cracks and spacing between cracks can be calculated by the same mechanical methods as described above. This cracking process will be completed until the occurring tensile stress doesn't exceed anymore the tensile strength. For the detailed description of this cracking process and the calculation of the series of cracks, reference is made to the literature by Houben (2008).

By using the above mechanical method, the crack pattern of cement stabilized sand and clay materials was calculated. For sand-cement material, Figure 8.10 and 8.11 present an example of the calculated results for two sand-cement mixtures with and without Rc additive, including the development of the tensile stress and tensile strength, the spacing between the cracks and the development of the width of the cracks. The calculation is based on the construction time (May 1st at 10 am), medium stress relaxation model, curing condition (CR 1) and value of the coefficient of friction 3 after the first cracks. In the calculation of the crack pattern, hours is chosen as the unit of time because the first crack occurs shortly after construction. A period of 360 days (a year) after construction is taken into account.

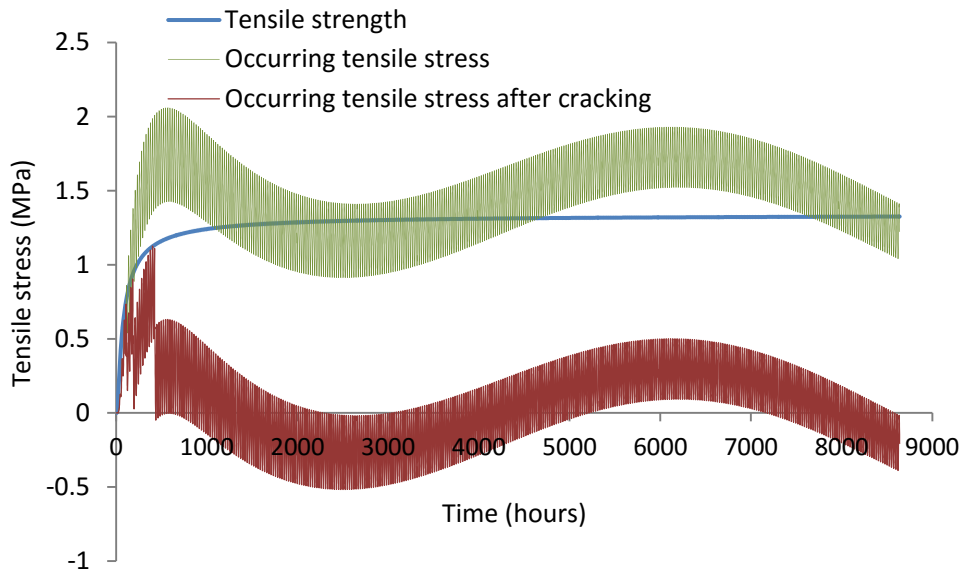


(a) Occurring tensile stress and tensile strength

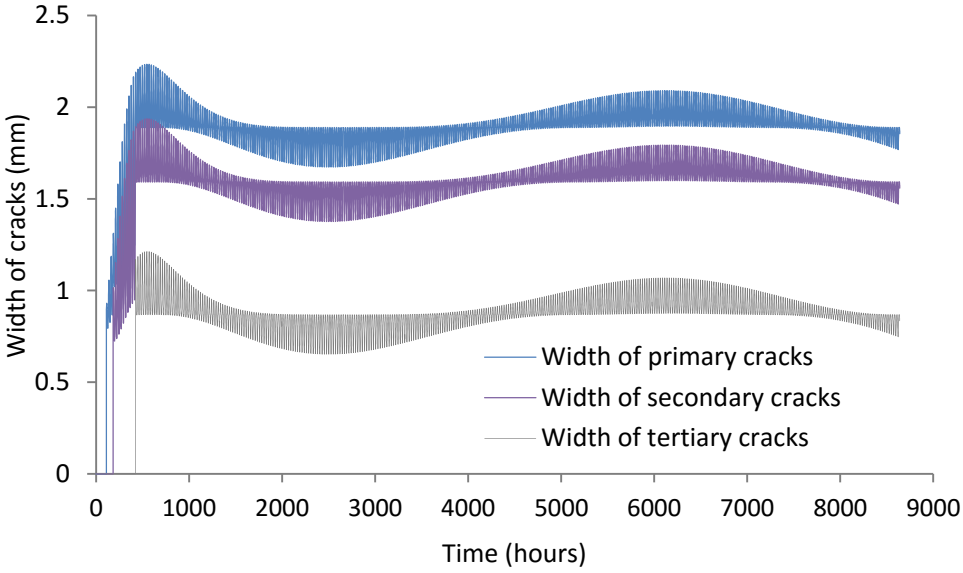


(b) Crack width

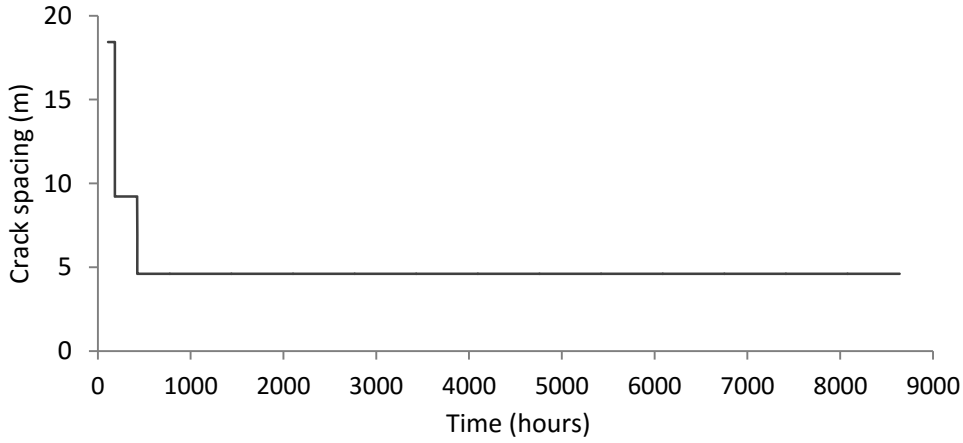


(c) Crack spacing

**Figure 8.10** Crack pattern of sand-cement mixture (0, 205) without Rc additive

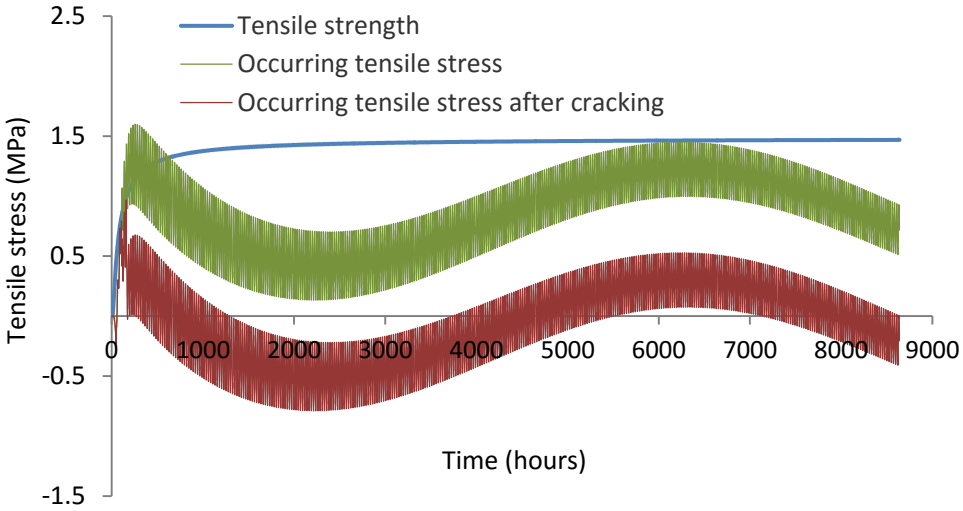


(a) Occurring tensile stress and tensile strength

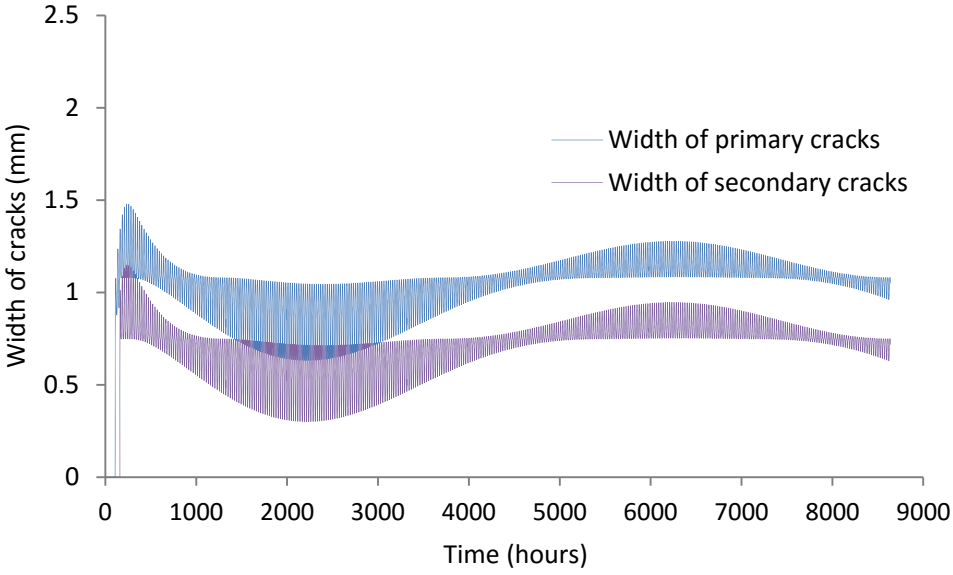


(b) Crack width

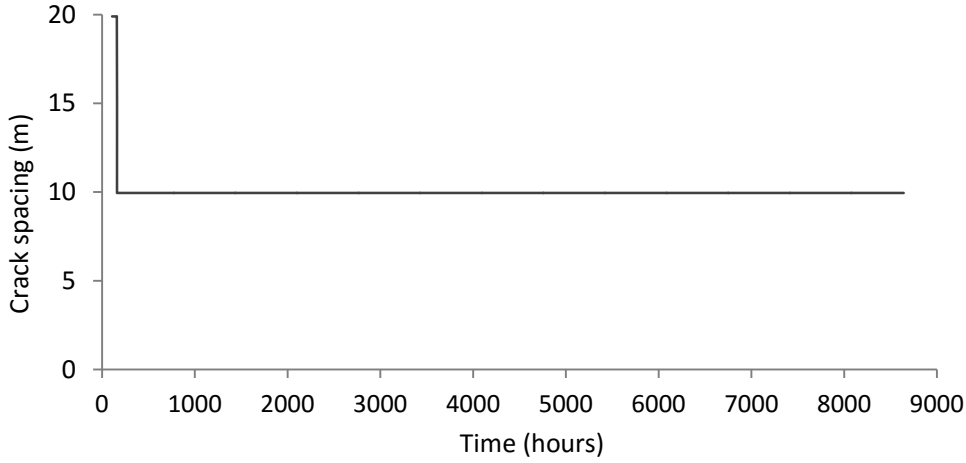


(c) Crack spacing

**Figure 8.11** Crack pattern of sand-cement mixture (1.9, 205) with Rc additive 1.9 kg/m$^3$

In Figure 8.10 and 8.11 the curves of occurring maximum tensile stresses (see green curves) are induced by the drying shrinkage of the materials and temperature change. After construction, the occurring tensile stress initially builds up rapidly due to the increased shrinkage of the materials. As the tensile stress exceeds the tensile strength, the primary cracks occur. After each series of cracks the occurring maximum tensile stress is reduced, see red curves. The variation of the daily and seasonal temperature causes the wave of the occurring tensile stress curve. The occurring maximum tensile stress exhibits a minimum value in summer and achieves maximum value shortly after construction and in winter. The first maximum tensile stress occurs due to the rapid development of shrinkage at early age which is hardly compensated by the slowly increasing seasonal temperature. The second maximum tensile stress is due to the low temperatures in winter. At longer term the general trend of the tensile stress curve tends to slightly decrease because of the influence of the stress relaxation of the materials.

For cement stabilized clay materials, the crack pattern was calculated, which showed that in all cases (three mixtures under two curing conditions), very severe cracking (final crack spacing << 0.5 m) is obtained, mainly due to the relatively large magnitude of drying shrinkage. Thus, calculation for the crack pattern of the clay-cement material is excluded from the following discussion.

The following section describes the transverse crack pattern of cement stabilized sand materials considering the influential factors of Rc additive contents, curing regimes, stress relaxation, construction date, the hour of construction on a day, the coefficient of friction between the base and the surrounding layers, and the amplitude of the daily temperature variation.

#### 8.3.3.1 Influence of Rc additive on the crack pattern of cement stabilized sand

Three sand-cement mixtures with different amounts of Rc additive, i.e. (0, 205), (1.9, 205) and (3.8, 205) were evaluated by comparing the transverse crack pattern. Table 8.3 lists the absolute values of the crack characteristics calculated for these three mixtures which were moist cured for 3 days.

The calculated results in Table 8.3 can be concluded as follows:

1) Use of Rc additive has a large influence on the transverse crack pattern. Without adding Rc additive, three series of cracks are predicted, resulting in the final crack spacing of 4.61 m, which is around 2 times smaller than for the mixtures with Rc additive.

2) The maximum crack width after one year is also reduced nearly by 50% by adding Rc additive in sand-cement mixtures.

3) The mixture with Rc content 3.8 kg/m$^3$ doesn't show more beneficial results. This mixture exhibits both, a somewhat smaller crack spacing and smaller crack width than the mixture with Rc content 1.9 kg/m$^3$, but the differences are not significant for practice.

**Table 8.3** Influence of Rc additive content on the crack pattern of sand-cement

| Items | | Rc additive content, kg/m$^3$ | | |
|---|---|---|---|---|
| | | 0 | 1.9 | 3.8 |
| Stress relaxation | | $R(t) = 2.22 \cdot t^{-0.25}$ | | |
| Construction time | | May 1 at 10 am | | |
| Curing regime | | Initial moist curing for 3 days | | |
| Primary cracks | Initial crack time, days | 4.6 | 4.5 | 3.5 |
| | Initial crack width, mm | 0.88 | 0.94 | 0.84 |
| | Crack spacing, m | 18.43 | 19.9 | 18.0 |
| Secondary cracks | Initial crack time, days | 7.7 | 6.7 | 4.6 |
| | Initial crack width, mm | 0.97 | 0.99 | 1.0 |
| | Crack spacing, m | 9.22 | 9.95 | 8.99 |
| Tertiary cracks | Initial crack time, days | 17.7 | No tertiary crack | No tertiary crack |
| | Initial crack width, mm | 1.16 | | |
| | Crack spacing, m | 4.61 | | |
| Final crack spacing (after one year) | | 4.61 | 9.95 | 8.99 |
| Maximum crack width (after one year) | | 1.85 | 1.04 | 0.98 |

As discussed in section 8.1, increasing the period of moist curing significantly reduces the total shrinkage deformation, and thus the occurring tensile stress might be reduced as well. Figure 8.12 illustrates the development of the occurring tensile stress and the tensile strength, based on the condition of moist curing for 28 days. Table 8.4 lists the calculated results for three mixtures with different Rc additive contents which are moist cured for 28 days.

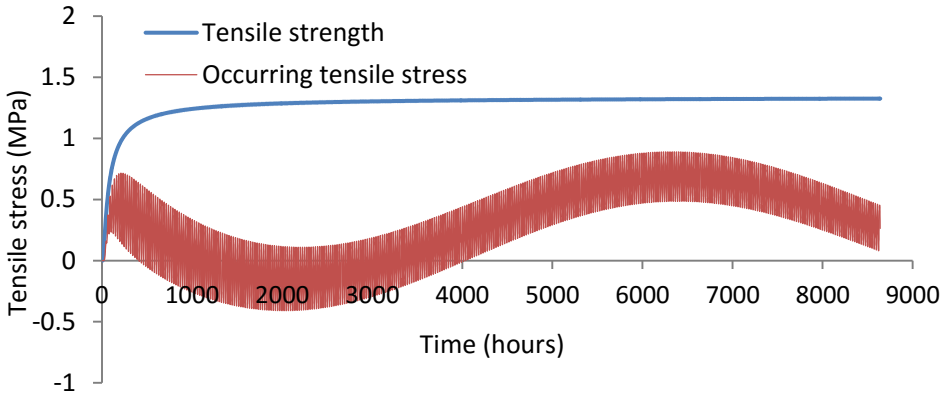


(a) Mixture (0, 205)

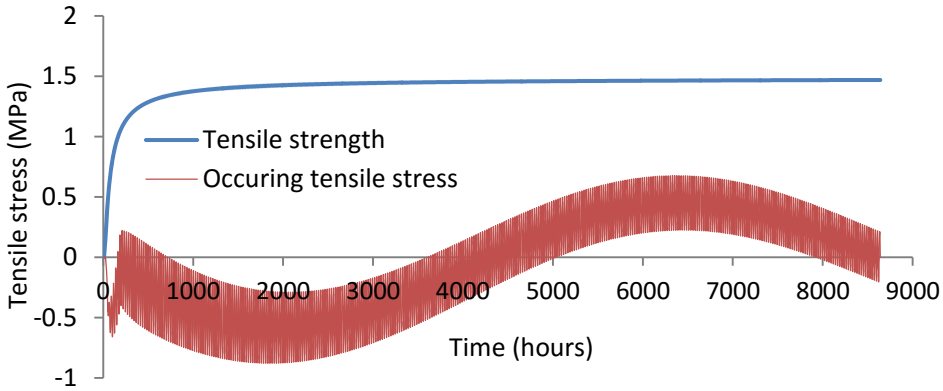


(b) Mixture (1.9, 205)

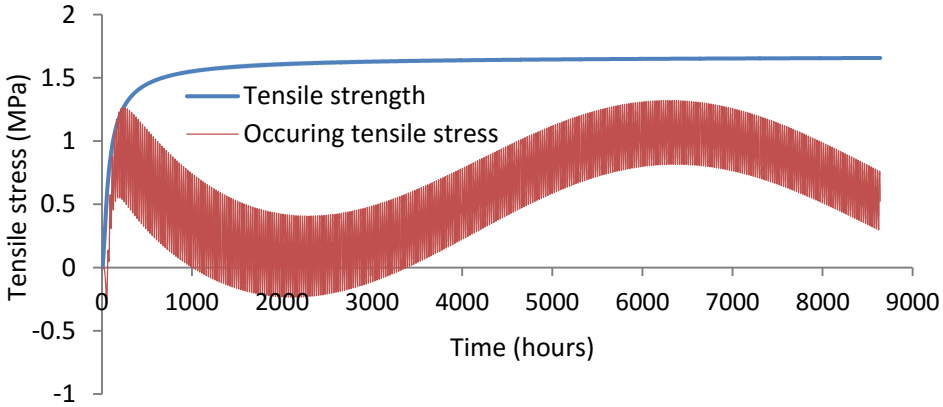


(c) Mixture (3.8, 205)

**Figure 8.12** Development of the occurring tensile stress and the tensile strength in sand-cement mixtures

As can be seen in Figure 8.12, the occurring tensile stresses of the mixtures without Rc and with Rc content 1.9 kg/m$^3$ are lower than the tensile strength through one year, so no cracks will occur. Besides, during the initial four days after construction, the mixture with Rc content 1.9 kg/m$^3$ experienced a small compressive stress due to the expansion of the material. Afterwards, the shrinkage strain of this mixture is almost 0, so the total occurring tensile stress mainly results from the temperature change. The

maximum tensile stress of this mixture that occurs in winter, is about 0.7 MPa, which is lower than the mixture without Rc additive (0.9 MPa) for the same curing period. Regarding the mixture with Rc 3.8 kg/m$^3$, primary cracks occur as the tensile stress exceeds the tensile strength around 6 days after construction. This means, in the case of a long period of moist curing, adding a high amount of Rc additive (i.e. 3.8 kg/m$^3$) doesn't give beneficial results for the transverse crack pattern.

**Table 8.4** Influence of Rc content on the crack pattern in sand-cement mixtures (28-day moist curing)

| Items | | Rc additive content, kg/m$^3$ | | |
|---|---|---|---|---|
| | | 0 | 1.9 | 3.8 |
| Stress relaxation | | $R(t) = 2.22 \cdot t^{-0.25}$ | | |
| Construction time | | May 1 at 10 am | | |
| Curing regime | | Moist curing for 28 days | | |
| Primary cracks | Initial crack time, days | – | – | 5.7 |
| | Initial crack width, mm | | | 1.26 |
| | Crack spacing, m | | | 25.8 |
| Final crack spacing (after one year) | | No cracks | No cracks | 25.8 |
| Maximum width of crack (after one year) | | | | 1.13 |

Comparing these two curing methods, it can be clearly noted that increasing the period of moist curing of the stabilized base can significantly reduce the occurring tensile stress and thereby the chance of cracking is greatly reduced.

In summary, the influence of Rc content on the crack pattern can be concluded as follows:

1) Adding a certain amount of Rc (1.9 kg/m$^3$) can reduce the amount of transverse cracks by 50% and reduce the crack width by 50%. However, increasing the Rc content by 2 times doesn't give more beneficial results regarding the transverse crack pattern.

2) The occurring tensile stress of the mixture with Rc 1.9 kg/m$^3$ is generally lower than that of the mixture without Rc additive regardless of the curing condition. That means adding a certain amount of Rc additive in sand-cement mixture may reduce the chance or rate of transverse cracking.

#### 8.3.3.2 Influence of stress relaxation on the crack pattern of cement stabilized sand

Stress relaxation is an unknown factor and it is postulated by equation 8-13, with three levels of lower, medium and higher relaxation, Figure 8.9. Table 8.5 lists the

calculated results of the crack pattern for three stress relaxation levels. Although the calculation is based on the assumption of the input parameters and might not be accurate for the realistic properties, analysis of the results intends to identify the sensitivity of this factor.

**Table 8.5** Influence of stress relaxation on the crack pattern in sand-cement mixture

| Items | | Stress relaxation | | |
|---|---|---|---|---|
| | | $R(t) = 1.89 \cdot t^{-0.20}$ | $R(t) = 2.22 \cdot t^{-0.25}$ | $R(t) = 2.59 \cdot t^{-0.30}$ |
| Mixture | | C=205 kg/m$^3$, Rc=1.9 kg/m$^3$ | | |
| Construction time | | May 1 at 10 am | | |
| Curing regime | | Initial moist curing for 3 days | | |
| Primary cracks | Initial crack time, days | 3.7 | 4.5 | 4.6 |
| | Initial crack width, mm | 0.67 | 0.94 | 1.08 |
| | Crack spacing, m | 15.6 | 19.9 | 21.4 |
| Secondary cracks | Initial crack time, days | 5.6 | 6.7 | No secondary crack |
| | Initial crack width, mm | 0.94 | 0.99 | |
| | Crack spacing, m | 7.8 | 9.95 | |
| Final crack spacing (after one year) | | 7.8 | 9.95 | 21.4 |
| Maximum crack width (after one year) | | 0.85 | 1.04 | 0.98 |

The results in Table 8.5 show that stress relaxation influences the crack pattern, due to the fact that it directly determines the development of the occurring tensile stress. When the stress relaxation is lower than the reference relaxation ($R(t) = 2.22 \cdot t^{-0.25}$), the occurrence time of the primary cracks is nearly one day earlier and the final crack spacing decreases from 9.95 m to 7.8 m, by 21%. In contrast, when the stress relaxation is higher, the primary cracks occur approximately at the same moment but the final crack spacing is more than two times larger because a high stress relaxation leads to a large release of the occurring tensile stress. In summary, the lower the stress relaxation, the earlier the primary cracks occur, the more cracks will appear and the smaller the final crack width. Provided that the crack spacing is at least 2 to 3 m, lower stress relaxation is the preferred situation, considering the load transfer, risk of reflective cracks, ingress of water, etc.

#### 8.3.3.3 Influence of construction time on crack pattern of cement stabilized sand

Construction time, including the different dates in the year and clock hour in the day, is taken into account in the analysis of the crack patterns.

Firstly, four different construction dates in one year are considered:

a) February 1, the lowest average daily temperature in the year;
b) May 1, average climate condition before summer;
c) August 1, the highest average daily temperature in the year;
d) November 1, the average climate condition before winter.

Table 8.6 presents the calculated results for these four different construction dates, calculated for the mixture with cement content 205 kg/m$^3$ and Rc 1.9 kg/m$^3$. To compare the influence of the construction date, the clock hour for construction remains the same, which is 10 am.

**Table 8.6** Influence of construction date on the crack pattern in sand-cement mixture

| Items | | Construction date | | | |
|---|---|---|---|---|---|
| | | Feb 1 10 am | May 1 10 am | Aug 1 10 am | Nov 1 10 am |
| Mixture | | C=205 kg/m$^3$, Rc=1.9 kg/m$^3$ | | | |
| Stress relaxation | | $R(t) = 2.22 \cdot t^{-0.25}$ | | | |
| Curing regime | | Initial moist curing for 3 days | | | |
| Primary cracks | Initial crack time, days | 3.8 | 4.5 | 3.8 | 3.7 |
| | Initial crack width, mm | 0.78 | 0.94 | 0.78 | 0.75 |
| | Crack spacing, m | 16.9 | 19.9 | 16.96 | 16.55 |
| Secondary cracks | Initial crack time, days | 5.7 | 6.7 | 5.7 | 5.67 |
| | Initial crack width, mm | 0.97 | 0.99 | 0.98 | 1.02 |
| | Crack spacing, m | 8.47 | 9.95 | 8.48 | 8.28 |
| Final crack spacing (after one year) | | 8.47 | 9.95 | 8.48 | 8.28 |
| Maximum crack width (after one year) | | 0.89 | 1.04 | 0.90 | 0.88 |

The construction dates on February 1, August 1 and November 1 lead to a very similar crack pattern, regarding the initial time of the cracks, the final crack spacing and crack width. However, if the construction is performed on May 1, the primary cracks occur nearly one day later and the final crack spacing is 1.5 m larger. This can be explained by the average daily temperature of May 1 which experiences an increasing trend (sine function), so that the thermal shrinkage will be less in the initial period after construction. The crack width is directly linked to the crack spacing: the larger the crack spacing, the wider the cracks but the differences are small. It can be concluded that the construction date has only a small effect on the final crack pattern.

Besides, one has to note that the development of the tensile strength (cured in the laboratory condition 20°C) of the material is adopted in this calculation, without considering the field conditions. For instance, if the construction is done in February, the cold winter temperature would delay the strength development. In contrast, also the occurring tensile stress develops slower due to the slower hydration process such as the development of the elastic modulus.

The thermal deformation is directly related to the actual temperature $T_2$ at the hour of construction, the construction hour can also influence the crack pattern. Table 8.7 gives the results of the crack pattern with respect to different construction hours, which is: 4 am (the lowest temperature), 10 am (the average temperature in one day), 4 pm (the highest temperature) and 10 pm (average temperature in one day), based on the construction date May 1.

**Table 8.7** Influence of construction hour on the crack pattern

| Items | | Construction hour | | | |
|---|---|---|---|---|---|
| | | May 1 4 am | May 1 10 am | May 1 4 pm | May 1 10 pm |
| Mixture | | C=205 kg/m³, Rc=1.9 kg/m³ | | | |
| Stress relaxation | | $R(t) = 2.22 \cdot t^{-0.25}$ | | | |
| Curing regime | | Initial moist curing for 3 days | | | |
| Primary cracks | Initial crack time, days | 5.0 | 4.5 | 3.4 | 4.1 |
| | Initial crack width, mm | 1.02 | 0.94 | 0.70 | 0.87 |
| | Crack spacing, m | 21.22 | 19.9 | 15.45 | 18.55 |
| Secondary cracks | Initial crack time, days | No secondary crack | 6.7 | 4.5 | 6.3 |
| | Initial crack width, mm | | 0.99 | 0.88 | 0.97 |
| | Crack spacing, m | | 9.95 | 7.73 | 9.28 |
| Tertiary cracks | Initial crack time, days | No tertiary crack | No tertiary crack | 8.5 | No tertiary crack |
| | Initial crack width, mm | | | 1.09 | |
| | Crack spacing, m | | | 3.86 | |
| Final crack spacing (after one year) | | 21.22 | 9.95 | 3.86 | 9.28 |
| Maximum crack width (after one year) | | 0.91 | 1.04 | 1.77 | 0.98 |

Table 8.7 shows that the construction hour has a very significant influence on the crack pattern. If the construction is performed on 4 am, only primary cracks occur and result in largest crack spacing and smallest crack width, which is the most preferable case. In contrast, when the construction is done at 4 pm (highest

temperature) in the afternoon, the most severe crack pattern occurs, leading to a reduced cracking spacing by 5 times and almost two times wider crack width. This phenomenon can be explained by the daily temperature variation. When the construction is done at 4 am which exhibits the lowest temperature, the base layer is subjected to thermal expansion due to the increased daily temperature. While in the case of the construction time at 4 pm, with highest temperature, the base layer is subjected to the thermal shrinkage shortly after construction due to the subsequent temperature decrease. However, the construction hours at 10 am and 10 pm result in a similar crack pattern due to the fact that at these two moments the average daily temperature occurs.

#### 8.3.3.4 Influence of the coefficient of friction on the crack pattern of sand-cement

When the stabilized base layer shrinks, friction forces occur between the base and the surrounding layers. Due to the equilibrium condition, the summation of the friction force is equal to the induced tensile stress of the base layer (George, 2002). Therefore, the coefficient of friction, expressed as ρ, determines the width of the cracks and the spacing of the cracks, see equations 8-18 and 8-19. Table 8.8 lists the calculated results of the crack pattern by varying the coefficient of friction. Three values of ρ were evaluated, i.e. 1.5, 3 and 6, representing lower, medium and higher friction levels, respectively.

**Table 8.8** Influence of the coefficient of friction on the crack pattern

| Items | | Coefficient of friction | | |
|---|---|---|---|---|
| | | 1.5 | 3 | 6 |
| Mixture | | C=205 kg/m$^3$, Rc=1.9 kg/m$^3$ | | |
| Stress relaxation | | $R(t) = 2.22 \cdot t^{-0.25}$ | | |
| Construction time | | May 1 at 10 am | | |
| Curing regime | | Initial moist curing for 3 days | | |
| Primary cracks | Initial crack time, days | 4.5 | 4.5 | 4.5 |
| | Initial crack width, mm | 1.88 | 0.94 | 0.47 |
| | Crack spacing, mm | 39.8 | 19.9 | 9.94 |
| Secondary cracks | Initial crack time, days | 6.7 | 6.7 | 6.7 |
| | Initial crack width, mm | 1.98 | 0.99 | 0.49 |
| | Crack spacing, m | 19.9 | 9.95 | 4.97 |
| Final crack spacing (after one year) | | 19.9 | 9.95 | 4.97 |
| Maximum crack width (after one year) | | 2.09 | 1.04 | 0.51 |

As can be seen in Table 8.8, friction between the base layer and the surrounding layers significantly influences the crack pattern which can be summarized as follows:

1) The higher the friction coefficient, the smaller the width of the cracks and the smaller the crack spacing.

2) The change of the crack width and crack spacing are linearly related to the change of the friction coefficient. However, the friction coefficient doesn't influence the initial time of the cracks as the friction only becomes active after the first cracks.

#### 8.3.3.5 Influence of the amplitude of daily temperature variation on the crack pattern of cement stabilized sand materials

In all the above calculations the amplitude of the daily temperature variation 4°C was adopted. That means if construction is done on May 1 (the average daily temperature is 14°C), the daily temperature of the base layer varies from 18°C to 10°C. If the amplitude increases to 8°C, the daily temperature will decrease to 6°C in the night. The large temperature drop might accelerate crack behavior. Herein the influence of the amplitude of daily temperature variation is taken into account. The calculated results based on four different amplitudes of the daily temperature variation are given in Table 8.9.

**Table 8.9** Influence of the amplitude of the daily temperature variation

| Items | | Amplitude of daily temperature variation, °C | | | |
|---|---|---|---|---|---|
| | | 2 | 4 | 6 | 8 |
| Mixture | | C=205 kg/m$^3$, Rc=1.9 kg/m$^3$ | | | |
| Stress relaxation | | $R(t) = 2.22 \cdot t^{-0.25}$ | | | |
| Construction time | | May 1 at 10 am | | | |
| Curing regime | | Initial moist curing for 3 days | | | |
| Primary cracks | Initial crack time, days | 4.6 | 4.5 | 3.7 | 3.6 |
| | Initial crack width, mm | 0.96 | 0.94 | 0.83 | 0.75 |
| | Crack spacing, mm | 20.16 | 19.9 | 17.37 | 16.34 |
| Secondary cracks | Initial crack time, days | No secondary cracks | 6.7 | 5.7 | 5.7 |
| | Initial crack width, mm | | 0.99 | 1.0 | 1.11 |
| | Crack spacing, m | | 9.95 | 8.68 | 8.17 |
| Final crack spacing (after one year) | | 20.16 | 9.95 | 8.68 | 8.17 |
| Maximum crack width (after one year) | | 1.07 | 1.04 | 0.94 | 0.85 |

The following conclusions can be drawn with respect to the influence of the amplitude of the daily temperature variation on the crack pattern:

1) The larger the amplitude of the daily temperature variation, the earlier primary cracks occur, the smaller the width of the cracks and the smaller the crack spacing. However, the variation of the crack width is very small.

2) In the case of the amplitude 2°C, only primary cracks occur because the small amplitude of the temperature variation leads to less temperature decrease and lower occurring tensile stress, so that the chance of subsequent cracks is reduced. However, as the amplitude increases from 4 to 8°C, the crack pattern seems quite similar.

## 8.4 Conclusions and recommendations

### 8.4.1 Conclusions

This Chapter evaluated the deformation behaviour of cement stabilized sand and clay base layers. The transverse crack pattern of the cement stabilized base was estimated.

**Shrinkage behaviour of cement stabilized sand and clay materials:**

The shrinkage of the cement stabilized sand and clay materials, cured in two different regimes, was measured and mathematical models were developed to estimate the shrinkage deformation as a function of time. Regarding the influence of the temperature variation, the coefficient of thermal expansion was measured for cement stabilized sand materials only. Three mixtures with the same cement content but different Rc additive contents were evaluated for these two behaviours. The principle findings are as follows:

(1) The shrinkage of sand-cement materials is influenced by the curing method and the Rc additive content. Adding the moderate amount of Rc additive can reduce the shrinkage when moist cured for 3 or 28 days. Longer periods of moist curing can substantially reduce the total shrinkage of cement stabilized sand materials.

(2) Adding Rc additive reduces the shrinkage of clay-cement materials and the higher the Rc content, the less shrinkage is observed, in both curing conditions. An increasing period of moist curing can also significantly reduce the total shrinkage of cement stabilized clay materials.

(3) The coefficient of thermal expansion was determined for cement stabilized sand materials (based on cement content 205 kg/m$^3$), which is $10\times10^{-6}/^{o}C$ at the age of 180 days, without influence of Rc additive content.

**Estimation of the transverse crack pattern:**

The transverse crack pattern of cement stabilized sand base layers was estimated by analyzing the development of the occurring tensile stress due to shrinkage and temperature variation, and the development of the tensile strength of the base materials. The crack pattern consisting of the time of occurrence of the cracks, the width and spacing of the cracks was calculated by a mechanical method. The principle conclusions are summarized as below:

(1) Adding Rc additive has a positive influence on the crack pattern of cement stabilized sand materials. Adding a certain amount of Rc additive reduces the width of the cracks and reduces the number of cracks approximately by 50%.

(2) Stress relaxation plays an important role in the crack pattern. The lower the stress relaxation, the earlier the primary cracks occur, the more cracks will appear and the smaller the final crack width.

(3) The construction date of the stabilized base has a minor influence on the crack pattern, showing similar crack width and spacing along with the initial time of occurrence.

In contrast, the construction hour has a significant impact on the crack pattern. Construction at 4 am with lowest daily temperature leads to the largest crack spacing and smallest crack width. In contrast, construction at 4 pm with highest daily temperature results in the most severe crack pattern, earliest time of cracks, smallest crack spacing and largest crack width.

(4) The coefficient of friction between the base layer and the surrounding layers influences the crack pattern. The higher the friction coefficient, the smaller the crack spacing and the smaller the width of the cracks. The change of the crack width and crack spacing are linearly related to the change of the friction coefficient.

(5) The amplitude of the daily temperature variation also influences the crack pattern. The larger the amplitude of the daily temperature variation, the earlier the primary cracks occur, the smaller the width of the cracks and the smaller the crack spacing.

(6) In the cement stabilized base, large crack width should be prevented. Provided that the crack spacing becomes not smaller than 2 to 3 m, a higher friction between

base and surrounding layers, adding a certain amount of Rc additive, a lower stress relaxation and construction during the colder periods of the day contribute to reduced crack width. Although more cracks will occur in some cases, the narrow cracks are usually tight enough that moisture intrusion into the base and/or subgrade layers is minimal (Gregory & Halsted, 2010).

Regarding the crack pattern of cement stabilized clay materials, based on this mechanical model the calculated results showed that in all cases (three mixtures under two curing conditions) very severe cracking is obtained (final crack spacing << 0.5 m), which is mainly due to the large drying shrinkage of the investigated clay.

### 8.4.2 Recommendations

The analysis of the crack patterns is based on a few assumed factors and very limited mixtures were evaluated. Therefore, in order to obtain a more precise prediction of the crack pattern of cement stabilized materials, further research is recommended to be done into the following aspects:

(1) Shrinkage measurements were conducted on only three mixtures of cement stabilized sand and clay materials with different amounts of Rc additive. Thus it is advised to measure the shrinkage properties on numerous mix compositions so that estimation models can be developed to predict the shrinkage behavior based on the amounts of cement and Rc additive.

(2) In the calculation of the crack patterns, the stress relaxation and the coefficient of friction are assumed values but they showed a large influence. Therefore, further research to determine the stress relaxation of cement stabilized materials with and without use of Rc additive and the coefficient of friction between base and surrounding layers is recommended.

(3) The influence of the cement content is not included in the analysis of the crack pattern. Since the cement content is a very influential factor, it is strongly recommended to evaluate the influence of the cement content on the crack pattern to obtain the optimum mixture design to prevent (as much as possible) transverse cracks.

(4) The estimated crack patterns are obtained based on a mechanistic method and the input parameters (e.g. tensile strength and modulus of elasticity) were obtained under laboratory conditions. However, Rc additive might have larger effect in the field condition. Thus, it is necessary to verify these obtained crack patterns on real road projects.

## References

Adaska, W.S. & D.R. Luhr. (2004). Control of reflective cracking in cement stabilized pavements, RILEM Publications.

Bofinger, H.E., H.O. Hassan & R.I.T. Williams (1978). The shrinkage of fine-grained soil-cement. TRRL supplementary report 398.

Chakrabarti, S., & Kodikara, J. (2003). Basaltic crushed rock stabilized with cementitious additives: compressive strength and stiffness, drying shrinkage, and capillary flow characteristics. Transportation Research Record: Journal of the Transportation Research Board, 1819(1), 18-26.

FHWA (2011). Coefficient of Thermal Expansion in Concrete Pavement Design ACPT Tech Brief-FHWA-HIF-09-015, U.S. Department of Transportation, Federal Highway Administration.

Houben, L.J.M. (2010). Model for transversal cracking in non-jointed plain concrete pavements as a function of the temperature variations and the time of construction. 7th International workshop on design and performance of sustainable and durable concrete pavements, Carmona, Spain.

George, K.P. (1968). Shrinkage characteristics of soil-cement. Research Record 255. Washington DC (Highway Research Board), pp.42-57.

George, K.P. (2002). Minimizing cracking in cement-treated materials for improved performance. No. R&D Bulletin RD123.

Gregory E. & Halsted, P.E. (2010). Minimizing Reflective Cracking in Cement Stabilized Pavement Bases. Annual Conference of the Transportation Association of Canada, Halifax, Nova Scotia.

Jahangirnejad, S., Buch, N., & Kravchenko, A. (2009). Evaluation of Coefficient of Thermal Expansion Test Protocol and Its Impact on Jointed Concrete Pavement Performance, ACI Materials Journal, pp. 64-71.

Nakayama, H., & Handy, R.L. (1965). Factors Influencing Shrinkage of Soil-Cement, Highway Research Record 86, Washington, D.C.

Thompson, M.R. (1998). Stabilized Base Properties (strength, modulus, fatigue) for mechanistic-based airport pavement design. University of Illinois at Urbana-Champaign, Illinois, USA.

Xuan, D.X. (2012). Cement Treated Recycled Crushed Concrete and Masonry Aggregates for Pavements. PhD dissertation, Delft University of Technology, Delft, the Netherlands.

# CHAPTER 9

# CONCLUSIONS AND RECOMMENDATIONS

The main objective of this research is to evaluate the effect of Rc additive on the properties of cement stabilized materials. An extensive research program consisting of laboratory tests and a field evaluation was conducted on cement stabilized soils with and without use of Rc additive. Different soil types were investigated. The main conclusions of this dissertation are summarized in this final Chapter and some recommendations are also given with respect to future research.

## 9.1 Conclusions

The test program in this study included testing the mechanical properties, a microstructure analysis, a field evaluation and analysis of the crack pattern. The main conclusions regarding each aspect are summarized and categorized as follows:

(1) Mechanical properties of cement stabilized materials

Laboratory tests including compression, indirect tensile, flexural tensile and fatigue tests were carried out to investigate the effect of Rc additive on the mechanical properties of cement stabilized materials. Two types of soil, sand (non-cohesive soil) and clay (cohesive soil), were stabilized by adding different cement and Rc additive contents (based on the dry mass of soil). Different curing times were also considered for each mixture. Based on the test results, the effect of variable factors was analyzed and estimation models for the mechanical strength were obtained. Additionally, four-point bending tests were performed to obtain the stiffness modulus and fatigue properties of all the mixtures.

The principle findings are summarized as below:

a) Mechanical properties of cement stabilized sand

- Cement and Rc additive both contribute to the mechanical strength of cement stabilized sand materials. Addition of Rc additive yields higher compressive and tensile strength. A higher Rc content generally leads to higher strength of cement stabilized sand. The strength improvement of using Rc is generally in a range of 10% to 30%.
- The mechanical strength of cement stabilized sand is also closely related to the curing time. The strength increases substantially from 3 to 7 days, and then steadily increases until 28 days, but after 28 days the strength remains almost constant. This is observed in most of these mixtures, and is applicable to compressive, indirect tensile and flexural tensile strength.
- Estimation models to predict the mechanical strength of cement stabilized sand materials are developed, based on the combined effect of cement and Rc contents, density of the specimen and the curing time. The effect of the Rc content on the mechanical properties is described by means of an exponential function.
- The stiffness modulus of the cement stabilized materials is strongly influenced by the applied strain level. As the strain increases, the stiffness modulus significantly decreases until failure. Addition of moderate amount of Rc additive seems to increase the strain level at which the beam specimen fails. Based on the calculation from the linear-elastic multilayer program, as the Rc content increases from 0.56 to 3.2 kg/m$^3$, the maximum bearing load of the base layer increases on average by 45%.
- The frequency of dynamic loading has no clear influence on the stiffness modulus of cement stabilized sand. The stiffness of the sand-cement materials remain nearly constant.
- Fatigue relations with the number of load cycles until failure as a function of the applied stress level or the initial strain level are obtained for all the tested mixtures. These fatigue relations are influenced by the mix design. The slope of the fatigue line is relatively large which indicates rather brittle behavior of the cement stabilized sand.

b) Mechanical properties of cement stabilized clay

- In stabilized clay materials the cement content is found to be the significant factor controlling the compressive and tensile strength. A higher cement content generally yields a higher strength. Increasing Rc additive content shows moderate strength improvement on stabilized clay with high cement content 251 kg/m$^3$.
- The compressive and tensile strength of cement stabilized clay materials keeps increasing as the curing continues. That is because after the cementitious reaction the pozzolanic reaction takes place and continues to contribute to further strength development.
- Estimation models to predict the mechanical properties of cement stabilized clay are obtained as a function of the cement and Rc contents, density of the specimen and the curing age. For this investigated type of clay, the Rc additive content is not found to be related to these models. The achieved models exhibit a good fit with the test data.
- The stiffness modulus of cement stabilized clay is influenced by the applied strain, i.e. the stiffness decreases until failure under increased strain. Compared with sand-cement material, the decreasing rate is however lower and most of the clay-cement mixtures are able to withstand a much higher strain level before breaking.
- The estimation model of the initial stiffness modulus of cement stabilized clay gives a positive influence of the cement and Rc additive contents. The results of strain at break and the flexural strength showed however large variation and no consistent correlation with the cement or Rc additive content was found for the investigated type of clay.
- The fatigue relations have been obtained for all the clay-cement mixtures. However, these fatigue relations showed a large scatter between mixtures and most of the relations exhibit rather low $R^2$. No consistent correlation with either cement or Rc content was obtained for this investigated type of clay.

(2) Micro-properties of cement stabilized materials

Micro-properties of cement stabilized materials using Rc additive were characterized by performing scanning electron microscopy (SEM) and X-ray diffraction (XRD)

analysis. Use of Rc additive in cement paste and cement stabilized materials were both evaluated. The major findings are concluded as follows:

- The mixtures of cement paste and clay-cement with different amount of Rc additive exhibit similar XRD patterns, including the peak position, relative intensity, width and shape of each diffraction peak. However, the portlandite peak of the cement paste mixtures with moderate amount of Rc additive exhibits slightly higher intensity which might indicate the higher amount of portlandite formed.
- The SEM images of cement paste showed that the mixtures with Rc additive seem to exhibit the more dense microstructure and less voids. Similarly, in sand-cement mixtures, adding Rc additive also seems to lead to more cement hydration products filling the voids between the sand particles which might explain the increased strength caused by use of Rc additive.
- The SEM images of cement stabilized clay showed different morphology of the two mixtures with and without Rc. The ettringite crystals are observed in the mixture with Rc additive at 3 and 28 days, but the mixture without Rc doesn't show the trace of ettringite crystals. This could be resulting from the reaction of clay-cement with the compounds in Rc additive.

(3) Field performance of cement stabilized materials

The field evaluation of cement stabilized materials comprises a wide range of soil materials. A cement stabilized road base was constructed by creating different test sections. Two independent variables, cement and Rc contents, were evaluated. The strength of the field cores was compared with the strength of laboratory-prepared specimens. Models were developed to predict the field compressive strength and indirect tensile strength. The main findings can be concluded as follows:

- Addition of Rc additive generally yields a higher compressive strength and indirect tensile strength for cement stabilized materials evaluated in the field study, in both field and laboratory conditions. The improvement of strength is dependent on the soil types.
- The field strength and the laboratory-strength are compared at the same maturity index due to the huge difference of the cement hydration progress in these two conditions. The compressive strength and indirect tensile strength of the field cores generally reach 30% to 70% of the strength obtained for the

laboratory-prepared specimens at equal maturity index. Besides, large variations of density and strength are found in all field sections.

- The strength obtained from the laboratory-prepared specimens showed a steady increase during 28 days. In contrast, the field cores didn't show obvious strength improvement as the age increases. This can be explained by the low temperatures in the field condition that resulted in a low maturity index during the period of 28 days.
- Based on the field results, regression models were developed to predict the compressive strength and the indirect tensile strength of cement stabilized materials in the field condition under consideration of the specific execution of these test sections.

(4) Transverse cracking behavior of cement stabilized materials

Shrinkage tests were performed on 3 sand-cement mixtures and 3 clay-cement mixtures. All mixtures had the same cement content, but 3 different Rc contents were applied. By means of a mechanical model the transverse crack pattern of a cement stabilized base layer was estimated. The most important findings are:

- Adding appropriate amount of Rc additive reduces the shrinkage of cement stabilized sand and clay materials. Especially for the clay soil, the higher the Rc additive content, the less shrinkage is observed. An increasing period of moist curing also significantly reduces the total shrinkage of cement stabilized materials.
- Based on the calculation results, the investigated cement stabilized clay base exhibits very severe cracking (final crack spacing << 0.5 m) in all cases (three clay-cement mixtures with and without Rc additive and under two curing conditions), which is mainly due to the large drying shrinkage of this stabilized clay.
- Adding Rc additive has a large influence on the crack pattern of cement stabilized sand materials. Adding a certain amount of Rc additive reduces both the width of the crack and the number of cracks by 50% approximately.
- For sand-cement materials, the lower the assumed stress relaxation of the cement stabilized sand base layer, the earlier the primary cracks occur, the more cracks will appear and the smaller the final crack width.

- The date of construction has limited influence on the crack pattern of cement stabilized sand base, but the hour of construction has a significant influence on the crack pattern.
- The coefficient of friction between the cement stabilized sand base layer and the surrounding layers influences the crack pattern. The higher the friction coefficient, the smaller the width of the cracks and the smaller the crack spacing.
- The larger the amplitude of the daily temperature variation, the earlier the primary cracks occur, the smaller the width of the cracks and the larger the number of cracks.
- In the cement stabilized base, large crack width should be prevented. Provided that the crack spacing becomes not smaller than 2 to 3 m, a higher friction between base and surrounding layers, adding a certain amount of Rc additive, a lower stress relaxation and construction during the colder periods of the day contribute to reduced crack width.

## 9.2 Recommendations

In order to gain more comprehensive knowledge on the effect of the Rc additive in cement stabilization, further research is recommended to be done into the following aspects:

- For sand soil, the mix compositions used in this research are relatively high, especially cement content, which is not corresponding to the practical application. Therefore the mixtures used in practice should be further investigated.
- In the central composite mix design, the moisture content is not considered as a variable factor. However, the moisture content is also an influential factor controlling the properties of cement stabilized materials. Thus, it is advised to investigate the effect of the moisture content on the properties of cement stabilized soil with combined effect of cement and Rc additive.
- The micro-study of using Rc in cement stabilized soil, including the SEM and XRD tests were only conducted on a few mixtures. It is advised to perform such tests on a large number of mixtures as well as a wide range of soil types, which can provide deep insight into the chemical and physical interaction in the Rc-cement-soil system.

- In the analysis of the crack pattern, stress relaxation and the coefficient of friction are assumed values but they have a large influence. Thus, it is essential to determine the stress relaxation of cement stabilized materials with and without use of Rc additive and the coefficient of friction with surrounding layers. Besides, the input parameters (e.g. tensile strength and modulus of elasticity) were obtained under laboratory conditions. Thus, it is necessary to verify these obtained crack patterns on real road projects.
- Analysis of the crack pattern was only limited to three sand-cement and three clay-cement mixtures with variable Rc additive contents without considering the influence of the cement content. Thus, it is very necessary to evaluate more mix compositions to identify the optimum mix design with appropriate cement and Rc additive contents to achieve a balance between the strength properties and the potential of cracking, which can be beneficial for the pavement design.

**Appendix A** Strength test data cement stabilized sand

Test data of compressive strength of cement stabilized sand

| Items | Mix variables | | 3-day | | 7-day | | 28-day | | 91-day | |
|---|---|---|---|---|---|---|---|---|---|---|
| | Rc | Cement | D | UCS | D | UCS | D | UCS | D | UCS |
| | kg/m³ | kg/m³ | kg/m³ | MPa | kg/m³ | MPa | kg/m³ | MPa | kg/m³ | MPa |
| $Rc_0C_0$-1 | 1.9 | 205 | 2076 | 6.38 | 2046 | 12.78 | 2053 | 17.0 | 2069 | 19.45 |
| $Rc_0C_0$-2 | 1.9 | 205 | 2056 | 7.82 | 2019 | - | 2036 | 18.13 | 2127 | 17.63 |
| $Rc_0C_0$-3 | 1.9 | 205 | 2051 | 6.3 | 2057 | 13.97 | 2027 | 20.51 | 2044 | 20.26 |
| $Rc_0C_{-a}$-1 | 1.9 | 140 | 1992 | 2.7 | 1989 | 5.79 | 1992 | 8.97 | 2026 | 11.55 |
| $Rc_0C_{-a}$-2 | 1.9 | 140 | 2011 | 3.51 | 2010 | 6.75 | 2031 | 11.03 | 2025 | 10.83 |
| $Rc_0C_{-a}$-3 | 1.9 | 140 | 1990 | 3.03 | 1985 | 6.43 | 2057 | 10.19 | 2016 | 9.71 |
| $Rc_aC_0$ -1 | 3.8 | 205 | 2104 | 9.99 | 2110 | 17.86 | 2087 | 18.35 | 2040 | 21.95 |
| $Rc_aC_0$ -2 | 3.8 | 205 | 2102 | 9.46 | 2086 | 16.1 | 2109 | 19.2 | 2091 | 23.58 |
| $Rc_aC_0$ -3 | 3.8 | 205 | 2091 | 9.71 | 2110 | 17.07 | 2081 | 18.06 | 2079 | 21.54 |
| $Rc_{-a}C_0$ -1 | 0 | 205 | 2052 | 4.45 | 2100 | 13.01 | 2068 | 15.95 | 2042 | 22.08 |
| $Rc_{-a}C_0$ -2 | 0 | 205 | 2055 | 4.45 | 2063 | 12.5 | 2071 | 17.19 | 2044 | 20.10 |
| $Rc_{-a}C_0$ -3 | 0 | 205 | 2024 | 5.71 | 2093 | 13.17 | 2060 | 14.73 | 2036 | 19.39 |
| $Rc_0C_a$-1 | 1.9 | 270 | 2128 | 13.47 | 2163 | 18.8 | 2140 | 20.06 | 2095 | 22.79 |
| $Rc_0C_a$-2 | 1.9 | 270 | 2141 | 14.27 | 2179 | 21.73 | 2131 | 22.73 | 2122 | 19.77 |
| $Rc_0C_a$-3 | 1.9 | 270 | 2150 | 14.31 | 2134 | 22.59 | 2123 | 19.72 | 2111 | 24.10 |
| $Rc_1C_{-1}$-1 | 3.2 | 159 | 2033 | 4.92 | 2027 | 11.2 | 2049 | 11.4 | 2033 | 15.12 |
| $Rc_1C_{-1}$-2 | 3.2 | 159 | 2059 | 5.55 | 2042 | 10.66 | 2034 | 14.3 | 2020 | 13.40 |
| $Rc_1C_{-1}$-3 | 3.2 | 159 | 2066 | 5.76 | 2044 | 11.51 | 2050 | 12.68 | 2025 | 14.45 |
| $Rc_1C_1$-1 | 3.2 | 251 | 2164 | 10.39 | 2159 | 19.05 | 2162 | - | 2140 | 28.72 |
| $Rc_1C_1$-2 | 3.2 | 251 | 2138 | 12.42 | 2162 | 17.93 | 2164 | 27.03 | 2166 | 25.38 |
| $Rc_1C_1$-3 | 3.2 | 251 | 2147 | 9.57 | 2151 | 18.95 | 2185 | 24.6 | 2160 | 31.47 |
| $Rc_{-1}C_1$-1 | 0.56 | 251 | 2158 | 10.25 | 2161 | 18.97 | 2087 | 23.36 | 2085 | 24.57 |
| $Rc_{-1}C_1$-2 | 0.56 | 251 | 2127 | 10.36 | 2087 | 14.93 | 2108 | 24.25 | 2111 | 21.46 |
| $Rc_{-1}C_1$-3 | 0.56 | 251 | 2124 | 10.14 | 2106 | 17.02 | 2089 | 23.69 | 2099 | 21.55 |
| $Rc_{-1}C_{-1}$-1 | 0.56 | 159 | 2103 | 6.06 | 1951 | 8.26 | 2010 | 10.97 | 1975 | 11.15 |
| $Rc_{-1}C_{-1}$-2 | 0.56 | 159 | 2106 | 5.23 | 1986 | 8.5 | 2011 | 12.03 | 1984 | 13.23 |
| $Rc_{-1}C_{-1}$-3 | 0.56 | 159 | 2114 | 5.81 | 1974 | 7.91 | 2026 | 10.35 | 1985 | 13.20 |

Test data of indirect tensile strength on cement stabilized sand

| Items | Mix variables | | 3-day | | 7-day | | 28-day | | 91-day | |
|---|---|---|---|---|---|---|---|---|---|---|
| | Rc | Cement | D | ITS | D | ITS | D | ITS | D | ITS |
| | kg/m³ | kg/m³ | kg/m³ | MPa | kg/m³ | MPa | kg/m³ | MPa | kg/m³ | MPa |
| $Rc_0C_0$-1 | 1.9 | 205 | 2056 | 0.96 | 2086 | 1.28 | 2049 | 1.55 | 2056 | 1.72 |
| $Rc_0C_0$-2 | 1.9 | 205 | 2070 | 0.93 | 2072 | 1.44 | 2118 | 1.93 | 2068 | 1.58 |
| $Rc_0C_0$-3 | 1.9 | 205 | 2063 | 0.94 | 2096 | 1.37 | 2085 | 1.59 | 2010 | 1.53 |
| $Rc_0C_{-a}$-1 | 1.9 | 140 | 2001 | 0.37 | 1986 | 0.81 | 1991 | 1.00 | 2026 | 0.94 |
| $Rc_0C_{-a}$-2 | 1.9 | 140 | 2003 | 0.43 | 1961 | 0.82 | 2012 | 1.08 | 1985 | 1.06 |
| $Rc_0C_{-a}$-3 | 1.9 | 140 | 2015 | 0.41 | 1987 | 0.85 | 1994 | 1.19 | 1973 | 0.75 |
| $Rc_aC_0$ -1 | 3.8 | 205 | 2121 | 0.86 | 2067 | 1.44 | 2090 | 1.83 | 2080 | 1.89 |
| $Rc_aC_0$ -2 | 3.8 | 205 | 2099 | 0.93 | 2106 | 1.49 | 2092 | 1.85 | 2077 | 2.03 |
| $Rc_aC_0$ -3 | 3.8 | 205 | 2112 | 0.96 | 2099 | 1.30 | 2099 | 1.68 | 2073 | 1.94 |
| $Rc_{-a}C_0$ -1 | 0 | 205 | 2076 | 0.72 | 2059 | 1.14 | 2064 | 1.68 | 2035 | 1.36 |
| $Rc_{-a}C_0$ -2 | 0 | 205 | 2052 | 0.61 | 2063 | 1.18 | 2064 | 1.56 | 2044 | 1.66 |
| $Rc_{-a}C_0$ -3 | 0 | 205 | 2052 | 0.67 | 2054 | 1.05 | 2047 | 1.50 | 2035 | 1.68 |
| $Rc_0C_a$-1 | 1.9 | 270 | 2134 | 1.33 | 2151 | 1.59 | 2093 | 2.13 | 2141 | 2.40 |
| $Rc_0C_a$-2 | 1.9 | 270 | 2121 | 1.05 | 2149 | 1.73 | 2112 | 1.89 | 2124 | 2.42 |
| $Rc_0C_a$-3 | 1.9 | 270 | 2160 | 1.05 | 2132 | 1.87 | 2101 | 1.81 | 2152 | 2.44 |
| $Rc_1C_{-1}$-1 | 3.2 | 159 | 2049 | 0.52 | 2048 | 1.17 | 2041 | 1.41 | 2031 | 1.61 |
| $Rc_1C_{-1}$-2 | 3.2 | 159 | 2065 | 0.59 | 2030 | 1.20 | 2020 | 1.14 | 2046 | 1.86 |
| $Rc_1C_{-1}$-3 | 3.2 | 159 | 2057 | 0.59 | 2045 | 1.17 | 2015 | 1.32 | 2058 | 1.52 |
| $Rc_1C_1$-1 | 3.2 | 251 | 2132 | 1.01 | 2165 | 1.83 | 2172 | 1.94 | 2120 | 2.60 |
| $Rc_1C_1$-2 | 3.2 | 251 | 2151 | 1.08 | 2167 | 1.88 | 2131 | 2.03 | 2122 | 2.89 |
| $Rc_1C_1$-3 | 3.2 | 251 | 2159 | 1.11 | 2156 | 1.95 | 2146 | 2.22 | 2136 | 2.40 |
| $Rc_{-1}C_1$-1 | 0.56 | 251 | 2107 | 1.00 | 2122 | 1.58 | 2112 | 2.06 | 2073 | 2.63 |
| $Rc_{-1}C_1$-2 | 0.56 | 251 | 2158 | 0.97 | 2122 | 1.62 | 2071 | 2.35 | 2083 | 2.18 |
| $Rc_{-1}C_1$-3 | 0.56 | 251 | 2097 | 0.89 | 2129 | 1.63 | 2084 | 1.97 | 2053 | 2.29 |
| $Rc_{-1}C_{-1}$-1 | 0.56 | 159 | 2104 | 0.77 | 1864 | 0.92 | 1967 | 1.04 | 1987 | 1.01 |
| $Rc_{-1}C_{-1}$-2 | 0.56 | 159 | 2094 | 0.83 | 1859 | 0.81 | 1978 | 1.07 | 1967 | 1.12 |
| $Rc_{-1}C_{-1}$-3 | 0.56 | 159 | 2106 | 0.76 | 1848 | 0.85 | 2079 | 0.80 | 2029 | 1.31 |

Test data of flexural tensile strength test on cement stabilized sand

| Items | Mix variables | | 3-day | | 7-day | | 28-day | | 91-day | |
|---|---|---|---|---|---|---|---|---|---|---|
| | Rc | Cement | D | FTS | D | FTS | D | FTS | D | FTS |
| | kg/m³ | kg/m³ | kg/m³ | MPa | kg/m³ | MPa | kg/m³ | MPa | kg/m³ | MPa |
| $Rc_0C_0$-1 | 1.9 | 205 | 1991 | 1.88 | 1973 | 2.72 | 1992 | 2.73 | 1902 | 2.91 |
| $Rc_0C_0$-2 | 1.9 | 205 | 2006 | 1.83 | 2000 | 2.48 | 1998 | 2.84 | 1945 | 2.94 |
| $Rc_0C_0$-3 | 1.9 | 205 | 1988 | 1.62 | 1973 | 2.30 | 1996 | 2.84 | 2031 | 3.26 |
| $Rc_0C_{-a}$-1 | 1.9 | 140 | 1918 | 1.24 | 1905 | 1.90 | 2012 | 2.11 | 1988 | 2.13 |
| $Rc_0C_{-a}$-2 | 1.9 | 140 | 1877 | 1.08 | 1898 | 1.97 | 2025 | 2.21 | 1965 | 2.23 |
| $Rc_0C_{-a}$-3 | 1.9 | 140 | 1855 | 1.12 | 1930 | 2.11 | 2033 | 2.31 | 1965 | 2.13 |
| $Rc_aC_0$ -1 | 3.8 | 205 | 1977 | 2.23 | 2022 | 2.99 | 1947 | 2.84 | 1949 | 3.33 |
| $Rc_aC_0$ -2 | 3.8 | 205 | 1976 | 1.76 | 1973 | 2.71 | 1988 | 3.09 | 1977 | 3.70 |
| $Rc_aC_0$ -3 | 3.8 | 205 | 2000 | 2.16 | 1978 | 2.86 | 1963 | 2.91 | 1980 | 3.98 |
| $Rc_{-a}C_0$ -1 | 0 | 205 | 1932 | 1.49 | 2016 | 2.51 | 2012 | 2.79 | 1976 | 4.01 |
| $Rc_{-a}C_0$ -2 | 0 | 205 | 1924 | 1.74 | 2001 | 2.56 | 2039 | 2.93 | 1991 | 3.61 |
| $Rc_{-a}C_0$ -3 | 0 | 205 | 1925 | 1.85 | 2036 | 2.60 | 2006 | 2.57 | 1999 | 4.10 |
| $Rc_0C_a$-1 | 1.9 | 270 | 2041 | 2.55 | 2047 | 2.94 | 2031 | 3.40 | 2051 | 4.27 |
| $Rc_0C_a$-2 | 1.9 | 270 | 2060 | 2.59 | 2089 | 3.24 | 2022 | 3.06 | 2066 | 4.55 |
| $Rc_0C_a$-3 | 1.9 | 270 | 2031 | 2.41 | 2089 | 2.99 | 2045 | 3.29 | 2035 | 4.27 |
| $Rc_1C_{-1}$-1 | 3.2 | 159 | 1990 | 1.56 | 1986 | 1.96 | 1906 | 2.48 | 1914 | 2.79 |
| $Rc_1C_{-1}$-2 | 3.2 | 159 | 2002 | 1.73 | 2012 | 2.18 | 1947 | 2.81 | 1922 | 2.53 |
| $Rc_1C_{-1}$-3 | 3.2 | 159 | 1995 | 1.43 | 2000 | 2.04 | 1939 | 2.68 | 1942 | 3.09 |
| $Rc_1C_1$-1 | 3.2 | 251 | 2053 | 3.12 | 2047 | 3.38 | 2051 | 3.58 | 2086 | 4.08 |
| $Rc_1C_1$-2 | 3.2 | 251 | 2094 | 2.86 | 2108 | 3.58 | 2059 | 3.62 | 2059 | 4.69 |
| $Rc_1C_1$-3 | 3.2 | 251 | 2091 | 2.73 | 2068 | 3.47 | 2094 | 3.69 | 2082 | 4.87 |
| $Rc_{-1}C_1$-1 | 0.56 | 251 | 1969 | 2.32 | 2020 | 3.16 | 2043 | 3.56 | 2012 | 4.27 |
| $Rc_{-1}C_1$-2 | 0.56 | 251 | 2000 | 2.48 | 2004 | 2.88 | - | - | 2004 | 4.69 |
| $Rc_{-1}C_1$-3 | 0.56 | 251 | 1992 | 2.20 | 2055 | 3.35 | 2000 | 3.54 | 2066 | 3.61 |
| $Rc_{-1}C_{-1}$-1 | 0.56 | 159 | 1914 | 1.60 | 1957 | 1.92 | 1988 | 2.04 | 1965 | 2.34 |
| $Rc_{-1}C_{-1}$-2 | 0.56 | 159 | 1902 | 1.59 | 1977 | 2.18 | 1945 | 2.25 | 1938 | 2.32 |
| $Rc_{-1}C_{-1}$-3 | 0.56 | 159 | 1930 | 1.76 | 1973 | 1.88 | 1949 | 2.04 | 2004 | 2.02 |

**Appendix B** Strength test data cement stabilized clay

Test data of compressive strength of cement stabilized clay

| Items | Mix variables | | 3-day | | 7-day | | 28-day | | 91-day | |
|---|---|---|---|---|---|---|---|---|---|---|
| | Rc | Cement | D | UCS | D | UCS | D | UCS | D | UCS |
| | kg/m$^3$ | kg/m$^3$ | kg/m$^3$ | MPa | kg/m$^3$ | MPa | kg/m$^3$ | MPa | kg/m$^3$ | MPa |
| $Rc_0C_0$-1 | 1.9 | 205 | 2142 | 3.94 | 2154 | 5.48 | 2136 | 7.19 | 2130 | 9.35 |
| $Rc_0C_0$-2 | 1.9 | 205 | 2153 | 4.3 | 2143 | 5.38 | 2137 | 7.51 | 2142 | 9.48 |
| $Rc_0C_0$-3 | 1.9 | 205 | 2146 | 4.2 | 2127 | 5.02 | 2138 | 6.86 | 2147 | 9.09 |
| $Rc_0C_{-a}$-1 | 1.9 | 140 | 2136 | 3.66 | 2133 | 4.06 | 2145 | 6.29 | 2132 | 7.17 |
| $Rc_0C_{-a}$-2 | 1.9 | 140 | 2141 | 2.93 | 2144 | 4.08 | 2132 | 5.91 | 2131 | 7.29 |
| $Rc_0C_{-a}$-3 | 1.9 | 140 | 2139 | 3.11 | 2139 | 4.55 | 2143 | 5.58 | 2134 | 7.22 |
| $Rc_aC_0$ -1 | 3.2 | 159 | 2163 | 3.09 | 2163 | 4.12 | 2130 | 5.74 | 2137 | 7.23 |
| $Rc_aC_0$ -2 | 3.2 | 159 | 2156 | 2.81 | 2160 | 3.84 | 2130 | 5.36 | 2154 | 7.5 |
| $Rc_aC_0$ -3 | 3.2 | 159 | 2160 | 2.81 | 2166 | 4.2 | 2139 | 5.54 | 2136 | 7.33 |
| $Rc_{-a}C_0$ -1 | 3.8 | 205 | 2149 | 3.14 | 2148 | 4.55 | 2141 | 7.0 | 2131 | 8.14 |
| $Rc_{-a}C_0$ -2 | 3.8 | 205 | 2148 | 3.46 | 2147 | 5.08 | 2143 | 7.86 | 2145 | 8.0 |
| $Rc_{-a}C_0$ -3 | 3.8 | 205 | 2138 | 3.25 | 2149 | 5.07 | 2144 | 7.69 | 2146 | 7.62 |
| $Rc_0C_a$-1 | 3.2 | 251 | 2154 | 5.08 | 2149 | 6.12 | 2257 | 10.87 | 2257 | 12.8 |
| $Rc_0C_a$-2 | 3.2 | 251 | 2144 | 4.9 | 2145 | 7.94 | 2252 | 11.15 | 2253 | 13.76 |
| $Rc_0C_a$-3 | 3.2 | 251 | 2149 | 5.47 | 2145 | 7.41 | 2251 | 10.95 | 2254 | 14.4 |
| $Rc_1C_{-1}$-1 | 1.9 | 270 | 2146 | 5.71 | 2135 | 8.63 | 2131 | 12.39 | 2136 | 14.39 |
| $Rc_1C_{-1}$-2 | 1.9 | 270 | 2144 | 6.3 | 2134 | 7.79 | 2137 | 13.13 | 2142 | 13.99 |
| $Rc_1C_{-1}$-3 | 1.9 | 270 | 2145 | 6.14 | 2143 | 8.47 | 2134 | 13.06 | 2128 | 14.42 |
| $Rc_1C_1$-1 | 0.56 | 251 | 2152 | 4.23 | 2138 | 6.38 | 2119 | 8.86 | 2128 | 11.7 |
| $Rc_1C_1$-2 | 0.56 | 251 | 2152 | 3.75 | 2139 | 6.26 | 2120 | 8.71 | 2133 | 11.28 |
| $Rc_1C_1$-3 | 0.56 | 251 | 2149 | 4.03 | 2151 | - | 2116 | 8.08 | 2113 | 11.3 |
| $Rc_{-1}C_1$-1 | 0 | 205 | 2141 | 3.8 | 2151 | 5.21 | 2163 | 8.1 | 2163 | 9.15 |
| $Rc_{-1}C_1$-2 | 0 | 205 | 2149 | 3.71 | 2147 | 5.23 | 2156 | 8.68 | 2160 | 10.06 |
| $Rc_{-1}C_1$-3 | 0 | 205 | 2143 | 3.68 | 2147 | 5.5 | 2160 | 7.63 | 2166 | 9.51 |
| $Rc_{-1}C_{-1}$-1 | 0.56 | 159 | 2137 | 3.4 | 2132 | 4.75 | 2139 | 6.68 | 2138 | 8.31 |
| $Rc_{-1}C_{-1}$-2 | 0.56 | 159 | 2131 | 3.47 | 2127 | 4.41 | 2145 | 6.75 | 2144 | 8.32 |
| $Rc_{-1}C_{-1}$-3 | 0.56 | 159 | 2141 | 3.36 | 2132 | 5.1 | 2142 | 6.75 | 2131 | 8.6 |

Test data of indirect tensile strength of cement stabilized clay

| Items | Mix variables | | 3-day | | 7-day | | 28-day | | 91-day | |
|---|---|---|---|---|---|---|---|---|---|---|
| | Rc | Cement | D | ITS | D | ITS | D | ITS | D | ITS |
| | kg/m³ | kg/m³ | kg/m³ | MPa | kg/m³ | MPa | kg/m³ | MPa | kg/m³ | MPa |
| $Rc_0C_0$-1 | 1.9 | 205 | 2150 | 0.62 | 2152 | 0.78 | 2136 | 1.16 | 2141 | 1.58 |
| $Rc_0C_0$-2 | 1.9 | 205 | 2138 | 0.61 | 2138 | 0.75 | 2137 | 1.50 | 2136 | 1.46 |
| $Rc_0C_0$-3 | 1.9 | 205 | 2153 | 0.64 | 2157 | 0.85 | 2137 | 1.34 | 2134 | 1.57 |
| $Rc_0C_{-a}$-1 | 1.9 | 140 | 2132 | 0.44 | 2138 | 0.71 | 2142 | 1.01 | 2139 | 1.20 |
| $Rc_0C_{-a}$-2 | 1.9 | 140 | 2130 | 0.41 | 2142 | 0.71 | 2136 | 0.90 | 2141 | 1.08 |
| $Rc_0C_{-a}$-3 | 1.9 | 140 | 2137 | 0.47 | 2136 | 0.69 | 2134 | 1.00 | 2136 | 1.10 |
| $Rc_aC_0$ -1 | 3.2 | 159 | 2155 | 0.42 | 2159 | 0.59 | 2139 | 0.72 | 2146 | 0.97 |
| $Rc_aC_0$ -2 | 3.2 | 159 | 2170 | 0.44 | 2162 | 0.55 | 2138 | 0.75 | 2145 | 1.01 |
| $Rc_aC_0$ -3 | 3.2 | 159 | 2160 | 0.41 | 2161 | 0.64 | 2131 | 0.75 | 2142 | 1.05 |
| $Rc_{-a}C_0$ -1 | 3.8 | 205 | 2157 | 0.52 | 2146 | 0.68 | 2152 | 1.21 | 2141 | 1.75 |
| $Rc_{-a}C_0$ -2 | 3.8 | 205 | 2160 | 0.46 | 2143 | 0.71 | 2145 | 1.18 | 2141 | 1.80 |
| $Rc_{-a}C_0$ -3 | 3.8 | 205 | 2148 | 0.54 | 2144 | 0.67 | 2149 | 1.07 | 2147 | 1.49 |
| $Rc_0C_a$-1 | 3.2 | 251 | 2149 | 0.68 | 2145 | 1.07 | 2255 | 1.90 | 2271 | 1.89 |
| $Rc_0C_a$-2 | 3.2 | 251 | 2142 | 0.75 | 2147 | 1.12 | 2261 | 1.73 | 2283 | 1.72 |
| $Rc_0C_a$-3 | 3.2 | 251 | 2155 | 0.66 | 2145 | 1.00 | 2258 | 1.99 | 2265 | - |
| $Rc_1C_{-1}$-1 | 1.9 | 270 | 2138 | 0.78 | 2124 | - | 2142 | 1.78 | 2147 | 1.99 |
| $Rc_1C_{-1}$-2 | 1.9 | 270 | 2132 | 0.71 | 2133 | 1.14 | 2144 | 1.86 | 2136 | 1.99 |
| $Rc_1C_{-1}$-3 | 1.9 | 270 | 2141 | 0.88 | 2130 | 1.16 | 2137 | 2.07 | 2141 | 1.99 |
| $Rc_1C_1$-1 | 0.56 | 251 | 2141 | 0.66 | 2151 | 0.86 | 2119 | 1.45 | 2125 | 2.04 |
| $Rc_1C_1$-2 | 0.56 | 251 | 2156 | 0.77 | 2148 | 0.88 | 2120 | 1.53 | 2124 | 1.99 |
| $Rc_1C_1$-3 | 0.56 | 251 | 2145 | 0.57 | 2148 | 1.02 | 2116 | 1.72 | 2114 | 1.64 |
| $Rc_{-1}C_1$-1 | 0 | 205 | 2159 | 0.61 | 2148 | 0.97 | 2155 | 1.29 | 2159 | 1.68 |
| $Rc_{-1}C_1$-2 | 0 | 205 | 2135 | 0.70 | 2155 | 0.89 | 2170 | 1.52 | 2162 | 1.91 |
| $Rc_{-1}C_1$-3 | 0 | 205 | 2138 | 0.59 | 2157 | 0.84 | 2160 | 1.03 | 2161 | 1.55 |
| $Rc_{-1}C_{-1}$-1 | 0.56 | 159 | 2139 | 0.49 | 2131 | 0.75 | 2131 | 0.98 | 2132 | 1.45 |
| $Rc_{-1}C_{-1}$-2 | 0.56 | 159 | 2136 | 0.50 | 2134 | 0.72 | 2129 | 1.13 | 2127 | 1.42 |
| $Rc_{-1}C_{-1}$-3 | 0.56 | 159 | 2127 | 0.46 | 2128 | 0.70 | 2137 | 1.23 | 2119 | 1.12 |

Test data of flexural tensile strength of cement stabilized clay

| Items | Mix variables | | 3-day | | 7-day | | 28-day | | 91-day | |
|---|---|---|---|---|---|---|---|---|---|---|
| | Rc | Cement | D | FTS | D | FTS | D | FTS | D | FTS |
| | kg/m³ | kg/m³ | kg/m³ | MPa | kg/m³ | MPa | kg/m³ | MPa | kg/m³ | MPa |
| $Rc_0C_0$-1 | 1.9 | 205 | 2160 | 1.76 | 2168 | 2.77 | 2156 | 2.98 | 2152 | 4.10 |
| $Rc_0C_0$-2 | 1.9 | 205 | 2168 | 1.66 | 2168 | 2.80 | 2152 | 2.96 | 2148 | 4.62 |
| $Rc_0C_0$-3 | 1.9 | 205 | 2172 | 1.64 | 2168 | 2.73 | 2152 | - | 2145 | 4.59 |
| $Rc_0C_{-a}$-1 | 1.9 | 140 | 2168 | 1.48 | 2145 | 2.21 | 2191 | 3.32 | 2148 | 3.26 |
| $Rc_0C_{-a}$-2 | 1.9 | 140 | 2156 | 1.43 | 2141 | 2.34 | 2203 | 3.39 | 2160 | 3.12 |
| $Rc_0C_{-a}$-3 | 1.9 | 140 | 2156 | 1.62 | 2148 | 2.56 | 2176 | 3.58 | 2152 | 2.51 |
| $Rc_aC_0$ -1 | 3.2 | 159 | 2156 | 1.56 | 2172 | 1.76 | 2125 | 2.62 | 2129 | 2.25 |
| $Rc_aC_0$ -2 | 3.2 | 159 | 2156 | 1.68 | 2168 | 1.52 | 2148 | 2.53 | 2148 | 2.67 |
| $Rc_aC_0$ -3 | 3.2 | 159 | 2145 | 1.44 | 2121 | 1.57 | 2148 | 2.04 | 2141 | 2.16 |
| $Rc_{-a}C_0$ -1 | 3.8 | 205 | 2148 | 1.41 | 2160 | 2.24 | 2141 | 4.50 | 2113 | 4.04 |
| $Rc_{-a}C_0$ -2 | 3.8 | 205 | 2152 | 1.52 | 2156 | 1.57 | 2137 | 4.41 | 2145 | 4.95 |
| $Rc_{-a}C_0$ -3 | 3.8 | 205 | 2156 | 1.38 | 2168 | 2.06 | 2133 | 4.12 | 2137 | 4.64 |
| $Rc_0C_a$-1 | 3.2 | 251 | 2160 | 2.51 | 2160 | 3.23 | 2172 | 4.20 | 2176 | 5.55 |
| $Rc_0C_a$-2 | 3.2 | 251 | 2148 | 2.16 | 2164 | 3.68 | 2168 | 4.24 | 2172 | 5.98 |
| $Rc_0C_a$-3 | 3.2 | 251 | 2156 | 2.20 | 2164 | 2.98 | 2168 | 4.12 | 2176 | 6.59 |
| $Rc_1C_{-1}$-1 | 1.9 | 270 | 2176 | 3.09 | 2141 | 2.84 | 2168 | 4.76 | 2176 | 5.95 |
| $Rc_1C_{-1}$-2 | 1.9 | 270 | 2152 | 2.67 | 2152 | 3.09 | 2172 | 4.25 | 2172 | 5.44 |
| $Rc_1C_{-1}$-3 | 1.9 | 270 | 2176 | 2.58 | 2164 | 3.35 | 2168 | 4.59 | 2160 | 4.27 |
| $Rc_1C_1$-1 | 0.56 | 251 | 2129 | 2.09 | 2156 | 2.93 | 2172 | 3.63 | 2152 | 5.02 |
| $Rc_1C_1$-2 | 0.56 | 251 | 2137 | 1.85 | 2164 | 2.91 | 2172 | 3.82 | 2172 | 5.39 |
| $Rc_1C_1$-3 | 0.56 | 251 | 2129 | 1.80 | 2125 | 2.23 | 2172 | 4.27 | 2160 | 5.67 |
| $Rc_{-1}C_1$-1 | 0 | 205 | 2141 | 1.80 | 2188 | 2.80 | 2156 | 3.82 | 2172 | 4.55 |
| $Rc_{-1}C_1$-2 | 0 | 205 | 2148 | 2.14 | 2176 | 2.78 | 2156 | 3.26 | 2168 | 4.43 |
| $Rc_{-1}C_1$-3 | 0 | 205 | 2148 | 1.97 | 2180 | 2.73 | 2145 | 3.70 | 2121 | 3.05 |
| $Rc_{-1}C_{-1}$-1 | 0.56 | 159 | 2137 | 1.90 | 2133 | 2.55 | 2152 | 3.75 | 2152 | 5.28 |
| $Rc_{-1}C_{-1}$-2 | 0.56 | 159 | 2141 | 2.20 | 2133 | 2.67 | 2156 | 3.66 | 2156 | 4.65 |
| $Rc_{-1}C_{-1}$-3 | 0.56 | 159 | 2141 | 1.50 | 2125 | 1.99 | 2164 | 3.68 | 2164 | 4.56 |

**Appendix C** Comparison of field strength and laboratory strength

(1) Compressive strength of the field cores and the lab-prepared specimens

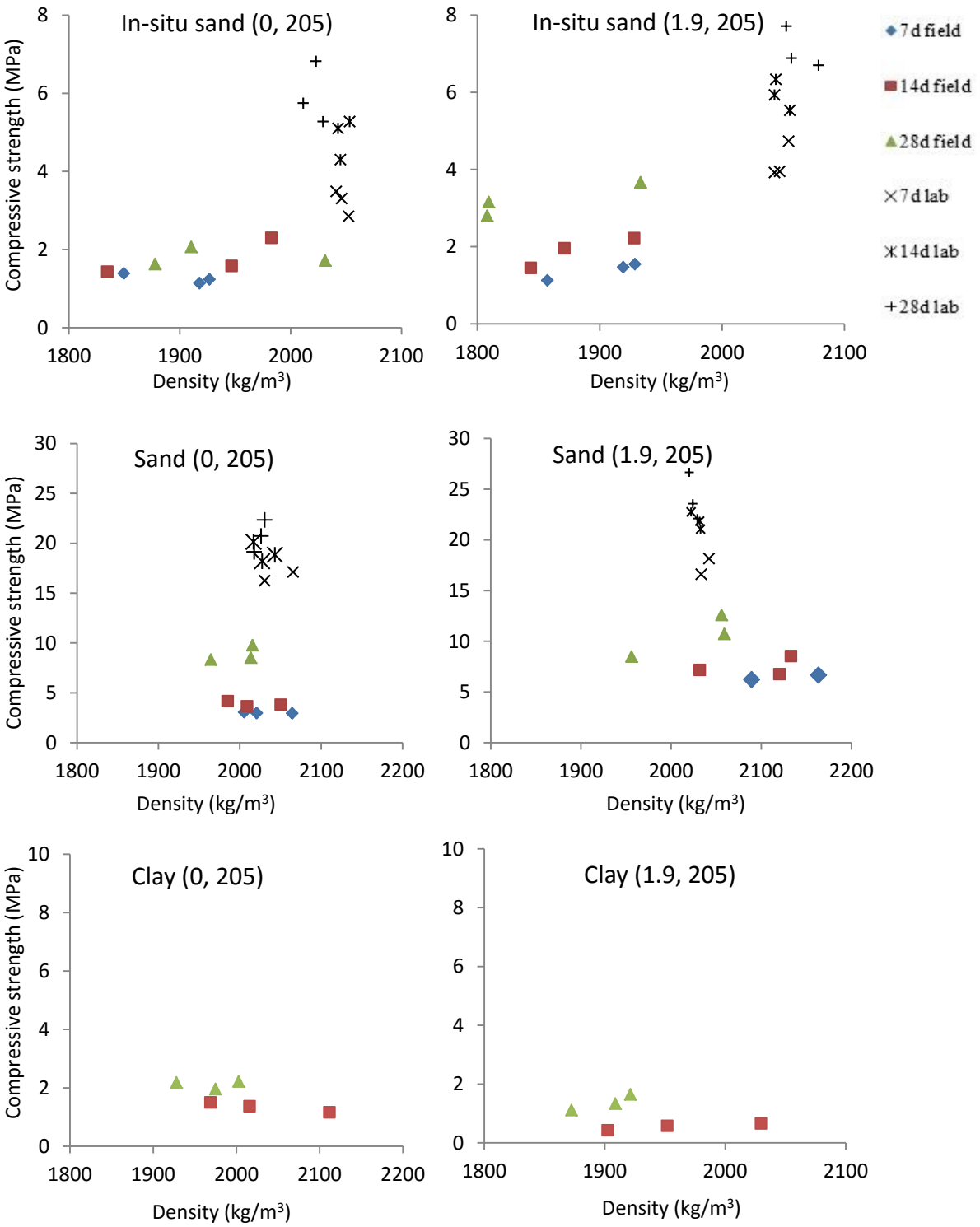

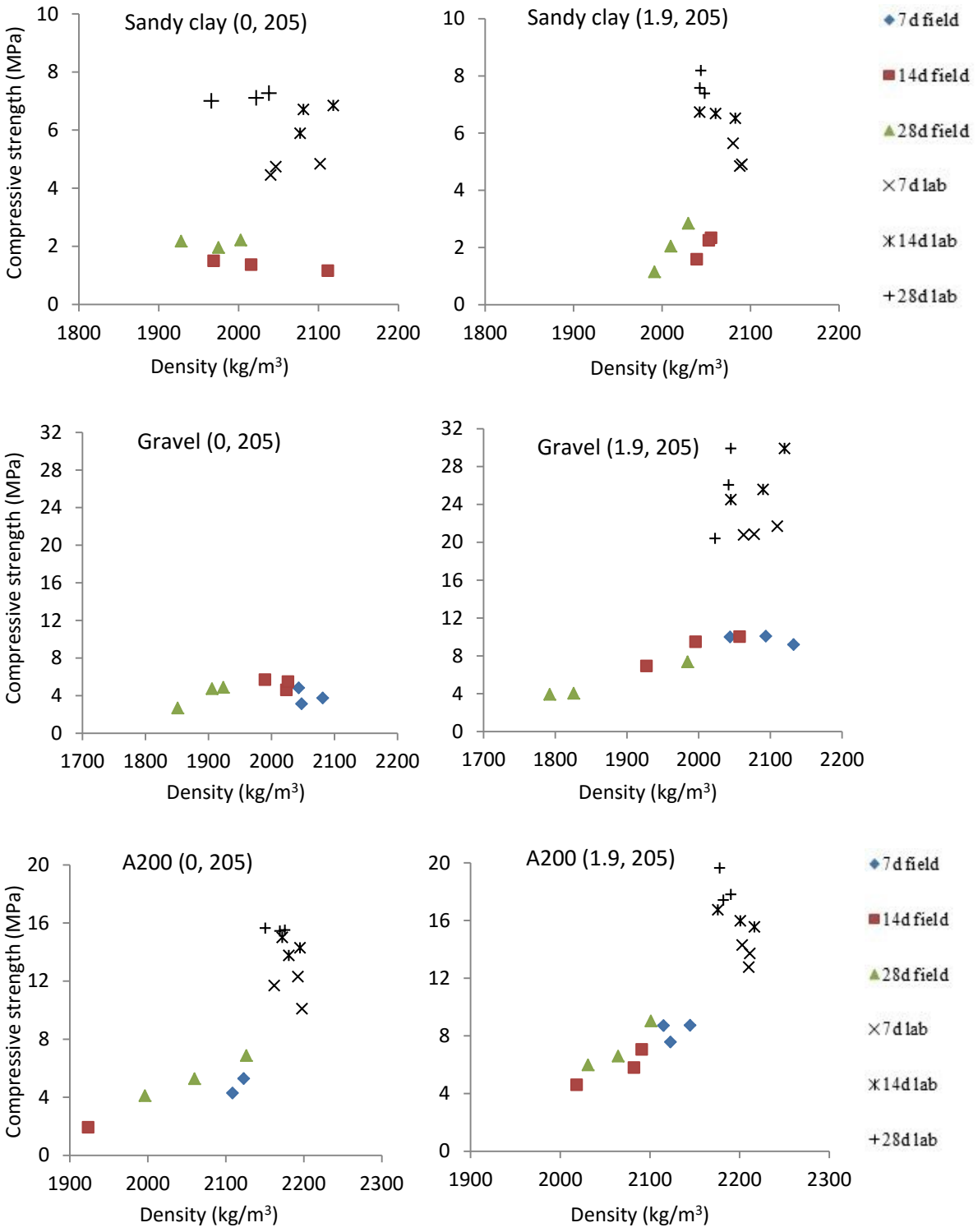
Sandy clay (0, 205)
Sandy clay (1.9, 205)
Gravel (0, 205)
Gravel (1.9, 205)
A200 (0, 205)
A200 (1.9, 205)
Compressive strength (MPa)
Density (kg/m³)
7d field
14d field
28d field
7d lab
14d lab
28d lab

(2) Indirect tensile strength of the field cores and the lab-prepared specimens

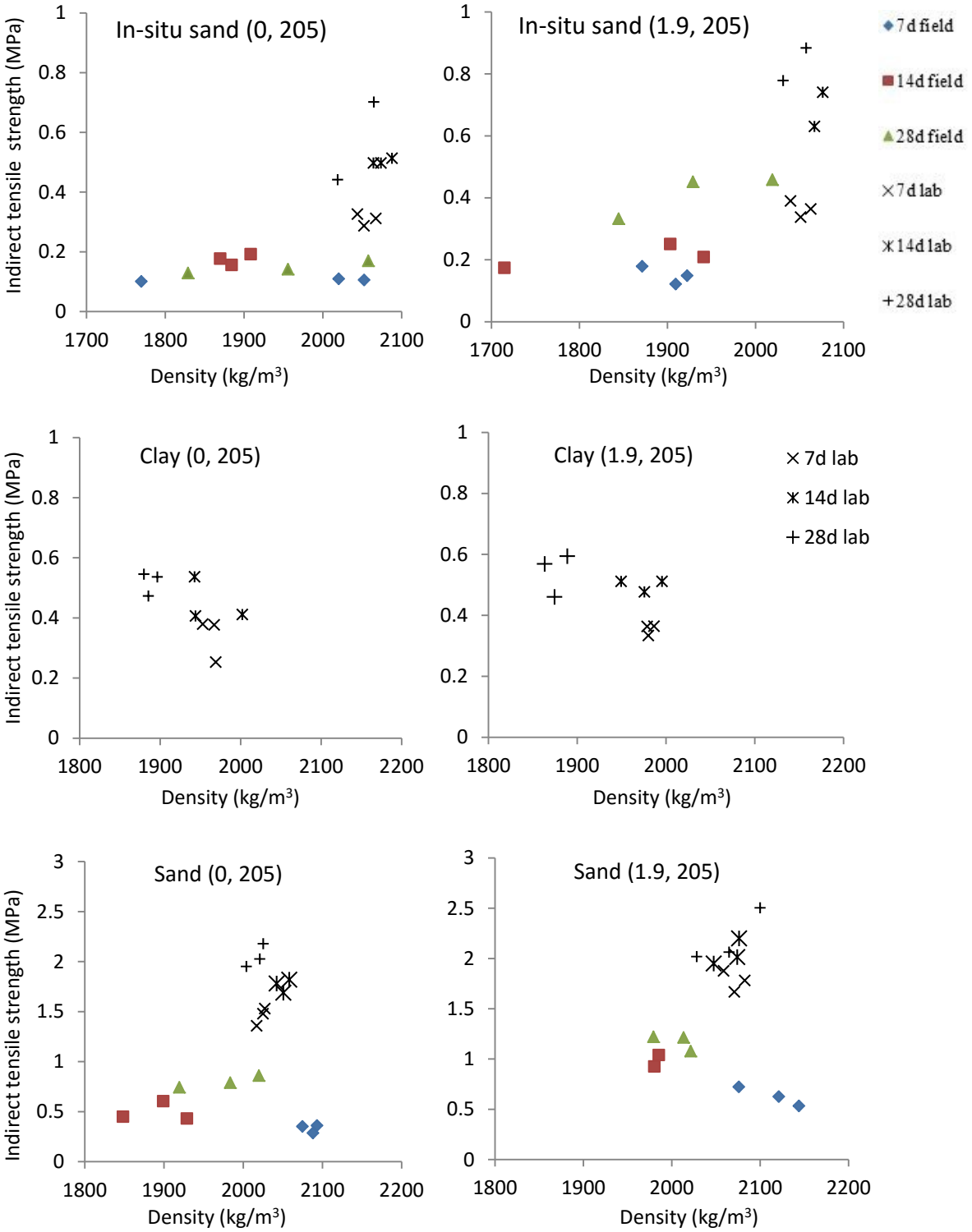

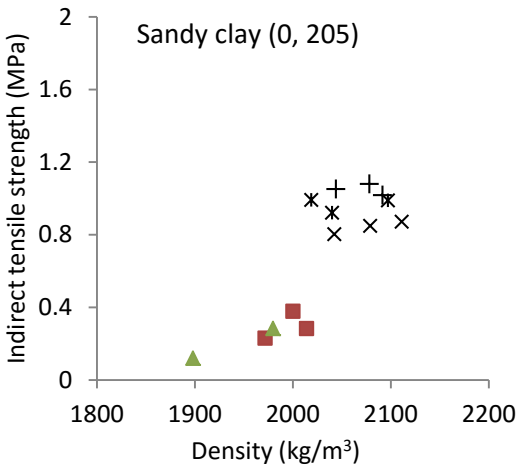
Sandy clay (0, 205)
Indirect tensile strength (MPa)
Density (kg/m³)
0
0.4
0.8
1.2
1.6
2
1800
1900
2000
2100
2200

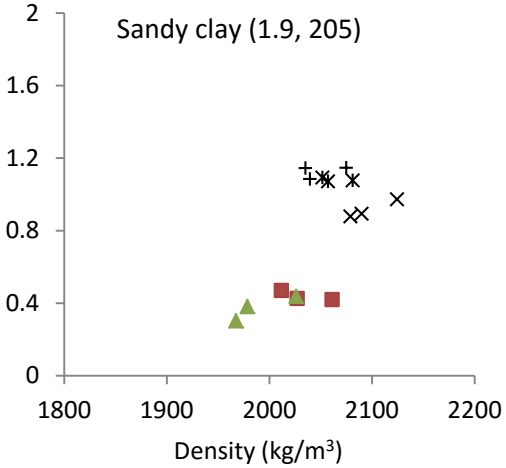
Sandy clay (1.9, 205)
Density (kg/m³)
0
0.4
0.8
1.2
1.6
2
1800
1900
2000
2100
2200

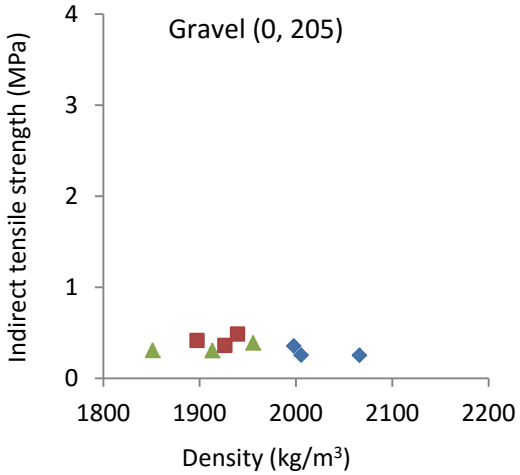
Gravel (0, 205)
Indirect tensile strength (MPa)
Density (kg/m³)
0
1
2
3
4
1800
1900
2000
2100
2200

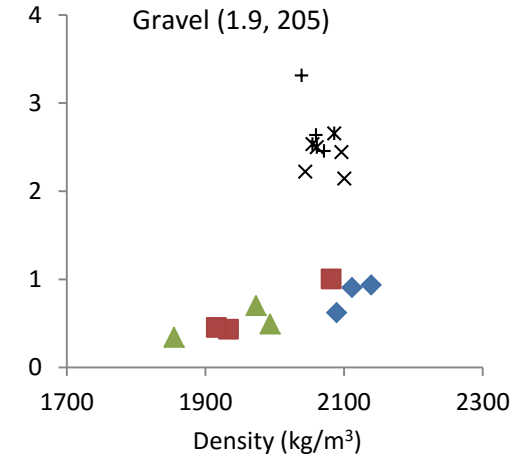
Gravel (1.9, 205)
Density (kg/m³)
0
1
2
3
4
1700
1900
2100
2300

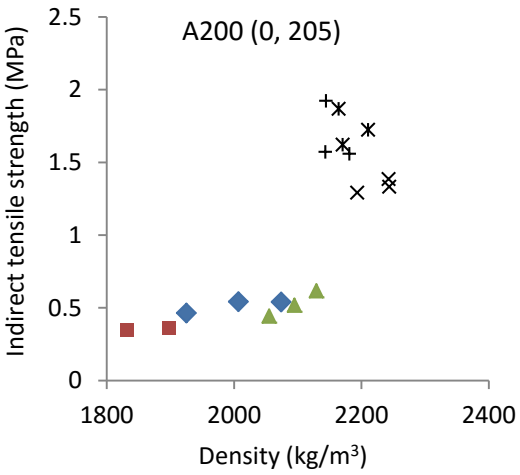
A200 (0, 205)
Indirect tensile strength (MPa)
Density (kg/m³)
0
0.5
1
1.5
2
2.5
1800
2000
2200
2400

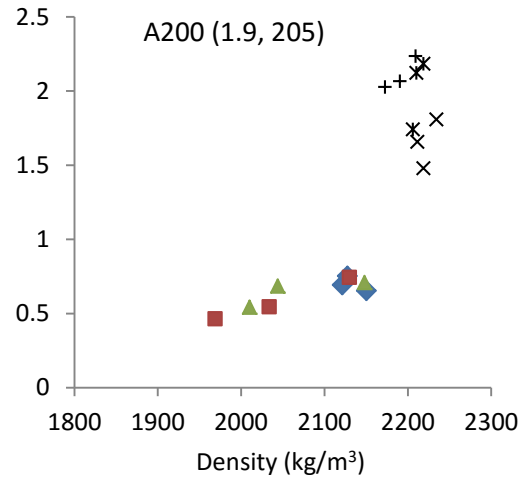
A200 (1.9, 205)
Density (kg/m³)
0
0.5
1
1.5
2
2.5
1800
1900
2000
2100
2200
2300